University of Glasgow

Defining the intrinsic and innate immune response to UV irradiated HSV-1 infection

Victor Iliev, BSc

School of Life Sciences,
College of Medical, Veterinary and Life Sciences,
University of Glasgow

Submitted in the fulfilment of the requirements of the
Doctor of Philosophy (PhD) degree in Virology

Submitted: December 2021

Abstract

Since the late 1960s UV irradiation of Herpesviruses has been used to study various aspects of cell biology, including the cellular immune response to virus infection. Previous studies have demonstrated that UV irradiation of herpesvirus virions strongly stimulates the type I and II IFN response to viral infection. However, the spatial and temporal kinetics of recruitment of immune signalling actuated in response to UV irradiated virus infection have remained poorly understood, due to limitations of viral DNA (vDNA) detection. Utilizing 5-Ethynyl-2'-deoxycytidine (EdC) labelling of HSV-1 DNA in combination with click chemistry, we were able to directly visualize vDNA and characterize the recruitment of host immune factors to infecting wild type (WT) or UV irradiated viral genomes. UV irradiation of HSV-1 virions induced the premature cytoplasmic release of vDNA in a microtubule-dependent manner. An increase in vDNA thymine dimer formation was observed that restricted genome decompacting once released from the capsid. HSV-1 genomes in the cytoplasm exhibited an enhanced recruitment of cGAS and STING following UV irradiation compared to non-UV irradiated cytoplasmic genomes. Depletion of cGAS led to the loss of STING recruitment, demonstrating a sequential recruitment of cellular PRRs. ChIP analysis further supported this finding as cGAS interaction with HSV-1 genomes was enhanced following UV irradiation, whilst STING demonstrated no interaction at all. Conversely, UV irradiation reduced frequency of recruitment of key PML-NB proteins to vDNA in the nucleus. ChIP analysis demonstrated the interaction between UV irradiated vDNA and PML to be significantly reduced compared to WT HSV-1 genomes. The click labelling was further extended to human Cytomegalovirus (hCMV) to investigate if these immune defences are conserved among Herpesviruses or HSV-1 specific. Collectively, our analysis shows multiple host factors to alter their respective recruitment and/or vDNA binding properties in response to infection following UV irradiation.

Table of Contents

List of Figures

List of Tables

Acknowledgements

This PhD was funded by the Medical Research Council as part of the Centre for Virus Research Postdoctoral Training Programmes, without whom I would not have been able to carry out this work. I would also like to thank the Centre for Virus research for the additional support as a consequence of the COVID-19 pandemic and its disruptions to my PhD.

I am extremely grateful to my PhD supervisor Dr. Chris Boutell for the endless amount of support both in my work and my professional development, shaping me into the opinionated young scientist I am now. I would like to extend my many thanks to the other members of the Boutell group both past and present. To Anne and Steven, I am eternally grateful for all the support you have provided me over the years. To Anne, I am also sorry and extremely thankful for the hundreds of coverslips you have processed! To Jo, Chris P. and Lauren, do not give up! A PhD is a true testament to your stubbornness, so keep going no matter what. Trust me it ends at some point, and you never have to go back. To all my former students I helped supervised, Joshua, Franciska, Chiara and Gordon, I am happy to see that only half of you decided on doing PhDs so I did manage to scare some of you, but you were a joy to teach. And to Sam, I am very thankful for all of the advice you gave me when I started and for showing me that you can be grumpy and approachable at the same time. Also, the trip to South Korea and Japan was my best holiday (so far) so cheers for that.

To all of my CVR friends, thanks for listening to all my moaning and supporting me in the many fits I have had over the years. It's good to know that there are people that will support you during your breakdowns. Specifically, Natalia, thank you for being my work wife and shared the good and the majority of the bad through this experience. Our coffee mornings were what made me come into work in the morning, before you know ….

COVID. Meredith, thank you for all of the sweets and cute notes you left at my desk. I am very grateful for all the help and advice you have given me and thank you for being an awesome assessor. Betty, even though it was unlucky circumstance you had to join my group I am grateful as it was a great time having you as a close colleague. You do know some gossip. Jack, Jamie, Steven, James thank you for all the laughs, pointless conversations and fun pub quizzes. Liz and Pippa, even though you moved on and completely forgot about me, I am no better. But it was fun having you there! And to Rute, thanks for the awesome 15 min corridor talks we had, they were always a pick-me-up even though once they resulted in me being locked up in my house for 3 days but at least it was a false coronavirus alert.

To my friends from Bulgaria: my three sisters – Madlen, Yanitsa and Olga. You are the loves of my life and I want you to know I am eternally grateful for the support and love you have given me and for always being a phone call away. My trips back home have always been amazing because of you, and I am happy I have you as friends for the rest of my life!

To my friends from Glasgow: my flatmates past and present, Svetoslava, Konstantina and Veronika, as well as my two neighbours Jaklyn and Krasimir, thank you for making the last four years and three months bearable! The number of crazy adventures and spontaneous trips have made the crazy at work seem normal. And thank you for at least reading this part of my thesis I appreciate it! I am also grateful to you for allowing me to vent for a million things and have given me advice for so many things. Also, all of those constant TKMaxx trips have me so much poorer so thank you for that.

Finally, I am incredibly grateful to my mother and grandmother for absolutely everything! If it wasn't for all the sacrifices, support and monetary investment I would not be writing these words right now or be

where I am! Thank you for all the support, love and interest for all that I do, even though you really have no idea as to what I do. I love you very much!

Author's declaration

The author declares that, except where explicit reference is made to the contribution of others, that this dissertation is the result of his own work and has not been submitted for any other degree at the University of Glasgow or any other institution.

List of abbreviations

ATRX	**Alpha-thalassemia mental retardation X-linked**
BHK	**Baby hamster kidney cells**
BSA	**Bovine Serum Albumin**
BrdU	**Bromodeoxyuridine**
cDNA	**Complementary DNA**
cGAMP	**Cyclic guanosine monophosphate–adenosine monophosphate**
cGAS	**cGAMP synthase**
ChIP	**Chromosome immunoprecipitation**
Coeff	**Coefficient**
Coloc	**Colocalization**
CSK	**Cytoskeletal buffer**
Ctrl	**Control**
CVSC	**Capsid vertex-specific component**
Daxx	**Human death-domain associated protein**
DMEM	**Dulbecco's Modified Eagle Medium**
DMSO	**Dimethyl sulfoxide**
DNA	**Deoxyribonucleic acid**
Ds	**Double strand**
E	**Early**
EdA	**5-Ethynyl-2'-deoxyadenosine**
EdC	**5-Ethynyl-2'-deoxycytidine**
EDTA	**Ethylenediaminetetraacetic acid disodium salt dihydrate**
EdU	**5-Ethynyl-2'-deoxyuridine**
EGTA	**Ethylene glycol tetraacetic acid**
ER	**Endoplasmic reticulum**
FCS	**Fetal calf serum**
FFU	**Foci Forming Unit**
FISH	**Fluorescent in situ hybridization**
gDNA	**Genomic DNA**
GMEM	**Glasgow's Modified Eagle Medium**
GuaHCl	**Guanidine Hydrochloride**

HCl	**Hydrogen chloride**
hCMV	**Human Cytomegaolivurs**
HEK-293t	**Human embryonic kidney cells immortalized by insertion of hTERT**
HEL	**Human embryonic lung**
HFF	**Human Foreskin Fibroblast cells**
HFt	**Human Fibroblasts immortalized by insertion of hTERT**
HHV	**Human herpesviruses**
Hpi	**Hours post-infection**
HS	**Human serum**
HSV	**Herpes Simplex Virus type**
HSV-1EdU	**EdU-labeled WT HSV-1**
hTERT	**Human telomerase reverse transcriptase**
HVEM	**Herpes virus entry mediator**
ICP	**Infected cell protein**
IE	**Immediate early**
IF	**Indirect immunofluorescence**
IFI16	**Interferon gamma inducible protein 16**
IFN	**Interferon**
IFNAR	**IFNα/ß receptor**
IL	**Interleukin**
IMR-90	**Human lung fibroblast cells**
IRF	**IFN-regulatory factor**
ISG	**IFN-stimulated gene**
ISGF3	**FN-stimulated gene factor 3**
ISRE	**Interferon-stimulated response element**
IU	**International unit**
JAK	**Janus-associated kinase**
K	**Lysine**
kDa	**Kilo Dalton**
L	**Late**
LATs	**Latency-associated transcripts**
M	**Molar**
MCP	**Major Capsid Protein**
MgCl2	**Magnesium chloride**

Mg	**Milligram**
Mj	**Microjoules**
Mm	**Millimolar**
Ml	**Milliliter**
MIEP	**Major Immediate Early Promoter**
Mm	**Millimeter**
MOI	**Multiplicity of infection**
MORC	**Microrchidia family CW-type zinc finger**
Mpi	**Minutes post-infection**
mRNA	**Messenger RNA**
miRNA	**Micro RNA**
Mx	**Myxovirus resistance protein**
NaCl	**Sodium Chloride**
Ng	**Nanogram**
Nm	**Nanometer**
NPC	**Nuclear Pore Complex**
NK	**Natural killer**
NLS	**Nuclear localization signal**
Ns	**Non-significant**
O.N.	**Over night**
Ori	**Origin of replication**
ORF	**Open reading frame**
PAGE	**Polyacrylamide gel electrophoresis**
PAMPs	**Pathogen-associated molecular pattern**
PBS	**Phosphate buffered saline**
PBST	**PBS Tween**
PFA	**Paraformaldehyde**
PFU	**Plaque forming unit**
PIAS	**Protein Inhibitor of Activated STAT**
PML	**Promyelocytic leukemia protein**
PML-NB	**PML-nuclear body**
PolyI:C	**Polyinosinic-polycytidylic acid sodium salt**
PRRs	**Pattern recognition receptors**
qPCR	**Quantitative polymerase chain reaction**
RIG	**Retinoic acid inducible gene**

RING	**Really interesting new gene**
RNA	**Ribonucleic acid**
RNase	**Ribonuclease**
RNF	**Ring finger protein**
RPE	**Retinal pigmented epithelial cells immortalized hTERT**
Rpm	**Revolutions per minute**
RT	**Reverse transcription**
SAOS	**Human bone osteosarcoma epithelial cells**
SCP	**Small Capsid Protein**
SD	**Standard deviation**
SDS	**Sodium dodecyl sulfate**
SENP	**SUMO-specific proteases**
SIM	**Sumo-interacting motif**
Sp1	**Specificity protein 1**
Sp100	**Speckled protein of 100 kDa**
STAT	**Signal transducers and activators of transcription**
STING	**Stimulator of interferon genes**
Ss	**Single strand**
SUMO	**Small ubiquitin-like modifiers**
TBK1	**TANK binding kinase 1**
TF	**Transcription factor**
TRIM	**Tripartite motif**
Ub	**Ubiquitin**
UL	**Unique long**
Us	**Unique short**
UV	**Ultraviolet**
U2OS	**Human bone osteosarcoma epithelial cells**
vDNA	**Viral DNA**
VP	**Virion protein**
VZV	**Varicella-zoster virus**
W	**Weighted**
WB	**Western blot**
WT	**Wild type**
X g	**Times gravity**
ZAP	**Zinc finger antiviral protein**

3D	**3 dimensional**
µg	**Microgram**
µl	**Microlitre**
µm	**Micromillimeter**
µM	**Micromolar**

1. Introduction

Host cells are under constant attack from pathogens and have developed multiple defence mechanisms to control infection to reduce the damage these pathogens cause. The cellular immune responses can be separated into 3 branches of the immune system: intrinsic, innate, and adaptive. Intrinsic immunity refers to a form of pre-existing cellular defence that is mediated by constitutively expressed cellular proteins (intrinsic restriction factors) that act to block viral replication immediately upon infection (Paludan et al., 2019; Yan & Chen, 2012). In contrast, the innate and adaptive arms of the immune system are upregulated in response to pathogen detection to confer a broadly neutralizing antiviral response that limits the propagation and spread of virus (Scherer & Stamminger, 2016; Yan & Chen, 2012; Hannoun, Maarifi & Chelbi-Alix, 2016).

These arms of the immune system are required to act in unison to confer efficient restriction of viral pathogens, a process heavily dependent on the recognition of specific Pathogen Associated Molecular Patterns (PAMPS) by cellular Pattern Recognition Receptors (PRRs) (Komatsu, Nagata & Wodrich, 2016; Abe, Marutani & Shoji, 2019; Ma, Ni & Damania, 2018; Yang & Shu, 2020). Correspondingly, viruses have evolved a variety of ways to evade or inhibit these pathways. The molecular basis of these interactions has been extensively studied (Abe, Marutani & Shoji, 2019; Ma, Ni & Damania, 2018). This literature review will focus on the cellular mechanisms utilized to detect and control Herpes Simplex Virus 1 (HSV-1) and Human Cytomegalovirus (hCMV) as well as the viral immune evasion strategies that combat these defences. Particular attention will be given to promyelocytic leukemia-nuclear body (PML-NB) constituent proteins and the cyclic GMP-AMP synthase (cGAS) and stimulator of interferon (IFN) genes (STING) proteins due to their key role in the detection and entrapment of DNA viruses and activating the innate immune responses during herpesvirus infection. These will be discussed in the context of UV irradiated herpesvirus or HSV-1 infection, as little is known about how UV inactivation

of herpesviruses results in enhanced immune activation (Hidmark et al., 2005; Marcus, Rojek & Sekellick, 2005).

1.1 Overview of HSV-1 infection

HSV-1 is ubiquitous within the human population, with an estimated 3.7 billion people infected under the age of 50 (67% of the population). Viral transmission occurs most commonly via direct physical contact with infected individuals who are shedding the virus, and the resultant infection is lifelong. Vertical transmission from seropositive mothers to their children during pregnancy has also been reported, with significant morbidity and mortality (Whitley & Baines, 2018; Kabani & Kimberlin, 2018). HSV-1 infection is typically asymptomatic or manifests as ulcers in or around the mouth ('cold sores'). Additionally, HSV-1 infections can lead to more severe and even life-threatening outcomes, for example viral encephalitis (Whitley & Baines 2018). Following lytic infection of mucosal epithelial cells, the virus infects neuronal cells of the sensory ganglia where the genomes establish a life-long latent infection. Periodic reactivation events cause HSV-1 lytic infection to recommence that enables transmission to new hosts (Held & Derfuss, 2011; Kabani & Kimberlin, 2018). Efficient antivirals are available for HSV-1, such as acyclovir, valacyclovir, and trifluridine (Birkmann & Zimmermann, 2016) , although resistance to some of these drugs has been reported (Frobert et al., 2014). This creates a need for the development of a vaccine, and although there are a number of vaccine candidates that have been trialled none of them have clinically approved to date (Johnston, Gottlieb & Wald, 2016).

1.2. Herpesviridae family

Both HSV-1 and hCMV belong to the Herpesviridae family of viruses with more than 130 known members. Nine of these are known to cause disease in humans (human herpesviruses or HHV) and are classified into three groups based on their biological characteristics, DNA sequence relatedness and cellular tropism: Alphaherpesvirinae, which includes HHV-1, -2 and -3 (HSV-1, HSV-2 and Varicella-zoster virus, respectively); Betaherpesvirinae, which includes HHV-5 (human Cytomegalovirus), -6A, -6B and -7; Gammaherpesvirinae, which includes HHV-4 and -8 (Epstein-Barr virus and Karposi Sarcoma-associated virus, respectively) (Knipe & Howley-Fields, 2013; Everett, 2014).

1.3. HSV-1 virion structure

The HSV-1 virion is largely spherical with a diameter of 186 nm, that can extend up to 225 nm when including the glycoproteins (Grünewald et al., 2003). Typical for Herpesviridae members, it is comprised of four main architectural components: the core, the capsid, the tegument, and the envelope (Figure 1). The core contains a single copy of the linear double stranded DNA genome, and it resides in a liquid-crystalline state as a toroid or spool structure, with the DNA strands being spaced approximately 2.6 nm apart (Furlong, Swift & Roizman, 1972; Booy et al., 1991; Everett, 2014). The complete genome sequencing of the HSV-1 strain '17' is 152 260 bp long with a 68.3% G+C composition (Mcgeoch et al., 1988; Kieff, Bachenheimer & Roizman, 1971; Bauer et al., 2013; Everett, 2014; Knipe & Howley-Fields, 2013). The viral genome is comprised of unique long and short regions (U_L and U_S, respectfully) flanked by inverted repeated ab and b'a', and ac and c'a sequences, respectively (Figure 1) (Mcgeoch et al., 1988; Bauer et al., 2013; Everett, 2014). The capsid is 125 nm in diameter, composed by 162 major structural protein subunits in a T=16 icosahedral lattice (Wildy et al., 1960). The major capsid proteins involved in the assembly of HSV-1 capsids

are VP5, VP26, VP19c, VP23, pre-VP22a and pre-VP21 (Trus et al., 1996). These capsomeres are sub-divided into 150 hexons that form the edges and faces of the capsids along with 11 pentons and 1 portal complex, through which the viral DNA enters and exits the capsid (Newcomb et al., 2001; Wildy et al., 1960; Everett, 2014; Knipe & Howley-Fields, 2013; Huet et al., 2016; Brown & Newcomb, 2011). The portal is cylindrical and is comprised of 12 copies of pUL6 (Newcomb et al., 2001; McElwee et al., 2018). The pentamers and hexamers are comprised of five and six copies of the major capsid protein VP5, respectively (Newcomb et al., 1993; Knipe & Howley-Fields, 2013; Everett, 2014). At the tip of every VP5 positioned at a hexon capsomere is a single copy of VP26 protein, accumulating to 900 copies of it per capsid (Booy et al., 1994; Newcomb et al., 1993; Everett, 2014; Knipe & Howley-Fields, 2013). The neighbouring capsomeres interact directly with heterotrimeric "triplexes" located at the local 3-fold symmetry and are composed of two subunits of VP23 and one subunit of VP19C (Zhou et al., 1994; Trus et al., 1996; Newcomb et al., 1993; Knipe & Howley-Fields, 2013; Everett, 2014). Additionally, Cryo-EM studies have discovered an extra capsid component that is adjacent to the triplexes and pentons, called the capsid vertex-specific component (CVSC) and is composed of UL17, UL25 and UL36, with the function of capsid stabilization during and after DNA packaging (Fan et al., 2015; Huet et al., 2016; Trus et al., 2007; Toropova et al., 2011; Cockrell et al., 2011; Conway et al., 2010). Procapsid maturation is carried out by the VP24 protease, which cleaves off the scaffolding proteins and plays a role in the initiation of procapsid angularization (Liu & Roizman, 1993; Loret, Guay & Lippé, 2008). The tegument layer is located in the space between the capsid and the envelope. The HSV-1 tegument is a large, highly asymmetric, and densely packed network of thousands of protein molecules. Proteomic analysis has identified 23 virally encoded tegument proteins that are acquired during tegumentation in the cytoplasm, specifically at the trans-Golgi network (Loret, Guay & Lippé, 2008; Granzow et al., 2001; Sugimoto et al., 2008; Turcotte, Letellier & Lippé, 2005). Tegument proteins play an important role during infection, including entry, initiation of viral gene expression, assembly and egress, as well as immune evasion (Table 1). Finally, the envelope is arranged as a lipid bilayer enclosing the tegument and contains 16 membrane proteins, 12 of which are glycoproteins that protrude externally

– gB-gE gG-gN. These are of particular importance as they are involved in the interaction between the virion and the host cell surface proteins required for entry (Reske et al., 2007).

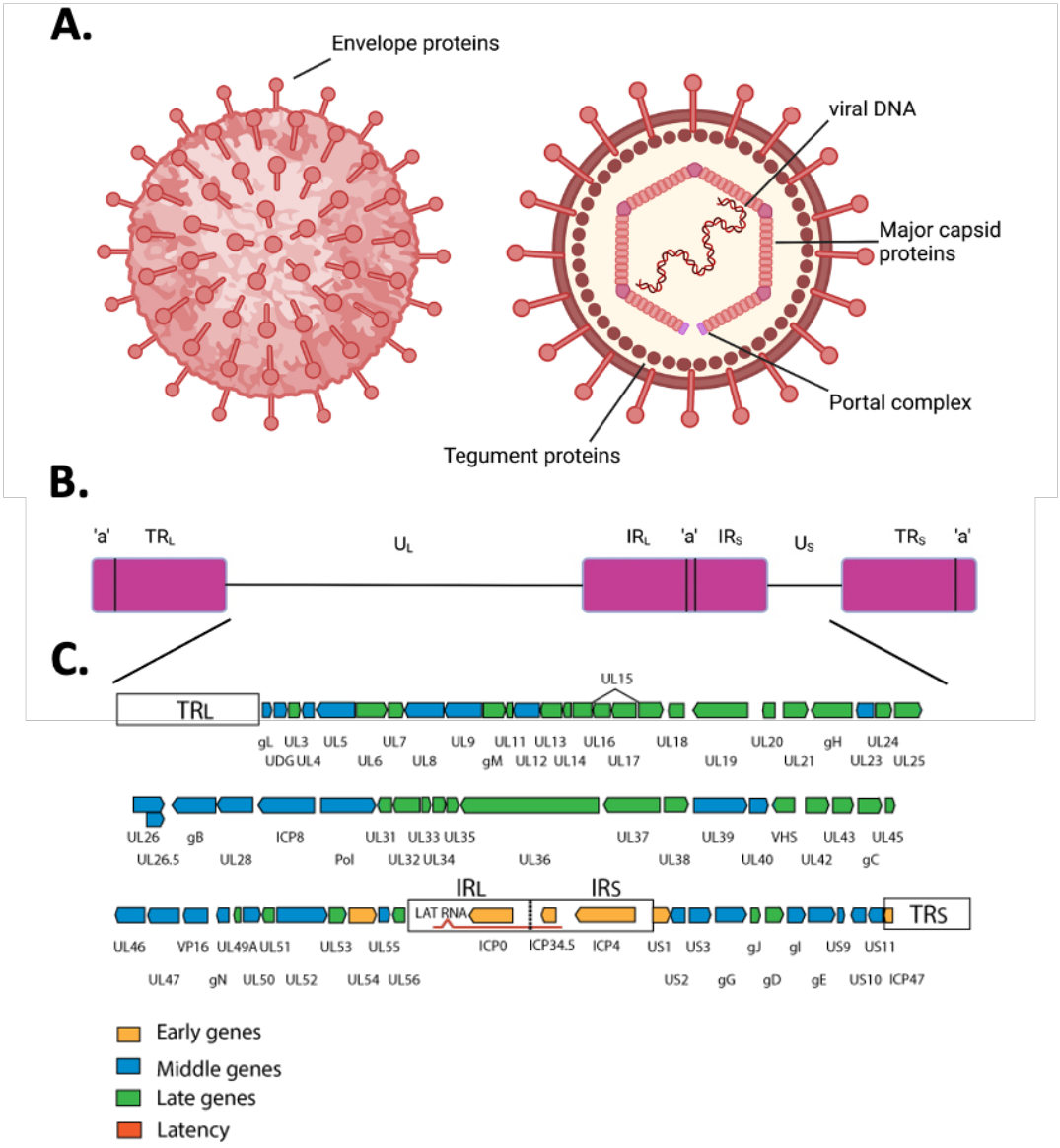

Figure 1. HSV-1 virion and genome structure.

(A) Cartoon representation of the HSV-1 virion, composed of viral genome, capsid, tegument and envelope. The dsDNA genome is enclosed on the capsid and surrounded by the tegument layer. The envelope is a lipid bilayer membrane that is decorated with glycoproteins. (B) Cartoon representation of the genome, showing the positions of the Unique short or long regions (U_S and U_L, respectfully) and the genome repeated sequences (R), labelled as Internal (I) or Terminal (T). The repeat sequence is indicated with 'a' (Everett, 2014). Images were created with Biorender.com. (C) Cartoon representation of all of the open reading frames (ORFs) of the HSV-1 genome. Colour coding of the ORFs to denote the temporal kinetics of expression of the individual viral proteins (ViralZone, 2012).

Tegument protein	Function
ICP0	Regulation of viral transcritpion and evasion of the immune system
ICP4	Regulation of viral transcritpion
ICP34.5	Regulates host translation, viral DNA replication and immuneresponse
pUL7	Mitochondrial regulatory function
pUL11	Maturation and capsid envelopment
pUL13	Protein kinase, tegument dissociation, regulates apoptosis andpUS3, inhibits IFN response
pUL14	Nuclear import, regulates apoptosis, nuclear targeting ofcapsids
pUL16	Secondary envelopment
pUL21	Secondary envelopment, regulates microtubule assembly
pUL23	Thymidine kinase, viral DNA replication
pUL36	Capsid transport, secondary envelopment, release of viral DNA,deubiquitinating activity
pUL37	Secondary envelopment, regulating viral transcription
pUL41	Regulates host/viral translation and immune response
pUL46	Secondary envelopment,
pUL47	regulates pUL48-dependenttranscription
pUL48	Secondary envelopment, regulating viral transcription
pUL49	Secondary envelopment, regulates microtubule assembly
pUL50	dUTPase, viral DNA replication
pUL52	Unknown
pUL55	Unknown
pUS2	Unknown
pUS3	Protein kinase, primary deenvelopment, tegumentdissociation, regulates actin assembly
pUS10	Unknown
pUS11	Regulates host translation, capsid transport

Table 1. HSV-1 key tegument proteins and their functions during viral infection. Adapted from (Kelly et al., 2009).

1.4. HSV-1 replication cycle

1.4.1 Attachment, fusion and nuclear delivery of viral DNA

The initial step of establishing viral replication in target cells is the attachment of the virus to the cell surface. There are several ways attachment may occur during the initial stages of infection: (i) gC and gB interact independently with heparan sulfate (HS) proteoglycans to promote initial attachment, (ii) gD interaction with one of several host receptors - herpes entry mediator (HVEM), nectin-1 or 3-0-sulfated heparan sulfate (Montgomery et al., 1996; Geraghty et al., 1998; Whitbeck et al., 1997; Shukla et al., 1999; Laquerre et al., 1998; Shieh et al., 1992; Campadelli-Fiume et al., 2012; Connolly et al., 2011).The differential use of all of these receptors could account the extensive viral tropism of HSV-1 to a large number of different cell types in culture. The exact mechanism of viral fusion with the cell membrane remains to be elucidated but is believed that gD binding to the cell receptor leads to the conformational change in the gH/gL complex that leads to the activation of gB. The concert acting of these glycoproteins results in the fusion of the viral envelope and cellular membrane, mediating viral capsid entry (Satoh et al., 2008; Avitabile, Forghieri & Campadelli-Fiume, 2007; Gianni, Amasio & Campadelli-Fiume, 2009; Connolly, Jardetzky & Longnecker, 2021). Entry of HSV-1 into HFF cells is reported to be via membrane fusion (Maurer, Sodeik & Grü, 2008). HSV-1 utilizes endocytosis as an additional mode of entry into target cells (Nicola et al., 2005; Milne et al., 2005; Nicola, 2016). Upon entry, cytosolic nucleocapsids exploit the cellular microtubule network to traverse the cell and reach the nucleus (Sodeik, Ebersold & Helenius, 1997). The HSV-1 capsid binds multiple microtubule proteins, such as dynein-1, dynactin, and kinesin-1, via the different structural features of the inner tegument and results in the directional transport of the capsid to the nucleus (Döhner, Nagel & Sodeik, 2005; Radtke et al., 2010), where an increase in empty capsids can be observe by Cryo-EM (Further et al., 1983; Miyamoto' And & Morgan, 1971). The viral tegument protein UL25 and the cellular protein importin-b play a key role

in the binding of the capsid to the cellular nuclear pore complex (NPC) (Pasdeloup et al., 2009). HSV-1 capsids dock to the NPC cytoplasmic filaments via Nup358 and Nup214 in an importin- b - and Ran- dependent manner (Pa¨ et al., 2000; Copeland, Newcomb & Brown, 2009a). VP1/2, encoded by UL36, is also important in this process (Copeland, Newcomb & Brown, 2009b) and its proteolytic cleavage is key for DNA release out of the capsid (Jovasevic, Liang & Roizman, 2008). The exact trigger for DNA release is still to be fully determined. Atomic force microscopy has shown HSV-1 genomes to be condensed rod-like structure and is hypothesised that the pressure-driven DNA ejection pushes the genome through the NPC (Shahin et al., 2006; Bauer et al., 2013). Once in the nucleus, the viral genomes have been shown to localize to cellular protein clusters, known as PML-NBs (discussed in a section further below) (Ishov & Maul, 1996).

1.4.2 Virus gene expression and DNA replication

Characteristic for all herpesviruses, HSV-1 gene expression is carried out in a temporally regulated cascade. The viral genes are classified into 3 temporal classes: immediate-early (IE; α), early (E; β) and late (L; γ) genes (Honess & Roizman, 1974). IE proteins are the first ones to be synthesized following nuclear entry. VP16 is a tegument protein that plays an important role in stimulating the expression of the IE proteins (Batterson, Roizman & Kovler, 1983). VP16 interacts with host cell factor-1 (HCF-1), allowing for its nuclear translocation (Laboissie`re & O'hare, 2000). Once transported to the nucleus, VP16 binds to Oct-1 and HCF-1 and forms a transcriptional regulatory complex that binds IE genes via its conserved DNA binding domain (Kristie & Sharp, 1990). This interaction enhances the transcriptional activity of the pre-assembled cellular machinery on the IE promoter regions to stimulate IE transcription (Fan et al., 2020; Simmen et al., 1997).

De novo synthesis of IE genes (ICP4, ICP0, ICP22, ICP27 and ICP47) promote the transcription of E genes. The viral ICP4 is shown to be the essential transcriptional regulator of this process. ICP4 is a DNA-binding protein that can, dependent on the target promoters, increase or decrease the transcription rate of specific genes via the RNA Polymerase II (Papavassiliou & Silverstein, 1990; Carrozza & Deluca, 1996; Smith et al., 1993). Additionally, ICP4 represses itself by binding to a repressor element in its own promoter to reduce its own and IE and E gene levels, stimulating the switch to L gene production (Muller, 1987). ICP27 is another essential regulatory viral protein for replication and the transcription of E and L genes during early timepoints of infection. It has been shown to directly interact with RNA Polymerase II along with ICP8 to regulate viral gene expression but also to modulate transcription through direct or indirect interactions with other viral regulatory regions or viral proteins (Olesky et al., 2005; Sacks et al., 1985; Uprichard & Knipe, 1996; Mcgregor et al., 1996; Samaniego, Webb & Deluca, 1995). Additionally, ICP27 has been shown to play an important role in viral intronless mRNA export by interacting with the RNA export factor Aly/REF (Sandri-Goldin, 1995; Chen, Sciabica & Sandri-Goldin, 2002). ICP0 acts together with cellular proteins to activate transcription and provide a favourable environment for viral protein synthesis and DNA replication. Expression of ICP0 induces the degradation of PML and dispersal of PML-NBs from vDNA (Everett, Boutell & Hale, 2013; Alandijany et al., 2018). Additionally, ICP0 induces the degradation and dispersal of multiple H3.3 chaperone molecules, for example HIRA, during independent phases of infection (Orzalli, DeLuca & Knipe, 2012; Orzalli, Broekema & Knipe, 2016; McFarlane et al., 2019; Goff et al., 2018). Consequently, this leads to the reduction of H3 acetylation and H3 loading on vDNA and promote transcription (Cliffe & Knipe, 2008; Lee, Raja & Knipe, 2016; Goff et al., 2018).

Once E gene products are synthesized, vDNA replication can commence. There are seven essential genes uncovered to be required for replication (Challberg, 1986): the origin binding protein (UL9) (Elias et al., 1986), the single stranded DNA binding protein ICP8 (Conley et al., 1981), the helicase-primase complex (UL5/UL8/UL52) and the vDNA polymerase

(catalytic subunit UL30 and its accessory factor UL42) (Purifoy, Lewis & Powell, 1977). HSV-1 DNA replication occurs in nuclear structures near PML-NB sites termed replication centres, where vDNA and replication proteins accumulate (Ishov & Maul, 1996; Uprichard & Knipe, 1996; Quinian, Chen & Knipe, 1984). Viral DNA replication is carried out by two modes: (i) theta replication begins following DNA entry into the nucleus, the linear DNA genome circularizes and the origin binding protein UL9 binds to one of three origins of replication (one copy of ori_L and two or ori_S) (Hardwicke & Schaffer, 1995) and begins to unwind the DNA. The ssDNA binding ICP8 is recruited to separated strands of the DNA and acts as a scaffolding protein by promoting the activity of the helicase-primase complex (le Gac, Villani & Boehmer, 1998; Falkenberg et al., 1997; Fierer & Challberg, 1992). The helicase-primase complex and the DNA polymerase are recruited onto the replication forks and leading-lagging strand synthesis commences (Wu,' et al., 1988). (ii) theta replication is then switched to a UL9-independent rolling circle mechanism where long concatemers are synthesized then cleaved into unit-length monomers by the viral terminase complex during packaging into pro-capsids (Rabkin & Hanlon, 1990). DNA replication along with ICP22 stimulates the production of L genes, which initiate capsid assembly and packaging.

1.4.3 Nucleocapsid assembly and egress

Virus capsid assembly is a multistep process and in vitro studies have identified VP5, VP19C, VP23, pre-VP22a and the maturational products of UL26 (VP21 and VP24) as the minimum proteins required for normal capsid formation (Newcomb,' et al., 1994; Newcomb et al., 1999, 1996). Once these components are synthesized in the cytoplasm, they are transported to the nucleus, where capsid assembly is carried out in large inclusion bodies (Spencer et al., 1998; Peng et al., 2010). This allows for the formation of the procapsid by the interaction of the major capsid protein VP5 and the scaffolding proteins, as well as the triplexes which stabilize the links between VP5 capsomeres. The maturation of the procapsid is achieved once the scaffolding proteins are removed from the structure,

allowing for the angulariazation and achievement of the polyhedral shape. These capsids are then filled with the concatemers of vDNA produced by the viral replication machinery by the terminase complex and cleaved into unit-length monomers, completing the assembly process (Yang, Homa & Baines, 2007; Heming, Conway & Homa, 2017).

Viral egress is a highly complex process as mature non-enveloped capsids need to exit the nucleus, traverse the cytoplasm and bud out of the infected cell. The biggest obstacle in this process is the egress from the nucleus, as it represents a formidable barrier to mature capsids. The current model proposes HSV-1 capsids to exit via an envelopment/de-envelopment/re-envelopment mechanism (Skepper et al., 2021; Mettenleiter & Minson, 2006; Mettenleiter, 2002). In this pathway mature capsids bud through the inner nuclear membrane, acquiring an envelope and form the primary enveloped virions within the nuclear lumen. This is mediated through the heterodimeric complex composed of UL31 and UL34. Following primary envelopment, these particles fuse with the outer nuclear membrane and are released in the cytoplasm (de-envelopment). Soon after, the inner tegument proteins are recruited and the capsids associate with the microtubule network (Radtke et al., 2010) for transport to the trans-Golgi network (Turcotte, Letellier & Lippé, 2005; Sugimoto et al., 2008). There, the outer tegument layer and bilipid envelope, containing the full complement of envelope proteins, are acquired and the mature viruses are released from the cell by exocytosis to infect neighbouring cells. Additionally, there is evidence that HSV-1 membrane acquisition maybe occurring in endocytic tubules instead of membranes of the secretory pathways, as inhibition of the endocytic pathway led to a retention of viral glycoproteins on the cell surface and a decrease of virus yields (Hollinshead et al., 2012). An overview of the HSV-1 replication cycle is shown in Figure 2.

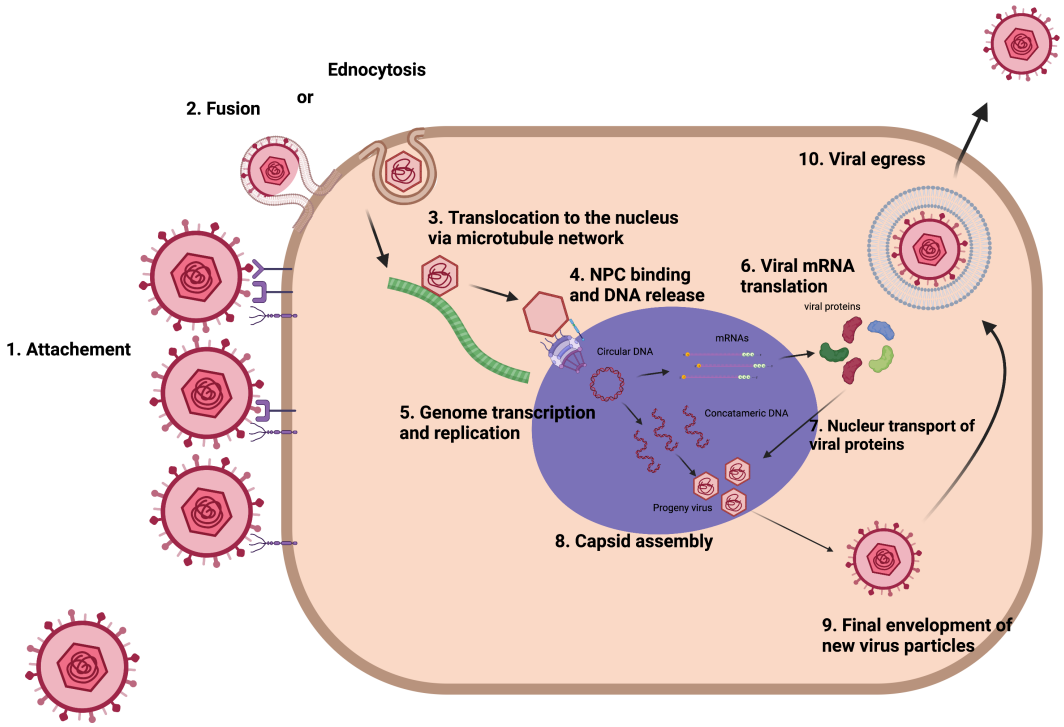

Figure 2. Overview of the HSV-1 life cycle.

The virus attaches via glycoproteins to the cellular receptors. It enters the cells via direct fusion of the viral envelope and the plasma membrane or endocytosis. The de-enveloped capsid is transported to the nuclear pores via the microtubule network, and the vDNA is ejected into the nucleus through the Nuclear Pore Complex. Theta replication and rolling circle are two suggested mechanisms for vDNA replication. Viral transcription results in the production of viral mRNAs that are escorted to the cytoplasm by ICP27 and translated into proteins. The capsid is assembled at sites adjacent to vDNA replication compartments allowing for the packing of vDNA into the capsid. The nucleocapsids bud through the nuclear membrane through an envelopment/de-envlopment/re-envelopment mechanism, transport through the cytoplasm, and fuse with the plasma membrane to egress. During the capsid maturation and egress steps, the nucleocapsid acquires tegument and envelope proteins, respectively. The release of mature progeny virions promotes attachment to adjacent cells, and the continuation of the cycle (Knipe & Howley-Fields, 2013). Image created with Biorender.com.

1.5. Viral latency

Primary HSV-1 infection occurs in epithelial and endothelial cells in the oral cavity that eventually leads to the axonal infection of sensory neurons feeding the sites of primary infection. These are usually the maxillary and mandibular branch of the trigeminal ganglion. The virus travels via retrograde transport to the neuronal cell body where it establishes a life-long latent infection in the nucleus (Theil et al., 2003; Stevens & Cook, 1971). Viral DNA (vDNA) is maintained as a circular episome and associates with nucleosomal chromatin, the epigenetic modification of which silences viral gene promoters leading to a block in viral transcription (Roizman, 2011). The only detectable transcripts are latency-associated transcripts (LAT). Their transcription leads to the production of primary micro RNAs (miRNAs), which act to render gene promoter regions transcriptionally inactive by the induction of heterochromatin formation and silencing the production of ICP0 and ICP4 (Wang et al., 2005; Kwiatkowski, Thompson & Bloom, 2009; Umbach et al., 2009, 2008). In addition to LATs and miRNAs being important for establishing latent infection, the cellular immune system has also been found to play a role in maintenance of HSV-1 latency. Prolonged chemokine and cytokine expression along with continued activation of CD8+ T cells have been reported to be important in maintaining latency (Khanna et al., 2003). HSV-1 is able to reactivate from latency in response to specific stimuli such as stress, exposure to UV, and tissue injuries (Bonneau, 1996; Hendricks et al., 2021; Roizman & Whitley, 2013). During reactivation, the LAT promoter is deacetylated, while the histones associated with lytic genes are acetylated, activating the onset of transcription and the onset of infection (Amelio et al., 2006; Du et al., 2011).

1.6. Host immunity to viral infection

In order to combat infection, cells have evolved a large array of mechanisms to detect and supress viral replication. The molecular details of the cellular immune response to herpesvirus infection have been extensively studied in the last few decades. The current understanding of the host immune response (intrinsic and innate) to HSV-1 is discussed below.

1.6.1 Host intrinsic immunity to HSV-1

The intrinsic immune response is mediated by constitutively expressed cellular restriction factors that act immediately and directly to limit viral infection. The presence of these molecules is a determining factor for the potential of cell lines to restrict infection independently of the activation of IFN-mediated innate immune defences permissive to infection (Alandijany et al., 2018). The use of HSV-1 lacking the key ICP0 protein has been instrumental in defining the characteristics of this arm of immunity, as the deletion of this protein resulted in the relief of degradation of a large number of intrinsic immune restriction factors such as PML-NB constituent proteins (Sacks & Schaffer, 1987; Stow & Stow, 1986; Boutell & Everett, 2013). Different cell lines show various levels of restriction to ICP0-null mutant HSV-1, ranging from ~1000-fold in diploid fibroblasts and keratinocytes to almost absent in osteosarcoma U2OS cells (Yao & Schaffer, 1995; Everett, Boutell & Orr, 2004). Additionally, the intrinsic immune response was saturable as increasing the MOI of the ICP0-null mutant relieved restriction and allowed for the virus to grow to levels comparable to the WT strain (Everett, Boutell & Orr, 2004; Rodríguez et al., 2020).

These findings have allowed for the identification of a range of different intrinsic restriction factors (Table 2). In this section some of the more relevant intrinsic host factors to HSV-1 will be discussed.

Protein	Function	Reference
PML	Essential for forming PML-NBs, which entrap viral genomes	Alandihany et al., 2018 Everett and Chelbi-Alix, 2007 Sahin Umut et al., 2014
Sp100	PML-NB component, which entrap viral genomes	Alandijany et al., 2018 Sternsdorf et al., 1995 Everett, 2006 / 2008
Daxx	PML-NB component, interacts with ATRX and promotes H3.3 loaidng onto vDNA to repress viral gene expression	Lin et al., 2006 Goldberg et al., 2010 Tang et al., 2004 Drané et al., 2010
ATRX	PML-NB component, interacts with Daxx and promotes H3.3 loaidng onto vDNA to repress viral gene expression	Tang et al., 2004 Li et al., 2017 Lukashchuk and Everett, 2010 Goldberg et al., 2010
MORC3	PML-NB component, influences recruitment of other components	Mimura et al., 2010 Sloan et al., 2016
PIAS1/4	PML-NB component, recruited to sites of vDNA, restriction of plaque formation	Brown et al., 2016 Conn et al., 2016
RNF8/RNF168	Recruted to adjacant sites of vDNA in cells at the edge of plaques, reduces gene expression	Lilley et al., 2010, 2011
Repressive histones (histones with repressive marks)	Recruit to infecting vDNA and induce the viral genome chromatinization and silencing, require chaperone molecules (e.g., HIRA, Daxx)	Rai et al., 2017 Cabral et al., 2018 Kent et al., 2004 Lee et al., 2006

Table 2. The role of intrinsic immune restriction factors in response to HSV-1 infection.

1.6.1.1 PML-NB constituent proteins

PML (promyelocytic leukaemia) nuclear bodies (NBs), also known as Nuclear Dot 10 (ND10), are small macro-molecular nuclear sub-structures that are ubiquitously expressed in all cells and contain many permanently or transiently associated proteins (Tavalai & Stamminger, 2009; Bernardi & Pandolfi, 2007). The list of proteins, that have been reported to be associated with PML-NBs is constantly growing. However, there are several key proteins that are constitutively expressed in normal diploid cells and are crucial to the structural formation of these dot-like structures. Promyelocytic leukaemia protein, or PML, is essential for the structure and integrity of NBs. Other proteins have been shown to associate with PML to form PML-NBs, such as Daxx, ATRX and Sp100 (Everett & Chelbi-Alix, 2007; Everett, 2006). The complexity of these dynamic foci is shown in their involvement in a variety of different cellular functions, such as oncogenesis, apoptosis, DNA damage response, and cellular immune response to virus infection (Bernardi & Pandolfi, 2007).

PML-NBs have also been shown to play a role in the regulation of intrinsic and innate immunity against DNA virus infection, including retroviruses such as HIV-1 (Scherer & Stamminger, 2016; Bernardi & Pandolfi, 2007; Kahle et al., 2016; Dutrieux et al., 2015). The first observation of the interplay between DNA viruses and PML NBs was made back in 1993 by Maul et al, who showed the disruption of PML-NBs in HSV-1 infection by the viral immediate early protein ICP0 (Maul, Guldner & Spivack, 1993). After years of extensive research, our understanding of the interplay between HSV-1 and PML has greatly improved (Tavalai & Stamminger, 2009; Scherer & Stamminger, 2016). Other DNA viruses have also been shown to interact with PML-NBs, for example adenovirus (Ishov & Maul, 1996), other herpesviruses, including human cytomegalovirus (hCMV) (Kelly, Driep & Wilkinson, 1995; Ishov, Stenberg & Maul, 1997) and papillomaviruses (Frappier, 2016). Although the details around these events are becoming clearer, many aspects of the functional interplay between PML-NBs and viral genomes remain to be resolved.

However, it is clear that PML-NBs play an important role in the temporal regulation of intrinsic and innate immune defences to DNA virus infection (Regad et al., 2001; Chee et al., 2003; Scherer et al., 2016; Alandijany et al., 2018).

1.6.1.1.1 Promyelocytic leukemia protein (PML)

PML is a member of the tripartite motif (TRIM)-containing protein family. These constitute of a conserved RING domain, one or two B box domains and a coiled-coil domain (Jaworska et al., 2020; Goodrum, 2016; Tao et al., 2008). The PML gene contains 9 exons and can be alternatively spliced giving rise to a large number of isoforms (PML I-PML VII) with variable C-termini. Dependent on the presence of a nuclear localization signal (NLS), PML isoforms are predominantly nuclear, but a cytoplasmic PML variant has been described – PML VII (Jensen, Shiels & Freemont, 2001). The different PML isoforms carry out distinct functions by interacting with numerous cellular proteins (Jensen, Shiels & Freemont, 2001). PML has been found to be heavily SUMOylated at different lysine residues, which regulates PML function (Kamitani et al., 1998b; Liang et al., 2016a; Cuchet et al., 2011). SUMOylation is essential for the recruitment of several PML-NB associated proteins, but not for the oligomerization of PML, which forms the PML-NB scaffold (Sahin Umut et al., 2014; Shen et al., 2006a; Zhong et al., 2000). PML has been found to undergo extensive post-translational modification (PTM) in response to different stimuli (e.g., oxidative stress), including ubiquitination, phosphorylation, and ISGylation, that affect PML stability, turnover and function (Hsu & Kao, 2018).

During HSV-1 infection, PML and other PML-NB components are rapidly recruited to the sites of nuclear infecting vDNA (Everett & Murray, 2005). Viral genome deposition is enough for the *de novo* re-localization of these cellular proteins and is independent of viral protein synthesis (Everett & Murray, 2005; Everett et al., 2006). Once recruited onto vDNA, these NB

factors entrap the viral nucleic acid prior to initiation of viral replication and repress the progress of viral transcription (Glass & Everett, 2013; Alandijany et al., 2018). During wild type HSV-1 infection this event is short-lived due to the expression of ICP0. ICP0 antagonizes PML-NBs (Everett & Murray, 2005) by its E3-Ub ligase-mediated activity that degrades PML (Vanni et al., 2012; Boutell, Sadis & Everett, 2002; Komatsu, Nagata & Wodrich, 2016). Consistent with this, HSV-1 mutants that fail to express ICP0 (ICP0-null mutant HSV-1; ΔICP0 HSV-1) form a stable association between the viral genome and PML-NBs, independently of the activation of IFN-mediated innate immune defences, as these genomes fail to express ICP0 to degrade PML and relieve the repression state of the viral DNA (Alandijany et al., 2018). Furthermore, it was shown that the depletion of single factors comprising the NBs or a combination of them rescued ICP0-null mutant virus replication to varying levels but had no effect on wild type HSV-1 infection (Glass & Everett, 2013; Everett et al., 2008). The recruitment of PML to nuclear HSV-1 DNA is dependent on the SUMOylation pathway (Cuchet-Lourenço et al., 2011), leading to the hypothesis that this initial host response to DNA virus infection may be mediated by the SUMOylation pathway (Boutell et al., 2011).

1.6.1.1.2 Sp100 (Speckled protein of 100 kDA)

Sp100 is a member of the Speckled protein family of chromatin "readers" and is predominantly localized with nuclear PML (Sternsdorf et al., 1995). Similarly to PML, Sp100 has a SUMO interacting motif (SIM), a SUMOyaltion acceptor site and is alternatively spliced giving rise to multiple isoforms with different functions (Negorev et al., 2006; Sternsdorf et al., 1999).

During infection, Sp100 is recruited onto viral genomes in the nucleus in a PML-independent manner and correlates with a repression of viral gene expression (Everett et al., 2006, 2008; Alandijany et al., 2018). Sp100

depletion increased the plaque formation of a ΔICP0 HSV-1 mutant but did not affect WT infection (Everett et al., 2008). Furthermore, double-depletion of both PML and Sp100 cumulatively enhanced plaque formation of ΔICP0 HSV-1, revealing the separate activity of these host proteins in repressing HSV-1 infection (Everett et al., 2008). Interestingly, the simultaneous depletion of both PML-NB proteins was not sufficient to increase plaque formation in ΔICP0 HSV-1 infection to match WT, suggesting that other restriction factors are also at play (Everett et al., 2008). The presence of SIM and not a SUMO modification site is required for Sp100A (the most abundant isoform) to localize to viral DNA (Cuchet-Lourenço et al., 2011).

1.6.1.1.3 Daxx (Human death-domain associated protein) and ATRX (Alpha-thalassemia mental retardation X-linked)

Daxx is a transcriptional repressor that interacts directly with various nuclear proteins. Daxx has two functionally important SIM domains (Santiago et al., 2009) that allow Daxx to localize to PML-NB (Lin et al., 2006). Daxx strongly interacts with ATRX via its helical bundle or 4HB domain (Tang et al., 2004; Li et al., 2017). The physical interaction with ATRX promotes the loading of histone variant H3.3 onto DNA (Research; P, 2010; Goldberg et al., 2010; Drané et al., 2010). Characteristic to PML-NB proteins, Daxx undergoes extensive post-translational modification to regulate its biological function (Mahmud & Liao, 2019).

Similar to PML and Sp100, Daxx is recruited to nuclear sites of HSV-1 DNA in a SIM-dependent manner (Lukashchuk & Everett, 2010; Glass & Everett, 2013; Cuchet-Lourenço et al., 2011). Depletion of Daxx has a positive effect on plaque formation of ΔICP0 HSV-1 but no significant effect on WT HSV-1 (Lukashchuk & Everett, 2010). Additionally, the reintroduction of Daxx to ΔICP0 HSV-1 infected cells completely reverses this phenotype that is mediated by its SIM domain (Cuchet-Lourenço et al., 2011). Daxx

recruitment to vDNA is PML- and Sp100-independent (Everett et al., 2006; Alandijany et al., 2018). Triple depletion of these proteins resulted in a significant relief of restriction and increased plaque formation of ΔICP0 HSV-1 mutant (approximately 100-fold) relative to single or double depletion (Glass & Everett, 2013). This additive effect still did not make up for the loss of the viral ICP0, suggesting that other restriction factors contribute to the cellular repression of ΔICP0 HSV-1 (Glass & Everett, 2013).

ATRX has also been shown to be a restriction factor of HSV-1 and localizes to parental genomes. However, this recruitment is dependent on Daxx, as ATRX failed to localize to viral DNA in Daxx-depleted cells (Lukashchuk & Everett, 2010). Additionally, Daxx reintroduction, but not ATRX-interaction domain Daxx mutant, restored the original phenotype and restriction of ΔICP0 HSV-1 was observed. Collectively, these data highlight the importance of the Daxx and ATRX interaction in the ATRX-mediated restriction of ΔICP0 HSV-1 infection (Lukashchuk & Everett, 2010).

1.6.1.1.4 SUMO (Small ubiquitin-related modifier)

SUMO is a small (~10-12 kDA) protein present in all eukaryotes. There have been 5 isoforms identified, designated SUMO1-5. SUMO1, SUMO2 and SUMO3 are constitutively expressed in all cells, with SUMO2/3 sharing ~95% amino acid sequence homology (differing only by two amino acids); and SUMO1 sharing ~45% amino acid identity with SUMO2/3 (Rivas et al., 2021a). SUMO2/3 can form polySUMO chains on targeted proteins by poly-SUMOylation (Tatham et al., 2001). SUMO1 does possess the ability to form chains. However *in vivo* studies have showed it appears to act as a chain terminator of other SUMO2/3 polychains (Kamitani et al., 1998a; Yang et al., 2006; Matic et al., 2008). SUMO4/5 have been found to be selectively expressed in specific cell types (Liang et al., 2016b; Baczyk et al., 2017). SUMO proteins are translated as inactive precursors, which maturate by truncation of the C-terminus to display the C-terminal -diglycine (-GG)

motif. This is carried out by a family of proteases called ubiquitin-like-protein specific proteases (SENPs) (Mukhopadhyay & Dasso, 2007). SUMOylation of proteins plays an important role in regulating various cellular processes, including intrinsic and innate immune defences (Rivas et al., 2021b). To this end, many viruses (including HSV-1) have evolved mechanisms to exploit this pathway to avoid the cellular immune defences (Imbert & Langford, 2021).

SUMOylation of different PML-NB proteins plays an important role in the formation of these nuclear structures (Takahashi et al., 2005a), specifically in the formation of the PML scaffold (Zhong et al., 2000; Takahashi et al., 2005b; Shen et al., 2006b). HSV-1 has evolved a mechanism where ICP0 targets a large number of SUMO modified proteins, including PML, for proteasome degradation by acting as a viral SUMO targeting E3 ubiquitin ligase (Boutell et al., 2011). This results in the disassembly of PML-NBs to promote the efficient initiation of viral infection (Boutell et al., 2011).

1.6.1.2 IFI16 (Interferon Gamma Inducible Protein 16)

IFI16 is a member of the family of PYHIN (Pyrine domain and two DNA-binding hematopoietic interferon-inducible nuclear proteins with 200-amino acid repeat (HIN-200) domain) proteins. IFI16 has been shown to localize to foci of HSV-1 DNA in the nucleus (Johnson, Chikoti & Chandran, 2013; Cuchet-Lourenço et al., 2013). Depletion of IFI16 enhances plaque formation of ΔICP0 HSV-1 mutant but does not affect WT HSV-1 infection (Cuchet-Lourenço et al., 2013; Orzalli et al., 2013; Merkl, Orzalli & Knipe, 2018). IFI16, similar to PML-NB constituent proteins, is targeted for proteasomal degradation by the HSV-1 ICP0 (Orzalli et al., 2013).

IFI16 has been identified as a PRR DNA sensor (Unterholzner et al., 2010). It has been shown to be predominantly nuclear, but also shuttle to the cytoplasm. Depending on its cellular localization it is able to activate different pathways to restrict the progress of viral infection. Initially, IFI16 was discovered as a cytoplasmic DNA sensor during HSV-1 infection, where IFI16 shuttled to the cytoplasm to bind cytosolic HSV-1 DNA. This interaction led to the activation of STING and IRF3, resulting in the production of IFNβ (Unterholzner et al., 2010; Horan et al., 2013). IFI16 has been shown to bind both ss and ds DNA (Jakobse et al., 2013). In the nucleus, IFI16 has been reported to play a role in the recruitment of PML and Daxx to viral genomes (Cuchet-Lourenço et al., 2013). There is also evidence of IFI16 being involved in the activation of the inflammasome signalling in response to herpesvirus infection (Kerur et al., 2011), as well as HSV-1 epigenetic silencing (Johnson et al., 2014; Orzalli et al., 2013).

1.6.2 Host innate immune response to HSV-1

Unlike intrinsic immunity, innate immune defences are upregulated in response to viral infection. This response can be separated in two phases: (i) detection of pathogen-associated molecular patterns (PAMPs) by the cellular pattern recognition receptors (PRRs); (ii) this recognition results in a cascade of signalling events that result in the downstream induction of type I interferons (IFN), proinflammatory cytokines and chemokines. These events are tightly regulated in a spatiotemporal manner by a variety of PTMs to ensure optimal activation and reduce inappropriate cellular and tissue damage that may lead to prolonged inflammation. The IFN response is classified into three types (type I, II, and III), dependent on the receptors utilized. In this section, the type I IFN response to HSV-1 infection, sensing and detection of viral components, IFN-signalling cascades, and IFN-induced restriction factors are discussed as they are more pertinent to DNA detection of foreign DNA and are part of the focus of this study.

1.6.2.1 Type I IFN response

The type I IFN response plays an important role during viral infection, to induce an antiviral state of cells that limits viral propagation and spread during HSV-1 infection. Mouse models unable to induce a type I IFN response (IFNAR KO or KO for type-I IFN receptor) are unable to control the spread of HSV-1 infection (Wilcox et al., 2016). The lack of the type I IFN receptors has shown to decrease survival rates in mice, and positively affect viral replication, viral dissemination and pathogenesis (Wilcox et al., 2016; Luker et al., 2003; Zawatzky et al., 1982; Leib et al., 1999). The induction of the type I IFN pathway is carried by different PRRs that recognize viral PAMPs and induce the production of type I IFNs, which in turn promote the induction of IFN stimulated genes (ISGs), that ultimately exert an antiviral effect.

1.6.2.2. Type I IFN signalling cascade

The canonical IFN pathway is mediated by the binding of IFNs to their appropriate receptors. Type I IFNs bind to the IFN α receptor (IFNAR), composed of two subunits – IFNAR1 and IFNAR2. These subunits are associated with tyrosine kinase 2 (TYK2) and janus activated kinase 1 (JAK1), respectfully. The binding induces the dimerization of these subunits and result in their autophosphorylation and subsequent tyrosine phosphorylation of signal transducers and activators of transcription 1 (STAT1) and STAT2. Once activated, STAT1 and STAT2 dimerize and subsequently form a complex with IRF9, termed ISG factor 3 (ISGF3), which binds the IFN-stimulated response element (ISRE) of ISG promoters (Figure 3) (Lurie & Platanias, 2005). This leads to the promoted expression of a large number of ISGs that act to inhibit viral infection through various different mechanisms.

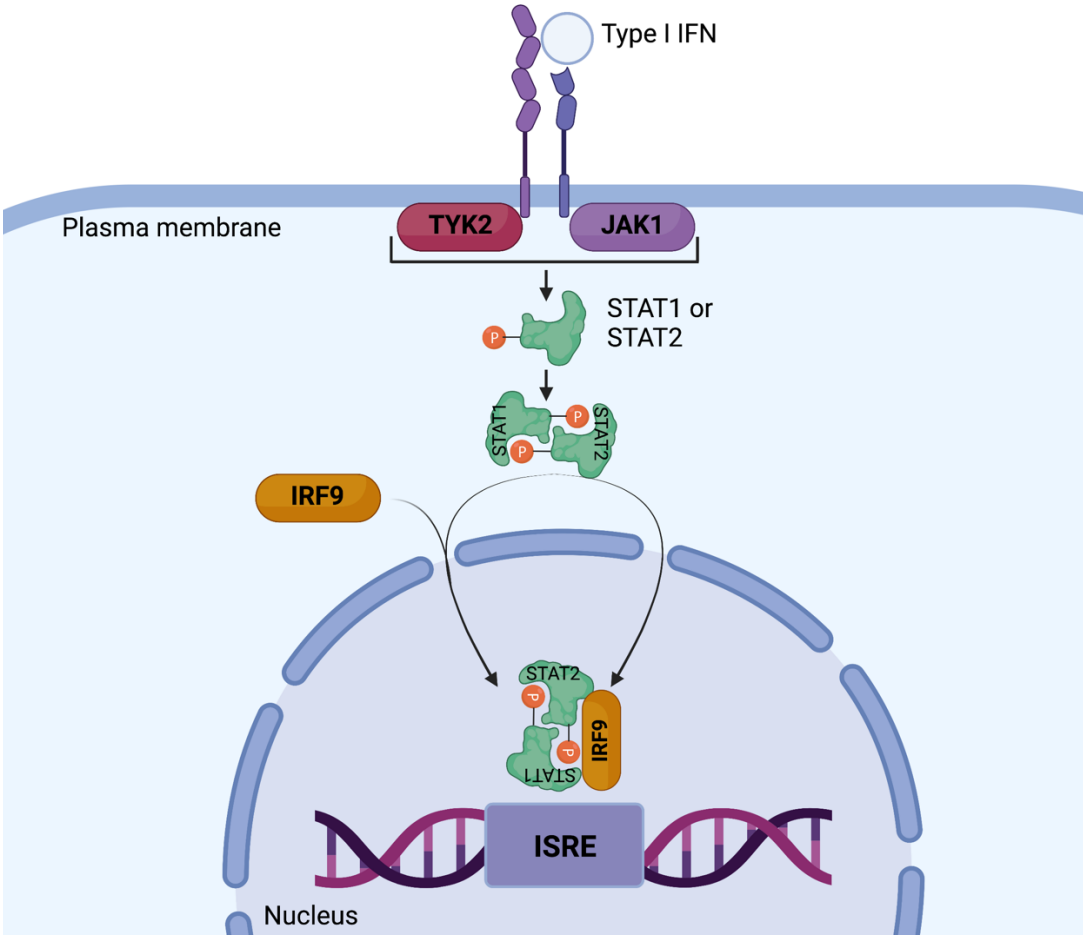

Figure 3. Type I IFN signalling pathway.

Type I IFNs produced by virus infected cells (IFNα and IFNß) bind to their receptors (IFNAR) on the cell surface of neighbouring cells. This leads to the activation of the JAK-STAT pathway. The phosphorylated STAT1 and STAT2 bind to IRF9 to form ISGF3, that translocates to the nucleus in order to induce the expression of ISGs (e.g., viperin, tetherin, ISG15) (Platanias, 2005).

1.6.2.3. ISG mediated antiviral response

While there is a large number of ISGs (>300) (de Veer et al., 2001), only a few have been found to have antiviral activity against HSV-1 (Taddeo, Esclatine & Roizman, 2002; Hu et al., 2016a). ISG15 was reported to be key to mounting an efficient IFN-response to HSV-1 in murine models, although a precise mechanism of the antiviral activity of ISG15 remains to be elucidated (Lenschow et al., 2007). Both of the Myxovirus resistance (Mx) proteins – MxA and MxB, have been shown to confer resistance to HSV-1 by inhibiting viral replication. MxA has been shown to inhibit viral replication, whilst MxB has been recently shown to be panherpesvirus restriction factor exerting its antiviral function through an unknown mechanism. (Ku et al., 2011; Schilling et al., 2018; Crameri et al., 2018). Viperin, tetherin and zing finger antiviral protein (ZAP) have also been found to restrict HSV-1 replication and are antagonized by the UL41 gene product vhs (virion-host shutoff protein), however this function is not targeted as vhs acts as an RNAse and destabilizes many mRNAs. Viperin and tetherin sequester the virions to the plasma membrane, preventing the capsid release in the cytoplasm, while ZAP targets HSV-1 mRNA for degradation. Vhs targets cellular mRNAs for degradation, therefore reducing the ISG products and inhibiting their antiviral properties (Zenner et al., 2013; Su, Zhang & Zheng, 2015; Shen et al., 2014). 2-5 olygoadenylate synthetase (OAS1) has also been found to be important in the restriction of HSV-1 in both mouse and human cells and is counteracted by Us11 (Al-Khatib et al., 2003; Sànchez & Mohr, 2007). Although these effector ISGs have been identified to repress HSV-1, this area remains understudied and requires further investigation.

1.6.2.4. Sensing and detection of HSV-1 by cellular PRRs

The activation of the type I IFN pathway is dependent on the sensing and detection of the viral PAMPs by cellular PRRs. There is a large number of proteins identified as PRRs, such as Toll-like receptors (TLRs) and RIG-I-

like receptors, that recognize different viral components, such as DNA (recognised by TLR9), RNA (recognised by RIG-I and MDA5) and viral glycoproteins (recognised by mannan-binding lectin) (Ma, Ni & Damania, 2018; Abe, Marutani & Shoji, 2019). Many of these adaptor molecules activate the same signalling cascades to induce a robust antiviral response. In this section the DNA sensing molecules involved in HSV-1 detection, excluding TLRs, are discussed as these have been previously implicated in the cytoplasmic sensing of HSV-1 genomes during infection (Horan et al., 2013; Sun et al., 2019).

1.6.2.4.1 The cGAS-STING plays a key role in the detection of foreign DNA

Cytosolic DNA is one of the most potent activators of a type I IFN response (Stetson & Medzhitov, 2006). Under normal conditions, DNA is stored within different organelles, such as mitochondria and the nucleus, but during viral infection the intracellular DNA levels are increased. The cytosolic DNA is recognised by the inactive molecule cGAS, which when bound to DNA undergoes a conformational change and produces the secondary messenger molecule cGAMP (Diner et al., 2013; Sun et al., 2013). cGAMP is detected by the ER-bound Stimulator of IFN Genes (STING), leading to the activation of STING by ubiquitination and STING oligomerization. This allows for STING to translocate to the Golgi via the ERGIC. (Zhang et al., 2013; Ishikawa & Barber, 2008a; Burdette et al., 2011a). During the trafficking processes, STING recruits the kinase TBK1 leading to its activation. This in turn leads to the phosphorylation and activation of IRF3, which dimerized and translocates into the nucles where it leads to the induction of downstream effector genes (ISGs) (Figure 4) (Hopfner & Hornung, 2020). The cGAS-STING pathway is also able to recognise self-DNA and the importance of this is being investigated in different health conditions, such as cancer and autoimmune diseases, as constitutive and systemic activation of this pathway leads to chronic inflammation and pathology (Gao et al., 2015; Corrales et al., 2015).

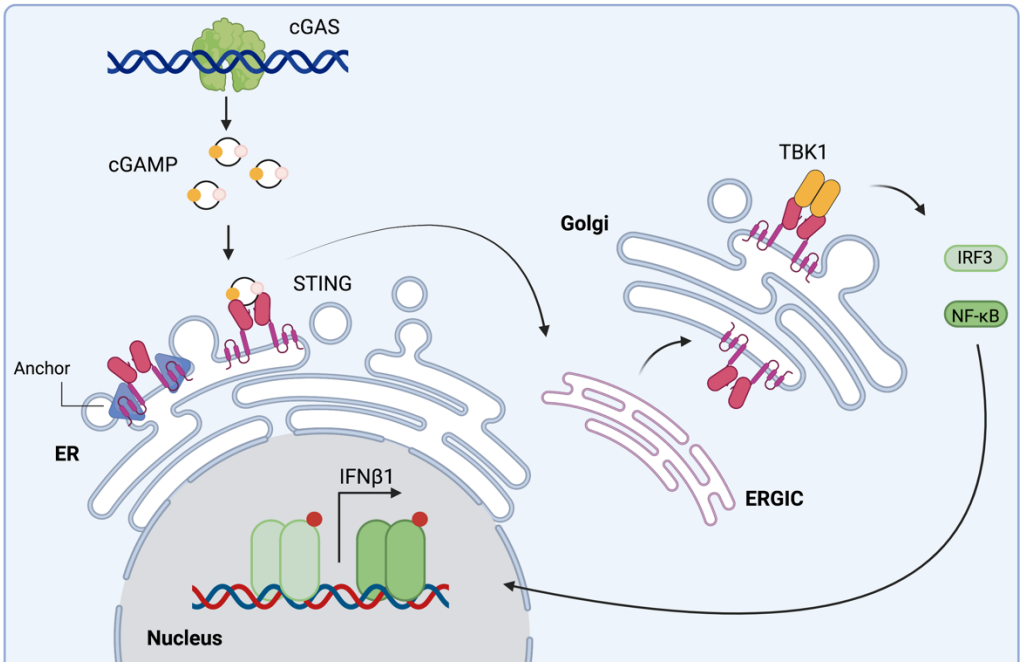

Figure 4. The cGAS-STING pathway.

On binding of dsDNA induces the activation of the enzymatic activity of cGAS and the production of cGAMP. cGAMP binds to STING and induces STING phosphorylation and translocation from the ER to the ERGIC. Once there STING binds and stimulates TBK1 autophosphorylation, that subsequently activates IRF3. The active form of IRF3 is a dimer that translocates to the nucleus and initiates the synthesis of type I IFNs

1.6.2.4.2. cGAS as a DNA sensor

Cyclic GMP-AMP synthase (cGAS) or C6otf150, is a ~520 kDa protein that was discovered through purification of cytosolic extracts, revealing it to be a DNA detector with a direct binding activity (Sun et al., 2013). Although initial studies suggested cGAS to be a cytosolic sensor, an increasing amount of evidence has shown cGAS to also reside in the nucleus and exert function there, such as chromatin retention and stabilization of other DNA sensors (Liu et al., 2018; Jiang et al., 2019; Orzalli et al., 2015). Structural studies have found that the DNA-binding of cGAS is length-dependent and sequence-independent (Andreeva et al., 2017; Luecke et al., 2017). The active form of cGAS is a dimer sandwiching two DNA molecules, however short DNA molecules support weak dimerization. Full activation and stabilization of the cGAS-DNA complex is achieved through oligomerization and formation of condensates, which is promoted by longer length of DNA molecules that support the binding of multiple cGAS monomers (Zhou et al., 2018; Du & Chen, 2018; Andreeva et al., 2017; Luecke et al., 2017). Once switched into an active state, cGAS catalyses the generation of 2,3-cGAMP from GTP and ATP in a two-step process at the same catalytic site. cGAMP then activates STING, leading to downstream signalling (Gao et al., 2013). The activity of cGAS is heavily modulated by PTM (Hopfner & Hornung, 2020).

Studies on DNA sensing carried out in macrophages have shown that the proteasome is involved in the degradation of the HSV-1 capsid and release of vDNA into the cytoplasm (Horan et al., 2013). cGAS was shown to be involved in the sensing of cytosolic HSV-1 DNA leading to a STING-dependent type I IFN response in macrophages and microglia (Reinert et al., 2016; Sun et al., 2019). However, the interaction between cGAS and HSV-1 has not been investigated in other primary cell types, such as epithelial cells or keratinocytes. Interestingly, there have been multiple reports of different HSV-1 proteins antagonising cGAS to overcome the

cellular immune response (Table 3) (Zhang et al., 2018; Huang et al., 2018; Ye et al., 2017; Xu et al., 2017; Su & Zheng, 2017a).

1.6.2.4.3. STING as a DNA sensor

Stimulator of IFN genes (STING; MITA; MPYS or ERIS) is a ~40 Kda dimeric transmembrane protein located at the ER. STING is critical for the TBK1-IRF3-mediated innate immune response to DNA viruses. STING knock out (KO) in mouse models results in enhanced susceptibility to HSV-1 infection and completely abolishes the IFNβ response (Ishikawa, Ma & Barber, 2009; Abe et al., 2013a; Ishikawa & Barber, 2008b). Under normal conditions STING forms a dimer, spanning the ER, that allows for the binding of TBK1. Phosphorylation of TBK1 under these conditions is inhibited by the steric hindrance in trans (Zhang et al., 2019; Shang et al., 2012). In response to cGAMP binding, STING is activated by undergoing a conformational change in the ligand site and translocates to the Golgi via the ER-Golgi intermediate compartment (ERGIC) (Burdette et al., 2011b; Sun et al., 2009). There, TBK1 binds and dimerizes, allowing for its phosphorylation and activation of STING. This is followed by the binding and activation of IRF3 and IRF3 dimerization that leads to its nuclear localization where it promotes IFN production and ultimately leads to the induction of ISGs (Shang et al., 2019; Zhong et al., 2008; Liu et al., 2015). STING has been shown to be able to directly bind DNA, however the functional consequence of this during infection has still to be described (Abe et al., 2013b).

Studies have shown that STING is important in the control of HSV-1 infection, as it is enriched in expression in fibroblasts. STING KO mice replicate higher viral titres, more severe pathology and enhanced viral spread (Parker, Murphy & Leib, 2015; Ishikawa & Barber, 2008b). In addition to the cGAS-STING PRR pathway, studies have found STING to inhibit HSV-1 infection through inflammasome activation (Wang et al., 2020), upregulation of tetherin (Royer & Carr, 2016), and other IFN-independent activities (Wu et al., 2020; Yamashiro et al., 2020). HSV-1 has also evolved

various mechanisms to evade STING-mediated antiviral activates through different viral proteins, such as VP11/VP12, VP1-2 and $\gamma_1$134.5 (Table 3) (Deschamps & Kalamvoki, 2017; Bodda et al., 2020; Pan et al., 2018; Christensen et al., 2016). Taken together, these data identify STING as an important host factor to HSV-1 infection.

Viral protein	Cellular protein	Method of antagonizing	Reference
UL37	cGAS	Deaminates cGAS at a specific site to inhibit the synthesis of cGAMP	Zhang et al., 2018
UL49	cGAS	Interacts with cGAS and inhibits its enzymatic activity	Huang et al., 2018
UL41	cGAS	Degrades cGAS RNA via its RNase activity	Su and Zheng, 2016
UL46	STING	Binds to STING and TBK1 to modulate the activity of STING	Deschamp and Kalamvoki, 2017
UL36	STING	Binds directly to STING and promotes the deubiquitination	Bodda et al., 2020
ICP34.5	STING	Binds to STING and disrupts the translocation from the ER to ERGIC	Pan et al., 2018
ICP27	STING	Interats with STING and TBK1	Christensen et al., 2016

Table 3. HSV-1 proteins that target the cGAS-STING pathway.

1.6.2.4.4. IFI16 as a DNA sensor

IFI16 was initially recognised as a cytosolic DNA sensing protein. IFI16 localized to HSV-1 vDNA and activated the type I IFN pathway via the STING-TBK1-IRF3 axis. The removal of IFI16, or its mouse orthologue p204, resulted in a net decrease in the type-I IFNβ response to HSV-1 infection. IFI16 binds to DNA with its two HIN domains, which allows for the formation of filamentous oligomers on DNA. This interaction is dependent on DNA length and structure (Morrone et al., 2013; Horan et al., 2013; Unterholzner et al., 2010). Additionally, there has been data on the interaction between cGAS and IFI16 in stimulating STING-mediated ISG induction in specific cell types (Diner et al., 2016; Almine et al., 2017; Orzalli et al., 2015; Morrone et al., 2013). IFI16 is predominantly nuclear and its association with HSV-1 DNA is transient during early timepoints of infection and as early as 30 mpi. IFI16 puncta as well as IFNβ and ISG production were lost in an ICP0-dependent manner (Everett, 2015; Diner et al., 2016; Orzalli et al., 2013). Recent studies have shown that productive infection is required for the nuclear activation of IFI16 in response to HSV-1 infection, as the drug inhibition of viral replication resulted in the inhibition of the induction of cellular ISGs, such as Mx1 (Alandijany et al., 2018).

1.7. Specificity protein 1 (Sp1) and its role in HSV-1 infection

Sp1 is a C_2H_2 type zinc finger protein and the founding member of the Sp family of proteins (Dynan & Tjian, 1983; Chu, 2012). Sp1 has been reported to be a ubiquitously expressed transcription factor and plays a role in regulating a large number of genes through transcriptional activation or repression. These dynamic changes in function can be attributed, at least in part, to the extensive Sp1 PTMs (Jackson et al., 1990; Chu, 2012). Sp1 has a high affinity for -GC or -GT promoter regions via the C-terminal zinc finger domains (Courey & Tjian, 1988) and is activated by interacting with $TAF_{II}110$ (Drosophila)/$TAF_{II}130$ (human orthologue) and cofactor required

for Sp1 (CRSP) via the N-terminal activation domain (Ryu et al., 1999; Hoey et al., 1993).

Multiple Sp1 binding sites have been identified on different HSV-1 genes and Sp1 has been shown to enhance replication of IE and E genes during infection (Pande, Petroski & Wagner, 1998; Tuan Nguyen-huynh & Schaffer, 1998; Gu, Huang & Hyward, 1995; Jones & Tjian, 1985). Sp1 gene activation is regulated by the viral ICP4 and an increase in Sp1 phosphorylation is observed during the switch from E to L phases of lytic replication. This resulted in the repression of Sp1 function (Imbalzanot & Delucat, 1992; Gu et al., 1993; Imbalzano, Coen & Delucal12, 1991; Kim & Deluca, 2002). However, more recent studies have suggested that Sp1 hyperphosphorylation is induced due to a global DNA damage response of infected cells rather that spatiotemporal regulation of the Sp1-dependent transcriptional functions (Iwahori et al., 2007, 2008).

1.8. UV light irradiation of HSV-1

UV irradiation is a well-established technique routinely used for inactivation of HSV-1 since the late 1960s and has been applied to studies investigating HSV-1 reactivation (Laycock et al., 1991; Dalai et al., 2002; Leblanc et al., 1999), cell transformation (Duff & Rapp, 1973; Davis' And & Kingsbury, 1976), vaccine development (Schneweis et al., 1981; Osorio & Ghiasi, 2003) and the potential use of UV viruses as vaccine adjuvants (Samudio et al., 2019, 2016). Studies involving UV treated viruses have showed that HSV-1 has decreased titers in fibroblasts and cells lacking DNA repair mechanisms (Rabson, Tyrrell & Legallais, 1969), reduced viral DNA polymerase activity (Fridlender et al., 1978), and delayed viral transcription in BHK cells (Eglin, Gugerli & Wildy, 1980). The delay was proposed to occur due to an event prior to replication (Ross, Cameron & Wildy, 1972; Fridlender et al., 1978). Electron microscopy studies in HeLa cells have contributed this to

impaired uncoating mechanisms (Miyamoto' And & Morgan, 1971). However, studies in BHK cells showed no difference in uncoating and attributed the delay in virus onset of infection to the inhibition of transcription due to pyrimidine dimers (Eglin, Gugerli & Wildy, 1980; Fridlender et al., 1978). This is in contrast to reports for other viruses, such as SARS-Cov 2, that are successfully inactivated following UV irradiation (Biasin et al., 2022, 2021). This difference can be explained by the difference in tolerance to UV irradiation by different viruses based off their nucleic acid composition, being RNA or DNA, or the specific wavelength of UV light (UV-A; UV-B; UV-C). Additionally, reports have been shown that UV irradiated HSV-1 is able to repair the damaged viral DNA via a recombination mechanism in a cell type dependent manner using the cellular DNA repair mechanisms (Hall, Featherston & Almy, 1980; Millhouse et al., 2012). It has been reported that UV-irradiated HSV-1 specifically enhances the activation of type I IFN-mediated immune response both in vitro and in vivo (Gary, Rosenberg & Louis, 1974; Taylor & O'brien, 1985; Hendricks et al., 1991; Eloranta, Sandberg & Alm, 1996). This stimulation of the innate immune system holds true for other DNA viruses, such as VACV (Delaloye et al., 2009) and RNA viruses, such as Influenza (Marcus, Rojek & Sekellick, 2005), upon UV irradiation. However, the precise mechanism of stimulation remains poorly investigated.

The damage induced to DNA by UV irradiation has been extensively researched over the last 70 years (Rorsch' et al., 1958; Beukers, Ijlstra & Berends, 1960). UV irradiation leads to the formation of various DNA lesions in response to UV exposure (Rastogi et al., 2010; Schreier, Gilch & Zinth, 2015). The main photoproducts are cyclobutene pyrimidine dimers (CPDs) and 6-4 photoproducts (Carell & Epple, 1998) and result in the alteration of DNA structure and base-pairing. These pyrimidine and purine dimers are formed between adjacent intrastrand bases.

1.9. Human Cytomegalovirus (hCMV)

HCMV is a member of the *Herpesviridae* family that has been shown to interact with PML-NBs during early points of infection (Ishov, Stenberg & Maul, 1997). As part of the work carried out, the spatiotemporal kinetics of recruitment of intrinsic immune factors to incoming hCMV genomes was investigated as a comparator and determine the conservation of these pathways between different Herpesviruses. In the following sections a brief introduction into the biology of hCMV relevant to the study is given.

Overview

Human Cytomegalovirus (hCMV) infection occurs in most individuals around the world with approximately 60% of adults in developed countries and 100% in developing countries test positive for IgG antibodies (WHO). HCMV can be acquired during different life stages: foetus, neonate, toddler, children or as an adult. Most infections are asymptomatic in healthy individuals with a competent immune system. However, in people with weakened or underdeveloped immune systems the infection can have a more severe outcome, including retinitis, pneumonia, hepatitis, and colitis. Congenital hCMV infection can have severe long-term effects, growth deficiencies, central nervous system complications and most commonly hearing loss (Griffiths, Baraniak & Reeves, 2015). HCMV can establish life-long infections through latency in the peripheral blood leukocytes and reactivation can occur with severe consequences in AIDS and transplant patients (Sinclair & Sissons, 2006).

Similar, to HSV-1, the hCMV particle (230 nm in diameter) is comprised of a core, containing the viral genome, surrounded by a less structured proteinaceous matrix (tegument) and finally surrounded by a lipid envelope decorated with glycoproteins. The hCMV genome is a linear double-stranded DNA molecule of 236 kbp in length (the largest of any herpesvirus). Because of its size, the genome DNA is more tightly packaged within a 130 nm capsid (Butcher et al., 1998a). The structure of the capsid, similar to that of HSV-1, is a T=16 icosahedral symmetry shell (Butcher et al., 1998a). The capsid is made of four viral structural proteins: the major capsid protein (MCP), the minor capsid protein (mCP), the minor capsid protein-binding protein (mC-BP) and the smallest capsid protein (SCP) (Gibson et al., 1996; Gibson, Baxter & Clopper, 1996; Gibson et al., 1984; Gibson, 1983). The MCP forms the pentons and hexons, with 150 hexons at the local six-fold symmetry axis, and 12 pentons located at the five-fold symmetry. The tips of the hexons are decorated with six copies of the SCP. At the position of three-fold symmetry and between the capsomeres are the heterotrimeric triplexes, formed from two copies of the mCP and one copy of the mC-BP. One of the pentamer positions is presumed to be occupied by the portal complex, through which the DNA enters and leaves the capsid. HCMV procapsid maturation occurs after the separation of scaffolding proteins from the surface of the capsid, allowing for angularization (Irmiere & Gibson, 1985). The tegument is composed of as many as 71 viral and cellular proteins (Varnum et al., 2004). The tegument is enclosed within the lipid bilayer envelope that is decorated by at least 19 viral glycoproteins (Varnum et al., 2004). The viral glycoproteins are essential for the complex process of viral attachment and entry into target cell and 5 have been showed to be essential for viral replication in vitro - gB,gM-gN and gH-gL (Mocarski et al., 2007).

Attachment, fusion and nuclear delivery of viral DNA

HCMV infects a large array of different cell types and has evolved to utilize one of two mechanisms of entering target cell: (i) direct fusion of the viral envelope with the host cell membrane at neutral pH (Compton, Nepomuceno & Nowlin, 1992) (ii) receptor-mediated endocytosis at low pH (for entry to specific cell types, such as epithelial cells) (Ryckman et al., 2006). This is due to the complex envelope protein composition of the virion, allowing for the characteristic wide host cell tropism (Varnum et al., 2004). The exact mechanism of viral attachment remains an active area of research, but several cellular proteins have been identified as entry requirements, such as heparan sulfate proteoglycans (HSPGs; initial tethering step by gM and gB) (Compton, Nowlin & Cooper, 1993; Kari & Gehrz, 1993), annexin II (gB receptor) (Taylort & Cooper, 1990; Pietropaolo & Compton, 1997), intergrin heterodimers $\alpha 2\beta 1$, $\alpha 6\beta 1$ and $\alpha V\beta 3$ (components of the cytoskeleton network bound via gB) (Wang et al., 2005b; Feire, Koss & Compton, 2004). The exact mechanism of the fusion step is also unclear. The current model suggests the initial tethering step of the virion to HSPGs mediated by gB and the gM/gN complex, followed by a secondary binding of gB-$\beta 1$ or epidermal growth factor receptor (EGFR). The exact mechanism of the secondary binding is yet to be discovered. Finally, gH/gL/gO along with gB mediate the fusion of the lipid membranes (Wang et al., 2005b; Feire, Koss & Compton, 2004). Transport of the capsid to the nucleus is mediated by the cellular microtubule network (Ogawa-Goto et al., 2003), where the genome is deposited.

Virus gene expression and DNA replication

HCMV genes are expressed in a temporally coordinated and regulated manor leading to the synthesis of three categories of viral genes: immediate-early (IE), early (E) and late (L). HCMV IE genes include the major IE proteins (MIE) IE1/IE2 (UL122/UL123) and auxiliary proteins, such as UL36-UL38, IRS1/TRS1 and US3. MIE are encoded by the ie1/ie2 genes, yielding four transcriptional products and are key for establishing hCMV infection. The ie1/ie2 gene contains a segment upstream of the TATA box containing binding sites for several transcription factors, such as NF-κB, Sp1 and CREB/ATF (Boshart et al., 1985) , allowing for the fast expression of these proteins. One of the products of ie1/ie2 is $IE1_{479aa}$ (IE1-72) which is a phosphoprotein that positively autoregulates expression from the gene and is essential during low moi infections (Mocarski et al., 1996). IE1-72 interacts along with $IE2_{579aa}$ (IE2-86) to regulate the expression of the E and L genes at a maximal activity of the promoters. IE2-86 is critical for viral replication as it has been shown to be a transactivator for several E and L proteins (Fortunato & Spector, 1999) or interact with other transcription factors (e.g. p53; (Fortunato et al., 1997; Sommer, Scully & Spector, 1994)). Additionally, IE2-86 represses the ie1/ie2 gene by binding to repressor sequences and contributing to the switch to E/L stages of infection (Pizzorno & Hayward, 1990).

The expression of E genes (more than 54 ORF) is dependent on the levels of functional IE proteins and occurs after 24 hpi. The E genes are further classified into two groups: E and E-L, dependent on the timeframe of expression (Fortunato & Spector, 1999). HMCV DNA replication occurs in the nucleus and is postulated to be carried out in a rolling circle mechanism with DNA circularization and the formation of head-to-tail concatemers (Mcvoy & Adler, 1994). Replication occurs at a single cis-acting lytic origin of replication (oriLyt) (Borst & Messerle, 2005), initially mediated by UL84 and IE2-86, and the viral replication machinery is recruited onto this site. Six proteins make up the replication machinery: the single-stranded DNA-

binding protein ppUL57, the helicase-primase complex (encoded by UL70, UL102 and UL105), the DNA polymerase (UL54) and the DNA polymerase processivity factor (UL44). The newly synthesized genomes mature through their inversion and cleavage at the pac1 and pac2 sites by the terminase complex (pUL56 and pUL89) (Mcvoy & Adler, 1994). The maturation of the progeny genomes along with the synthesis of L genes triggers virion assembly and packaging.

Nucleocapsid assembly and egress

The initial step in nucleocapsid assembly is the recruitment of pUL86 to the scaffolding protein AP pUL80.5 (pre-cursor to the Assembly Protein) in the cytoplasm and their subsequent translocation to the nucleus. Once there, these complexes oligomerise with the assistance of AP and form the hexon-penton capsomeres and along with pUL85-pUL86 and pUL48.5 assemble the procapsid. (Butcher et al., 1998b) These package the viral DNA genomes, finish maturation and travel through the nucleus. Similar to HSV-1, hCMV travels through the cell in an envelopment/de-envelopment/re-envelopment mechanism. The viral nuclear egress complex (heterodimer of pUL50 and pUL53) transport the capsids through the nuclear membranes with the help of the pUL97 kinase phosphorylation of nuclear lamin A/C. (Sharma et al., 2014, 2015; Lye et al., 2015). This disrupts the nuclear lamina and allows for the capsid to travel to the nuclear lumen, acquiring a primary envelope, which is then lost when budding through the outer nuclear membrane and released into the cytosol. The tegument and primary envelope are acquired in the viral assembly complex (vAC), which is located near the nucleus (Sanchez et al., 2000). Once these components are acquired the virions bud into cytoplasmic vesicles, where they acquire their final components of the viral envelope with the help of pUL99 and exit the cell (Figure 5) (Silva et al., 2003).

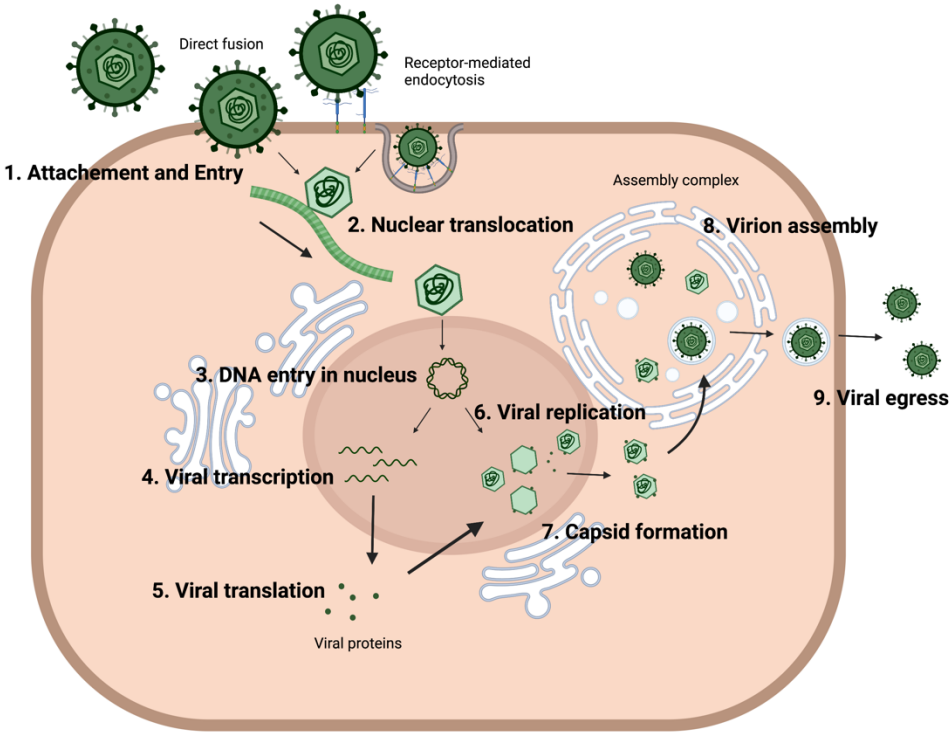

Figure 5. Overview of the hCMV life cycle.

(A) Infectious particles enter the cell through interaction with cellular receptors. Capsid and tegument proteins are delivered to the cytosol. (B) The capsid travels to the nucleus, where the genome is delivered and circularized. Tegument proteins regulate host cell responses and initiate the temporal cascade of the expression of viral I immediate early (IE) genes, followed by delayed early (DE) genes, which initiate viral genome replication, and late (L) genes. (C) Late gene expression initiates capsid assembly in the nucleus, followed by nuclear egress to the cytosol. Capsids associate with tegument proteins in the cytosol and are trafficked to the viral assembly complex (AC) that contains components of the endoplasmic reticulum (ER), Golgi apparatus and endosomal machinery. The capsids further acquire tegument and viral envelope by budding into intracellular vesicles at the AC. (D) Enveloped infectious particles are released along with non-infectious dense bodies.

PML

During HCMV infection parental genomes have been shown to associate with PML-NBs (Ishov, Stenberg & Maul, 1997). This interaction, however, is only observed within a narrow timeline during early infection, prior to the de novo expression of IE1 (Wilkinson et al., 1998; Korioth et al., 1996). The structure of SUMOylated PML allows for the recruitment of other factors, which ultimately form a condensed chromatin repressive environment around the IE1 promoter and halting viral infection (Woodhall et al., 2006). Furthermore, studies have showed that PML knockdown enhances infection, whilst transient expression reverses the phenotype (Tavalai et al., 2006). In order to circumvent the restriction of PML and PML-NBs, HCMV has evolved a mechanism to target PML and cause PML-NB to disassemble (Korioth et al., 1996; Wilkinson et al., 1998; Ahn & Hayward, 1997). The viral IE1 has been shown to directly interact with PML and abrogate the de novo SUMOylation of PML, and therefore disrupting the integrity of the nuclear bodies (Lee et al., 2004; Hou et al., 2017; Schilling et al., 2017; Reuter et al., 2021). Unlike the proteasome-dependent degradation of PML by ICP0 during HSV-1 infection (Everett et al., 2006), IE1 does not degrade PML, but induces the accumulation of mono-SUMOylated PML (Korioth et al., 1996; Hou et al., 2017; Ahn & Hayward, 1997).

Sp100

As a major component of PML-NB Sp100 has also been found to be a restriction factor for HCMV infection. Knockdown of Sp100 resulted in the increased plaque formation of HCMV and this effect was cumulative if combined with KD of PML or Daxx (Tavalai et al., 2011; Adler et al., 2011) Additionally, it was also demonstrated that Sp100 might also exert an

antiviral function during hCMV latency, as an increase in latent gene products was observed in cells in the absence of Sp100 (Tavalai et al., 2011). The exact mechanism of the restriction remains to be elucidated. Similar to PML, it is proposed that Sp100 is deSUMOylated by the viral IE1 protein to disrupt the structure of PML-NBs and its antiviral function (Mu¨ller & Dejean, 1999).

Daxx and ATRX

Daxx knockdown has been shown to have a positive effect on hCMV plaque formation and the reintroduction of Daxx to reverse this phenotype (Tavalai, Rechter & Stamminger, 2008). Daxx silences IE expression through the function of an additional histone deacetylase, which induces a transcriptionally inactive chromatin state at the major IE promoter (MIEP) (Saffert & Kalejta, 2006; Woodhall et al., 2006). The depletion of ATRX in the absence of the viral antagonist pp71 resulted in a relief in restriction, providing evidence about its restrictive contribution, although the exact mechanism is still unknown (Lukashchuk et al., 2008). HCMV has evolved a way to bypass the restriction of the Daxx/ATRX histone chaperone complex, which exerts its activity immediately after nuclear entry and prior to IE expression. The tegument protein pp71 translocates to the nucleus and localizes at Daxx and PML-NBs (Ishov, Vladimirova & Maul, 2002; Cantrell & Bresnahan, 2005). Daxx is degraded by pp71 in a proteasome-dependent ubiquitin-independent manner (Hwang & Kalejta, 2007). The direct interaction between the two proteins is required in order for this event to occur (Hofmann, Sindre & Stamminger, 2002; Ishov, Vladimirova & Maul, 2002; Cantrell & Bresnahan, 2005). Additionally, pp71 was found to increase the SUMOylation of Daxx, although the functional relevance of this is still to be determined (Hwang & Kalejta, 2009). To induce effective removal of repression, pp71 specifically targets ATRX for displacement, prior to targeting Daxx for degradation (Lukashchuk et al., 2008).

1.10. Rationale and aim of the project

Intrinsic and innate immune responses play crucial roles in the antiviral response to HSV-1 that lead to the cellular restriction of viral infection. Multiple different viral proteins have evolved to target and antagonize these mechanisms at various steps. These interactions between viral genomes and the different cellular immune factors have been investigated to a degree. However, these lines of study leave a lot of questions unanswered with regards to the molecular mechanism of intrinsic and innate immune responses. For example, (i) are they spatially separated or induced in the same cellular compartments, (ii) are they equally activated during infection or is one preferred over the other, (iii) are the same proteins involved in the detection of HSV-1 or do they differ based on the immune arm activated in response to infection, and (iv) are these antiviral immune defences conserved for herpesviruses or are the HSV-1 specific?

With the advancement of DNA labelling, a method using Cu catalysed orthogonal labelling of nucleic acids with azydes or alkynes has been optimised for the monitoring of HSV-1 DNA trafficking and the proteins it interacts during infection (Alandijany et al., 2018; Sekine et al., 2017; Wang et al., 2013). This method has allowed for the visualization of viral genomes using direct-fluorescent microscopy to examine the interactions between host immune factors and HSV-1 DNA, instead of indirect methods (e.g., fluorescent-tagging of DNA binding proteins) (Everett, 2015; Glass & Everett, 2013; Komatsu et al., 2015) which requires the onset of viral replication and protein production. Additionally, this method does not require extensive sample processing, harsh denaturing conditions or high MOIs inherent to other techniques like Fluorescent in situ hybridization (FISH) and Bromodeoxyuridine (BrdU)-labelling, that ultimately saturate virus host interactions that prevent accurate spatiotemporal analysis (Everett et al., 2007; Jensen, 2014; Glauser et al., 2007). In order to further investigate the interactions between different intrinsic and innate immune

factors and HSV-1 DNA upon viral genome deposition, it was necessary to circumvent the synthesis and action of different viral proteins that may abrogate or inhibit the cellular immune defences in response to viral infection. To this end we utilized a UV irradiated HSV-1 virus model, that is known to be inactivated and induces the innate immune response of cells.

The main objectives of this project were as follows:

(1) Investigate the temporal recruitment of intrinsic immune factors (PML-NB protein component proteins) to UV irradiated HSV-1 genomes.

(2) Characterize the temporal recruitment of cellular PRRs factors (DNA sensing molecules IFI16, cGAS/STING) to UV irradiated HSV-1 genomes

(3) Evaluate the differences driving the differential recruitment of intrinsic and innate immune factors to HSV-1 vDNA.

(4) Develop and optimize a click chemistry protocol for hCMV to evaluate the conservation of the cellular intrinsic immune response during herpesvirus infection.

2. Materials

Table 4. Types of cells and cellular growth conditions used

Name	Type	Growth and maintenance media	Maintenance conditions
BHK	Baby hamster kidney cells	Glasgow modified Eagle's medium (GMEM) supplemented with 10% fetal calf serum (FCS), 10% tryptose phosphate broth, 100 units/ml penicillin, and 100 µg/ml streptomycin	All cell lines were maintained at 37°C with 5% CO2.
HEK 293T	Human embryonic kidney 293 cells immortalized hTERT	Dulbecco's Modified Eagle Medium (DMEM) supplemented with 10% FCS, 100 units/ml penicillin, and 100 µg/ml streptomycin	
U20S	Human bone osteosarcoma epithelial cells		
IMR-90	Human lung fibroblast cells		
HFFF	Human foreskin fibroblasts cells		
RPE	Retinal pigmented epithelial cells immortalized hTERT	Dulbecco's modified Eagle's medium supplemented with 10% FCS, 0.5 µg/ml hygromycin, 100 units/ml penicillin, and 100 µg/ml streptomycin	
HFt	Human foreskin fibroblasts immortalized hTERT		

Table 5. Cell culture media and reagents commonly used throughout this study

Reagent's name and abbreviations	Provider	Catalogue or reference number
Bovine serum albumin (BSA)	Sigma-Aldrich	A3294
Citifluor AF1	Electron microscopy Sciences	17970
DAPI	Sigma-Aldrich	D9542
Dimethyl sulfoxide (DMSO)	Sigma-Aldrich	D2650
DL-Dithiothreitol (DTT)	Sigma Aldrich	D0632
Dulbecco's Modified Eagle Medium (DMEM)	Life Technologies	41966-029
EDTA DISODIUM SALT DIHYDRATE (EDTA)	Fisher Scientific	D/0700/60

Ethylene glycol-bis(β-aminoethyl ether)-N,N,N',N'-tetraacetic acid(EGTA)	BDH	28672
Dulbecco's Phosphate Buffered Saline (PBS)	Sigma-Aldrich	D1408
Fetal Calf serum (FCS)	Life Technologies	10270-106
Formaldehyde	Sigma-Aldrich	f8775
Giemsa	VWR	350864X
Glasgow's MEM (GMEM)	Life Technologies	11710035
Glycine	VWR	101196X
Guanidine Hydrochloride (GuaHCl)	Sigma Aldrich	G3272
HEPES	Sigma-Aldrich	H3375
Human serum (HS)	MP Biomedicals	2931149
Lipofectamine® LTX with Plus™ Reagent	Sigma-Aldrich	15338100
Magnesium chloride (MgCl2)	Sigma-Aldrich	M8266
Methylated Spirit (IDA 99), 99% (v/v), Pure, (Industrial Methylated Spirit, 74 0.P.)	ThermoFisher	M/4450/17
NP-40	Sigma-Aldrich	9016-45-9
NuPAGE™ MES SDS Running Buffer	ThermoFisher	NP0002
NuPAGE™ MOPS SDS Running Buffer	ThermoFisher	NP0001
NuPAGE™ Transfer Buffer	ThermoFisher	NP0006-1
Polybrene	Sigma Aldrich	H9268
Poly-D-lysine hydrobromide	Sigma Aldrich	P7405
Polyinosinic–polycytidylic acid sodium salt Poly I:C	Sigma	P1530
Poly(dA:dT)	Invivogen	tlrl-path
Sodium Chloride (NaCl)	VWR	27810.295
Sodium dodecyl sulfate (SDS)	VWR	442444H
Sucrose	Sigma-Aldrich	S7903
Triton X-100	Promega	H5142
True blue HRP substrate	KPL	50-78-02
Trypsin	Life Technologies	15090-046
Tween 20	Biorad	170-6513
Urea	Sigma-Aldrich	U0631
Versene	E and O Laboratories	BM0400
5-Ethynyl-2'-deoxycytidine, (EdC)	Sigma-Aldrich	T511307
7-Deaza-7-ethynyl-2'-deoxyadenosine (EdA)	Jena Bioscience	CLK-099

Name and Abbreviation	Provider and catalogue number	Preparation
Hygromycin	Invitrogen 10687-010	Stored at 4° C
Interferon beta (IFNβ)	Calbiochem 407318	Suspended in Milli-Q H2O Aliquoted and store at -70° C
MG132	Calbiochem 474790	Suspended in DMSO Aliquoted and store at -20° C
Nocodazole	Sigma-Aldrich M1404	Suspended in DMSO Stored at 4° C
Penicillin/ streptomycin (P/S) solution	Life Technologies 15140122	Aliquoted and store at -20° C
Puromycin	Sigma-Aldrich P8833	Suspended in Milli-Q H2O Aliquoted and store at -20° C Stock concentration: 5 µg/ml

Table 6. Commonly used drugs, preparation, and storage.

Antibody	Species	Manufacturer	Dil. used in WB*	Dil. used in IF*	Dil. Used in ICC*	Dil. used in DotBlot*	Dil. used in ChIP*
Actin	Rabbit	Sigma, A5060	1:1000	N/A	N/A	N/A	N/A
ATRX	Mouse	Santa Cruz, sc-55584	N/A	1:500	N/A	N/A	N/A
α-Tubulin	Mouse	Cell Signalling,	N/A	1:1000	N/A	N/A	N/A
cGAS	Rabbit	Proteintech	1:1000	1:50	N/A	N/A	N/A
	Mouse	Sigma	1:1000	1:50	N/A	N/A	N/A
	Mouse	Santa Cruz, sc-515777	N/A	N/A	N/A	N/A	1 µg
CMV	Mouse	Abcam (ab2595)	N/A	N/A	1:1000	N/A	N/A
Daxx	Rabbit	Upstate, 04-445	1:500	1:500	N/A	N/A	N/A
H3	Rabbit	Abcam, ab1791	N/A	N/A	N/A	N/A	1 µg
ICP0 (11060)	Mouse	(Everett et al. 1993b)	1:10000	1:1000	N/A	N/A	N/A
ICP4 (58S)	Mouse	(Showalter et al. 1981)	1:500	N/A	N/A	N/A	N/A
IE2	Mouse	Millipore	N/A	1:1000	N/A	N/A	N/A
IFI16	Mouse	Abcam, ab55328	N/A	1:1000	N/A	N/A	N/A
PML	Rabbit	Bethyl Laboratories, A301-167A	1:2000	1:1000	N/A	N/A	N/A
PML	Mouse	Abcam, ab96055	N/A	1:1000	N/A	N/A	N/A
pp65	Mouse	Acris Abs, BM3259	N/A	1:100	N/A	N/A	N/A
Mx2	Rabbit	Sigma-Aldrich	1:500	1:50	N/A	N/A	N/A
Sp1	Rabbit	Abcam (ab227383)	1:300	1:1000	N/A	N/A	N/A
SP100	Mouse	GeneTex, GTX131569	N/A	1:500	N/A	N/A	N/A
STING	Rabbit	Proteintech	1:1000	1:500	N/A	N/A	1 µg
	Mouse	NovusBio	N/A	1:50	N/A	N/A	N/A
SUMO1	Rabbit	Abcam, ab32058	N/A	1:100	N/A	N/A	N/A
SUMO2/3	Rabbit	Abcam, ab3742	N/A	1:1000	N/A	N/A	N/A
Tymine Dimer	Mouse	Abcam, ab10347	N/A	N/A	N/A	1:250	N/A
Ubiquitin	Mouse	Invitrogen, eBioP4D1 (P4D1)	1:1000	N/A	N/A	N/A	N/A
VP5 (DM165)	Mouse	(McClelland et al. 2002)	1:500	N/A	1:300	1:250	N/A

Table 7. List of Primary antibodies used.

Antibody	Origin	Manufacturer	Assay and dilution
Rabbit IgG (H+L) Alexa-Flur 488	Donkey	Life Technologies, A21206	Immunofluorescence (IF) staining (1:1000)
Rabbit IgG (H+L) Alexa-Flur 647	Donkey	Life Technologies, A31573	
Mouse IgG (H+L) Alexa-Flur 488	Donkey	Life Technologies, A21202	
Mouse IgG (H+L) Alexa-Flur 488	Donkey	Life Technologies, A31571	
Rabbit IgG (H+L) Dylight 680	Goat	Thermo Scientific, 35568	Western blot (1:10000
Rabbit IgG (H+L) DyLight 800	Goat	Thermo Scientific, 35571	
Rabbit IgG (H+L) Dylight 680	Goat	Thermo Scientific, 35518	
Rabbit IgG (H+L) Dylight 800	Goat	Thermo Scientific, 35521	
Anti-mouse IgG-Peroxidase Ab	Goat	Sigma Aldrich, A4416	Immuno-staining plaque assay (1:1000)

Table 8. List of Secondary antibodies used.

Primer/Probe	Sequence	Provider
HSV-1 Us3 Fwd	5'-GATTGGGGCCACGGGATTTA	Sigma-Aldrich
HSV-1 Us3 Rev	5'-GGGGGTAATCTGGATGGCTG	
HSV-1 Us3 Probe	5'-[Cyanine5]CGATCCACGGAGCGCTCACC[BHQ3]	
HSV-1 UL36 Fwd	5'-AAGAGGTGACGCGCTTACAA	
HSV-1 UL36 Rev	5'-GTAACAGGCGCGGATCAGTA	
HSV-1 UL36 Probe	5'-[6FAM]CTGTCGCGACGCTACGTGCA[BHQ1]	
IFNb	Hs01077958_s1 (assay ID); 4331182 (catalogue N)	Invitrogen

Table 9. List of primer/probes used.

Oligo Name	Sequence	Target	Provider
cGAS	**AAGTGCGACTCCGCGTTCAG** **FWD** CACCGAAGTGCGACTCCGCGTTCAG **REV** CTTCACGCTGAGGCGCAAGTCCAAA	exon 1 3' end, fwd	Sigma-Aldrich
Sp1	**CAGGCTCGAAGTAGCAGCAC** **FWD** CACCGCAGGCTCGAAGTAGCAGCAC **REV** CGTCCGAGCTTCATCGTCGTGCAAA	exon 2 3' end, fwd	
STING	**CGGGCCGACCGCATTTGGGAGGG** **FWD** CACCGCGGGCCGACCGCATTTGGGA **REV** CGCCCGGCTGGCGTAAACCCTCAAA	exon 4 centre, rev	

Plasmid	Description	Provider
pSpCas9n(BB)-2A-Puro (PX462) V2.0	Cas9n (D10A nickase mutant) from S. pyogenes with 2A-Puro, and cloning backbone for sgRNA (V2.0)	Addgene
pVSV-G	Vector used for expression of vesicular stomatitis virus envelope protein	BD Biosciences
pCMV delta R.8.91	Lentivirus helper vector that contains reverse transcriptase polymerase (pol), capsid protein (gag), regulatory proteins (Rev), and CMV promoter	Addgene

Table 10. Table of guide RNAs and plasmids used for CRISPR-Cas9 gene editing.

3. Methods

3.1. Cell culture

3.1.1. Cell growth, maintenance, and passaging

Cells were maintained and grown in T75 cell culture flasks (Nunc Fisher Scientific UK Ltd) in the appropriate media as described above. These flasks were kept in incubators at 37°C and 5% CO_2. When cells were confluent (80-90% confluent) they were washed twice with 4ml Versene, followed by an incubation with 1 ml of trypsin at 37°C until cells were detached from the surface of the flask. These cells were then re-suspended in 9ml of the appropriate medium before they were placed in new flasks (passaging) or plated for experimentation.

3.1.2. Cell seeding

The total number of cells in flasks was determined using a Neubauer haemocytometer counting chamber and a light microscope. These cells were then seeded in the appropriate plate (12 or 24-well plates) in a total volume of 0.5-1 ml of cell culture medium. In the instance of confocal microscopy analysis, 13 mm glass coverslips were added to the wells prior to addition of cell culture medium. For these experiments 24 well plates were always used. The seeding density would vary between cell types but would range from 1 x 10^5 to 2 x10^5 cells/well. The seeded cells were incubated overnight to allow settling before any further experimentation was carried out.

3.2. CRISPR-Cas-9 lentivirus-based method of generating STING, cGAS- and Sp1- KO cells

3.2.1. Lentivirus stock generation

Transformation of competent bacteria and propagation of plasmid DNA were conducted by Steven McFarlane. For generation of lentivirus stocks, HEK-293T cells (2 X 10^6 cells) were seeded onto 60 mm dishes and incubated overnight at 37ºC in 5% CO_2. Guide RNAs were designed suing ChoChop but only the successful guide RNAs were included in the materials. pSpCas9 plasmid (3 µg) expressing a non-targeting control, STING-targeting, cGAS-targeting or Sp1-targetting guide RNA, plus pVSV-G (3 µg) plasmid and pCMV-DR8.91 helper plasmid (3 µg) were added to 250 µl of serum-free DMEM. PLUS reagent (8 µl) was added to the plasmid mixture and incubated for 15 minutes at room temperature. After incubation, serum-free DMEM (250 µl) and lipofectamine (12 µl) were added to the plasmid-reagent plus mixture and allowed to incubate for 15 minutes at room temperature. The culture medium of HEK-293T cells was removed and saved as "conditioned medium". Serum-free medium (850 µl) was added to the prepared plasmid-PLUS reagent-lipofectamine mixture prior to adding the entire volume to the cells and incubating at 37ºC for 3 hours. Then, 3 ml conditioned medium were added, and incubated at 37ºC for 4 hours. Following incubation, the medium was replaced by 4 ml of fresh DMEM supplemented with 30% FCS. Lentivirus stocks were harvested when cells showed severe cell death, typically 48 hrs post-transfection. Lentivirus stocks were filtered using 0.45 µm filter and used immediately or stored at -70ºC.

3.2.2. Lentivirus transduction of cells

HFt cells were seeded at 1 X 10^6 cells in 60 mm dishes and incubated overnight at 37ºC in 5% CO_2. For each infection, 1 ml of lentivirus

supernatant containing 1 µl of polybrene was added to the cell monolayer. The infected plates were kept at 37ºC in 5% CO_2 incubator for 1 hour with rocking every 5-10 minutes. Following the infection, the lentivirus-containing medium was discarded and replaced by antibiotic selection medium (HFt media containing puromycin at 1 µg/ml) and then passaged with continuous puromycin maintenance (0.5 µg/ml). The level of mRNA and protein expression was monitored by qPCR, IF and Western blotting. All experiments were repeated on independent batches of depleted cells.

3.3. Viruses

3.3.1. Protocol for growing of HSV-1 virus stocks

BHK cells were seeded at 1 X 10^6 cells per 60 mm dish and incubated overnight at 37ºC with 5% CO_2. Cells were infected with WT HSV-1 (Glasgow 17syn+ strain) at an MOI of 0.001 PFU/cell in 500 µl of serum-free DMEM provided by Chris Boutell (Alandijany et al., 2018). During viral absorption, the plates were rocked every 5-10 minutes for one hour to ensure equal distribution of the virus across the cell monolayer. Following the absorption, cells were overlaid with complete medium and incubated at 37ºC with 5% CO_2. The infected cells were checked on every 24 hrs for cytopathic effect, hallmark of progressive infection. Virus was harvested from supernatant when a severe cytopathic effect was observed, typically around 3 to 4 days post-infection. The cell-released virus was clarified by low-speed centrifugation at 1500 rpm for 10 minutes in a centrifuge to remove cell debris and resuspended in normal DMEM, supplemented with FCS at a final concentration of 10% to promote virus stability when frozen down. Virus stocks were aliquoted, snap frozen on dry ice, and stored at -70ºC.

3.3.2. Growth of hCMV virus stocks

IMR-90 cells were seeded in T75 flasks and incubated overnight at 37ºC with 5% CO_2. Cells were infected with hCMV (AD169) at an MOI of 0.01 PFU/cell in 2.5 ml of serum-free DMEM provided by Thomas Shenk (Yu et al., 2002). During viral absorption, the plates were rocked every 5-10 minutes for one hour to ensure equal distribution of the virus across the cell monolayer. Following the absorption, cells were overlaid with complete medium and incubated at 37ºC with 5% CO_2. Virus was harvested from supernatant when a severe cytopathic effect was observed, typically around 12-18 days post-infection. The cell-released virus was clarified by low-speed centrifugation at 1500 rpm for 10 minutes in a centrifuge to remove cell debris and resuspended in normal DMEM, supplemented with FCS at a final concentration of 10% to promote virus stability when frozen down. Virus stocks were aliquoted, snap frozen on dry ice, and stored at -70ºC.

3.3.3. Growth of EdC-labelled HSV-1 virus stocks.

RPE cells were used to grow EdC-labelled viruses as described previously (Alandijany et al., 2018). Cells were infected with HSV-1 at an MOI of 0.001 PFU/cell in a total volume of 2.5 ml DMEM containing 0.2% FCS at 33ºC with 5% CO_2. The flasks were rocked every 5-10 minutes for one hour. Following viral absorption, 3.5 ml of DMEM containing 0.2% FCS were added to each flask making a total of 6 ml per flask. At 24 hrs post-infection, EdC was added to a final concentration of 1 μM per flask. Then, a fresh pulse of EdC (1 μM) was added every 24 hrs for three days. When cells showed an extensive cytopathic effect, the yields were collected and combined in a 50 ml corning tubes. In order to remove cell debris, the tubes were centrifuged at 1500 RPM for 10 minutes at 4ºC. Supernatants

containing labelled cell-released virus were filtered through 0.45 µm filter to remove small debris. To remove any free EdC nucleotides within the virus prep, which would interfere with downstream microscopy, supernatants were processed with an illustra NAP-25 column (17085201, GE Healthcare) as per manufacturer's protocol. Purified virus stocks were aliquoted into working volumes and snap frozen on dry ice and further stored at -70ºC. The viral preparations were titrated in U2OS cells (described below).

3.3.4. Growth of EdC/A-labelled hCMV virus stocks

IMR-90 cells were used to grow EdC/A-labelled hCMV viruses. Cells were grown in T75 flasks and infected with AD169 hCMV at an MOI of 0.01 PFU/cell in a total volume of 2.5 ml DMEM at 37ºC with 5% CO_2. The flasks were rocked every 5 minutes for one hour. Following viral absorption, a further 2.5 ml of DMEM was added to the flask. These were left until advanced CPE could be seen, changing the DMEM media every 4-5 days. Once advanced infection could be seen, labelling of the virus was done using 200µl of DMEM with 5 µM final concentration of EdC/A (2.5 µM EdC + 2.5 µM EdA). Label pulsing was done daily until virus harvesting, which varied between stocks. When the virus was ready to be harvested, the flask supernatant was spun at 1500 rpm for 10 mins and then aliquoted and stored at -70ºC.

3.3.5. UV irradiation of HSV-1

UV irradiation of HSV-1 virus stocks was carried out every time prior to infection in a UVP CL-1000 Shortwave Ultraviolet Crosslinker (235 nm wavelength; 11798211, Thermo Fisher), unless otherwise stated. The UV dose that was used was 0.1 mJ/cm^2 for 30/60/180 seconds as indicated. A secondary UV source used was the shortwave UV lamp from the Microbiology Safety Cabinet (254 nm wavelength), used in tissue culture. The length of

irradiation was 5/10/15/30 minutes; however, the exact dose of UV irradiation cannot be determined by this method.

3.3.6. Titration of virus stocks

All virus stocks (WT HSV-1, HSV-1^{EdC}, HSV-1^{EdC} VP26 GFP) were titrated in U2OS cells. Cells were seeded overnight at a density between 1.5-2.5 X 10^5 cells per well in a 24-well plate. The virus stocks were prepared in 10-fold dilution series in serum-free DMEM prior to infection. Cells were then infected with virus inoculum of 100µl. During the absorption period, the plates were rocked every 5-10 minutes for one hour. Following the virus incubation step, cells were overlaid with DMEM supplemented with 10% FCS and 2% human serum (HS) and incubated at 37°C with 5% CO_2. The infected cells were checked regularly for viral plaques which were observed typically 48 to 72 hours post-infection. The plates were processed with Giemsa staining (described below), and the plaques were counted under a plate microscope. Then, viral titers were calculated using the following formula:

$$PFU/ml = Number\ of\ plaque * dilution\ factor * 10\ (used\ 100\mu l\ inoculum)$$

MOI (PFU/cell) was estimated based on the virus titre and the number of cells. Irrespective of the cell types to be infected, the MOI was estimated based on the virus titre determined on U2OS cells.

HCMV stocks were titrated using one of two methods: (i) immunostaining of plaques assay, (ii) foci forming assay (both explained below). Depending on the titration assay performed, HFt or IMR-90 cells were used, respectively.

3.4. Assays

3.4.1. Giemsa staining

Media was discarded from the wells containing virus-infected cells prior to the addition of Giemsa stain (500 µl/well). Following a 3-5 min incubation the plates were thoroughly washed with water to remove stain and left to airdry. Plaque numbers were then obtained with the help of a light microscope.

3.4.2. Immunostaining of plaques assay

Cells were seeded in 12 or 24-well plates and incubated at 37°C in 5% CO_2 overnight before further manipulations. Cells were inoculated with either a serial dilution or fixed MOI (PFU/cell as indicated) of WT or UV-irradiated HSV-1 (length indicated by number of seconds) in a total volume of 150/100 µl serum-free DMEM, respectively. Plates were rocked every 5 min for 1 h prior to removal of inoculum and overlay with complete medium containing 2% HS. At the indicated time post-infection, the media was removed, and the cells were washed three times with PBS. Cells were simultaneously fixed and permeabilized in PBS containing 1.8% formaldehyde and 0.1% 10x Triton, followed by blocking in PBS-tween (PBST) containing 5% skimmed milk for 30 minutes at room temperature. Cells were sequentially incubated for 60 minutes at room temperature with primary antibodies (indicated per experiment), followed by IgG–peroxidase secondary antibody. Three washes with PBST were performed following each antibody incubation. Finally, True Blue Peroxidase stain was added and incubated until the colour was developed. Plates were then washed three times with PBST, PBS, and distilled water. The number of plaques was counted under a plate microscope.

For hCMV, IMR-90 cells were seeded in a 24-well plate and incubated at 37°C with 5% CO_2 overnight prior to any further manipulation. The infection followed the same protocol as above with the difference being that infected cells were incubated for 96 hours prior to staining.

3.4.3. Foci forming assay (FFA)

HFt cells were seeded in 24-well plates and incubated overnight at 37°C and 5% CO_2. Following this, cells were inoculated with a serial dilution of virus stock of hCMV EdC/A in a total volume of 100µl serum-free DMEM. During the incubation with the virus, plates were rocked every 5 mins for 1 hour prior to the removal of the inoculum and overlay with complete DMEM. After 16-24hrs the media was removed, and the cells were washed three times with PBS. Cells were simultaneously fixed and permeabilized in PBS containing 1.8% formaldehyde and 0.1% 10x Triton, followed by 3 washes with PBS. Blocking was carried out for 30 mins at room temperature using PBS containing 2% filtered FCS. Cells were sequentially incubated for 60 minutes at room temperature with primary antibodies diluted in blocking solution, followed by Alexa 555 conjugated secondary antibodies. Three washes with PBS + 2% FCS were performed following each antibody incubation. A final wash with PBS and three washes with H_2O were carried out after the secondary antibody incubation. The plates were imaged using Celigo Image Cytometer (Nexcelom). Viral titres were calculated using the following formula:

$$FFU/ml = Number\ of\ \text{foci} * dilution\ factor$$

3.4.4. DotBlot assay

A 0.2 µm nitrocellulose membrane (Amersham, 15249794) was gridded using a pencil and 2 µl of virus stock was slowly added onto the

membrane and left to completely dry. The membrane was then incubated in blocking solution (PBST + 5% Marvel) for 1 h at room temperature. Following the block, membranes were incubated for 1 h in blocking solution containing primary antibodies at room temperature on a tube roller. The incubation was carried out in the dark. The membranes were washed with three 5 min washes with PBST and then incubated with secondary antibodies for 1 h. After that, another three 5 min washes with PBST and one 5 min wash with PBS were applied on the membrane. Membranes were imaged on an Odyssey Infrared Imager (LiCor). The intensity of protein bands was quantified with Odyssey Image Studio Software.

3.4.5. Virion genome release assay

13-mm coverslips were pre-treated with Poly-D-lysine for 60 mins. Chilled TNE buffer was mixed along with neat stock of virus preparation and protein denaturant Guanidine hydrochloride (2mM final concentration; Sigma; G3272) and incubated for 1 hour on ice. Following incubation, 75% ice-cold MeOH was mixed along with the virion solution (~60% final concentration) and added to the coverslips. The coverslips were incubated at 4ºC for 60-90 min. After the drying period, virions were fixed/permeabilised using PBS+ 5% PFA+ 0.5% Triton-x-100 for 10 min and washed twice with PBS. Samples were blocked, using filter sterilised PBS, containing 2% Foetal Calf Serum (FCS). Virion released genomes were detected by click chemistry, using a Click-iT Plus EdU Alexa Fluor 555 imaging kit for 30 min at room temperature (ThermoFisher Scientific, C10638), following manufacturer's instruction. Immunofluorescence imaging was then carried out using the Airyscan of the Zeiss 880 Confocal Microscope.

3.4.6. Sodium dodecyl sulphate-polyacrylamide gel electrophoresis (SDS-PAGE) and Western blotting

Cells were washed twice with PBS before whole cell lysates were harvested in a 1.5X boiling mix (SDS-PAGE loading buffer containing 4 M urea and 50 mM DTT). Harvested lysates were either used immediately or snap frozen and stored at - 20° C. Samples were boiled for 10 minutes in a water bath prior to loading. Wells were loaded with 15-20 µl of whole cell lysates. PageRuler prestained NIR protein ladder was used as a reference marker for molecular mass. Proteins were resolved by SDS-PAGE on Novex 4-12% Bis-Tris gel (Invitrogen NP0322BOX) using either NuPAGE MOPs (1X) or NuPAGE MES (1X) running buffer. Gels were run at 120 volts until the dye front reached the bottom of the gel. Separated proteins were electro-transferred for 1 hr at 30 volts onto Hybond-ECL 0.2 µm nitrocellulose membranes for western blotting. Protein transfer was conducted using Novex NuPAGE transfer buffer (1X) containing 10% methanol. Membranes were blocked for 1 hour at room temperature in filtered PBS supplemented with 5% FCS (PBS-FCS). Primary and secondary antibody incubations were performed in filtered PBST–FCS (PBS-FCS supplemented with 0.1% Tween-20) at the desired antibody dilution (Table 10 and 11). Membranes were washed three times in PBS supplemented with 0.1% Tween-20 (PBST) for 10 min following each antibody incubation. Prior to scanning, membranes were washed two times in PBS and two times in distilled water. Membranes were imaged on an Odyssey Infrared Imager (LiCor) and analysed with Odyssey Image Studio Lite software.

3.4.7. Click chemistry, indirect IF staining, and confocal microscopy

3.4.7.1. Fixation and permeabilization

Coverslips were washed twice with 500 µl of cytoskeleton (CSK) buffer (10 mM HEPES (pH 7.0), 100 mM NaCl, 300 mM sucrose, 3 mM $MgCl_2$, 5 mM EGTA) prior to fixation and permeabilization in 500µl of CSK buffer containing both 1.8% formaldehyde and 0.5% Triton-X100 for 10 minutes at room temperature. Cells were washed twice in 750 µl of CSK buffer, and then blocked in PBS containing 2% FCS (PBS-FCS) for at least 1 hour at room temperature or overnight (O.N.) at 4 ºC.

3.4.7.2. CLICK chemistry and detection of EdC signals

Detection of the EdC-labelled or EdC/EdA-labelled virus was conducted using Click-iT® Plus EdU Alexa Fluor 555 Imaging Kit (ThermoFisher Scientific, C10638) according to the manufacturers' instructions. Each ml of reaction solution contained 880 µl of 1X Click-iT® reaction buffer, 20 µl of copper protectant, 2.5 µl of Alexa Fluor® picolyl azide, and 100 µl of reaction buffer additive. Click chemistry was always conducted directly prior to indirect IF staining.

3.4.7.3. Indirect IF staining protocol

Primary and secondary antibody incubations were performed at room temperature and in the dark. Following a 60-minute incubation with 35µl of the primary antibody at the desired dilution (Table 10), coverslips were washed three times with PBS-FCS prior to a 60-minute incubation with both the secondary antibody and DAPI. The secondary antibodies used were Alexa 488, 555, and 647 conjugated donkey anti-rabbit, and anti-mouse IgG (Table 11). Coverslips were washed three times with PBS-FCS followed by three washes with distilled water. Coverslips were allowed to air dry prior

to mounting on glass slides using Citifluor AF1 mounting medium. Clear nail varnish was used to seal the edge of coverslips to the slides.

3.4.7.4. Confocal microscopy, image analysis, and three-dimensional (3D) image reconstitution

The samples were examined using a Zeiss LSM880 confocal microscope using the 63x Plan-Apochromat oil immersion lens with 408, 488 nm, 543 nm and 633 nm laser lines. Zen black software (Zeiss) was used for capturing Z-series images, generating cut mask channels, exporting the maximum intensity projection images, and determining the weighted (w.) colocalization coefficient. Imaris (Bitplane) software was used to generate 3D images.

3.4.8. Quantitative reverse-transcriptase polymerase chain reaction (qRT-PCR)

3.4.8.1. RNA preparation

RNA extraction was conducted using RNeasy Plus Mini Kit (Qiagen) according to manufacturer's instructions. Cells were washed twice with PBS, harvested in 200 µl Buffer RLT Plus, snap frozen, and either used immediately or stored at -20 °C. The cell lysate was vortexed for 30 seconds and centrifuged for 3 minutes at the maximum speed (17000 X g). The supernatant was carefully removed, transferred to a gDNA Eliminator spin column, and centrifuged for 30 seconds at 8000xg. The column was discarded, and 180 µl of 70% ethanol were added to the flow-through. The entire volume was transferred to an RNeasy spin column and centrifuged for 15 seconds at 8000xg. The flow-through was discarded, and 700 µl of Buffer RW1 were added to the column, followed by centrifugation for 15 seconds at 8000xg. The flow-through was discarded, and 500 µl of Buffer

RPE were added to the column, followed by centrifugation for 15 seconds at 8000xg. The last step was repeated. In order to dry the membrane, the RNeasy column was placed in a new 2 ml collection tube and centrifuged at 17000xg for 1 minute. Finally, 30 µl of RNase-free water were added, and the column was centrifuged for 1 minute at 8000xg to elute RNA. Extracted RNA was used immediately for complementary DNA (cDNA) synthesis or stored at -20 °C.

3.4.8.2. cDNA synthesis

Reverse transcription (RT) of cellular RNA to cDNA was performed using TaqMan Reverse Transcription Reagent Kit (Life Technologies, catalogue number N808-0234). Purified RNA was reverse transcribed in a total volume of 20 µl of reaction mix containing 2 µl of RT buffer (1x), 4.4 µl of MgCl2 (5.5 mM), 4 µl of dNTPs (2mM), 1 µl of Oligo dT, 0.4 µl of RNase inhibitor (8 U), 0.5 µl of multiscribe reverse transcriptase (25 U), and 6.7 µl of RNase-free water. RNA template was sequentially incubated at 25 °C for 10 minutes for primer annealing, at 37°C for 60 minutes for extension, and at 95 °C for 5 minutes for RT inactivation.

3.4.8.3. Quantitative real-time PCR

cDNA was amplified using target and control-specific primer/probe mixes (Table 12). Each sample was run in triplicate as a singleplex reaction in a total volume of 20 µl per reaction. Each reaction contained 1 µl of primer/probe mix, 10 µl of TaqMan fast universal mix (ThermoFisher Scientific, catalogue number 4352042), 7 µl of RNase-free of H2O, and 2 µl of cDNA. RT-PCR cycling condition as follows: a cycle of denaturation at 95

ºC for 20 seconds, and 40 cycles of annealing at 95 ºC for 3 seconds, and extension at 60 ºC for 30 seconds.

3.4.8.4. Analysis of qPCR data

Data were analysed using applied biosystems 7500 fast real-time PCR system software. The level of mRNA for host gene under investigation was normalized to GAPDH mRNA level, internal control, using the method. Normalized values were expressed relative to the normalized level of mRNA in a control sample (as indicated in the figure legends).

3.4.9. Chromatin immunoprecipitation quantitative real-time PCR (ChIP-qPCR)

3.4.9.1. Chromatin extraction and crosslinking

Chromatin extraction was conducted using Chromatin Extraction Kit (ab117152, Abcam) following manufacturer's protocol. Media was aspirated off and cells were placed on ice and UV crosslinked in a UVP CL-1000 Ultraviolet Crosslinker at the specified UV dose. Following UV crosslinking, working lysis buffer was added (200 µl/10^6 cells) and cells were resuspended into a 1.5 ml Eppendorf tube. These were subsequently incubated on ice for 10 mins, prior to a 10 sec vigorous vortex. Cells were then spun for 5 min in an Eppendorf centrifuge at 5000 rpm and 4ºC. Supernatant was then carefully discarded, and the pellet was resuspended in working extraction buffer (50µl/10^6 cells). The mixture was left to incubate for a further 10 mins with occasional vortex. Following this, cells were carefully resuspended and sonicated at 20 sec ON/ 15 sec OFF for 6 mins (roughly 10 pulses). Finally, extracts were spun at 12 000 rpm at 4ºC for 10 mins, prior to moving the supernatant to a new Eppendorf and

discarding the pellet. Chromatin buffer was added to the samples at a 1:1 ratio and 10% of the sample was put aside as input. These samples were either snap-frozen at -70ºC or immediately used for immunoprecipitation.

3.7.9.2. Chromatin Immunoprecipitation (ChIP)

The DNA concentration of UV crosslinked samples was measured using a NanoDrop. Chromatin Immuno-precipitation was carried out using the CIP Kit Magnetic-One Step (ab156907, Abcam). A final concentration of 5-10 µg of chromatin was used for individual ChIP reactions, dependent on the quality of the chromatin extraction. Following manufacturer's guidance, samples were mixed in an Eppendorf with ChIP buffer, magnetic beads and antibody of interest (1µg) to a final reaction volume of 200µl. Samples were then incubated on a tube rotator overnight at 4ºC. Once the samples were ready to be processed, the tubes were placed on a DynaMag magnetic tube stand (12321D, Abcam) and left for 1-2 mins to allow the beads to aggregate at the wall of the tube. The supernatant was discarded and the tubes were removed from the stand in order for the beads to be gently washed with 200µl of cold 1x Wash buffer. The samples were returned to the magnet stand and the wash process was repeated 4 times. An additional wash step was carried out using 200µl of Extraction buffer. Finally, the beads were mixed with 40µl of Extraction buffer and Proteinase K (39µl + 1µl, respectively). The samples were then placed at 65ºC and incubated for 15 mins. This was followed up by a 5 min incubation at 95ºC. The samples were placed on the magnet stand for the supernatant, containing the DNA, to be extracted and stored at -20ºC or used immediately for RT-qPCR. Inputs were processed parallel to the samples, by diluting them 1/10 with 88µl of Extraction buffer and 2.5µl of Proteinase K. The inputs were heat incubated in the same conditions as the samples.

3.7.9.3. Real time quantitative PCR (RT-qPCR)

DNA was amplified using target and control-specific primer/probe mixes (Table 12). Each sample was run in triplicate as a singleplex reaction in a total volume of 20 µl per reaction, as described above.

3.7.9.3. Analysis of RT-qPCR data

Data were analysed using applied biosystems 7500 fast real-time PCR system software. The level of mRNA for the viral gene under investigation was normalized to the input levels of the sample, using the Percent Input method.

3.8. Data plotting and statistical analysis

GraphPad Prism 7.02 was used for plotting the data and calculating P values. T-test or Mann-Whitney U-test was used to determine statistical significance (as indicated in the figure legends).

4. UV irradiation of HSV-1 results in the premature uncoating of vDNA in the cytoplasm

4.1. Overview

UV irradiation of HSV-1 has been used for decades for investigating the innate immune response to virus infection (Taylor & O'brien, 1985; Hendricks et al., 1991; Eloranta, Sandberg & Alm, 1996). However, the exact mechanism as to why UV irradiation promotes the activation of IFN-mediated innate immune defences remains to be elucidated. Following membrane fusion and cellular uptake, capsids have been shown to be able to be transported to the nucleus along the microtubule network (Sodeik, Ebersold & Helenius, 1997; Radtke et al., 2010). It is a possibility that some viral capsids may disassociate from the microtubules and release the vDNA prematurely in the cytoplasm via the proteasome (Miyamoto' And & Morgan, 1971; Horan et al., 2013). Direct tracking of vDNA during infection is now possible through ethynyl-modified deoxynucleoside labelling combined with click chemistry (El-Sagheer & Brown, 2010). Labelling of DNA virus genomes, such as adenovirus and papillomavirus, has been reported (Wang et al., 2013; Broniarczyk et al., 2015). The click chemistry-based method relies on the incorporation of nucleoside analogues into the newly synthesized DNA of replicating viruses. The alkynes on the labelled DNA react with the azides of fluorescent dyes in a copper (I)-catalyzed reaction and result in fluorescence. This type of DNA labelling does not require harsh manipulation of the sample, unlike FISH or BrdU-labelling, and results in an enhanced specificity and sensitivity of DNA detection (Chehrehasa et al., 2009; Salic & Mitchison, 2008). Our lab has optimized a protocol of EdC-labelling of HSV-1 genomes and purification of high titre virus stocks of labelled WT 17+ HSV-1 (HSV-1^{EdC}). Labelling was carried out in RPE cells infected at an MOI of 0.001 PFU/cell combined with pulse labelling with EdC (0.5 μM) at 24 hr intervals. Once advanced cytopathic effect was observed, the virus was harvested, purified through a NAP column (removing free EdC label in the viral supernatant) and titrated (section

3.3.3.). This protocol has been previously utilized to investigate the spatiotemporal recruitment of nuclear intrinsic immune factors to HSV-1 infecting DNA (Alandijany et al., 2018).

In this chapter a combination of EdC labelling of HSV-1 genomes and indirect immunofluorescence confocal microscopy was used to characterize viral genome localization within infected cells following infection with non-UV or UV irradiated HSV-1 virions. This was done during early stages of infection (90 mpi) and under infection conditions of MOI 3 PFU/cell. UV irradiation of HSV-1 resulted in the inhibition of plaque formation and protein production following infection. Microscopy observations revealed a dose-dependent cytosolic premature uncoating of UV irradiated HSV-1 genomes. Multiple UV sources demonstrated that this phenotype was reproducible and irrespective of the UV source. Additionally, the involvement of the cellular proteasome and microtubule network was explored in relation to the cytoplasmic deposition of HSV-1 genomes.

4.2. Results

4.2.1. Direct visualization of EdC-labelled HSV-1 genomes

EdC-labelling of HSV-1 allowed for the detection of input viral genomes, prior to vDNA replication and viral protein production. This method has been previously published from our group and others to investigate protein recruitment to vDNA as early as 30 mpi (minutes post-infection) (Sekine et al., 2017; Alandijany et al., 2018). To check if the virus stocks have been labelled successfully, HSV-1^{EdC} virions were annealed to Poly-D-lysine treated coverslips at 4^{o}C. Click chemistry was utilized to detect the viral DNA. To examine the specificity of the detected signal, virus was incubated in the presence of either DMSO (negative control) or

2M guanidine hydrochloride (GuaHCl), a protein denaturant that disrupts the structural integrity of capsids to expose the genomes.

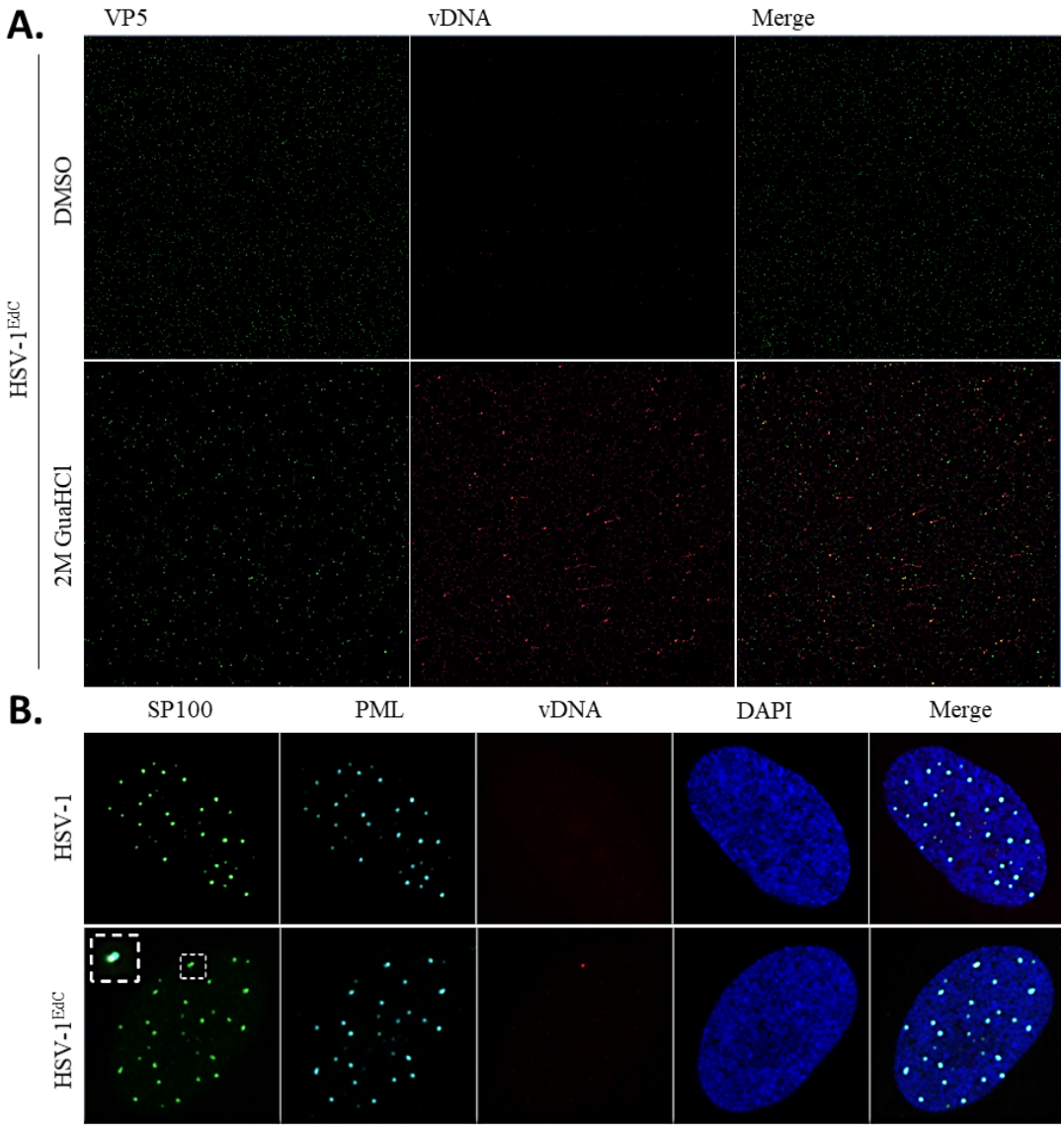

Figure 6. Sensitive and specific visualization of infecting viral DNA using EdC-labelling of genomes in combination with click chemistry.

(A) HSV-1^{EdC} was prepared on coverslips and incubated with either DMSO or 2M GuaHCl. Samples were fixed after 60 mins of addition of the virus and stained for the capsid protein VP5 (green), whilst vDNA was detected by click chemistry (red). Representative confocal image of a field of view showing the release of genomes in the presence or absence of a protein denaturant that disrupts the capsid. (B) HFT cells seeded on coverslips were infected with either unlabelled HSV-1 or HSV-1^{EdC} virus at an MOI of 3 PFU/cell. Cell monolayers were fixed and permeabilized at 90 mpi (minutes post infection). vDNA (red) was visualized by click chemistry. Nuclei were stained by DAPI. Additional staining controls were nuclear proteins Sp100 (green) and PML (cyan). Representative confocal image showing nuclei containing viral genomes.

Detection of labelled DNA signal was specific for HSV-1^{EdC} as only faint signal was detected in the control sample, where the capsids remained intact (Figure 6A). In the GuaHCl treated samples foci of vDNA could be observed, indicative of the release of the genome from the high pressurized capsid and was absent in the DMSO control. To further test the signal specificity, HFt cells were seeded onto coverslips and infected with either HSV-1 or HSV-1^{EdC} at an MOI of 3 PFU/cell. Samples were fixed at 90 mpi and stained for PML and Sp100, PML-NB component proteins reported to localize to nuclear HSV-1 DNA (Alandijany et al., 2018). DNA signal detected was specific for the HSV-1^{EdC} infected HFt cells, localizing to both PML-NB proteins, and was absent in the non-labelled HSV-1 infected cells (Figure 6B). This allows for click chemistry to be utilized for viral genome visualization both *in vitro* and *in vivo*.

4.2.2. UV-irradiated HSV-1 is unable to form plaques or produce viral proteins

UV inactivation of viruses is a common technique used in virology (Schneweis et al., 1981; Osorio & Ghiasi, 2003). These viruses have been shown to be slowed down in initiating infection by 16-24 hours and induce a strong type I IFN response (Eglin, Gugerli & Wildy, 1980; Taylor & O'brien, 1985; Hendricks et al., 1991; Eloranta, Sandberg & Alm, 1996). To assess the protein production profile of UV irradiated HSV-1 virus, we assessed the ability of the virus to form plaques and initiate protein expression. HFt cells were infected with either non-UV or UV irradiated HSV-1 (0.1 mJ/cm^2 for varying lengths of UV irradiation – 30, 60 and 180 seconds) in a 10-fold dilution series. Infected cell monolayers were incubated for 16-24 hours prior to ICC staining and plaque counting. Plaque staining for VP5 (viral late protein) was only detectible in the non-UV virus infection. As little as 30 sec of UV irradiation was enough to stop the virus from forming detectable plaques (Figure 7).

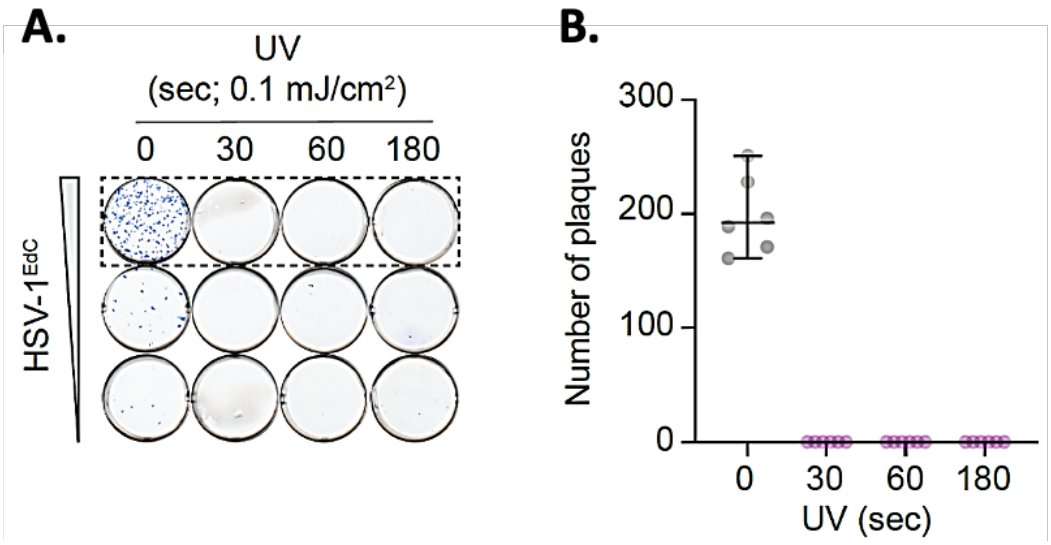

Figure 7. UV irradiation of HSV-1 abolishes viral plaque formation in HFt cells.
HFt cells were seeded overnight prior to infection with non-UV or UV-irradiated HSV-1 (as indicated) at a 10-fold dilution series. After an hour of viral adsorption, cells were overlaid with media containing 2% HS. At 24 hours post-infection, cells were fixed and permeabilized, and immunostained for HSV-1 plaque formation using an anti-VP5 monoclonal antibody. (A) The number of plaques (blue) was counted manually under a plate microscope. (B) Graph showing the plaque count for the selected row of wells on the right (dashed line).

In order to determine if UV irradiation inhibited the onset of viral replication, we next investigated viral protein expression. HFt cells were infected with non-UV or UV irradiated HSV-1 at an MOI of 3 PFU/cell for 8 hours prior to lysate extraction and WB analysis for ICP4, ICP0 and UL42. To determine if IE gene expression was occurring, PML was also used as an internal control as it is rapidly degraded by ICP0. Actin was used as a loading control. Relative expression levels were measured using Image Studio Lite software. Protein levels differed between the two types of infection. Non-UV irradiated HSV-1 expressed ICP0 (IE), ICP4 (IE) and UL42 (E) proteins and PML could be observed to be degraded. UV irradiated HSV-1 infected cells exhibited the same protein expression profile as mock infected cells, with no visible detection of viral proteins or PML degradation, suggesting a failure to initiate IE gene expression (Figure 8). Additionally, cells seeded onto coverslips were infected under the same conditions and stained for ICP0 to determine the percentage of antigen positive cells. Relative to non-UV irradiated HSV-1, where 80% of cells were ICP0 positive, UV irradiated HSV-1 infected cells exhibited no ICP0 production (Figure 9). These data suggest that UV irradiation of HSV-1 inhibits viral IE protein production.

In order to confirm that UV irradiated virus could enter into infected cells, we measured the type I IFN response. It has been reported that UV-irradiated HSV-1 specifically enhances the activation of type I IFN-mediated immune response both in vitro and in vivo (Gary, Rosenberg & Louis, 1974; Taylor & O'brien, 1985; Hendricks et al., 1991; Eloranta, Sandberg & Alm, 1996). To this end, we measured the levels of mRNA of IFNβ produced in HFt infected cells in a time course experiment (Figure 10). Non-UV HSV-1 did not induce IFNβ production in infected HFts. Conversely, UV HSV-1 successfully induced the production of IFNβ transcripts, which accumulated over time (Figure 10). These data suggest that UV irradiated HSV-1 is successfully entering cells and induces a type I IFN-mediated immune response.

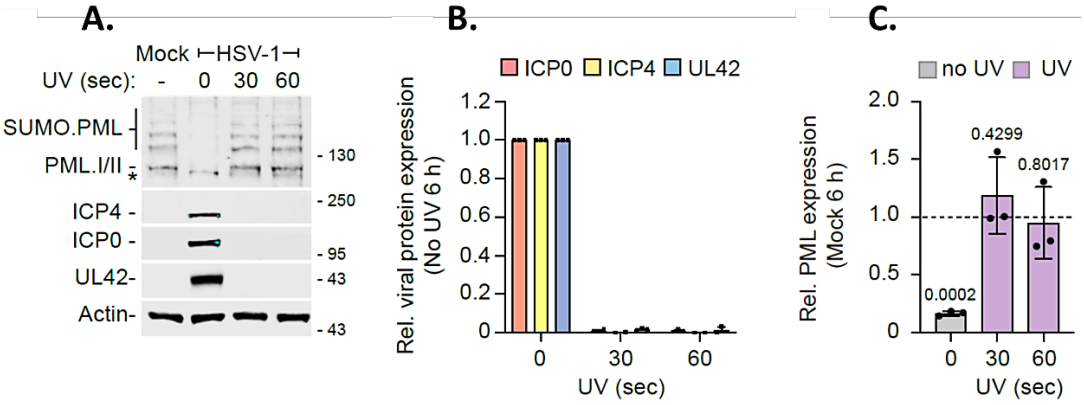

Figure 8. UV-irradiation of HSV-1 inhibits viral protein production and viral PML degradation. HFt cells were seeded overnight then infected with either non-UV or UV-irradiated HSV-1 (UV irradiation length indicated in secs) at an MOI of 3. Whole cell lysates were collected at 6 hpi, and protein levels were measured by Western blot. (A) Western blot showing the levels of PML, ICP4, ICP0, UL42 and actin in whole cell lysates. (B) Quantitation of viral protein levels (as in A) normalized to their respective actin loading control. Values expressed relative to the normalized non-UV irradiated HSV-1 infected cells. n=3; SD shown. (C) Quantitation of cellular PML expression levels (as in A). Values normalized to their respective actin loading controls and expressed relative to their normalized levels in mock infected HFt cells (dotted line = 1). n=3, SD shown. P value shown; student t-test.

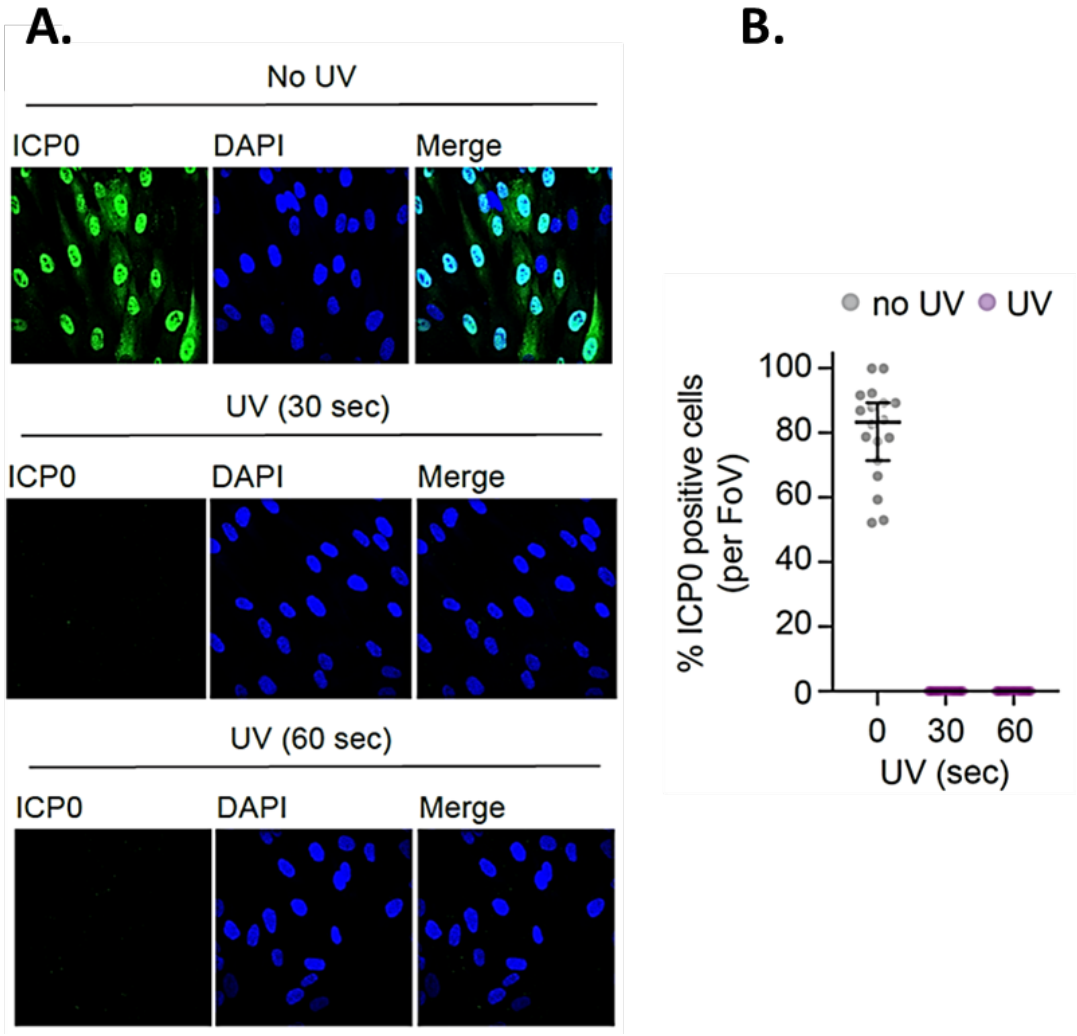

Figure 9. UV-irradiation of HSV-1 abrogates viral ICP0 protein production.

HFt cells were seeded overnight on coverslips then infected with either non-UV or UV-irradiated HSV-1 (length of UV irradiation indicated in secs) at an MOI of 3. Cells were fixed and permeabilized 6 hpi and assessed for the production of viral ICP0 (green). Nuclei were visualized by DAPI stain (blue). (A) Representative confocal images stained for ICP0 and DAPI. (B) Scatter plot showing the percentage (%) of ICP0 positive cells per Field of View (FoV). Individual points derived from 3 independent experiments.

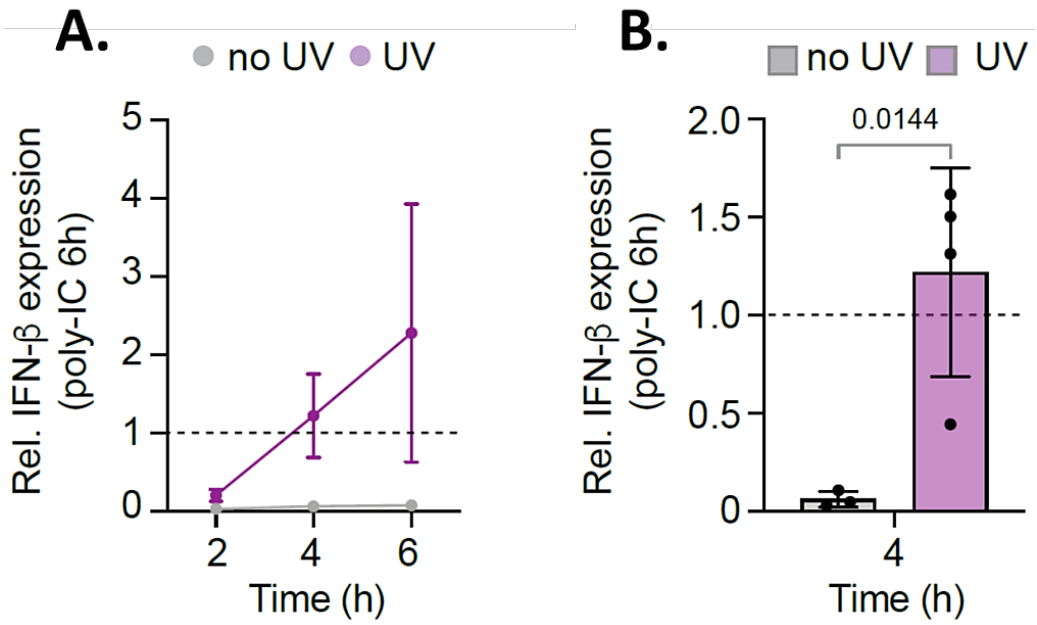

Figure 10. UV-irradiated HVS-1 induces the production of IFNß.

HFt cells were seeded overnight prior to infection with either non-UV or UV-irradiated HSV-1 (30 sec irradiation) at an MOI of 3. Cellular lysates were collected at the indicated times and processed by RT-qPCR to measure the levels of IFNß mRNA transcript levels. (A) Graph showing a time course of mRNA levels of IFNß normalized to control poly-IC treated cells at 6 hpi. n=4, means and SD shown. (B) Bar graph showing the difference between IFNß expression at 4h (as in A). N=4, SD shown; P value shown; student t-test.

4.2.3. UV irradiation causes the premature cytoplasmic uncoating of HSV-1 genomes

Electron microscopy studies of UV irradiated HSV-1 virions have shown the accumulation of capsids in the cytosol, 97% of which contained DNA (Miyamoto' And & Morgan, 1971). This observation is consistent with published data that has shown a delay in HSV-1 protein production following UV irradiation that was due to an event occurring prior to replication (Ross, Cameron & Wildy, 1972; Fridlender et al., 1978). However, the influence of UV irradiation on vDNA localization during HSV-1 infection has not been directly examined. We therefore applied click chemistry to visualize the localization of HSV-1^{EdC} labelled genomes following UV irradiation (Figure 11A). Since click chemistry is compatible with indirect IF imaging, it was possible to investigate the localization of vDNA under low MOI conditions at early time points of infection (90 mins post addition of virus).

HFt cells were infected with either non-UV or UV irradiated HSV-1^{EdC} (irradiated using a short UV wavelength crosslinker - 235 nm) at an MOI of 3 PFU/cell. The cells were fixed at 90 mpi and click staining was utilized to detect vDNA. HSV-1^{EdC} genomes were readily detected under both irradiation conditions, with majority of non- UV irradiated HSV-1 DNA being nuclear and the majority of UV irradiated HSV-1 DNA being cytoplasmic (Figure 11A and Figure 12A). Notably, a decrease in the number of detectable genomes was observed in a UV dose-dependent manner (Figure 11B). Interestingly, when the genome area was measured using Fiji software, a difference in genome size upon UV-irradiation could also be detected in a dose-dependent manner (Figure 11C). Quantitation of viral genome location demonstrated that in non-UV irradiated HSV-1 infection roughly 70% of genomes reached the nucleus (Figure 12B). This observation was consistent with published electron microscopy data that found 70% of capsids to have injected the viral DNA in the nucleus after 1 hour (Miyamoto' And & Morgan, 1971). Conversely, UV-irradiation of 30 and 60 secs decreased the HSV-1 genomes in the nucleus down to 60% and 50%, respectively (Figure 12B). Despite the decreased number of overall detectable genomes,

the ratio of nuclear:cytoplasmic viral DNA remained consistent (Figure 12C). These data suggested that UV irradiation induces the premature uncoating of HSV-1 genomes in the cytoplasm, thereby inhibiting the initiation of nuclear infection.

To determine if this phenotype was due to the source of UV irradiation an additional irradiation method was tested. Instead of using a shortwave UV crosslinker (235 nm wavelength), UV irradiation of HSV-1 virus was carried out with the shortwave UV lamp of a Microbiological Safety Cabinet (MSC; 254 nm wavelength) for varying lengths of time – 5,15 and 30 mins. Similar to UV crosslinker irradiation MSC UV irradiated HSV-1 inhibited plaque formation upon UV treatment (Figure 13). Additionally, MSC UV irradiated HSV-1 exhibited a cytoplasmic deposition genome phenotype in a UV dose-dependent manner (Figure 14A). Quantitation of microscopy images demonstrated UV irradiation decreased nuclear genome accumulation down to 30% following 30 min UV irradiation (Figure 14D). The increase in cytosolic genome deposition and reduction of nuclear HSV-1 genomes again correlated to the length of UV irradiation. The total number of HSV-1 genomes were affected by the MSC UV irradiation (Figure 14B), with only 30 genomes visualised per field of view following 30 min UV irradiation, representing a 60% drop in detectable vDNA foci. This data was consistent with previous experiments utilizing UV crosslinker irradiation (Figure 11B). Finally, the genome area decreased following UV irradiation in a UV dose-dependent manner (Figure 14C). The 30 min timepoint could not be quantified as the number of detectable genomes was too low to apply statistical analysis. Collectively this data show that UV irradiation of HSV-1 induces the premature release of viral genomes into the cytoplasm independently of UV light source. Thus, for the remainder of the study we used 30 sec UV irradiated HSV-1 (UV crosslinker).

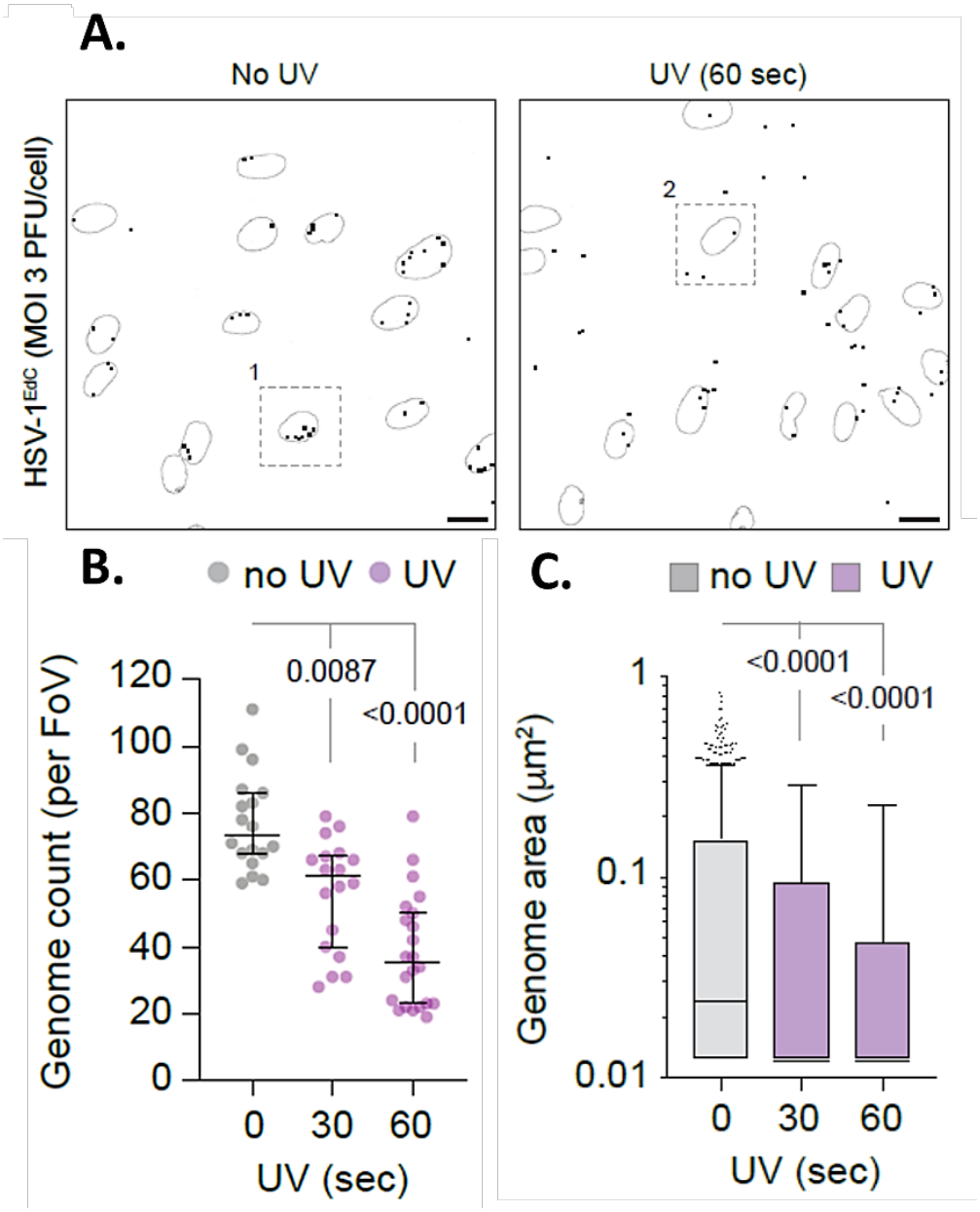

Figure 11. UV irradiation of HSV-1 influences genome localization and size.

HFt cells were seeded overnight prior to infection with either non-UV or UV irradiated HSV-1^{EdC} at an MOI of 3 PFU/cell. Cell monolayers were fixed and permeabilized at 90 mpi. Viral DNA was visualized with click chemistry. Nuclei were stained with DAPI stain (blue). (A) Representative field of view of outlines of non-UV or UV irradiated (60 sec) HSV-1 infected HFt nuclei. IF images were processed with ImageJ to show outlines. (B) Number of genomes per FoV. Boxes: 25th to 75th percentile range; black line: median; whiskers: 5th to 95th percentile range. n=3 fields of view per condition derived from a minimum of 3 independent experiments conducted in duplicate. P value shown; One-way ANOVA (Kruskal-Wallis). (C) Quantitation of the genome area (µm2). Boxes: 25th to 75th percentile range; black line: median; whiskers: 5th to 95th percentile range. n≥500 genome foci per condition derived from a minimum of 3 independent experiments conducted in duplicate. P value shown; One-way ANOVA (Kruskal-Wallice).

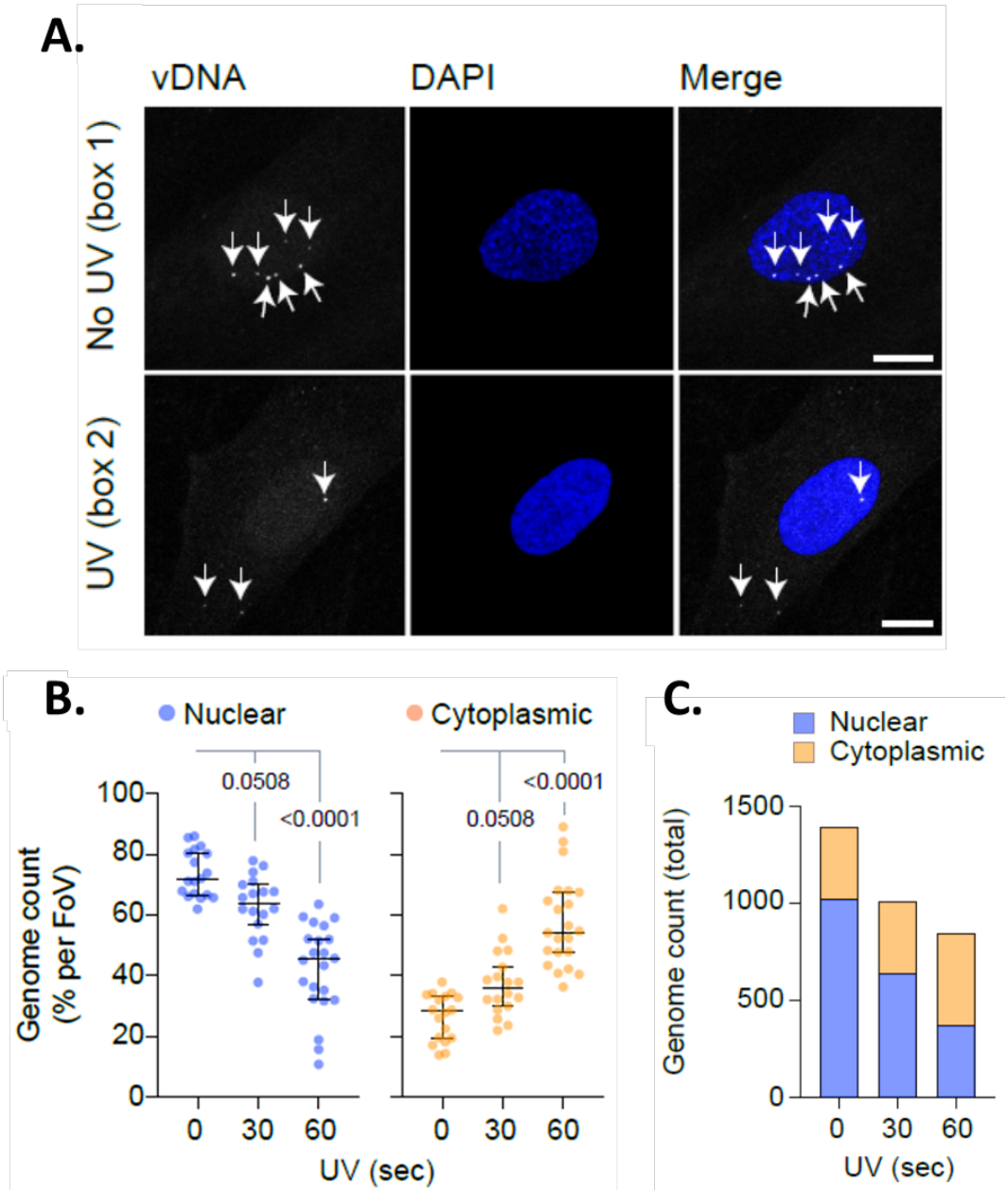

Figure 12. UV irradiation of HSV-1 induces the premature cytoplasmic deposition of viral genomes.

HFt cells were seeded overnight prior to infection with either non-UV or UV irradiated HSV-1 at an MOI of 3 PFU/cell. Cell monolayers were fixed and permeabilized at 90 mpi. Viral DNA was visualized with click chemistry. Nuclei were stained with DAPI stain (blue). (A) Representative confocal microscopy images showing premature uncoating of HSV-1 DNA upon UV irradiation. Viral DNA highlighted by white arrows. Non-UV irradiated HSV-1 HFts in box 1 and UV irradiated HSV-1 HFts in box 2. (B) Quantitation of the genome distribution (nuclear or cytoplasmic) per field of view in percentage (%). Individual points shown; black line: median; whiskers: 5th to 95th percentile. n=3 fields of view per condition derived from a minimum of 3 independent experiments conducted in duplicate. ns (not significant value shown; One-way ANOVA (Kruskal-Wallis). (C) Total genome distribution per FoV. n≥900 genome foci per condition derived from 3 independent experiments conducted in duplicate.

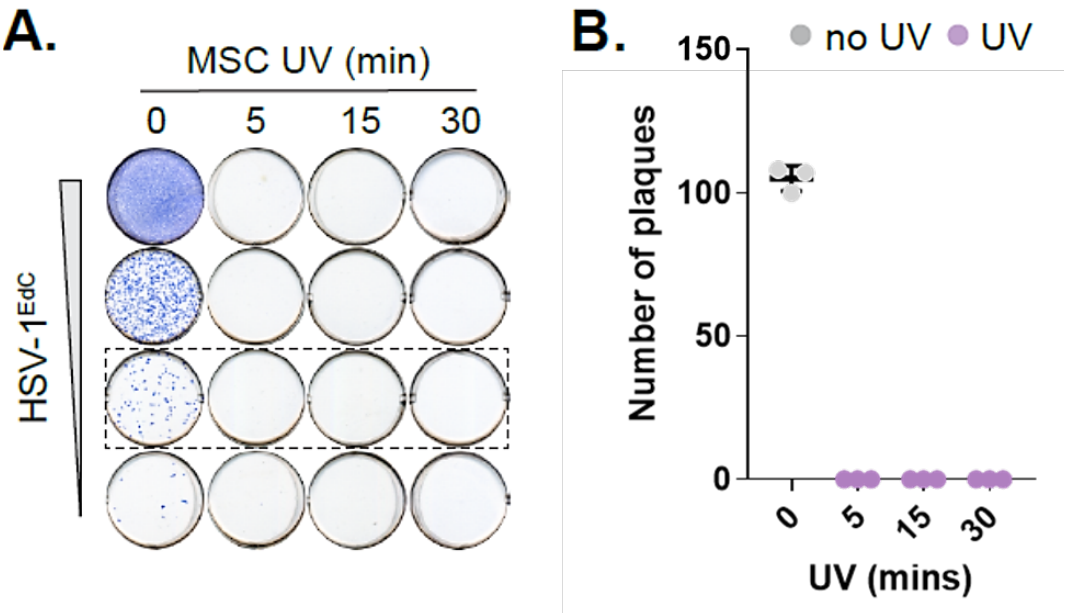

Figure 13. MCS (shortwave) UV irradiation of HSV-1 abolishes viral plaque formation in HFt cells. HFt cells were seeded overnight prior to infection with either WT HSV-1 or UV-irradiated HSV-1 (UV HSV-1; MSC UV irradiation duration indicated in min) at a 10-fold dilution series. After an hour of viral adsorption, cells were overlaid with media containing 2% HS. At 24 hours post-infection, cells were fixed and permeabilized, and immunostaining plaque assay was conducted. (A) The number of plaques (blue) was counted manually under a plate microscope. (B) Graph showing the plaque count for the selected row of wells on the right (dashed line).

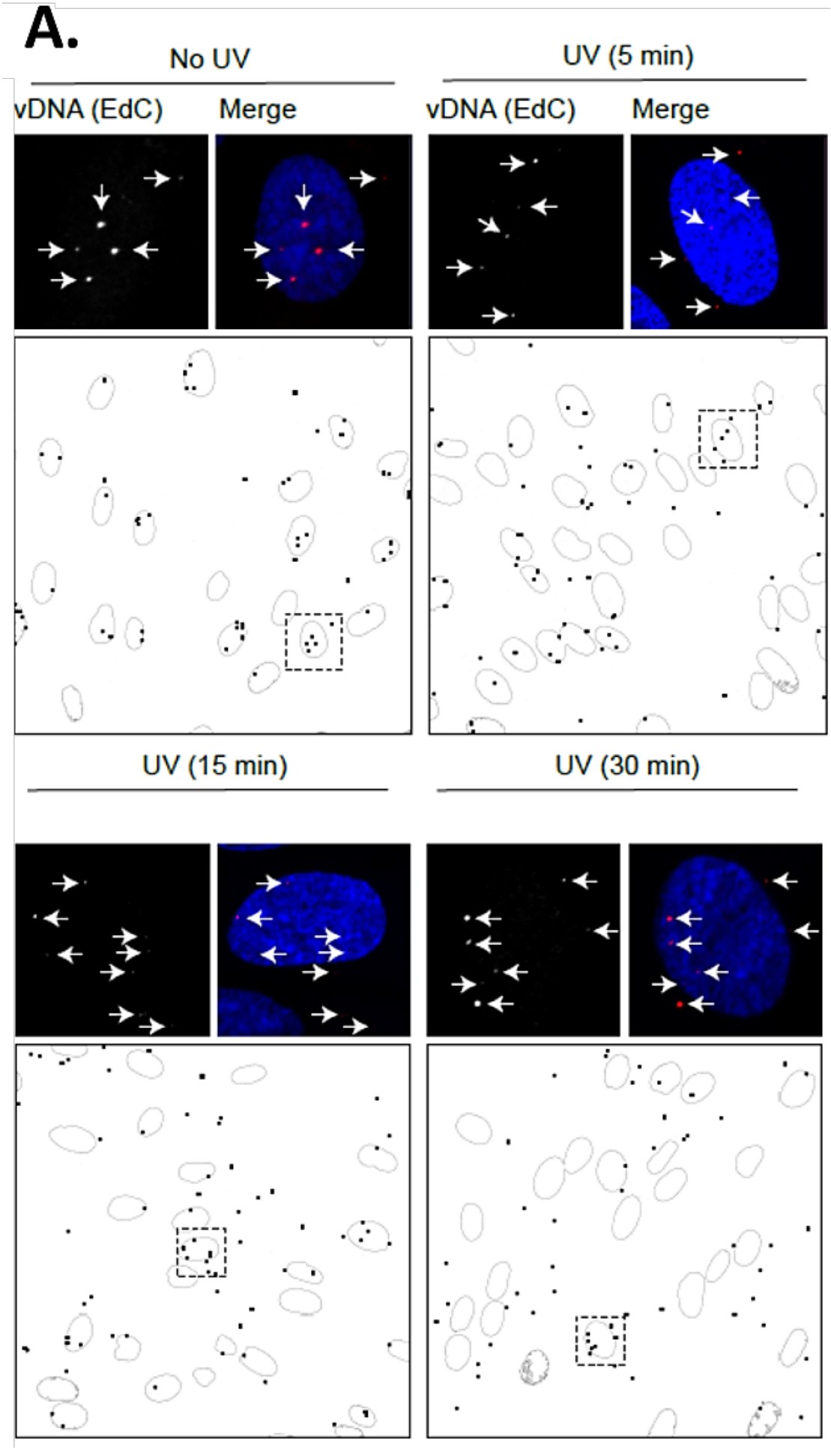
A.
No UV
UV (5 min)
vDNA (EdC)
Merge
vDNA (EdC)
Merge
UV (15 min)
UV (30 min)

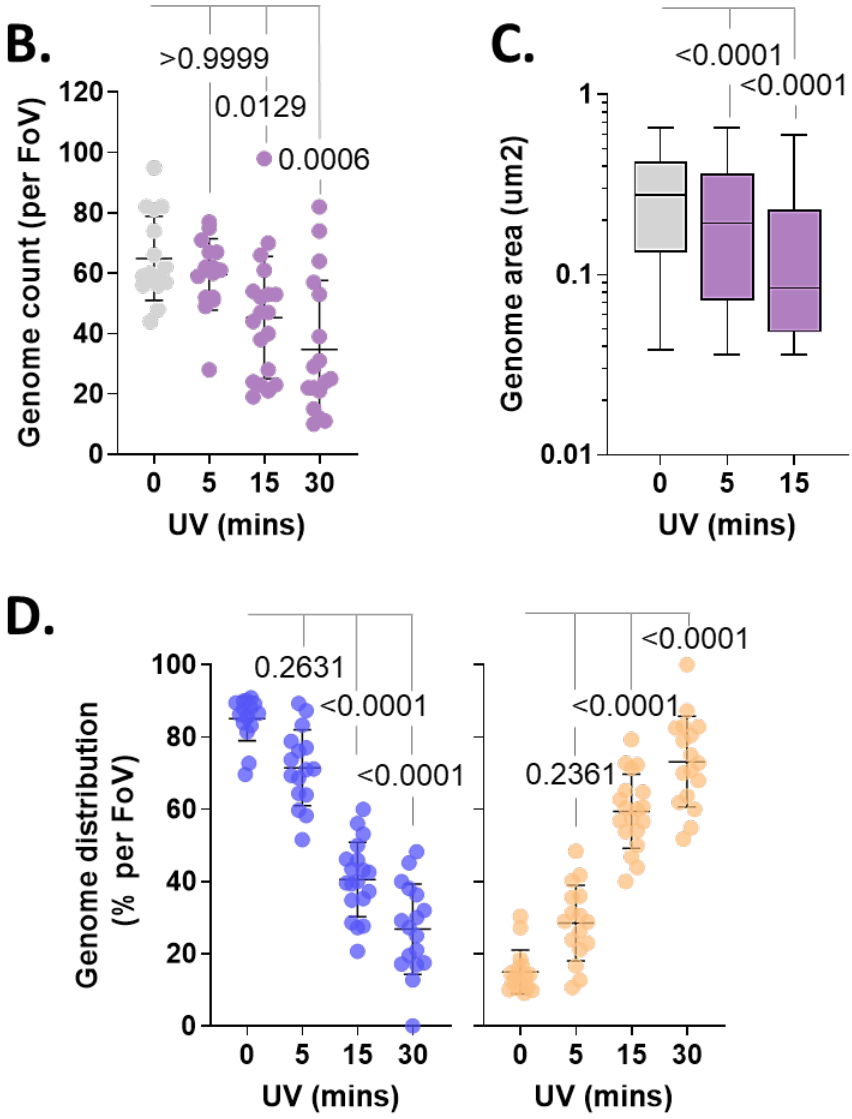

Figure 14. UV irradiation causes the premature uncoating of HSV-1 genomes in the cytosol. HFt cells were seeded overnight prior to infection with either non-UV or UV irradiated HSV-1^{EdC} (MSC UV irradiation as indicated) at an MOI of 3 PFU/cell. Cell monolayers were fixed and permeabilized at 90 mpi. Viral DNA was visualized with click chemistry. Nuclei were stained with DAPI stain (blue). (A) Representative confocal microscopy images showing premature uncoating of HSV-1 DNA upon UV irradiation. IF images were processed with ImageJ to show outlines. Area of interest indicated by dashed lines. Viral DNA highlighted by white arrows. (B) Number of genomes per FoV. Boxes: 25th to 75th percentile range; black line: median; whiskers: 5th to 95th percentile range. n=3 fields of view per condition derived from a minimum of 3 independent experiments conducted in duplicate. P>0.05 ns (not significant); P value shown; One-way ANOVA (Kruskal-Wallice). (C) Quantitation of the genome area (μm2). Boxes: 25th to 75th percentile range; black line: median; whiskers: 5th to 95th percentile range. n≥500 genome foci per condition derived from a minimum of 3 independent experiments conducted in duplicate. P value shown; One-way ANOVA (Kruskal-Wallis). (B) Quantitation of the genome distribution (nuclear or cytoplasmic) per FoV in percentage (%). Boxes: 25th to 75th percentile; black line: median; whiskers: 5th to 95th percentile. n=3 fields of view per condition derived from a minimum of 3 independent experiments conducted in duplicate. P>0.05 ns (not significant); P value shown; One-way ANOVA (Kruskal-Wallis).

4.2.4. The cellular proteasome does not play a role in the cytoplasmic release of UV irradiated HSV-1 genomes

The proteasome plays an important role in the turnover of cellular proteins by targeting Ubiquitin conjugated proteins for degradation. HSV-1 infection of macrophages has showed that the proteasome plays a role in targeting the viral capsids for degradation in the cytoplasm, leading to the release of vDNA (Horan et al., 2013). In turn, cytoplasmic genome release promoted detection by cellular PRRs (e.g., cGAS) and activation of innate immune signalling cascades and the establishment of an antiviral state (Sun et al., 2019). We investigated if the proteasome played a role in premature release of UV irradiated HSV-1 genomes. Cells were treated with the proteasome inhibitor MG132 (5μM) prior to infection with non-UV or UV irradiated HSV-1^{EdC} at an MOI of 3PFU/cell. Inhibition of the proteasome did not affect HSV-1 genome distribution, irrespective of UV irradiation (Figure 15A). Quantitation of the genome localization showed a consistent decrease in nuclear distribution and increase in cytosolic deposition of vDNA, consistent with previous data (Figure 15B). The efficacy of MG132 to block the 26s proteasome was checked by Western Blot for the presence of high molecular weight (HMW) ubiquitin (Ub) conjugates, which get degraded by the proteasome rapidly. The addition of MG132 resulted in the accumulation of HMW Ub conjugates, confirming the inhibition of the proteasome by the inhibitor (Figure 15C). Similar results were observed independently of UV irradiation (Figure 16). From this data we can conclude that the proteasome does not play a role in mediating the cytoplasmic deposition of HSV-1 genomes following UV irradiation.

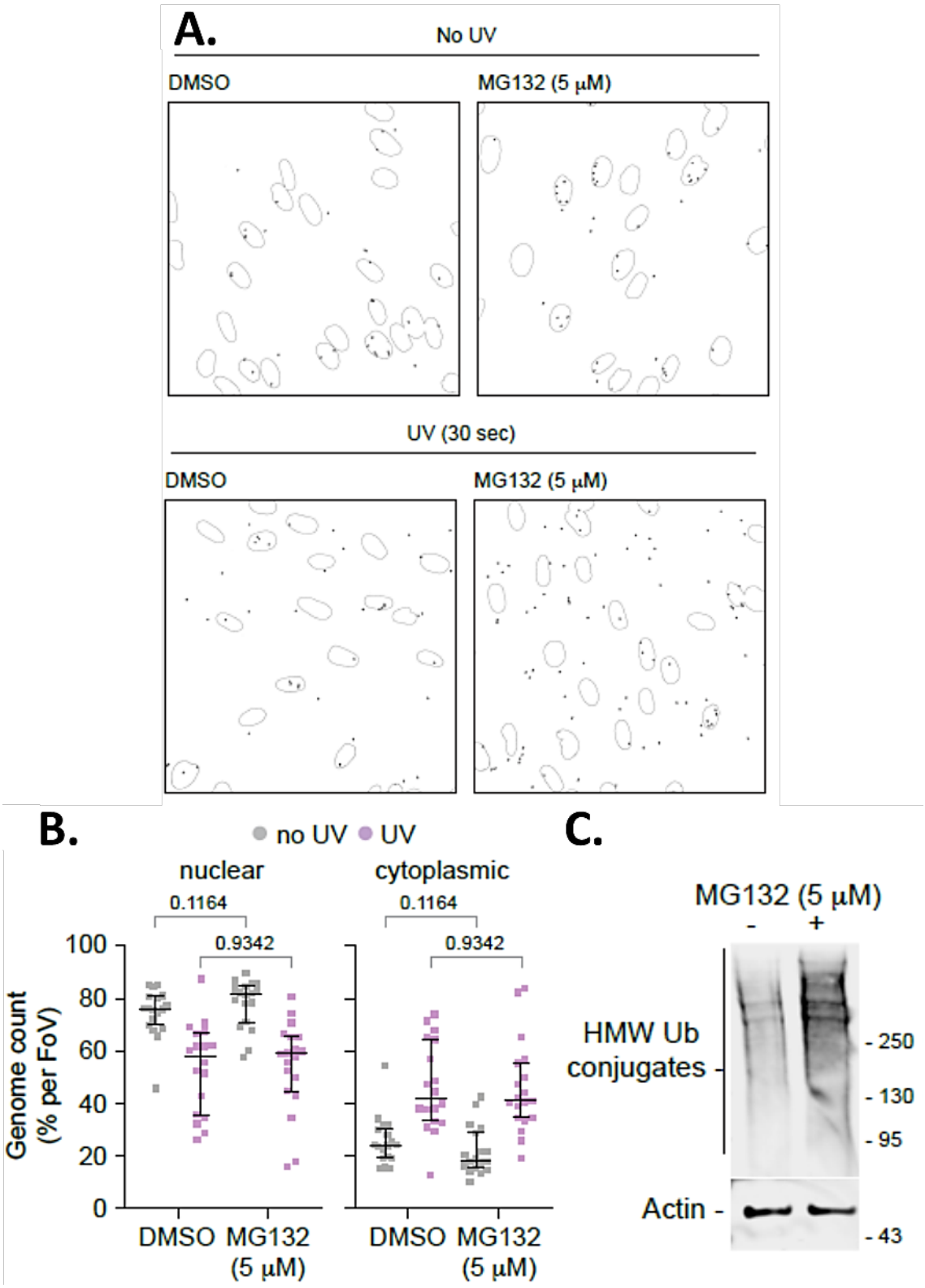

Figure 15. The cellular proteasome does not mediate the cytosolic deposition of UV irradiated HSV-1 genomes.

HFt cells were seeded overnight prior to treatment with DMSO or MG132 (5 μM). Cells were infected with either non-UV or UV irradiated HSV-1^{EdC} at an MOI of 3 PFU/cell. Cell monolayers were fixed and permeabilized at 90 mpi. Viral DNA was visualized with click chemistry. Nuclei were stained with DAPI (blue). (A) Representative confocal microscopy images showing premature uncoating of HSV-1 DNA upon UV irradiation in cells treated with DMSO or MG132. IF images were processed with

ImageJ to show outlines. (B) Quantitation of the genome distribution (nuclear or cytoplasmic) per FoV in percentage (%). Individual points shown; black line: median; whiskers: 5th to 95th percentile. n=3 fields of view per condition derived from a minimum of 3 independent experiments conducted in duplicate. P value shown; Mann-Whitney *U*-test. (C) Western blot analysis of whole cell lysates derived from HFt treated with DMSO or MG132 and probed for Ub conjugates and actin as loading control. Mass markers are shown.

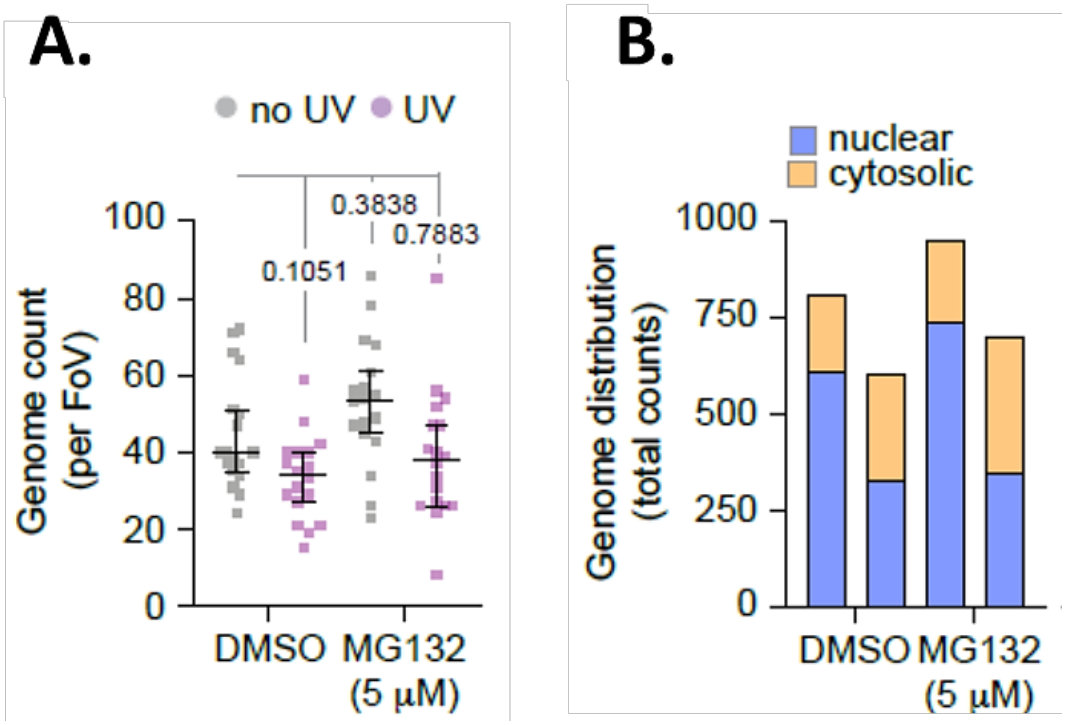

Figure 16. MG132 proteasome inhibitor does not affect genome distribution or detection.
HFt cells were seeded overnight prior to treatment with DMSO or MG132 (5 µM). Following this, cells were infected with either non-UV or UV irradiated HSV-1EdC at an MOI of 3 PFU/cell. Cell monolayers were fixed and permeabilized at 90 mpi. Viral DNA was visualized with click chemistry. Nuclei were stained with DAPI (blue). (A) Number of genomes per FoV. Boxes: 25th to 75th percentile range; black line: median; whiskers: 5th to 95th percentile range. n=3 fields of view per condition derived from a minimum of 3 independent experiments conducted in duplicate. P value shown; One-way ANOVA (Kruskal-Wallis). (B) Total genome distribution per FoV. n≥600 genome foci per condition derived from 3 independent experiments conducted in duplicate.

4.2.5. Disruption of the cellular microtubule network induces the cytosolic release of HSV-1 genomes

HSV-1 capsids utilize the cellular microtubule network to traverse the cytoplasm to reach the nucleus (Sodeik, Ebersold & Helenius, 1997). We hypothesized that UV irradiation may affect the stable attachment of capsids to microtubules. To test this hypothesis, a microtubule inhibitor was used to determine the involvement of the microtubule network to prevent the premature uncoating of HSV-1 genomes. HFt cells were pre-treated with increasing concentrations of nocodazole (inhibitor of microtubule polymerization) and infected with either non-UV irradiated HSV-1^{EdC} or UV irradiated HSV-1^{EdC} at an MOI of 3 PFU/cell (Figure 17A). DMSO treated cells were used as controls. The number of cytosolic genomes increased in a nocodazole concentration-dependent manner irrespective of UV irradiation, doubling at 10 μM nocodazole when compared to the control (Figure 17B and C). A significant reduction in nuclear and increase in cytoplasmic HSV-1 genomes to comparable levels was observed in cells pre-treated with nocodazole, irrespective of UV irradiation when compared to the DMSO control. (Figure 18). These data provide some evidence that the microtubule network may play a role in mediating the cytoplasmic deposition of vDNA following UV irradiation. However, the exact mechanism as to how these capsids fall off or fail to stably associate with the microtubules remains to be determined.

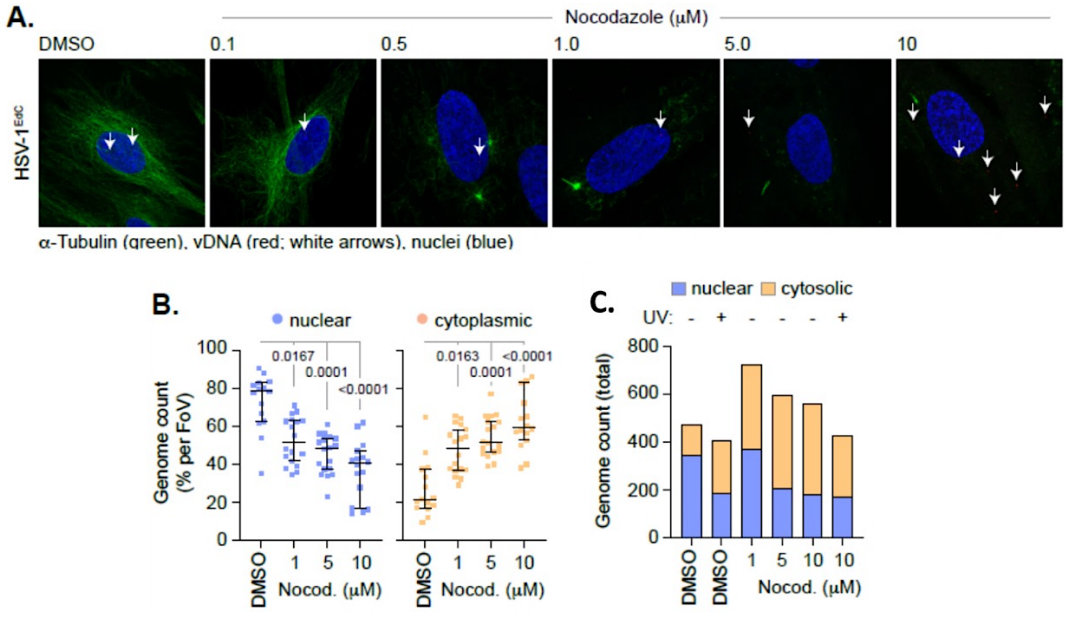

Figure 17. Cellular microtubule network stabilises HSV-1 capsids from prematurely releasing viral genomes.

HFt cells were seeded overnight prior to treatment with DMSO or increasing concentrations of Nocodazole (μM). Cells were infected with either non-UV or UV irradiated HSV-1^{EdC} at an MOI of 3 PFU/cell. Cell monolayers were fixed and permeabilized at 90 mpi. Viral DNA was visualized with click chemistry. Nuclei and microtubules were stained with DAPI (blue) and α-tubulin (green), respectively. (A) Representative IF images of HSV-1^{EdC} infected HFt cells treated with DMSO or Nocodazole. Viral DNA localization highlighted with white arrows. (B) Quantitation of the genome distribution (nuclear or cytoplasmic) per FoV in percentage (%). Boxes: 25th to 75th percentile; black line: median; whiskers: 5th to 95th percentile. n=3 FoV per condition derived from a minimum of 3 independent experiments conducted in duplicate. P value shown; One-way ANOVA (Kruskal-Wallis). (B) Total genome distribution per field of view. n≥400 genome foci per condition derived from 3 independent experiments conducted in duplicate.

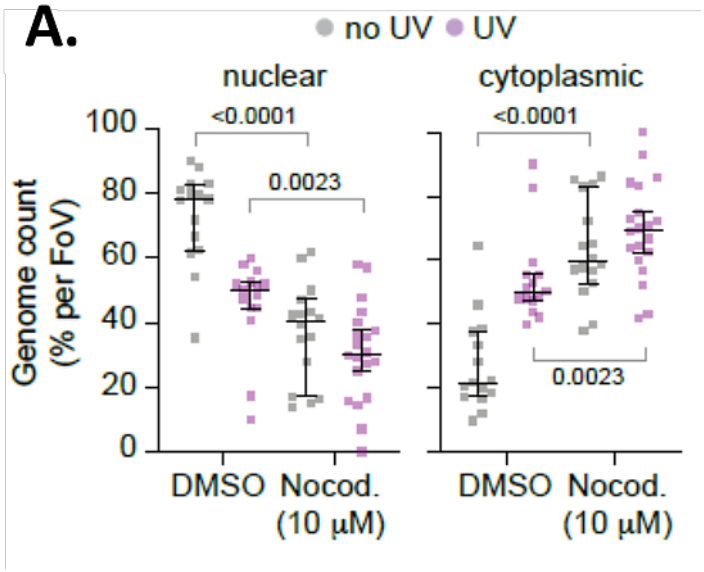

Figure 18. Microtubule depolymerisation induces the cytoplasmic release of HSV-1 DNA irrespective of UV irradiation.

HFt cells were seeded overnight prior to treatment with DMSO control or Nocodazole (10 μM). Following this, cells were infected with either non-UV or UV irradiated HSV-1^{EdC} at an MOI of 3 PFU/cell. Cell monolayers were fixed and permeabilized at 90 mpi. Viral DNA was visualized with click chemistry. Nuclei were stained with DAPI stain (blue). Quantitation of percentage vDNA localization per FoV. Individual values plotted; median with SD shown. n=3 fields of view per condition derived from a minimum of 3 independent experiments conducted in duplicate. P value shwon; Mann-Whitney *U*-test.

4.3. Summary

UV irradiation is a method routinely utilized for HSV-1 inactivation since the late 1960s. UV irradiation has been shown to affect nuclear capsid transport, thus delaying viral transcription and reducing titres; although the exact mechanism was unknown (Rabson, Tyrrell & Legallais, 1969; Fridlender et al., 1978; Eglin, Gugerli & Wildy, 1980). Lately, studies identified UV irradiation to induce the accumulation of pyrimidine dimers, as UV light leads to the induction of DNA damage of intrastrand bases (Ross, Cameron & Wildy, 1972; Miyamoto' And & Morgan, 1971; Eglin, Gugerli & Wildy, 1980; Fridlender et al., 1978; Goodsell, 2001; Rastogi et al., 2010). The use of UV irradiated virus has been utilized in countless studies investigating the immune responses to HSV-1. However, it remains unclear where UV irradiated genomes localize during infection due to the limitations of DNA detection. Utilizing a previously reported protocol for click labelling of HSV-1 DNA provided a non-invasive assay to investigate the localization of UV irradiated HSV-1 genomes under low MOI conditions (Figure 6) (Alandijany et al., 2018).

UV irradiated virus is able to penetrate the cell as efficiently as non-irradiated viruses (Ross, Cameron & Wildy, 1972). Electron microscopy of UV irradiated HSV-1 showed the accumulation of DNA filled viral capsids in the cytoplasm following entry into cells (Miyamoto' And & Morgan, 1971), although the resultant difference in capsid uncoating could not be sufficient to explain the delay in replication (Rabson, Tyrrell & Legallais, 1969; Fridlender et al., 1978; Eglin, Gugerli & Wildy, 1980). The microscopy observations in this study showed for the first time the genome distribution of HSV-1 following UV irradiation (Figures 12 and 14). UV irradiation of HSV-1 inhibits plaque formation and initiation of replication as no viral proteins could be observed even after 24h of infection (Figures 7, 8 and 9) (Ross, Cameron & Wildy, 1972; Eglin, Gugerli & Wildy, 1980; Fridlender et al., 1978). UV irradiated HSV-1 genomes were prematurely released into the cytosol in a UV-dose dependent and UV source-independent manner (Figures 12 and

14). This observation falls in line with EM data, showing an increase in cytosolic viral core-containing capsids following UV irradiation (Miyamoto' And & Morgan, 1971). The increased number of viral genomes deposited in the cytosol could account for the decrease in protein production and initiation of replication (Eglin, Gugerli & Wildy, 1980; Ross, Cameron & Wildy, 1972). A small proportion of UV irradiated HSV-1 genomes reach the nucleus, but were insufficient to establish infection, potentially due to the accumulation of DNA damage on the viral genome (Eglin, Gugerli & Wildy, 1980). The number of detectable genomes was observed to decrease in a UV-dose dependent manner (Figure 12 and 14), consistent with previous studies that have reported a similar decrease in detectable viral capsids following UV irradiation (Miyamoto' And & Morgan, 1971; Eglin, Gugerli & Wildy, 1980). Additionally, as bio-orthogonal nucleic acid labelling requires for the alkyne group to be accessible for the fluorophore-bound azide molecule to bind, it cannot be disregarded that the interaction could be disrupted by the crosslinking effect of UV light resulting in the reduced number of detectable genomes within infected cells (Figure 14). Nevertheless, the proportion of nuclear:cytosolic genome localization falls within the model of disruption of initiation of viral infection happening at a pre-replication step (Ross, Cameron & Wildy, 1972; Fridlender et al., 1978). UV irradiated HSV-1 also initiated a stronger type I IFN immune response when compared to WT infection (Figure 10) (Taylor & O'brien, 1985; Hendricks et al., 1991; Eloranta, Sandberg & Alm, 1996). Studies in macrophages have showed that the proteasome plays a role in the ubiquitin-mediated degradation of the cytoplasmic capsids, releasing the viral DNA and initiating the IFN immune response via cellular PRRs, such as IFI16, cGAS and DDX41 (Horan et al., 2013; Sun et al., 2019). This would represent an attractive model, where UV irradiation increases the cytoplasmic release of viral DNA via the targeted ubiquitination of HSV-1 capsids that in turn increases the cellular PRR DNA sensing signalling to initiate an IFN immune response. Contrary to macrophages, our data in fibroblasts showed the proteasome not to play a role in degrading cytoplasmic capsids, as chemical inhibition of the proteasome did not have an effect on the levels of detectable cytosolic HSV-1 DNA, irrespective of UV irradiation (Figures 15 and 16). The difference in mechanism could be due to the variation of the levels of the

26s proteasome expression, as myeloid cells express the 26s proteasome genes to higher levels than fibroblasts (Human Protein Atlas). Following entry into the cell, HSV-1 capsids exploit the microtubule network to traverse the cytoplasm and reach the nucleus (Sodeik, Ebersold & Helenius, 1997). Microtubule disruption has been shown to reduce capsid transport leading to lower viral titres (Kristensson et al., 1986; Sodeik, Ebersold & Helenius, 1997). Consistent with these reports, nocodazole pre-treatment of cells significantly increased the number of cytoplasmic genomes independently of UV irradiation (Figures 17 and 18). Although this provides evidence for the involvement of the microtubule network in the stabilisation of HSV-1 capsids, the exact mechanism remains unknown and warrants further investigation. Certainly, one possibility is the disassociation of UV irradiated HSV-1 capsids during transport via the microtubule network, indicative of the changes in the capsid protein interactions involved in mediating this transport, such as UL34 and VP26, following UV irradiation (Reynolds et al., 2002; Döhner, Nagel & Sodeik, 2005).

In summary, the data presented in this chapter reveals direct evidence demonstrating UV irradiation of HSV-1 virions to induce the premature uncoating of HSV-1 DNA during cytosolic transport. This in turn results in the activation of the type I IFN response. Nevertheless, there is a small population of UV irradiated HSV-1 genomes that reach the nucleus that are unable to initiate infection.

5. Nuclear immune regulators are differentially recruited to HSV-1 genomes following UV irradiation

5.1 Overview

Intrinsic immunity is one of the first lines of cellular defence in response to infection. This arm of immunity is mediated by constitutively expressed restriction factors that act immediately and directly to limit infection. One of the most well studied intrinsic immune responses to HSV-1 infection relates to component proteins that reside within PML-NBs (Scherer & Stamminger, 2016; Tavalai & Stamminger, 2009). During HSV-1 infection, core PML-NB components, such as PML, Sp100 and Daxx, are rapidly recruited to infecting genomes within minutes of nuclear infection. Once localized to vDNA, these restriction factors entrap HSV-1 genomes and repress the initiation of viral transcription (Everett & Murray, 2005; Everett et al., 2006; Glass & Everett, 2013; Alandijany et al., 2018). This interaction during WT HSV-1 infection is transient, as the expression of the viral ICP0 protein leads to the ubiquitin-mediated proteasomal degradation of PML, resulting in the dispersal of other core PML-NB constituent proteins that colocalize with vDNA (Everett & Murray, 2005; Vanni et al., 2012; Boutell, Sadis & Everett, 2002; Komatsu, Nagata & Wodrich, 2016; Glass & Everett, 2013).

In the previous chapter UV irradiation led to a switch in the subcellular localization of HSV-1 genomes from the nucleus to the cytoplasm. We concluded that UV irradiation induces the premature uncoating of HSV-1 viral capsids in a UV dose-dependent manner. However, a small population of UV irradiated genomes were observed to reach the nucleus. In this chapter, we investigated the recruitment of core PML-NB constituent proteins to non-UV and UV irradiated HSV-1 genomes. Our data show UV irradiation of HSV-1 impairs the recruitment of PML-NB component proteins to vDNA independent of the UV light source. These data suggest that UV irradiation of vDNA directly influences the recruitment of nuclear

restriction factors to HSV-1 genomes. For comparison, we examined the recruitment of the nuclear PRR IFI16. We show IFI16 to not stably localize to HSV-1 DNA irrespective of UV irradiation. Utilizing ChIP, we show UV irradiation of HSV-1 DNA led to a decrease in the interaction of PML with vDNA. We observed an increase in thymine dimer formation within vDNA that restricted genome decompacting upon release from the viral capsid. This change in the structure of the DNA could account for reduced recognition and binding of PML to vDNA. These findings suggest that changes to vDNA structure induced by UV irradiation directly influence the ability of multiple nuclear restriction factors to localize to vDNA upon nuclear infection.

5.2. Results

5.2.1. UV irradiation of HSV-1 virions impairs the recruitment of PML-NB host factors to vDNA within the nucleus

The use of EdC-labelled input genomes and indirect immunolabelling has allowed for to detailed investigation into the recruitment of different host restriction factors and PRRs to infecting vDNA at early timepoints of infection (≤90 mpi). Utilizing Zen software to measure the weighted (w.) colocalization coefficient between cellular proteins of interest and vDNA, enabling accurate quantitation (Alandijany et al., 2018). The values range from 0 (no colocalization) to 1 (perfect colocalization).

HFt cell monolayers were infected under the same conditions as described in Chapter 1. CLICK chemistry and indirect IF staining were utilized to visualize vDNA and the colocalization of PML-NB proteins PML, Daxx and Sp100 to nuclear infecting genomes (Figure 19A). Consistent with previous reports (Alandijany et al., 2018), Sp100 and Daxx colocalized with PML (w. colocalization coefficient >0.7) in mock infected cells (Figure 19A). In both non-UV and UV irradiated HSV-1^{EdC} infected cells, Sp100 and Daxx retained a high degree of colocalization to PML (w. colocalization coefficient >0.7), comparable to that observed in mock infected cells (Figure 19A). In contrast, all three proteins exhibited reduced recruitment to UV irradiated vDNA (Figure 19A). These microscopy observations were confirmed by quantitative analysis (Figure 19C). The stability of the PML-NBs during infection was unaffected, demonstrating the decrease in localization to vDNA was due to UV irradiation of the viral genome as opposed to a cellular response to the detection of DNA damage (Figure 19D). Collectively these data showed that UV irradiation of HSV-1 DNA affects the ability of PML-NBs to recognize nuclear infecting HSV-1 genomes that results in the significantly lower levels of recruitment of core PML-NB constituent proteins to vDNA.

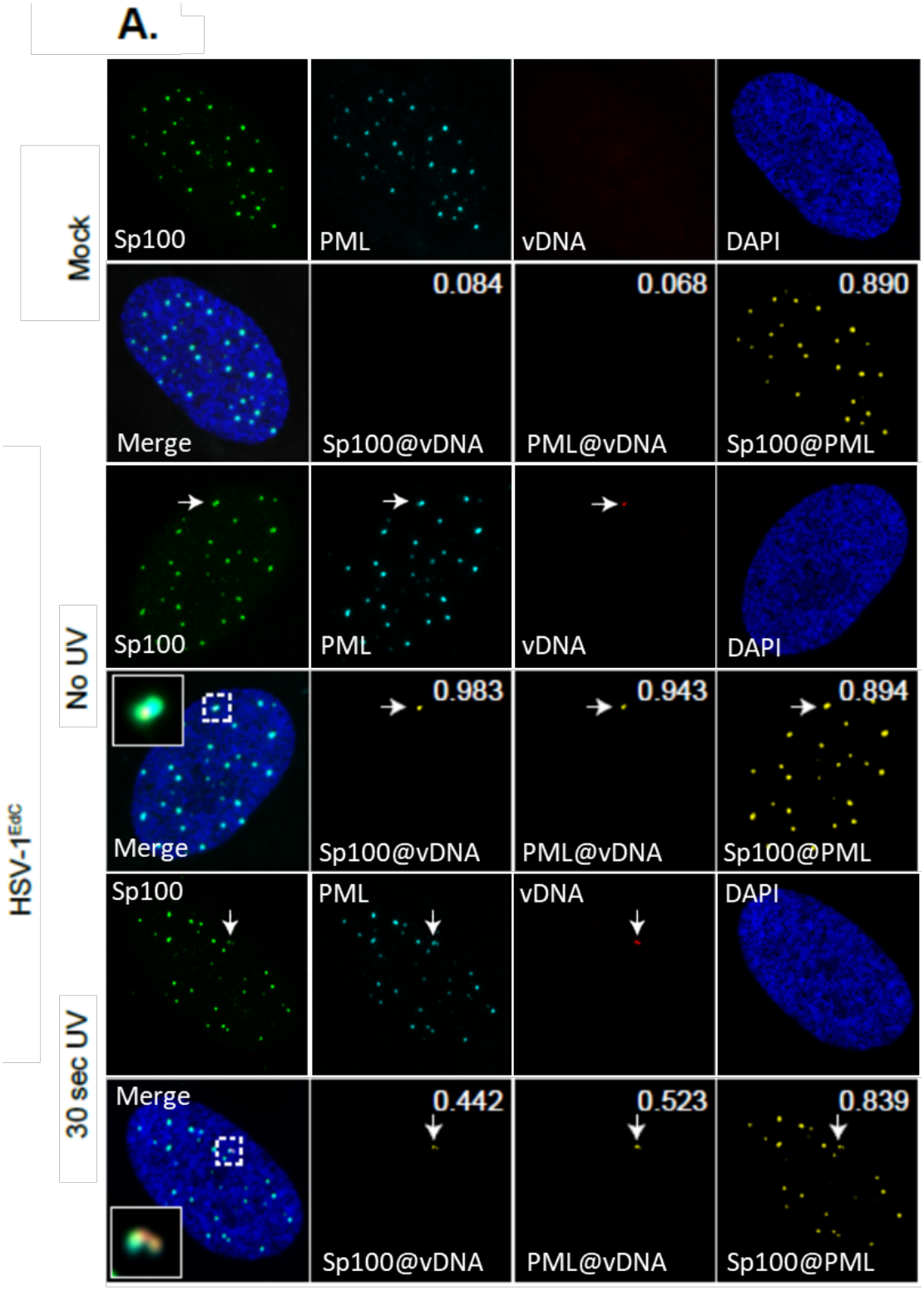
A.
Mock
HSV-1EdC
No UV
30 sec UV
Sp100
PML
vDNA
DAPI
Merge
Sp100@vDNA
PML@vDNA
Sp100@PML
0.084
0.068
0.890
0.983
0.943
0.894
0.442
0.523
0.839

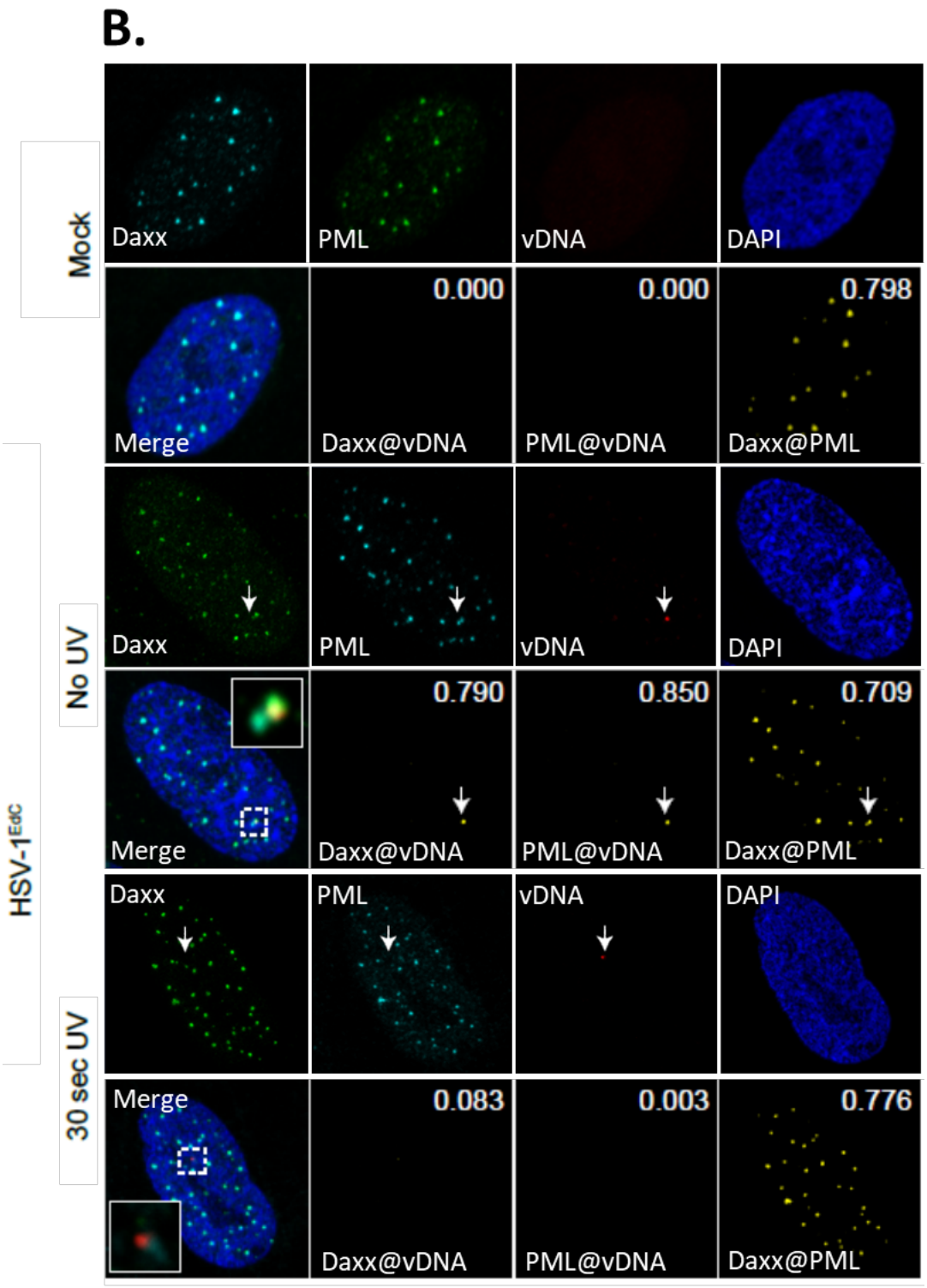

C. and D. NEXT PAGE

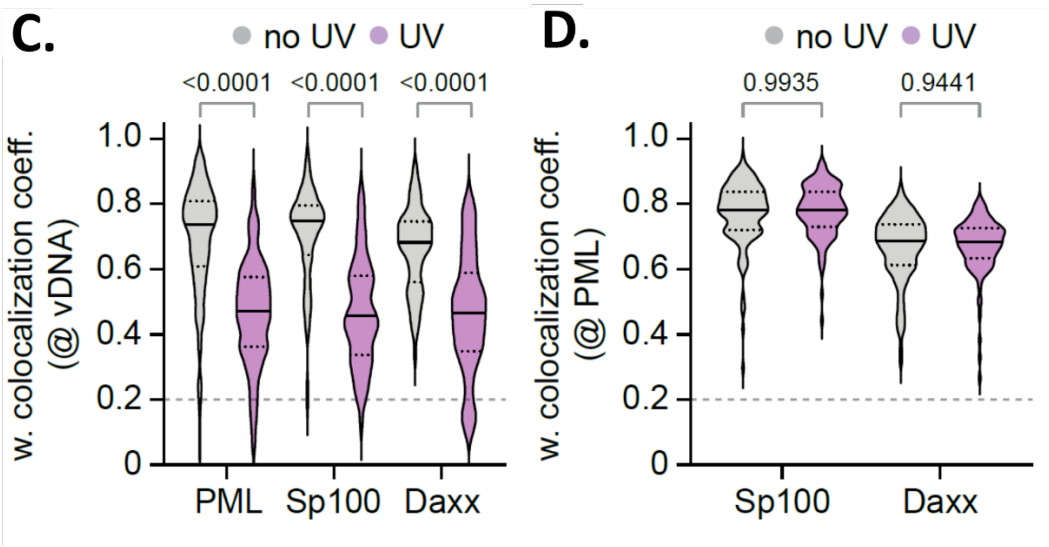

Figure 19. UV irradiation of HSV-1^{EdC} impairs the recruitment of PML-NB constituent proteins to infecting viral genomes.

HFt cells were mock infected or infected with ≤3 PFU/cell of non-UV or UV irradiated HSV-1. Cells were fixed and permeabilized at 90 mpi. Labelled viral DNA was detected by CLICK chemistry. Sp100, Daxx, and PML were detected by indirect immunofluorescence. Nuclei were stained with DAPI. (A and B) Localization of Sp100 or Daxx (green) and PML (cyan) to nuclear infecting viral genomes (red). White boxes show regions of interest. Cut mask (yellow) highlights colocalization between cellular proteins of interest and vDNA or proteins of interest themselves. W. colocalization coefficients shown. (C) Quantitation of protein recruitment to infecting vDNA or (D) Sp100/Daxx colocalization with PML at 90 mpi. Black line: median weighted (w.) colocalization coefficient; dashed lines: 95% CI shown. n>100 nuclei per sample population derived from a minimum of three independent repeats. P value shown; Mann-Whitney *U*-test.

In order to determine if this phenotype was attributable to the source of UV irradiation, the analysis was repeated using MSC shortwave UV irradiated HSV-1. Quantitation demonstrated a similar decrease in the recruitment of PML, Daxx and Sp100 to vDNA in a UV-dose dependent manner (Figure 20A). Notably, an increase in w. colocalization coefficient of the core PML-NB proteins and vDNA (5 min) could be observed (Figure 20B). This could be due to a difference in the efficiency of the virus infection in this set of experiments. Sp100 and Daxx localization to PML was also unaffected by the presence of either virus, demonstrating that the introduction of damaged vDNA into the nucleus to not significantly influence the localization of PML-NB constituent proteins to PML itself (Figure 20B). We concluded that UV irradiation of HSV-1 DNA, impairs the recruitment of PML-NB proteins to nuclear infecting viral genomes.

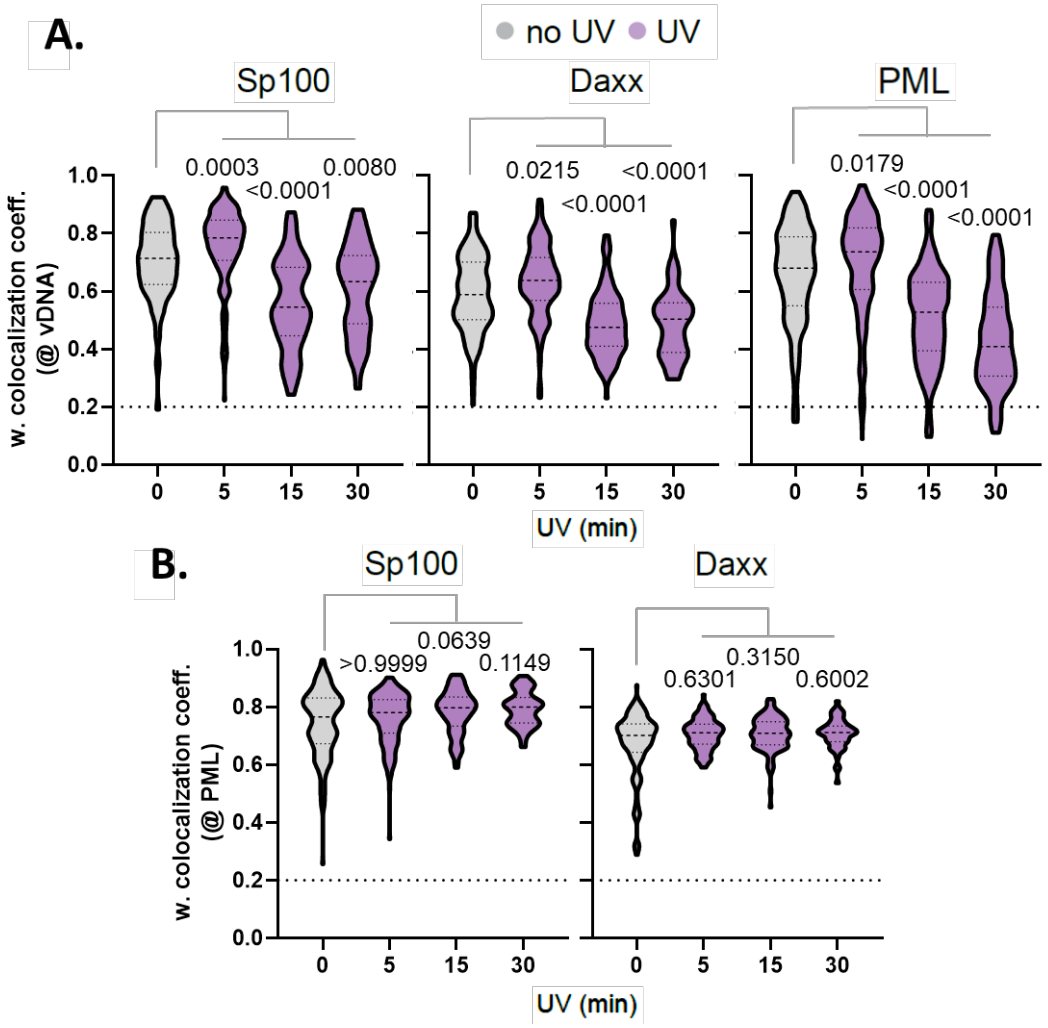

Figure 20. MSC (shortwave) UV irradiation of HSV-1^{EdC} impairs the recruitment of PML-NB constituent proteins to infecting viral genomes.

HFt cells were mock infected or infected with 3 PFU/cell of non-UV or UV HSV-1^{EdC}. Cells were fixed and permeabilized at 90 mpi. Labelled viral DNA was detected using click chemistry. Sp100, Daxx and PML were detected by indirect immunofluorescence. Nuclei were stained with DAPI. (A) Quantitation of cellular protein recruitment to vDNA or (B) Sp100 or Daxx colocalization with PML. Violin plots. Black line: median weighted (w.) colocalization coefficient; dashed lines: 95% CI. n>80 nuclei per sample population derived from a minimum of three independent repeats. P value shown; Mann-Whitney *U*-test.

5.2.2. Cellular PRR IFI16 does not stably localize to vDNA irrespective of UV irradiation

IFI16 has been reported to act as a DNA sensor that interacts with ssDNA and dsDNA (Morrone et al., 2013; Jønsson et al., 2017). The cytoplasmic-nuclear shuttling of this protein allows for the activation of different antiviral mechanisms, including the STING/IRF3 axis of the type I IFN pathway, nuclear inflammasome activation, and chromatin repression of viral genomes (Unterholzner et al., 2010; Jakobse et al., 2013; Kerur et al., 2011; Johnson et al., 2014; Orzalli, DeLuca & Knipe, 2012). However, most of these studies were carried out using indirect methods of vDNA detection. Recent studies using click chemistry to detect viral genomes have shown that productive infection was required to induce an IFI16-dependent IFN response (Alandijany et al., 2018). Herein we investigated the recruitment profile of IFI16 to both cytoplasmic and nuclear genomes to investigate its role in the IFN response to HSV-1 infection upon UV irradiation. In line with previous evidence (Alandijany et al., 2018), no recruitment of IFI16 to vDNA was observed at 90 mpi irrespective of UV irradiation, where IFI16 nuclear distribution remained largely diffuse (Figure 21A). Quantitative analysis confirmed the lack of recruitment of IFI16 to viral genomes localized in the cytoplasm or nucleus (Figure 21B). PML localisation was used as a positive control and displayed comparable levels to previous data (Figure 21B). IFI16 has been reported to be degraded by ICP0 (Orzalli, DeLuca & Knipe, 2012). However, UV irradiated HSV-1^{EdC} inhibit the expression of viral IE proteins (Figure 8 and 9) excluding any effect of ICP0 on its recruitment to vDNA. Given previous studies demonstrating the need for active viral replication for the activation of IFI16, the lack of recruitment of IFI16 to HSV-1 DNA is consistent with previous studies (Alandijany et al., 2018). However, our data demonstrates the UV irradiation of HSV-1 genomes does not promote a DNA replication independent mechanism of IFI16 recruitment to damaged DNA. Notably, we cannot rule out potentially transient interactions due to the fixed timepoints of analysis. Collectively, we concluded that IFI16 was

not stably recruited to HSV-1 DNA upon UV irradiation and is unlikely to mediate innate immune response to UV irradiated HSV-1.

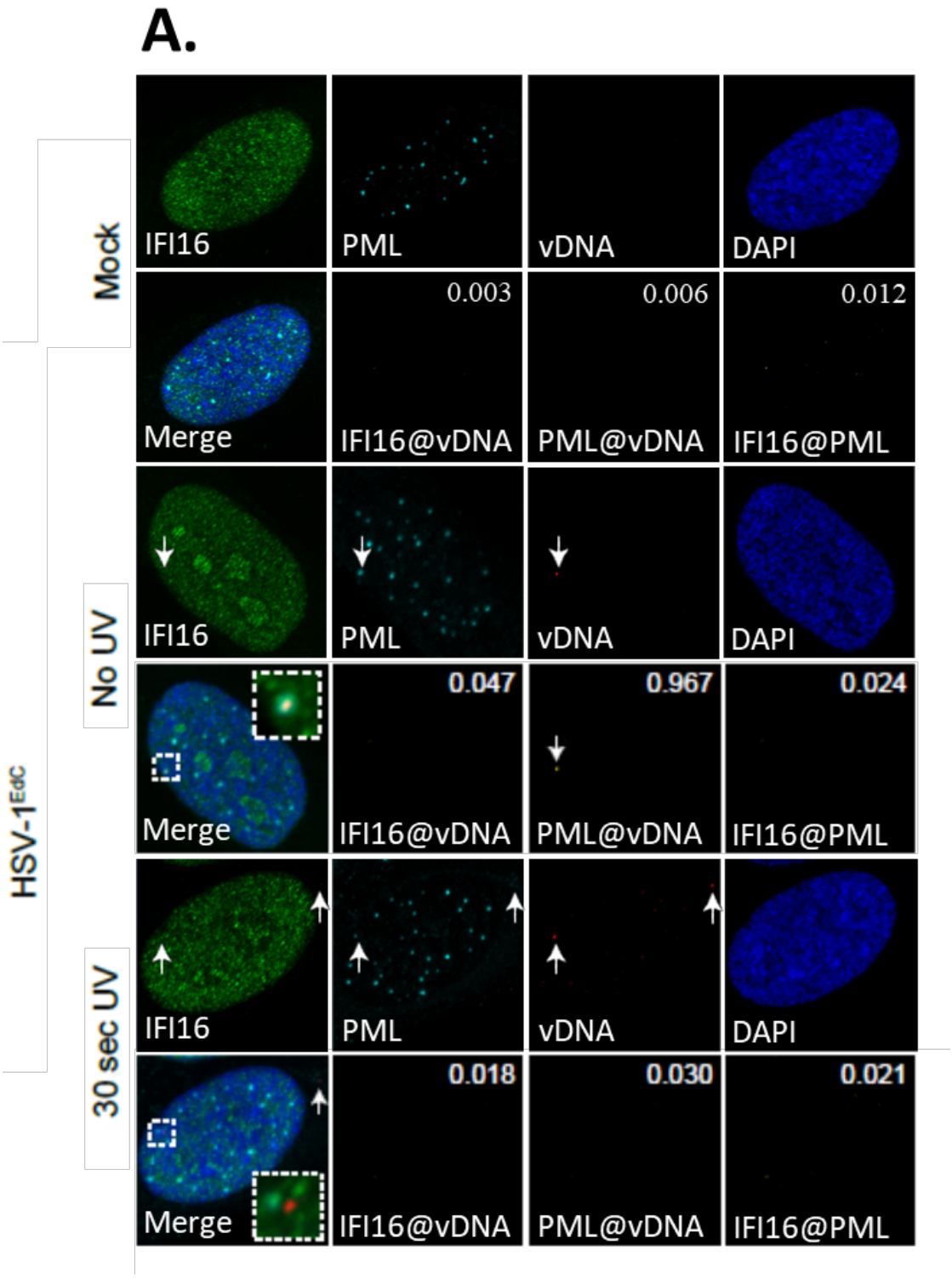

B. CONTINED ON NEXT PAGE.

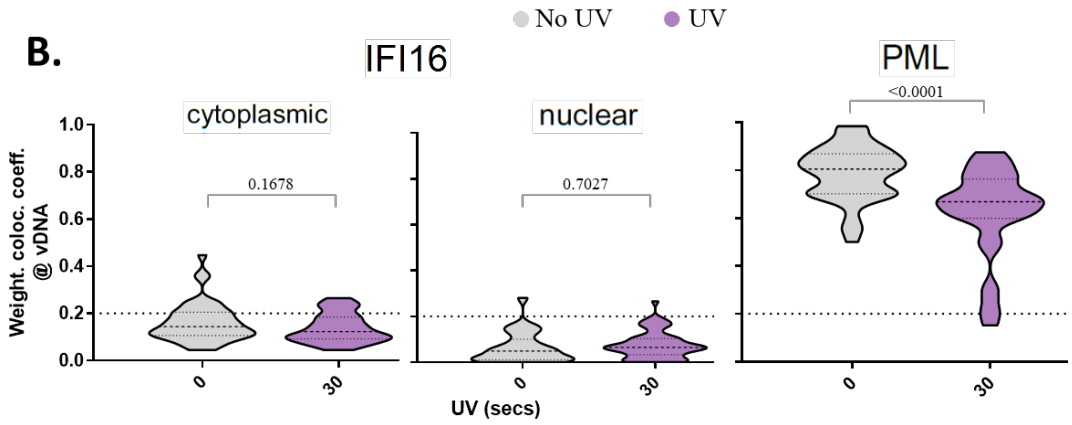

Figure 21. IFI16 does not stably localize to infecting HSV-1^{EdC} genomes irrespective of UV irradiation.

HFt cells were mock infected or infected with 3 PFU/cell of non-UV or UV irradiated HSV-1. Cells were fixed and permeabilized at 90 mpi. Labelled vDNA (red) was detected by click chemistry. IFI16 and PML were detected via indirect immunofluorescence. Nuclei were stained with DAPI. (A) Localization of sub-nuclear recruitment of IFI16 (green) and PML (cyan) to infecting viral genomes (red). White boxes show zoomed areas of interest. Cut mask (yellow) highlights the regions of colocalization between the cellular proteins of interest and non-UV or UV irradiated HSV-1 genomes. White arrows used to indicate vDNA foci. Weighted colocalization coefficient shown. (B) Quantitation of cellular IFI16 or PML recruitment to infecting HSV-1 vDNA in either the cytosol or the nucleus. Violin plots. Black line: median weighted (w.) colocalization coefficient; dashed lines: 95% CI. n>50 nuclei per sample population derived from a minimum of three independent repeats. P value shown; Mann-Whitney *U*-test.

5.2.3. UV irradiation of HSV-1 reduces the PML interaction with vDNA

PML is the major scaffolding protein of PML-NBs and plays an important role in the initial suppression of HSV-1 replication. The exact mechanism of PML recognition of vDNA is still unknown, which may occur directly through interaction with vDNA or indirectly through other PML-NB associated proteins. As the previous results demonstrated a reduction in the level of PML recruitment to UV irradiated HSV-1 DNA, we investigated if PML directly interacted with vDNA by ChIP.

To robustly detect PML interaction with vDNA, a SPOT tag, which is a 12-amino acid peptide tag that is readily recognised by a single domain antibody (nanobody), was inserted to flag the PML gene (Virant et al., 2018). HFt cells expressing doxycyclin inducible SPOT-tagged PML (SPOT PML) were kindly generated by Steven McFarlane. SPOT PML protein was only detectable following a 6hr induction with doxycycline (Dox) and not expressed in untreated cells (Figure 22C). The addition of the SPOT tag did not affect the localization of PML to PML-NBs within the nucleus of cells (Figure 22A). Quantitative analysis showed that SPOT PML was detected at PML-NBs (w. colocalization coefficient ≥0.9) (Figure 22B). These cells were then used in a series of ChIP-qPCR experiments that utilize high affinity SPOT nanobody coupled to magnetic beads to examine if PML interacted directly with vDNA (Figure 23). SPOT PML HFts were pre-treated with Dox for 6hr prior to infection with non-UV or UV irradiated HSV-1 at an MOI of 3 PFU/cell for 90 mins. The ChIP was performed with the total SPOT PML and IgG (negative control) in parallel. qPCR analysis was carried out using two independent probes to detect Us3 and UL36. These genes were selected to identify close to complete genomes as the loci are located in the centre and 3' end of the genome, respectfully. The input of non-UV or UV irradiated HSV-1 was equivalent, as shown by the ΔCT value for both viral genes examined (Figure 23A). The fraction of non-UV irradiated HSV-1 DNA associated with SPOT PML was consistent and significantly above IgG background. UV irradiation of the HSV-1 DNA resulted in a significant decrease of the fraction of viral genomes associated with SPOT PML,

although those interactions were still above IgG background (Figure 23B). Cells not treated with Dox or not crosslinked were utilized as additional negative controls (Figure 23C). From this data we concluded that PML interacts directly with HSV-1 genomes upon nuclear entry, and that this interaction is negatively affected by UV irradiation of the vDNA. These data are consistent with our microscopy observations (Figure 19 and 20), which show UV irradiation to reduce the colocalization of PML with vDNA. The specific mechanism by which UV irradiation inhibits PML interaction with vDNA requires further investigation. However, we identify for the first time PML to directly interact with vDNA upon nuclear infection.

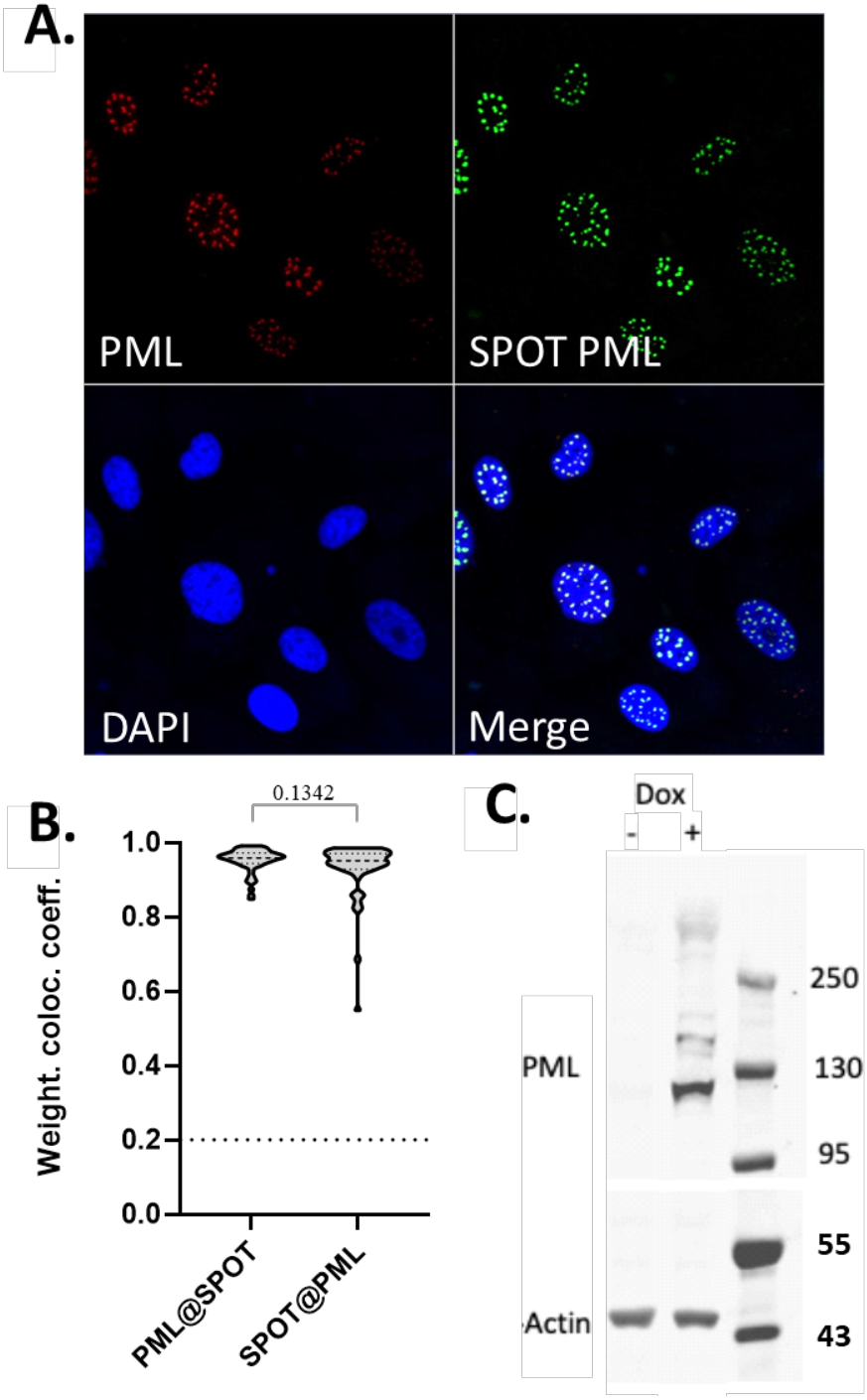

Figure 22. SPOT-tagged PML localizes to PML-NBs.

SPOT PML HFts were seeded overnight prior to a doxycycline induction for 6hr. PML and SPOT PML were detected by indirect immunofluorescence. Nuclei were visualized by DAPI staining. (A) Representative confocal image of sub-nuclear localization of endogenous (red) and SPOT (green) PML. (B) Quantitation analysis of recruitment of endogenous and SPOT PML to each other. Violin plots. Black line: median weighted (w.) colocalization coefficient; dashed lines: SD. n>70 nuclei per sample population derived from a minimum of three independent repeats. P value shown; Mann-Whitney *U*-test. (C) Western blot showing the levels of SPOT PML and actin (as a loading control) in whole cell lysates derived from SPOT PML HFt cells that have (+) or have not been (-) pre-treated for 6 hours with doxycycline (Dox). Membranes were probed for SPOT tag using a SPOT nanobody.

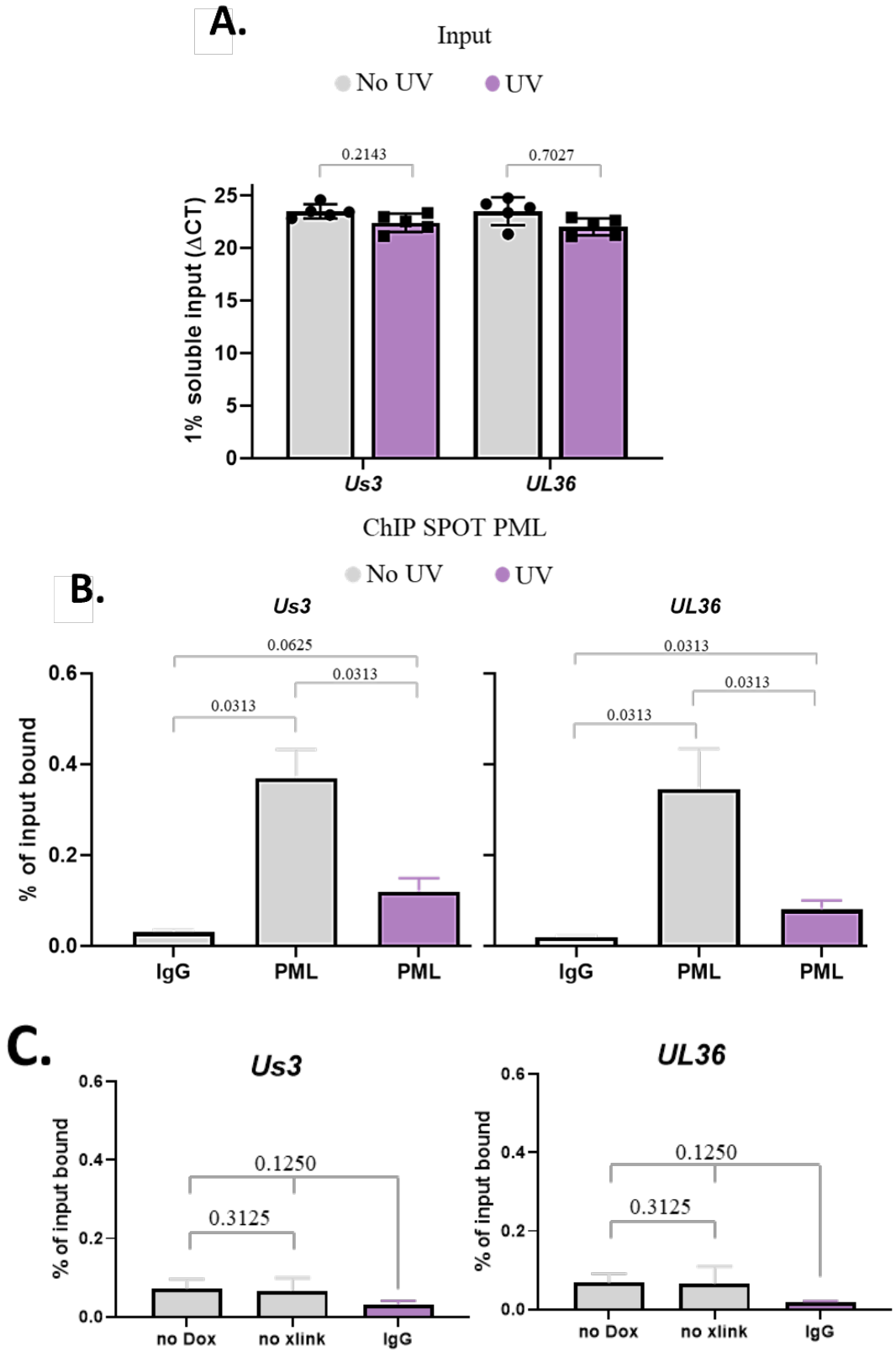

Figure 23. UV irradiation of HSV-1 decreases the PML interaction with vDNA.

SPOT PML HFts were seeded overnight prior to a doxycycline induction for 6 hr followed by infection with either non-UV or UV irradiated HSV-1 at an MOI of ≤3 PFU/cell. Cells were UV crosslinked at 90 mpi and chromatin extracted. Immunoprecipitation was carried out using SPOT and IgG antibodies. Relative levels of HSV-1 DNA bound to immunoprecipitated proteins was measured by qPCR using Us3 and UL36 specific primers. (A) Bar graphs showing the ΔCT value of the input chromatin extracts

from HFt cells infected with non-UV or UV irradiated HSV-1. Individual points shown, black lines: mean. Data was pooled from 5 independent repeats. P value shown; Paired student *t* test. (B) Bar graphs showing the percentage of viral DNA bound to PML or IgG. Mean and standard error of the mean shown; Data pooled from 5 independent repeats. P value shown; Paired one-tailed non-parametric Wilkoxin test. (C) Bar graphs showing the level of viral DNA bound to PML in the absence of doxycycline or UV crosslinking. Mean and standard error of the mean shown. Data pooled from 5 independent repeats. P value shown; Paired one-tailed non-parametric Wilkoxin test.

5.2.4. UV irradiation inhibits the genome decompaction of vDNA following uncoating

UV irradiation of HSV-1 virions led to a decrease in detectable genome area in a dose-dependent manner (Figure 11 and 14). UV irradiation has been shown to induce Pyrimidine and Purine intrastrand dimers between adjacent DNA strands (Goodsell, 2001; Rastogi et al., 2010). This led to the hypothesis that UV irradiation of HSV-1 genomes may induce crosslinking of DNA strands through the formation of pyrimidine dimers, preventing genome decompaction potentially effecting its recognition by PML-NBs. To this end, we utilized a cell-free virion genome release assay protocol to stimulate vDNA release from the capsid in the presence of the protein denaturant Guanidine Hydrochloride (GuaHCl). Viral DNA was visualized via click chemistry and genome measurements calculated using ImageJ. Both non-UV and UV irradiated HSV-1 genomes were successfully ejected from the capsid, whereas that decompaction was absent in the UV irradiated HSV-1 DNA samples (Figure 24A and C). Genome measurements demonstrated a reduction in the number of DNA strands of UV irradiated genomes, suggesting a reduction in genomes compaction efficiency (Figure 24B). The number of genomes analysed for each condition was comparable for both conditions (Figure 24C). Dot Blot analysis demonstrated UV irradiation to induce the formation of thymine dimers (TD) in a dose-dependent manner (Figure 25A), with almost a 3-fold increase TD formation observed after 60 sec UV irradiation, compared to non-UV irradiated HSV-1 (Figure 25B). Collectively these data suggests that the formation of pyrimidine dimers affect the ability of HSV-1 to effectively decompact its genome upon capsid release. Thus, UV irradiation induces a restriction in genome decompaction of infecting vDNA that leads to a loss in PML recognition of vDNA. Additional study is required to determine if a lack of access to a specific DNA sequence or altered 3D structure of the target DNA inhibits PML detection of vDNA.

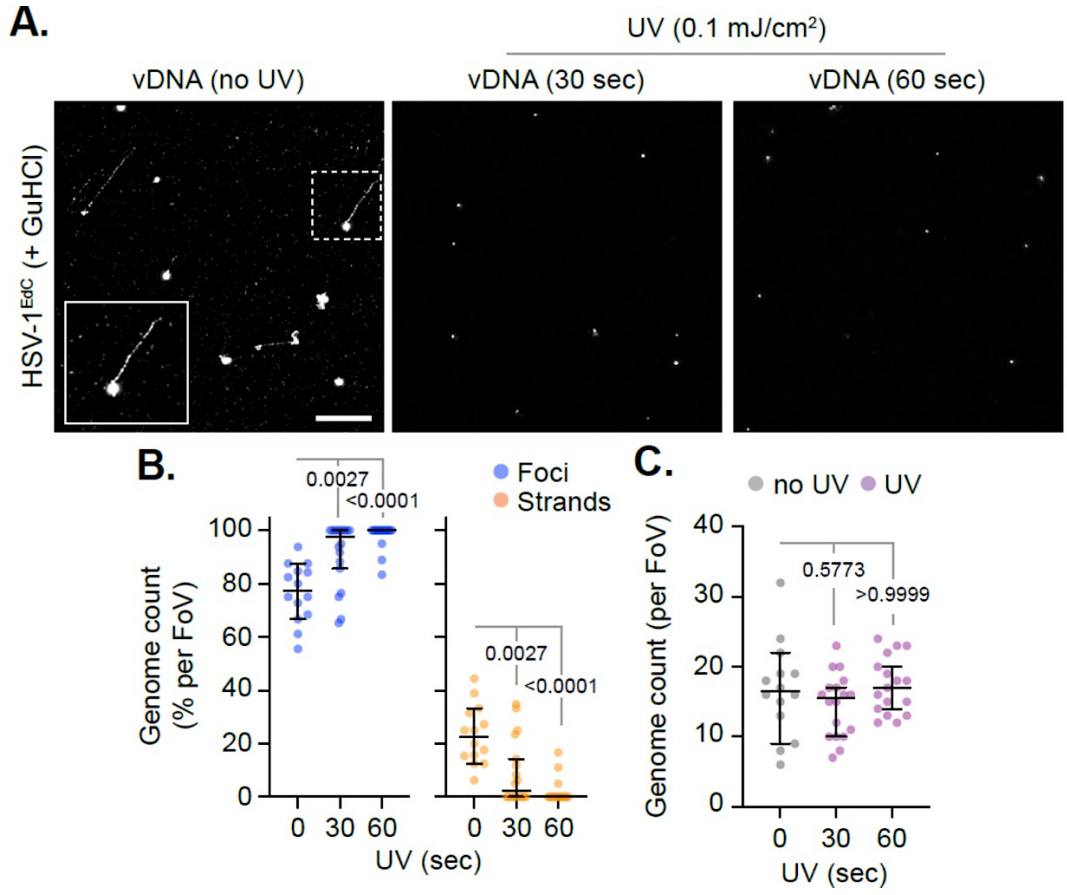

Figure 24. UV irradiation of HSV-1 abrogates genome decompaction.
Neat non-U or UV irradiated HSV-1^{EdC} virus was annealed to coverslips, pre-treated with Poly-D lysine, in the presence or absence of Guanidine hydrochloride (GuaHCl). vDNA were detected by click chemistry and Airy scan imaging. (A) Representative confocal images of viral DNA from non-UV or UV irradiated HSV-1^{EdC}. (B) Quantitation of percentage of DNA strands and compact genomes (foci) per field of view (as in A). n=3, means and SD shown. P value shown; One-way ANOVA. (C) Number of observable non-UV or UV irradiated HSV-1 viral genomes per field of view (as in A). n=3, mean and SD shown. P value shown; One-way ANOVA.

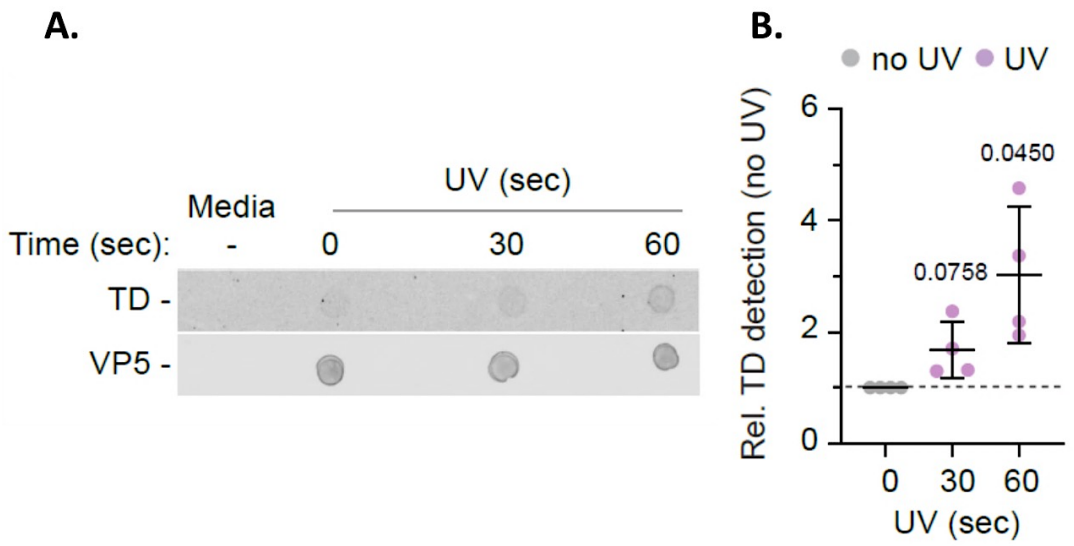

Figure 25. UV irradiation of HSV-1 causes the accumulation of TD in the vDNA.

Virus stock of non-UV or UV irradiated HSV-1^{EdC} was blotted on 0.2µm nitrocellulose paper and probed for TD and VP5 (capsid protein) in a DotBlot assay. (A) Representative blot of neat virus for the presence of Thymine Dimers (TD) and viral capsid protein VP5 (loading control). Media samples represent negative control. (B) Quantitation of TD presence in samples (as in A). n=4, SD shown. Values normalized to their respective VP5 control and expressed relative to their normalized levels in HSV-1 no UV virus stock. P value shown; one sample t test against a hypothetical mean of 1.

5.3. Summary

PML-NBs play a key role in regulating intrinsic and innate immune defences to herpesvirus infection (Alandijany et al., 2018). However, the role of these nuclear bodies in mediating the cellular immune response to UV irradiated virus infection has not been investigated. In Chapter 1, we showed UV irradiation of HSV-1 to induce the premature uncoating of genomes in the cytoplasm in a microtubule-dependent manner, which resulted in the induction of a strong type I IFN response. A percentage of UV irradiated viral genomes were delivered to the nucleus. In this chapter we assess the interaction between nuclear intrinsic immune factors and UV irradiated vDNA.

PML-NB constituent proteins, such as PML, Sp100, and Daxx, have been shown to localize to infecting viral genomes in the nucleus and to have a role in restricting HSV-1 IE transcription (Glass & Everett, 2013; Everett & Murray, 2005; Everett, 2006; Cuchet-Lourenço et al., 2011, 2013). These interactions are transient, as WT HSV-1 expresses ICP0 that antagonizes PML-NBs by targeting various key components for Ub-mediated proteasomal degradation (Vanni et al., 2012; Boutell, Sadis & Everett, 2002; Zheng, Samrat & Gu, 2016; Everett et al., 2006; Everett, Boutell & Orr, 2004; Boutell & Everett, 2013; Everett et al., 2008; Lukashchuk & Everett, 2010). Previous studies have also investigated the interaction between PML-NBs and HSV-1 genomes by click chemistry (Sekine et al., 2017; Alandijany et al., 2018). The microscopy observations in this chapter fall in line with these previous reports, showing that non-UV irradiated HSV-1 genomes recruit key components of PML-NBs (Sp100, Daxx, PML) as early as 90 minutes post-addition of virus (Figures 19). Upon UV irradiation, however, HSV-1 genomes that reach the nucleus exhibit reduced colocalization with PML-NB components (Figures 19). This effect was directly attributable to UV irradiation independently of UV light source (Figure 20). Studies have shown that PML itself can associate with cellular ssDNA molecules in response to exogenous DNA damage and PML-NBs can sequester DNA molecules during DNA processing events associated

with DNA synthesis (Jul-Larsen et al., 2004; Bøe et al., 2006). This evidence for direct interaction between PML and vDNA is supported by our ChIP-qPCR analysis (Figure 23). The interaction between PML and vDNA was inhibited upon UV irradiation of HSV-1 virions (Figure 23), indicating that the DNA damage induced to the genome is inhibitory to its recognition by PML and potentially other PML-NB constituent proteins (e.g., Sp100 and Daxx). Since the exact recognition mechanism of viral DNA by PML-NBs remains unknown, the disruption of vDNA recognition by PML-NBs by UV irradiation may result from a variety of different reasons. Genome size was shown to be affected by UV irradiation, demonstrated by the change of genome area presented in the previous chapter, suggesting the decompaction of viral genomes was affected (Figure 11). DNA damage induced by UV has been well documented. The formation of DNA damage due to exposure to UV light has been established, with the main photoproducts being cyclobutene pyrimidine dimers (CPDs) and 6-4 photoproducts, ultimately resulting in the alteration of base-pairing and DNA structure. In conjunction to these findings, our data demonstrates the UV-dose dependent accumulation of thymine dimers in the vDNA (Figure 25), resulting in the compromised structure of HSV-1 genomes represented by the inability of the vDNA to decompact following capsid release (Figure 24). This change in HSV-1 genome conformation could potentially mask or block a PML-NB specific binding site present in the decompacted state of the vDNA. Equally the specific three-dimensional structure maybe required for the efficient binding of PML and is inaccessible due to the crosslinking of the DNA strands. Further investigation is required to determine the nature of the recognition of HSV-1 DNA by PML.

In summary, the data presented in this chapter shed light on the interaction between PML-NB proteins and HSV-1 genomes. UV irradiation of HSV-1 severely affects the recruitment and interaction of PML and other PML-NB constituent proteins to vDNA, indicating that nuclear genome delivery alone is not sufficient to initiate an intrinsic antiviral immune response to HSV-1 infection. These data also demonstrate that PML-NB proteins physically associate with vDNA, likely through specific binding

requirements that require viral genome decompaction upon nuclear infection.

6. Cytoplasmic immune factors are differentially recruited to HSV-1 genomes following UV irradiation

6.1. Overview

Activation of the type I IFN pathway is dependent on the recognition of PAMPs, such as vDNA, by cellular PRRs (Ma, Ni & Damania, 2018; Abe, Marutani & Shoji, 2019). The majority of PRRs have been shown to reside in the cytosol, with reports demonstrating that some PRRs can also be localized in the nucleus, such as cGAS and IFI16 (Orzalli et al., 2015). The data presented has demonstrated the increase in cytosolic deposition of HSV-1 genomes following UV irradiation in a dose dependent manner. Additionally, UV irradiation of HSV-1 virions induced a much stronger innate immune response compared to the non-UV irradiated virus infection. These findings raised the question as to what specific PRRs were involved. To this end, we focused on investigating well characterized PRR proteins of the type I IFN pathway to determine their relative localization to cytosolic HSV-1 genomes. PML was included as a negative control. Additional cytosolic HSV-1 restriction factors were also investigated to determine if they played a role in mediating the IFN response to UV irradiated HSV-1.

Consistent with previous reports (Sun et al., 2019), our data demonstrated that cGAS was recruited to sites of HSV-1 vDNA in the cytosol. UV irradiation of HSV-1 caused an enhanced recruitment of not only cGAS but STING as well. This is interesting, as the canonical pathway currently describes STING as an ER anchored molecule that interacts with the secondary messenger molecule cGAMP produced following cGAS recognition of DNA (Sun et al., 2009; Reinert et al., 2016; Wu et al., 2013). Additionally, STING recruitment to cGAS was also enhanced following UV irradiation of HSV-1, and was absent in cGAS KO HFt cells, suggesting cGAS localization to infecting cytosolic genomes is a pre-requisite for the recruitment of STING. This is further supported by ChIP experiments, showing direct cGAS

interaction with vDNA being enhanced following UV irradiation, whilst STING demonstrated no interaction at all despite being reported to interact with DNA directly (Abe et al., 2013b). The increased interaction and recruitment can be a direct or indirect result of the accumulated DNA damage on viral genomes. To address the latter we investigated the recruitment of other restriction factors that may sterically inhibit the binding of cGAS, such as IFI16 but found no colocalization at HSV-1 DNA, in agreement with a recent report that IFI16 localizes to actively replicating genomes (Alandijany et al., 2018), even though it has been shown that IFI16 can interact with both cGAS and STING (Unterholzner et al., 2010; Johnson et al., 2014; Orzalli et al., 2015). Sp1, a transcription factor involved in HSV-1 replication, colocalized with vDNA within the cytoplasm during non-irradiated HSV-1 infection that was inhibited following UV irradiation. This gave evidence suggesting steric hindrance could potentially prevent cGAS and STING from localizing to vDNA due to the presence of other competing host factors. However, in Sp1 KO cells, neither cGAS nor STING were recruited to sites of HSV-1 DNA. These findings, along with data presented in the previous chapter, present preliminary evidence for a complex series of events and interactions that enhance the activation of innate immune signalling in response to UV irradiated virus infection. The data presented here may explain the enhanced levels of activation of the IFN response in UV irradiated virus infected cells and highlight the importance of carefully interpreting data using UV irradiated viruses to study the cellular immune response to infection, which is not as simple as currently portrayed in the literature.

6.2. Results

6.2.1. Recruitment of cytoplasmic PRRs cGAS and STING to HSV-1 DNA is enhanced upon UV irradiation

The cGAS-STING pathway and its role in DNA detection of viruses has been extensively studied. It has been reported that cGAS is involved in the detection of cytosolic HSV-1 DNA, which leads to the activation of the STING-IRF3 axis and IFN expression (Sun et al., 2019). Additionally, numerous HSV-1 proteins have been shown to antagonize different steps of the cGAS-STING pathway during infection (Table 3) (Pan et al., 2018; Deschamps & Kalamvoki, 2017; Bodda et al., 2020; Christensen et al., 2016; Huang et al., 2018; Su & Zheng, 2017b; Zhang et al., 2018). Data presented in Chapter 4, demonstrated an increase in the cytosolic deposition of HSV-1 genomes following UV irradiation. Thus, we decided to investigate the recruitment of DNA sensing molecules to HSV-1 genomes in the cytoplasm, specifically cGAS and STING, to determine if UV irradiation of HSV-1 DNA influenced their role in mediating the IFN response to HSV-1 infection. HFt cells were seeded overnight and infected with either non-UV irradiated or UV irradiated HSV-1 and fixed/stained for IF processing at 90 mpi. The cellular PRRs cGAS and STING and HSV-1 genomes were readily detectable in the cytosol of infected cells (Figure 26A and B). PML and IFI16 were used as reference controls for indirect IF staining to detect any changes in localization. To accurately compare the weighted coloc. coeff., an average area (calculated mean area of 30 nuclei) was used to take measurements from the cytosol containing the target genome and excluding nuclear signal. This enabled comparison between cells that show variance in the surface area of the cytoplasm (i.e., normalizing the number of pixels taken over a range of images that are used as a basis for w. coloc. coeff.). Interestingly, both cGAS and STING were recruited more efficiently to cytoplasmic genomes following infection with UV irradiated HSV-1, compared to non-irradiated HSV-1. There was no significant localization of either protein to vDNA in the nucleus. PML exhibited a similar profile of

decreased nuclear association to HSV-1 genomes following UV irradiation, with no localization observed to vDNA in the cytosol. IFI16 was not detectably recruited to vDNA in either location (Figure 26). These data provide evidence that both cGAS and STING may interact directly with infecting vDNA, contrary to the canonical pathway currently described in the literature. Additionally, cGAS has been reported to populate the nucleus and to play a role in stabilizing IFI16 during HSV-1 infection (Orzalli et al., 2015), but this was not observed in these experiments; highlighting the cytosol as a potentially exclusive cellular compartment for PRR detection in HFt cells following UV irradiation of HSV-1.

To further validate these observations, we identified a mouse monoclonal antibody against STING that enabled dual staining experiments with cGAS (Figure 27). A similar profile of enhanced recruitment to cytosolic UV irradiated HSV-1 genomes was observed for both cGAS and STING when compared to non-UV irradiated HSV-1 cytosolic genomes, albeit to lower levels. Interestingly, STING recruitment to cGAS could also be observed during HSV-1 infection and was enhanced upon UV irradiation (Figure 27B). Collectively, these results suggested that the cGAS-STING pathway maybe acting via a previously unreported mechanism, with STING having a more direct acting role than previously thought.

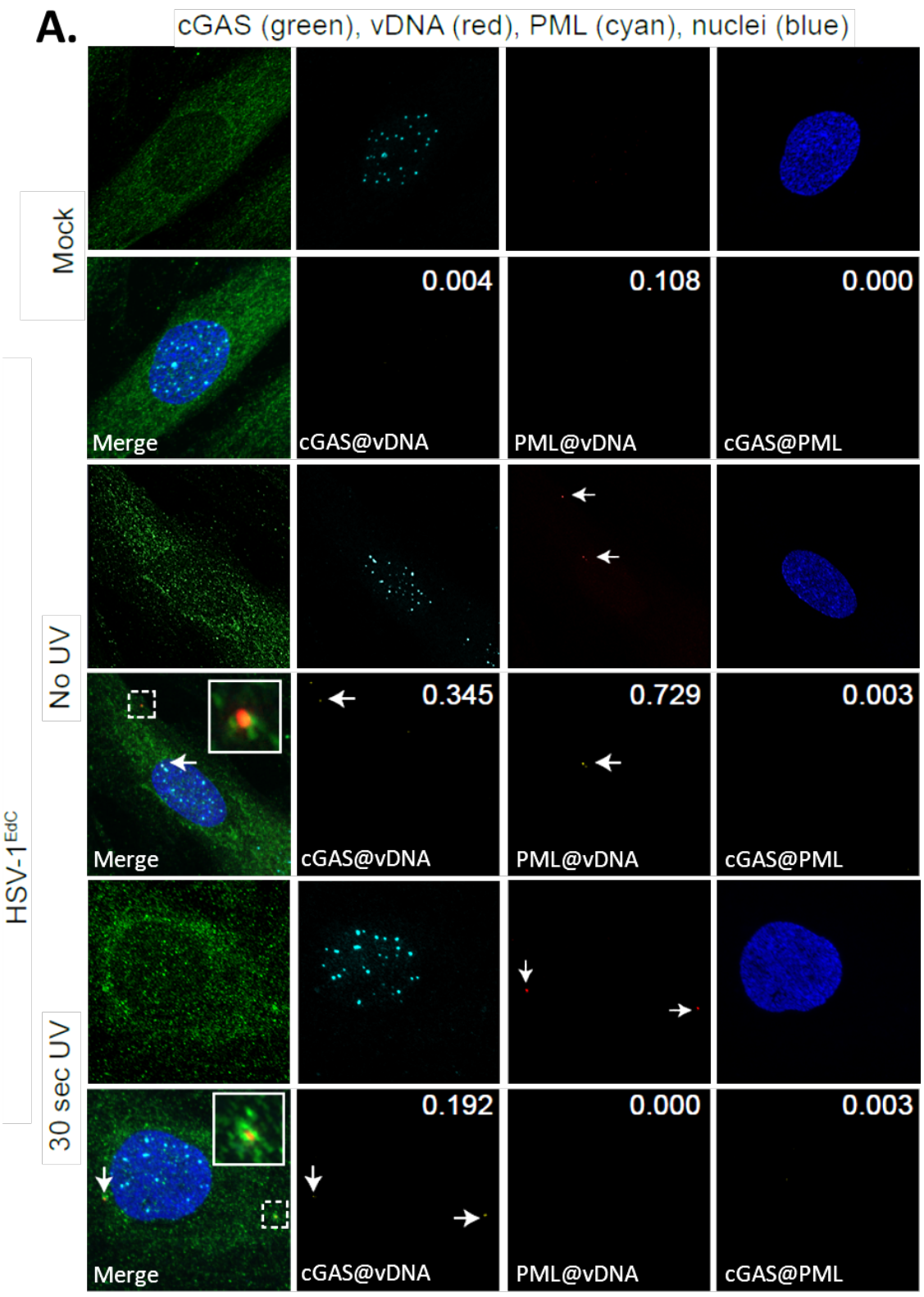
A.
cGAS (green), vDNA (red), PML (cyan), nuclei (blue)
Mock
No UV
30 sec UV
HSV-1EdC
Merge
cGAS@vDNA
PML@vDNA
cGAS@PML
0.004
0.108
0.000
0.345
0.729
0.003
0.192
0.000
0.003

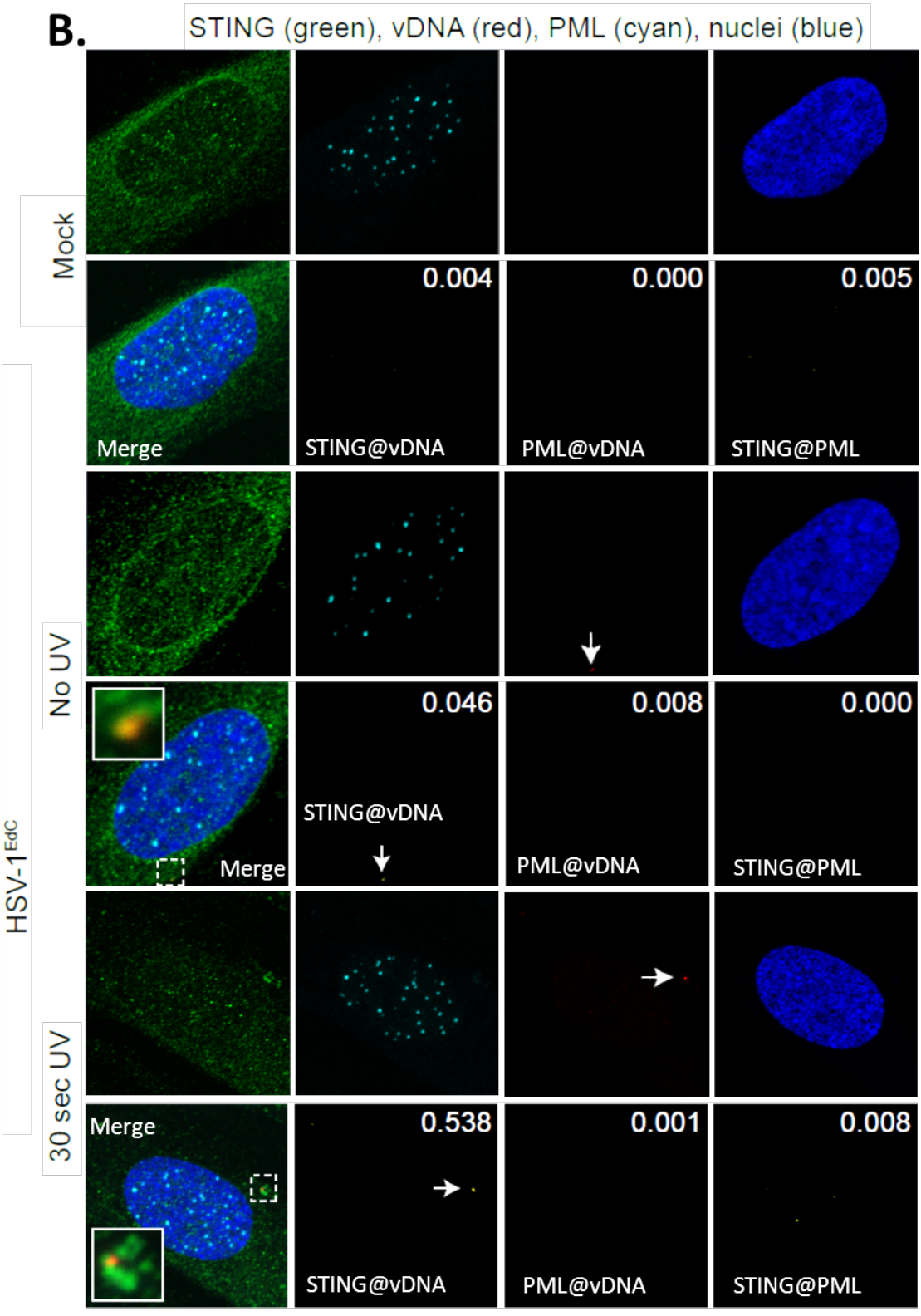
B.
STING (green), vDNA (red), PML (cyan), nuclei (blue)
Mock
HSV-1EdC
No UV
30 sec UV
Merge
STING@vDNA
PML@vDNA
STING@PML
0.004
0.000
0.005
0.046
0.008
0.000
0.538
0.001
0.008

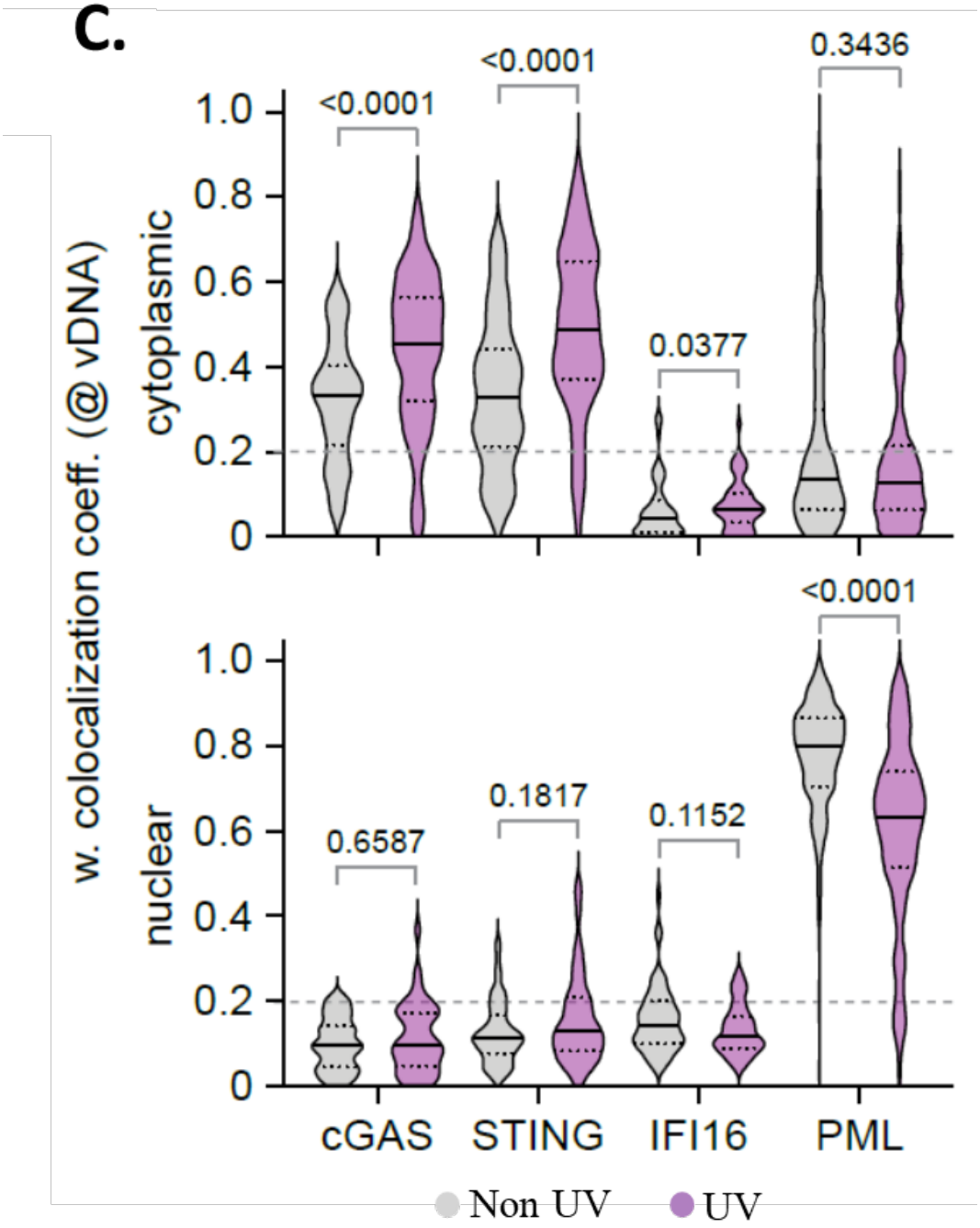

Figure 26. UV irradiation of HSV-1 enhances the recruitment of cGAS and STING to cytosolic vDNA.

HFt cells infected with 3 PFU/cell of HSV-1^{EdC} or UV HSV-1^{EdC}. Cells were fixed and permeabilized at 90 mpi. vDNA was detected using click chemistry. STING, cGAS and PML were detected via indirect immunofluorescence. Nuclei were stained with DAPI. (A and B) Localization of cGAS or STING (green) and PML (cyan) to cytosolic viral genomes (red), indicated by white arrows. White boxes show zoomed areas of interest. Cut mask (yellow) highlights the regions of colocalization between the cellular proteins of interest and non-UV or UV irradiated HSV-1^{EdC} genomes. Weighted colocalization coefficient shown. (C) Quantitation of cellular protein recruitment to infecting vDNA in the cytoplasm or nucleus at 90 mpi. Black line: median weighted (w.) colocalization coefficient; dashed

lines: SD. n>100 nuclei per sample population derived from a minimum of three independent repeats. P value shown; Mann-Whitney *U*-test.

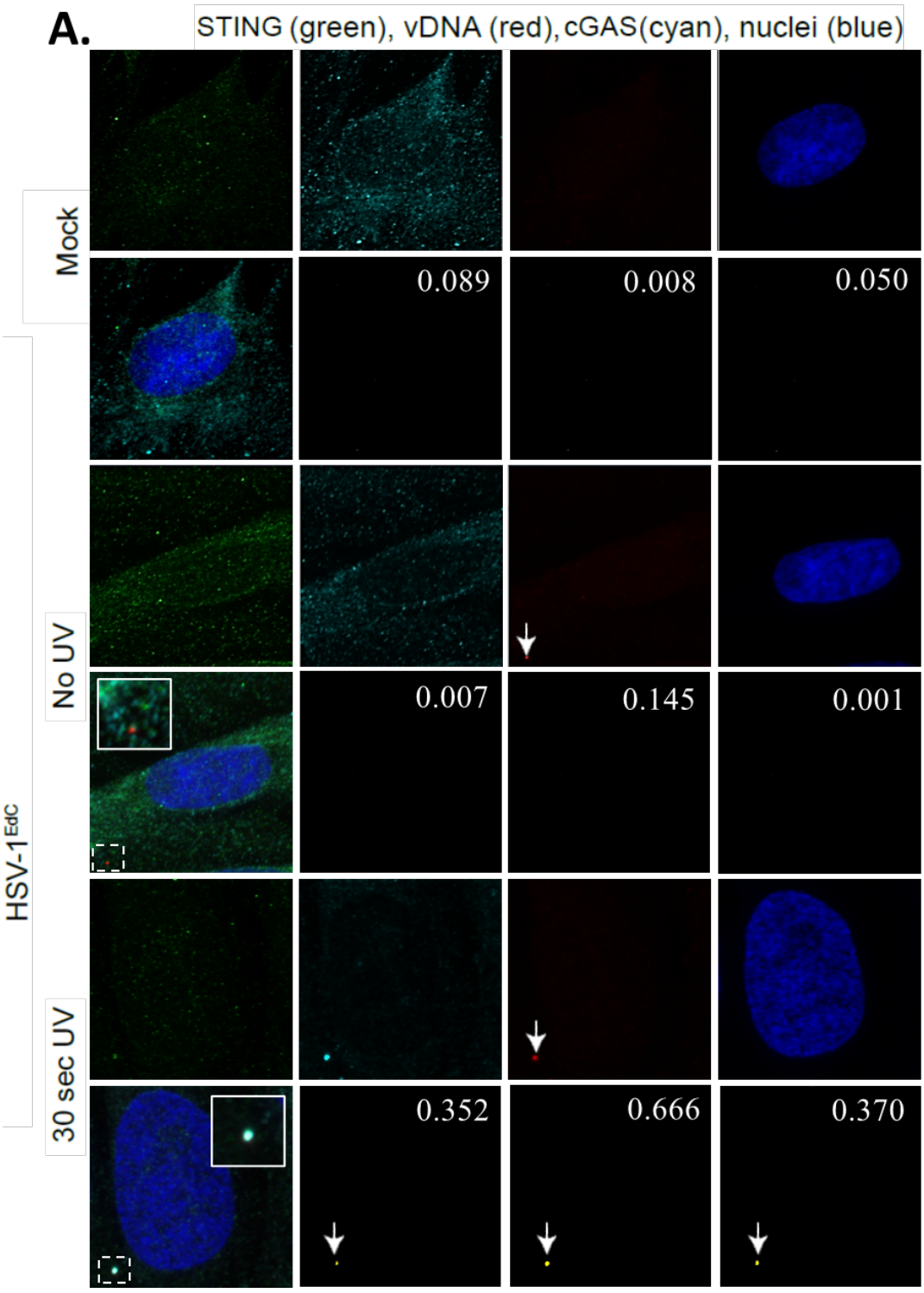

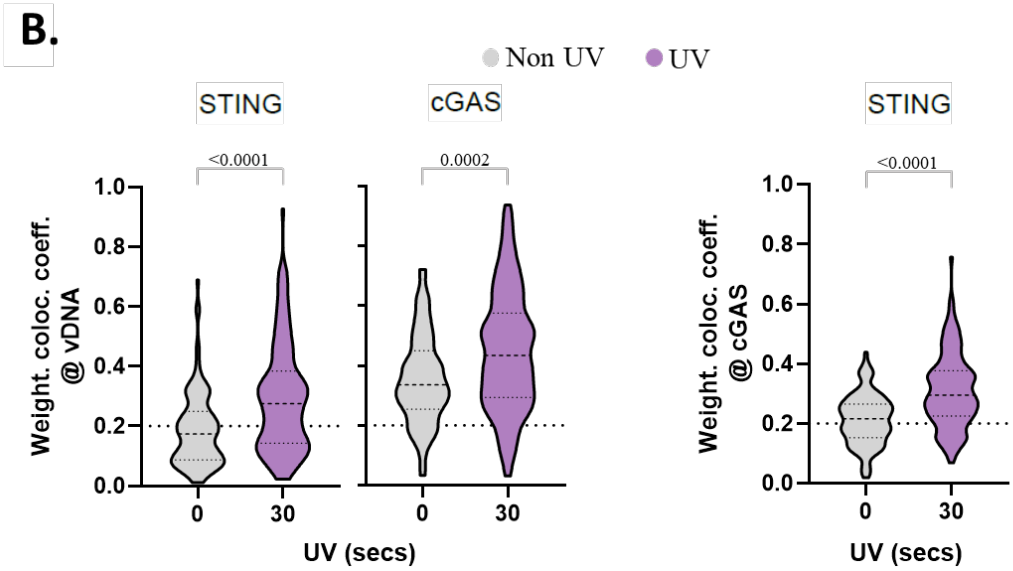

Figure 27. UV irradiation of HSV-1 enhances the recruitment of cGAS and STING to cytosolic vDNA.

HFt cells were infected with 3 PFU/cell of non-UV or UV HSV-1. Cells were fixed and permeabilized at 90 mpi. Infecting labelled viral DNA was detected using click chemistry. STING and cGAS were detected via indirect immunofluorescence. Nuclei were stained with DAPI. (A and B) Localization of STING (green) and cGAS (cyan) to cytosolic viral genomes (red), indicated with white arrows. White boxes show zoomed areas of interest. Cut mask (yellow) highlights the regions of colocalization between the cellular proteins of interest and non-UV or UV irradiated HSV-1 genomes. Weighted colocalization coefficient shown. (C) Quantitation of cellular protein recruitment to infecting vDNA or each other in the cytoplasm at 90 mpi. Black line: median weighted (w.) colocalization coefficient; dashed lines: SD. n>120 nuclei per sample population derived from a minimum of three independent repeats. P value shown; Mann-Whitney *U*-test.

6.2.2. Super-resolution analysis of the interaction between cGAS/STING and vDNA

In the canonical pathway cGAS is activated by recognizing and binding to DNA, which leads to the production of the signalling molecule cGAMP. STING has been described as an ER-bound protein that interacts with the signalling molecule cGAMP, which induces STING's translocation to the ERGIC that activates TBK1 and IRF3. Our preliminary data suggest that STING may directly localize to sites of cytoplasmic vDNA in association with cGAS, which was enhanced following UV irradiation of HSV-1. We therefore examined the physical distances between cGAS, STING, and vDNA using super high-resolution imaging.

Super high-resolution imaging confirmed our previous analysis, with cGAS and STING being readily detectable at vDNA (Figure 28A and B). Quantification revealed that the number of cGAS foci present in the vicinity of the HSV-1 genomes not to change following UV irradiation (typically 1 foci per genome). However, the number of STING foci almost doubled during infection with UV irradiated HSV-1 compared to non-UV irradiated HSV-1 infection (Figure 28C). Colocalization analysis was also performed using the Pearson coefficient (Figure 28D). The colocalization of cGAS to non-UV irradiated vDNA was high as indicated by the Pearson coefficient (mean of 0.9) and did not change following UV irradiation. In contrast, the colocalization of STING with vDNA increased upon UV irradiation (mean of 0.2 to 0.4), although this colocalization was signlificantly less than observed with cGAS (Figure 28D). When looking at the distance between foci, we separated them into two groups for our analysis; touching (foci that made direct contact with vDNA) and proximal (foci that have no contact with vDNA). There was no significant change in the distance between vDNA and cGAS or vDNA and STING upon UV irradiation of HSV-1 relative to no irradiation. However, cGAS localized in closer proximity to vDNA than STING (Figure 28E). There was no significant change in the distance of proximal cGAS or STING foci to vDNA following UV irradiation (Figure 28E). Notably, the volume of the HSV-1 DNA did not show any significant change in this

analysis compared to results presented in Chapter 2 (Figure 12 and 23). However, this may reflect differences in the population size between each analysis. Collectively these data demonstrate that the recruitment of cGAS to vDNA does not change upon UV irradiation. However, an enrichment in STING foci can be observed at sites in close proximity to vDNA, although the distance of these foci to vDNA is greater than that of cGAS. These data suggest a role for cGAS in the recruitment of STING to vDNA during HSV-1 infection that is dependent on UV irradiation.

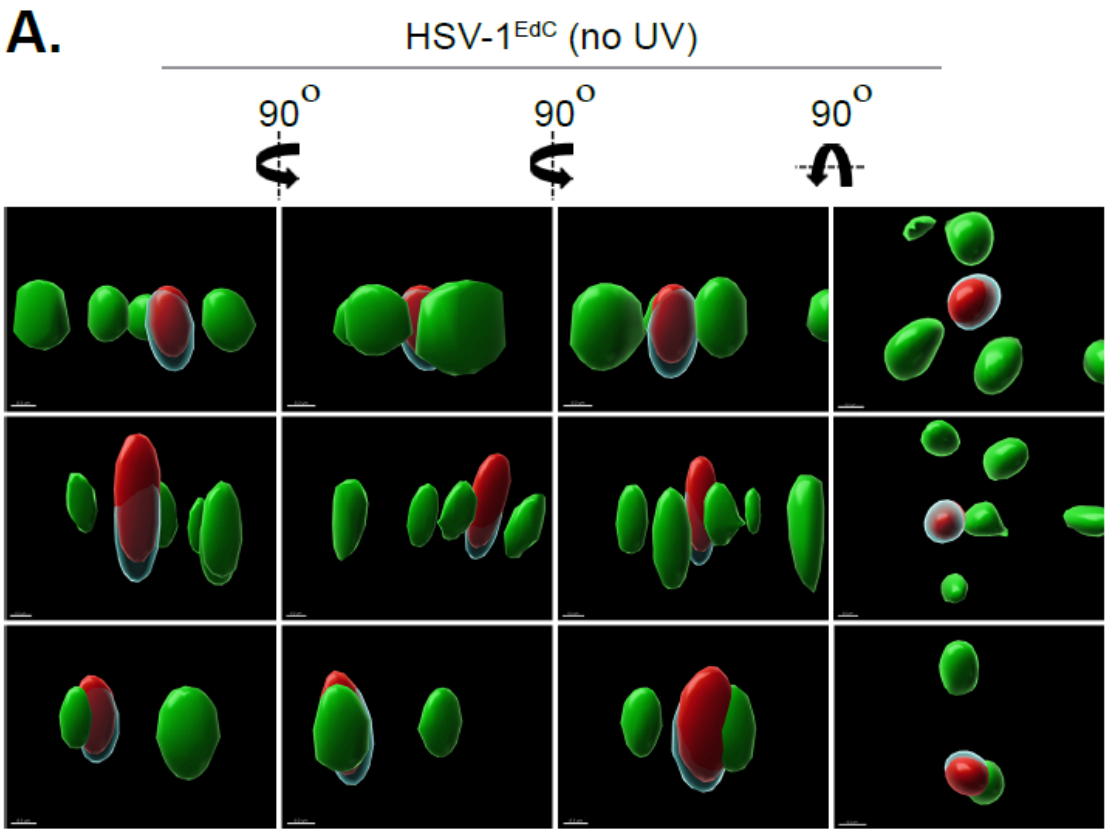

STING (green), vDNA (red), cGAS (cyan)

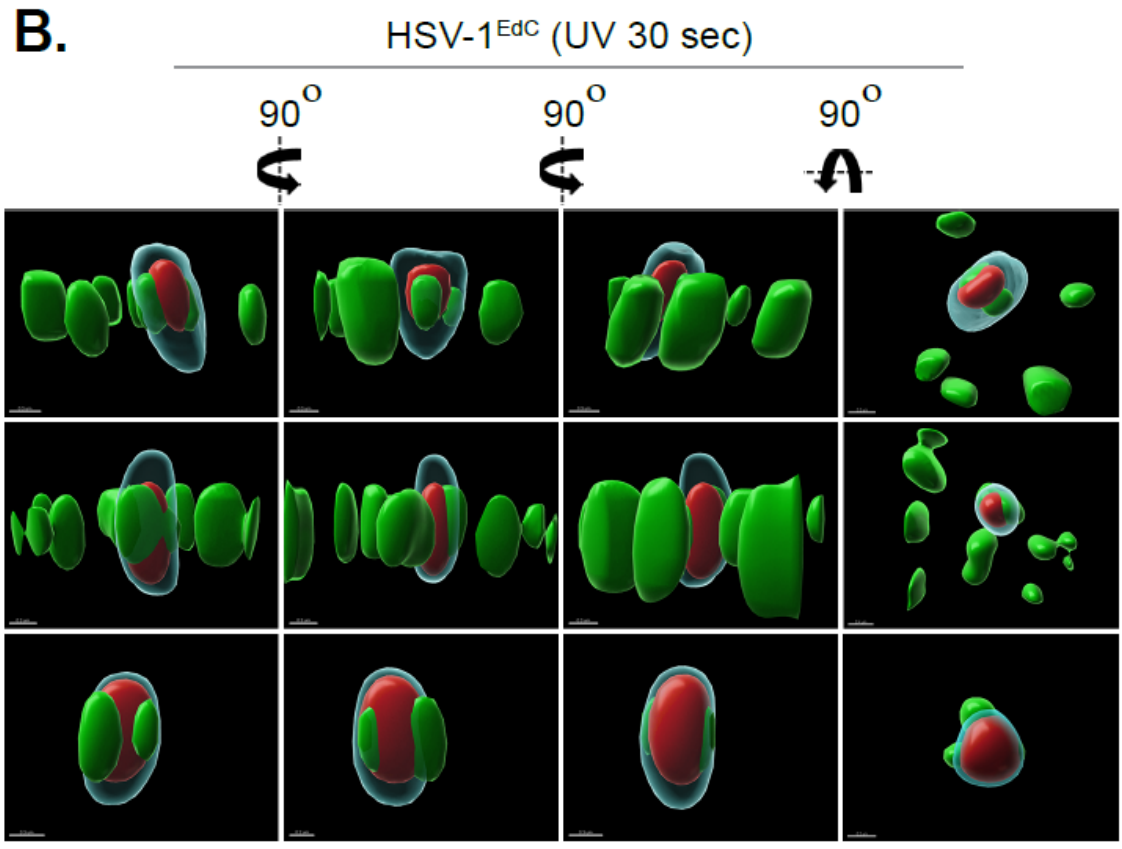

STING (green), vDNA (red), cGAS (cyan)

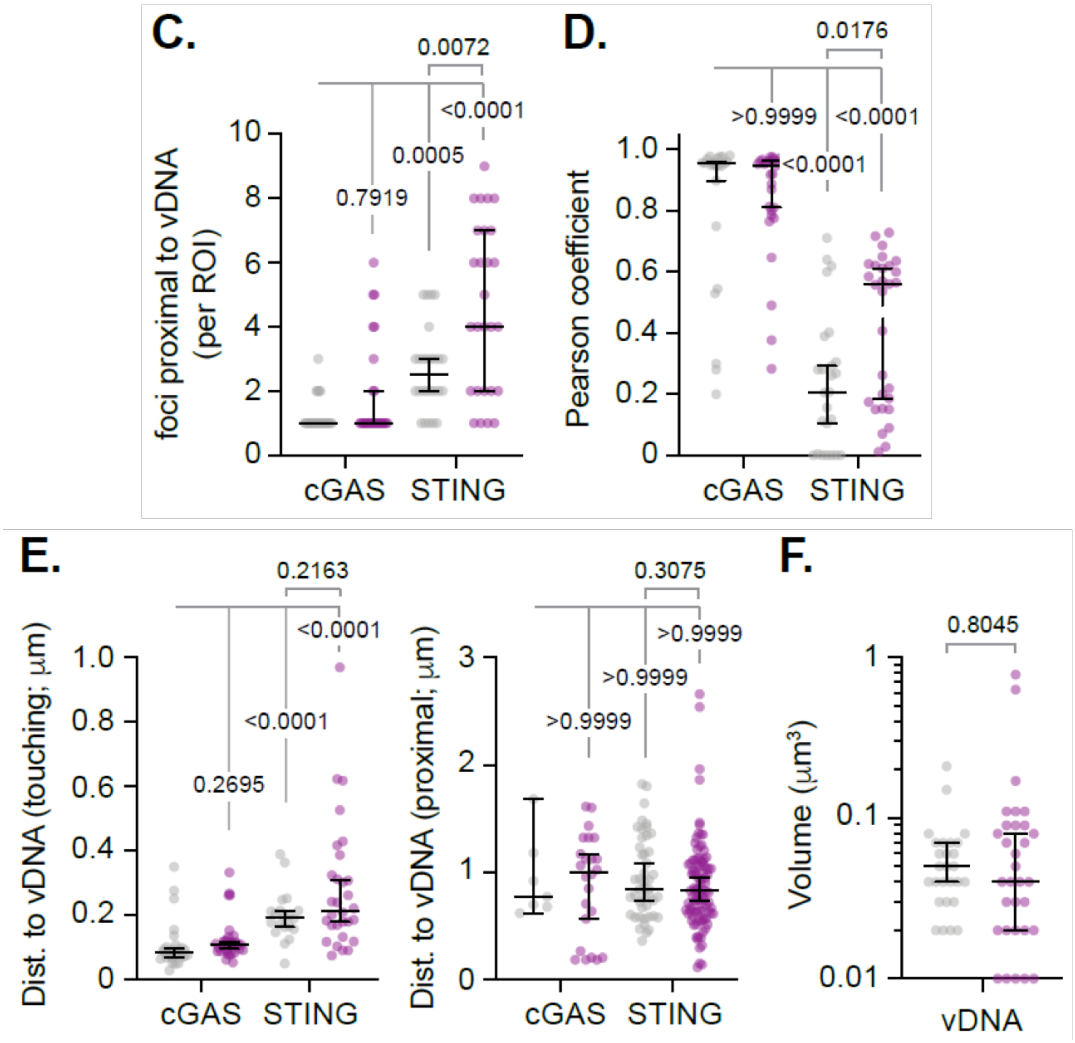

Figure 28. cGAS is more closely and efficiently recruited onto HSV-1 genomes in comparison to STING.

HFt cells were infected with 3 PFU/cell of non-UV or UV irradiated HSV-1. Cells were fixed and permeabilized at 90 mpi. vDNA was detected using click chemistry. STING and cGAS were detected via indirect immunofluorescence. Nuclei were stained with DAPI. Super-resolution Images were rendered and analysed using Imaris Imaging Software. Individual genomes represented by illustrated points. Representative 3D images of localization of STING (green) and cGAS (cyan) recruitment to non-UV (A) or UV (B) irradiated HSV-1 genomes (red). Black arrows indicate direction of the 90-degree rotation of the image. Area for analysis taken at 2µm^3 per genome (C) Quantitation of number of signal foci proximal to vDNA per region of Interest (ROI). Mean with 95% CI shown. n>30 individual viral genomes derived from a minimum of three independent repeats. P value shown; One-way ANOVA (Kruskal-Wallis test). (D) Quantitation of host factor colocalization with vDNA using Pearson coefficient. Mean with 95% CI shown. n>30 individual genomes derived from a minimum of three independent repeats. P value shown; One-way ANOVA (Kruskal-Wallis test). (E) Quantitation of the distance between host factors and vDNA. Touching is representative of direct contact with vDNA; proximal is representative of no contact. Mean with 95% CI shown. n>30 individual genomes derived from a minimum of three independent repeats. P value shown; One-way ANOVA (Kruskal-Wallis test). (F) Quantitation of volume of vDNA (as in C-E). Mean with SD shown. n>30 individual genomes derived from a minimum of three independent repeats. ns=not significant, Mann-Whitney *U* test.

6.2.3. The type-I IFN response to UV irradiated HSV-1 is mediated by the cGAS/STING pathway

Mouse and rabbit animal models have shown that UV irradiated HSV-1 virions induces a strong innate immune response compared to non-UV irradiated HSV-1 virions, which induced no IFN production, in serum samples at 24 hours post inoculation. This response was preferentially mediated by the type I and II IFN pathways (Taylor & O'brien, 1985; Hendricks et al., 1991; Eloranta, Sandberg & Alm, 1996; Gary, Rosenberg & Louis, 1974). Based on these reports and the data presented on cGAS and STING recruitment to UV irradiated HSV-1 DNA in the cytoplasm, we investigated the involvement of cGAS and STING in mediating the type-I IFNβ response. To this end, we utilized HFt cells that were KO for STING or cGAS. A Non-Targeted Control (NTC) gRNA was used as a negative control. The level of KO was assessed by Western Blot, which showed 70-80% successful knock down of the targeted genes (Figure 29). HFt cells were seeded overnight prior to infection with non-UV or UV irradiated HSV-1 at an MOI of 3 PFU/cell or mock infected. mRNA was extracted at 6 hr post infection and IFNβ levels were analysed by qPCR. PolyI:C, a synthetic dsRNA analogue molecule, was used as a positive control for IFNβ stimulation. In NTC cells, UV irradiated HSV-1 induced a significantly higher IFNβ response compared to non-UV irradiated HSV-1. The levels of IFNβ mRNA were significantly lower in both cGAS and STING KO cells and comparable to mock treated cells (Figure 30). These data show the importance of both PRRs, cGAS and STING, in mediating the type I IFN response to UV irradiated HSV-1 infection, which is weaker in WT HSV-1 infection due to the expression of multiple viral immune evasion antagonists (Table 1).

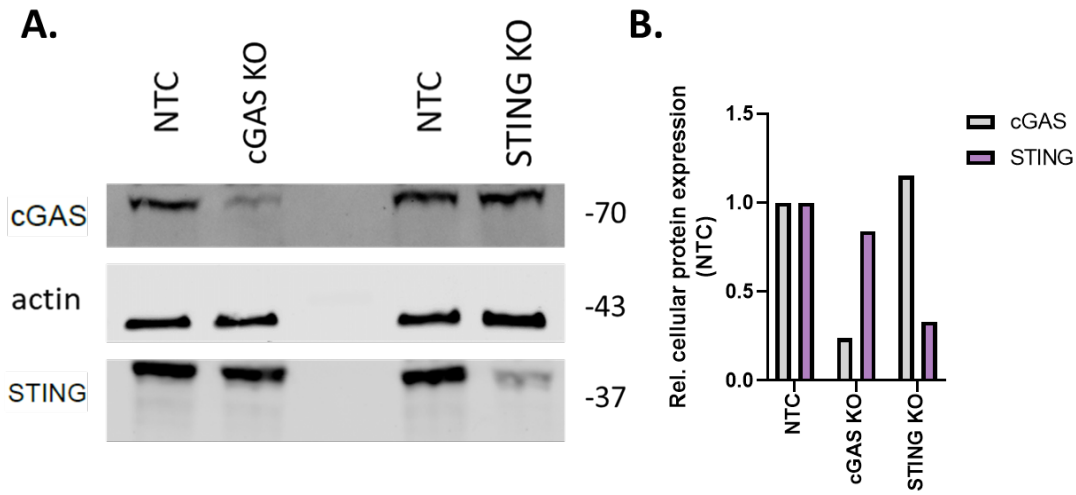

Figure 29. Knock-down of cGAS and STING.

HFt cells were CRISPR-Cas-9 gene edited with guide RNAs that targeted either cGAS or STING gene loci. A Non-Targeted Control (NTC) gRNA was used as a negative control. (A) Western blot showing the levels of cGAS, STING and actin (as a loading control) in whole cell lysates derived from NTC, cGAS KO and STING KO HFt cells. Membranes were probed for cGAS and STING to determine the level of knock-down in their respective KO cell. (B) Bar graph showing the relative protein expression of cGAS and STING in their respective KO cell lines. Values were normalized to NTC actin.

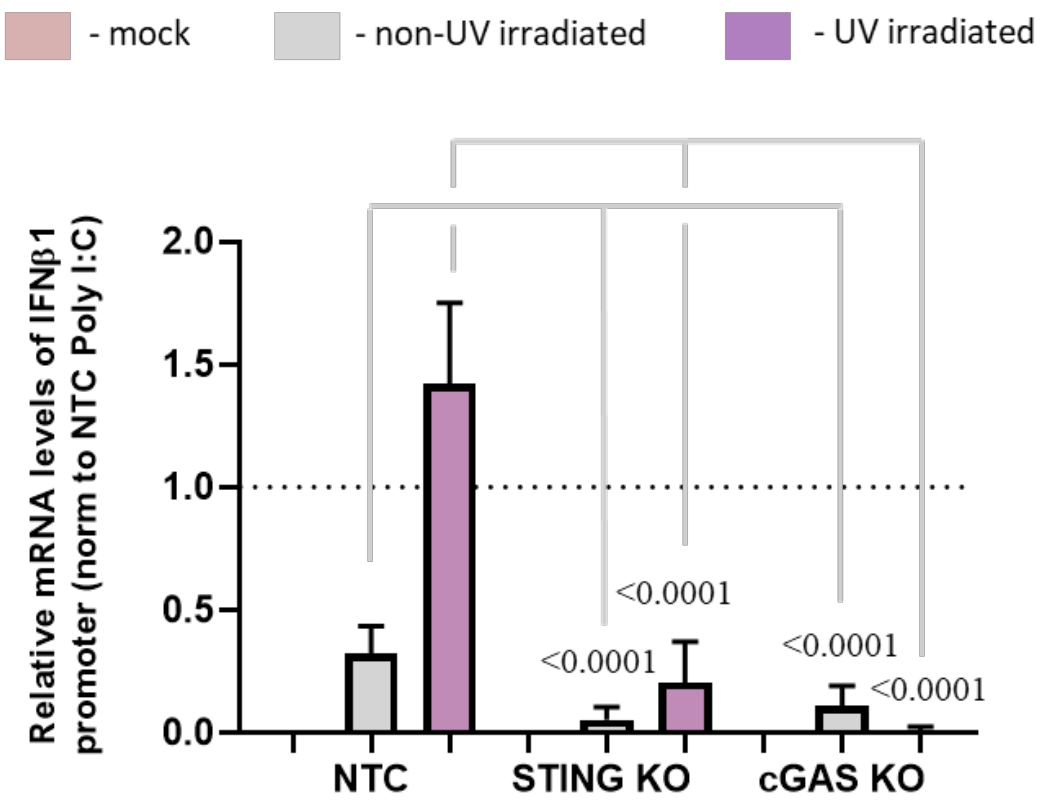

Figure 30. cGAS and STING are required for IFN-β induction during HSV-1 infection.

NTC or cGAS/STING KO HFt cells were seeded overnight prior to infection with non-UV or UV irradiated HSV-1 at an MOI of 3 PFU/cell. Cells were harvested at 6 hrs post-infection and mRNA was extracted. Bar graphs show the levels of IFNβ mRNA. mRNA transcript levels were measured by qRT-PCR and values normalized to GAPDH, using the threshold cycle (ΔΔCT) and expressed relative to mRNA levels of NTC cells treated with PolyI:C (dotted line). Results were derived from three independent experiments. Mean with SD shown. P value shown; Paired non-parametric Wilcoxon t-test.

6.2.4. cGAS localization to UV treated HSV-1 genomes is required for the recruitment of STING

The close association of STING to cGAS at vDNA and increased accumulation of STING foci proximal to vDNA upon UV irradiation raised the question as to whether these PRR proteins were sequentially recruited to vDNA. To answer this question, the localization profiles of cGAS and STING to vDNA was investigated in cGAS KO cells to check if STING recruitment was cGAS-dependent or if it independently recruited prior (Figure 31). HFt NTC or cGAS KO cells were seeded overnight prior to infection with non-UV or UV irradiated HSV-1 at an MOI of 3 PFU/cell (Figure 32A). Enhanced levels of colocalization of cGAS and STING to vDNA was observed in NTC cells infected with UV irradiated HSV-1 (w. coloc. coeff. of ≤0.3) compared to non-UV irradiated HSV-1 infected cells (w. coloc. coeff. of ≤0.15). There was also an increase in the colocalization of STING at cGAS in these cells, similar to our previous observation (Figure 27). As expected, KO of cGAS led to a reduction in cGAS at vDNA. A reduction in the level of STING recruitment of STING to vDNA in the absence of cGAS was also observed (Figure 32B). To ensure only cGAS KO cells were included, cGAS positive cells were excluded from the single cell analysis. These data suggests that cGAS may be playing a role in the recruitment of STING to HSV-1 DNA in the cytosol. This interaction is absent during infection with non-UV irradiated HSV-1, which may be due to active viral antagonism of the cGAS/STING pathway (Table 1). The recruitment of STING by cGAS could be through a direct chaperoning activity, another mediator protein that interacts with cGAS, or cGAMP synthesized by cGAS following DNA binding. Further investigation is required to elucidate the specifics of this interaction.

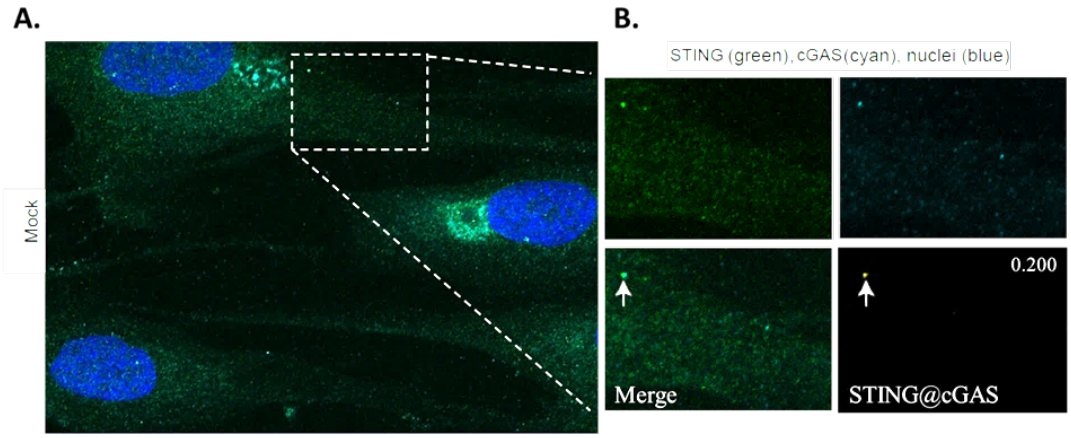

Figure 31. Quantitation analysis of cytoplasmic localization of host factors.
HFt cells were seeded on glass coverslips overnight prior to fixing and permeabilization at 90 mpi. STING and cGAS were detected by indirect immunofluorescence. Nuclei were stained with DAPI. (A) Cytoplasmic areas of interest (dashed line box) were cropped out using a pre-set area, equivalent of the average size of a nucleus of an HFt cell. (B) Standard colocalization analysis was then performed. Cut mask (yellow) highlights the regions of colocalization between the cellular proteins of interest, further indicated by white arrows. Weighted colocalization coefficient shown.

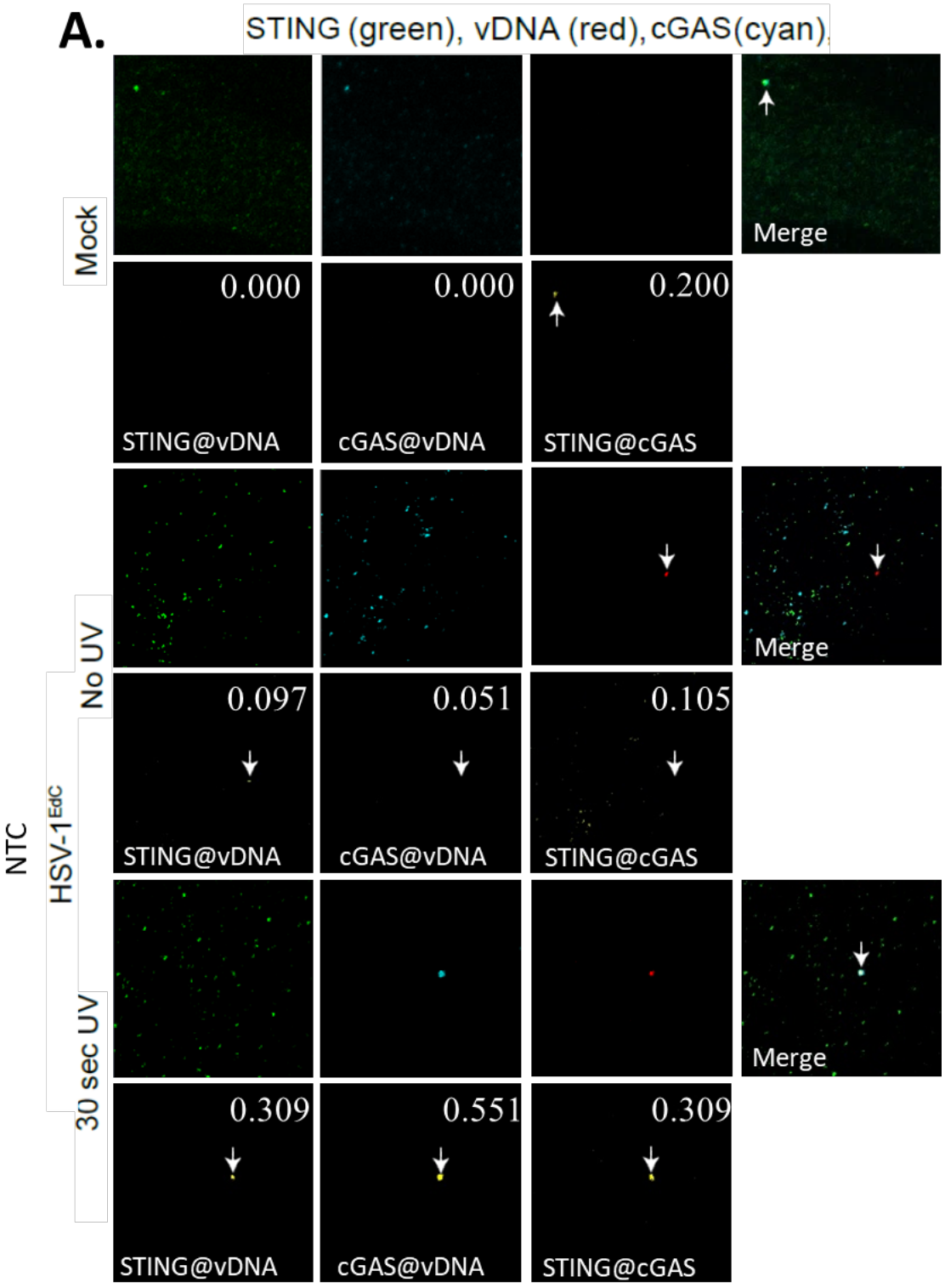
A.
STING (green), vDNA (red), cGAS(cyan),
Mock
NTC
HSV-1EdC
No UV
30 sec UV
Merge
0.000
STING@vDNA
0.000
cGAS@vDNA
0.200
STING@cGAS
Merge
0.097
STING@vDNA
0.051
cGAS@vDNA
0.105
STING@cGAS
Merge
0.309
STING@vDNA
0.551
cGAS@vDNA
0.309
STING@cGAS

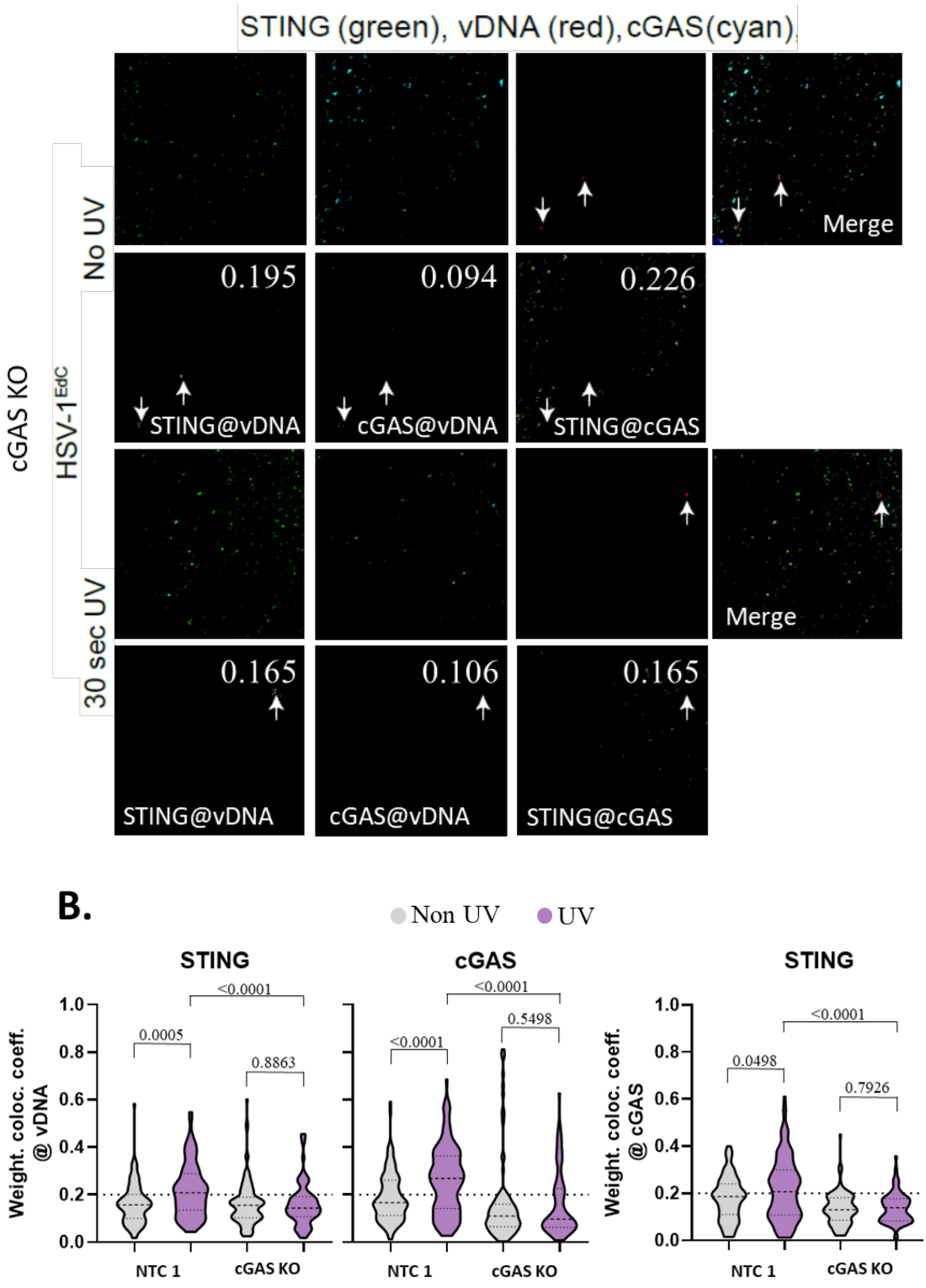

Figure 32. cGAS localization to UV treated HSV-1 genomes is required for the recruitment of STING.

NTC or cGAS KO HFt cells were infected with 3 PFU/cell of non-UV or UV irradiated HSV-1. Cells were fixed and permeabilized at 90 mpi. vDNA was detected using click chemistry. STING and cGAS were detected by indirect immunofluorescence. Nuclei were stained with DAPI. FoV were derived from cell cytosol. (A) Localization of STING (green) and cGAS (cyan) to cytosolic viral genomes (red). Cut mask (yellow) highlights the regions of colocalization between the cellular proteins of interest

and non-UV or UV irradiated HSV-1 genomes. Weighted colocalization coefficient shown. White arrows indicate individual HSV-1 genome foci. (B) Quantitation of cellular protein recruitment to infecting vDNA or each other in the cytoplasm at 90 mpi. Black line: median weighted (w.) colocalization coefficient; dashed lines: SD. n>80 nuclei per sample population derived from a minimum of three independent repeats. P value shown; Mann-Whitney *U*-test.

6.2.5. UV irradiation of HSV-1 enhances cGAS interaction with vDNA

cGAS has been identified as a DNA sensing molecule that directly interacts with DNA in a sequence length-dependent manner (Sun et al., 2013; Andreeva et al., 2017; Luecke et al., 2017). As we had observed an increase in cGAS and STING recruitment to vDNA following UV irradiation, we next investigated the interaction of these two endogenous PRRs with vDNA by ChIP-qPCR. HFt cells were seeded overnight prior to infection with non-UV or UV irradiated HSV-1 at an MOI of 3 PFU/cell. Samples were processed for chromatin extraction at 90 mpi and the IP performed using rabbit polyclonal antibodies raised against cGAS or STING. Non-immune IgG was used as a negative control. The bound vDNA was measured as a percentage of the soluble input DNA using two independent primer probe sets that detect Us3 and UL36 by qPCR. The input of non-UV and UV irradiated HSV-1 was equivalent, as determined by the ΔCT value for both viral genes (Figure 33A and B). The fraction of non-UV irradiated HSV-1 DNA associated with cGAS was consistent and at similar levels as the IgG background. Interestingly, UV irradiation of HSV-1 resulted in the significant increase of the fraction of viral genomes associated with cGAS, with these interactions significantly above IgG background (Figure 33A). On the other hand, endogenous STING was not observed to interact with HSV-1 DNA as the fraction of viral genomes associated with STING was comparable to background levels (Figure 33B). Collectively these data demonstrated that there is a direct interaction between cGAS, but not STING, with HSV-1 DNA that is enhanced upon UV irradiation. These findings correlate with our microscopy observations, which suggested that cGAS promotes the recruitment of STING to vDNA independently of STING. Whether the enhanced levels of interaction observed between cGAS and vDNA occurs as a result of increased binding affinity or increased numbers of cytosolic genomes following the UV irradiation remains to be determined.

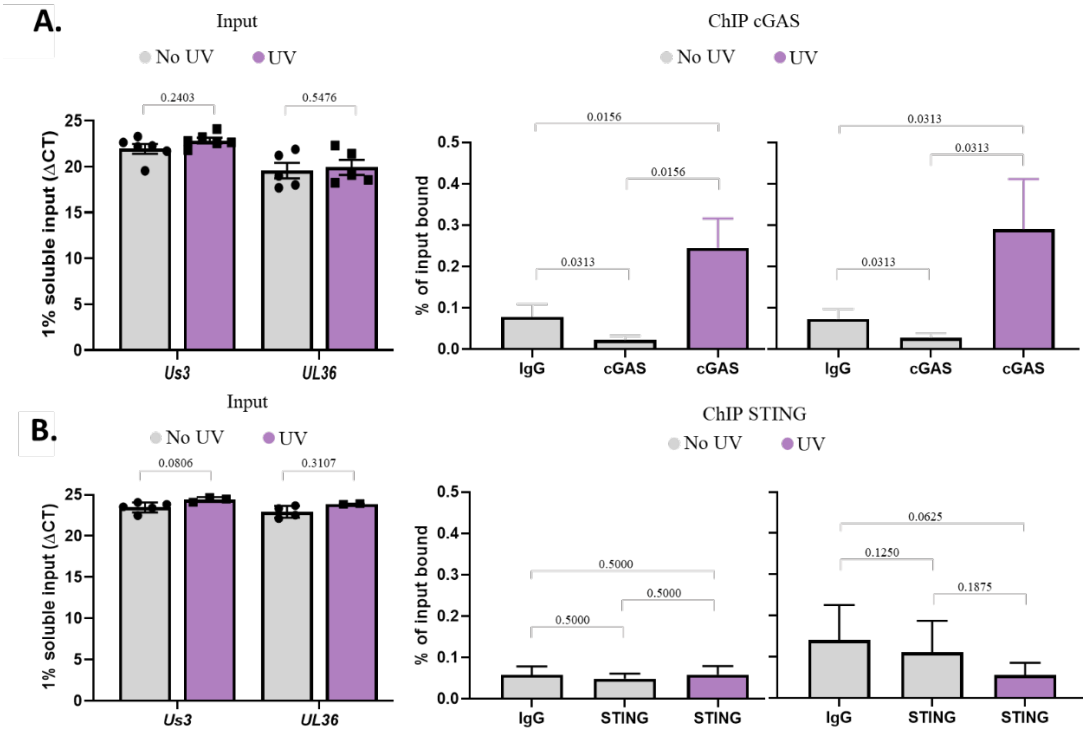

Figure 33. UV irradiation of HSV-1 enhances cGAS, but not STING interaction with vDNA.
HFts were seeded overnight prior to infection with non-UV or UV irradiated HSV-1 at an MOI of 3 PFU/cell. Cells were UV crosslinked at 90 mpi and chromatin extracted. Immunoprecipitation was carried out using cGAS, STING, and IgG (negative control) antibodies. Relative levels of HSV-1 DNA bound to the target proteins was measured by qPCR using primer-probes that recognize Us3 and UL36 viral sequences. (A) Bar graphs (left) showing the ΔCT value of the input virus for both non-UV and UV irradiated HSV-1. Individual points shown, black lines: mean. Data was pooled from 5 independent repeats. P value shown; Paired student *t* test. Bar graphs (right) showing the percentage of vDNA, bound to cGAS or IgG. Mean and standard error of the mean shown; Data pooled from 5 independent repeats. P value shown; Paired one-tailed non-parametric Wilcoxon test. (B) Bar graphs (left) showing the ΔCT value of the input virus for both non-UV and UV irradiated HSV-1. Individual points shown, black lines: mean. Data was pooled from 5 independent repeats. Paired student *t* test; P>0.05 ns (not significant). Bar graphs (right) showing the percentage of viral DNA, bound to STING or IgG. Mean and standard error of the mean shown; Data pooled from 5 independent repeats. P value shown; Paired one-tailed non-parametric Wilcoxon test.

6.2.6. Sp1 recruitment to cytoplasmic HSV-1 DNA is inhibited upon UV irradiation

Sp1 is a cellular transcription factor that has been reported to enhance IE and E gene expressions, as these genes contain multiple Sp1 binding sites (Pande, Petroski & Wagner, 1998; Tuan Nguyen-huynh & Schaffer, 1998; Gu, Huang & Hyward, 1995; Jones & Tjian, 1985). Given that recruitment of both cGAS and STING was increased following UV irradiation (Figures 26 and 27), it raised the hypothesis that there might be steric hindrance between cGAS and an unidentified cellular factor(s). To this end, we investigated the recruitment of Sp1 to HSV-1 genomes in the nucleus and cytosol. HFt cells were seeded overnight prior to infection with non-UV irradiated or UV irradiated HSV-1 at an MOI of 3 PFU/cell. PML was used as a positive control (Figure 34A). In the nucleus, Sp1 was not recruited to vDNA by 90 mpi, whereas PML showed characteristic recruitment to HSV-1 DNA that was reduced upon UV irradiation (Figure 34B). In contrast, cytoplasmic Sp1 was observed to associate with non-irradiated HSV-1 genomes at 90 mpi (w. coloc. coeff. of ≤0.6). This association was reduced following UV irradiation of HSV-1, potentially due to thymine dimers formation abrogating genome decompaction and Sp1 binding to vDNA (Figure 34B). Collectively, these data demonstrate cytosolic DNA to bind multiple cellular proteins that inhibit or influence PRR detection of viral PAMPs. These data suggest that UV irradiation may enhance cGAS detection of vDNA through impaired binding of other host factors that actively compete for vDNA binding in the cytosol. Whether this mechanism of competitive DNA binding/steric inhibition occurs in the nucleus too remains to be determined.

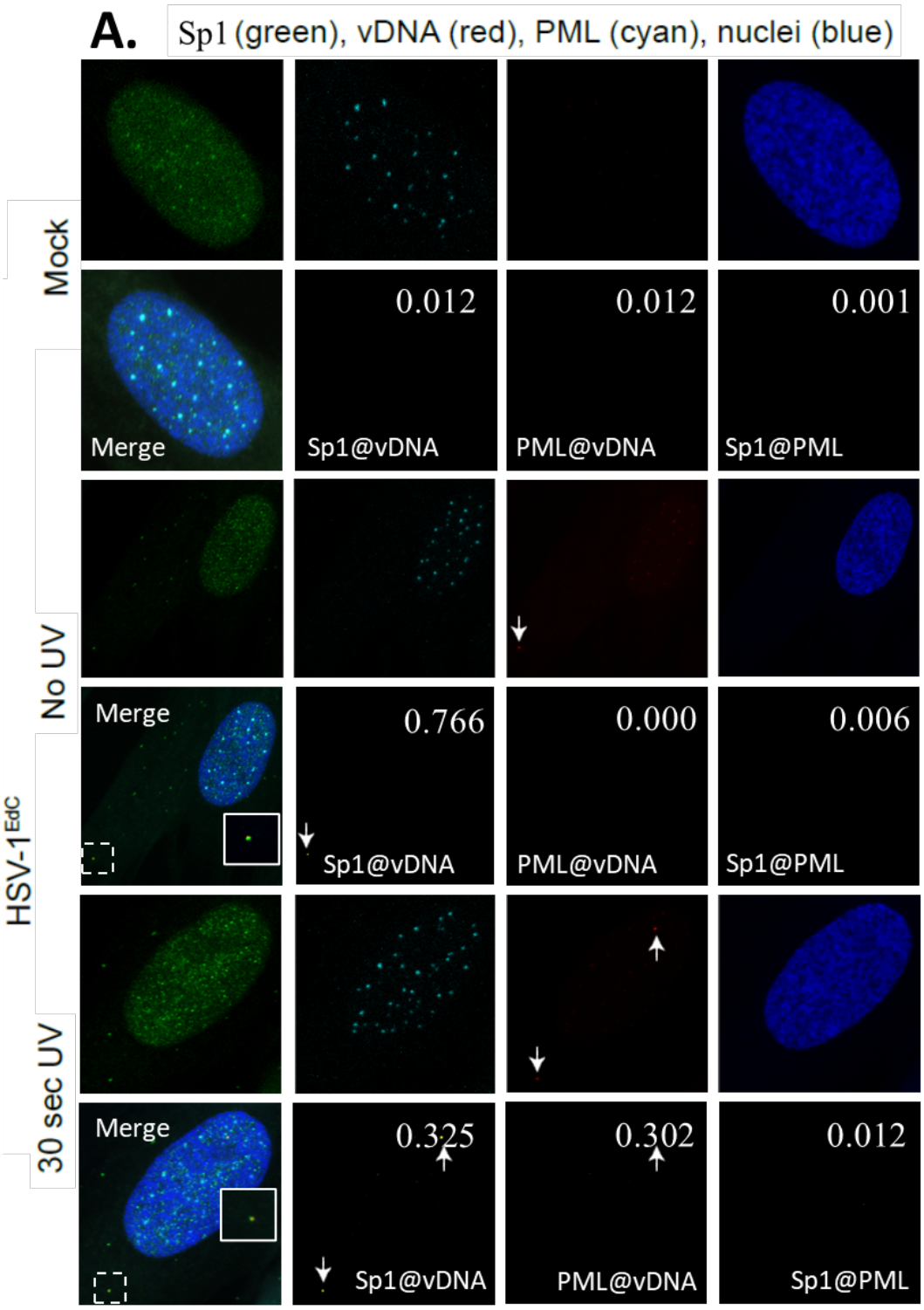
A.
Sp1 (green), vDNA (red), PML (cyan), nuclei (blue)
Mock
No UV
30 sec UV
HSV-1EdC
Merge
0.012
Sp1@vDNA
0.012
PML@vDNA
0.001
Sp1@PML
Merge
0.766
Sp1@vDNA
0.000
PML@vDNA
0.006
Sp1@PML
Merge
0.325
Sp1@vDNA
0.302
PML@vDNA
0.012
Sp1@PML

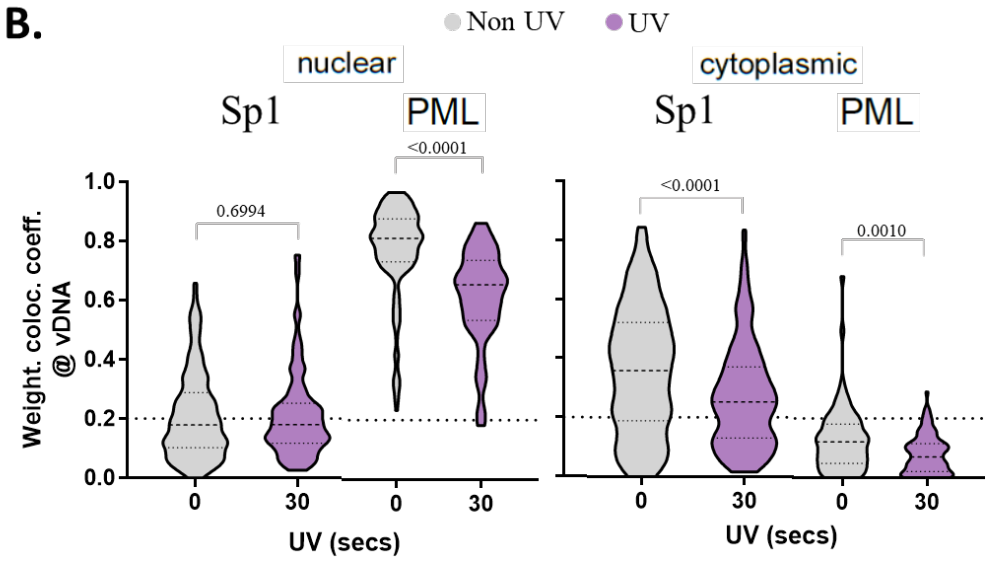

Figure 34. Sp1 localization to HSV-1 genomes is decreased following UV irradiation.
NTC or cGAS KO HFt cells were infected with 3 PFU/cell of non-UV or UV irradiated HSV-1. Cells were fixed and permeabilized at 90 mpi. vDNA was detected using click chemistry. STING and cGAS were detected by indirect immunofluorescence. Nuclei were stained with DAPI. (A) Localization of Sp1 (green) and PML (cyan) to infecting viral genomes (red), indicated with white arrows. Cut mask (yellow) highlights the regions of colocalization between the cellular proteins of interest and non-UV or UV irradiated HSV-1 genomes. Weighted colocalization coefficient shown. White arrows indicate individual HSV-1^{EdC} genome foci. (B) Quantitation of cellular protein recruitment to infecting vDNA or each other in the cytoplasm at 90 mpi. Black line: median weighted (w.) colocalization coefficient; dashed lines: SD. n>50 nuclei per sample population derived from a minimum of three independent repeats. P value shown;; Mann-Whitney *U*-test.

6.2.7. KO of Sp1 affects the recruitment of cGAS and STING to HSV-1 genomes

The recruitment profile of Sp1 in HSV-1 infected HFt cells presented some evidence for our hypothesis that a cellular protein may sterically inhibiting the binding of cGAS and STING to non-UV irradiated vDNA in the cytosol. To further test this, we decided to investigate the localization of cGAS and STING during HSV-1 infection in Sp1 KO cells. To this end, HFt cells were CRISPR-Cas 9 gene edited to disrupt the Sp1 gene expression. However, as Sp1 is an important cellular transcription factor required for cellular growth and division, the Sp1 KO cell line was derived through clonal selection due to difficulties with bulking of the transformed HFt cells. The KO of Sp1 was assessed by western blotting (Figure 35A and B). NTC was used as an accompanying internal control. NTC or Sp1 KO HFt cells were seeded overnight prior to infection with either non-UV or UV irradiated HSV-1 at an MOI of3 PFU/cell. Samples were fixed and processed at 90 mpi. Click and IF were utilized to detect vDNA and the cellular PRRs (cGAS and STING), respectively (Figure 36A). In NTC cells, cGAS and STING were recruited at low levels to non-UV irradiated HSV-1 DNA and this recruitment was enhanced following UV irradiation of the virus, in line with our previous observations (Figure 36A). Quantitative analysis of Sp1 KO infected cells showed that there was no recruitment of either cGAS or STING to HSV-1 DNA foci, irrespective of UV irradiation (Figure 36A and B). Additionally, STING failed to colocalize with cGAS during HSV-1 infection as demonstrated by the low weight. coloc. coeff. (<0.2) (Figure 36B). These observations prove our hypothesis to be null, as these data suggest that localization of Sp1 to sites of vDNA foci may be a requirement for the recruitment of cGAS, and thereafter STING during HSV-1 virus infection. The decrease in Sp1 localization to HSV-1 genomes following UV irradiation and enhanced recruitment of cGAS and STING demonstrate that even a weaker interaction between Sp1 and vDNA may be sufficient to recruit the cellular PRRs. However, western blot analysis of Sp1 KO cells (Figure 36A and B) demonstrated that Sp1 may play an important transcriptional role in the expression of cGAS, as cGAS protein levels were reduced in the absence of Sp1. This would explain the reduced cGAS recruitment to cytoplasmic

HSV-1 DNA and therefore the further recruitment of STING. Additional experimentation is required to determine if Sp1 regulates the expression of cGAS during HSV-1 infection.

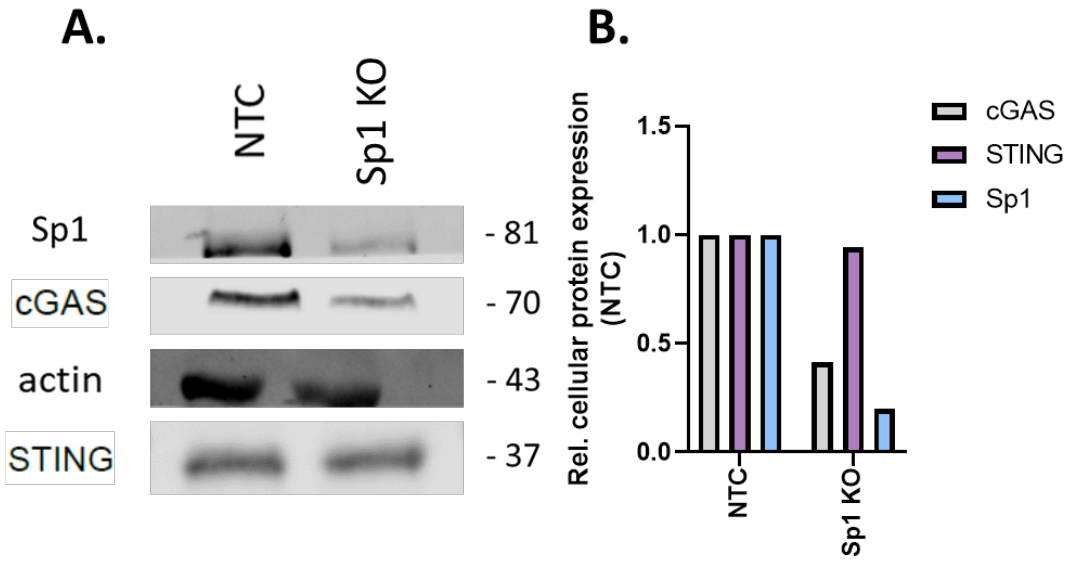

Figure 35. Knock-down of Sp1.

HFt cells were CRISPR-Cas 9 gene edited with guide RNAs to target the Sp1. A Non-targeted Control (NTC) gRNA was used as a negative control. (A) Western blot showing the levels of Sp1, cGAS, STING and actin (loading control) in whole cell lysates derived from NTCs or Sp1 KO HFt cells. Membranes were probed for Sp1 to determine the level of knock-down in the KO cell lines and cGAS or STING to evaluate their protein expression. (B) Bar graph showing the relative protein expression of Sp1, cGAS and STING in either cell line (as in A), normalized to their respective levels in NTC cells.

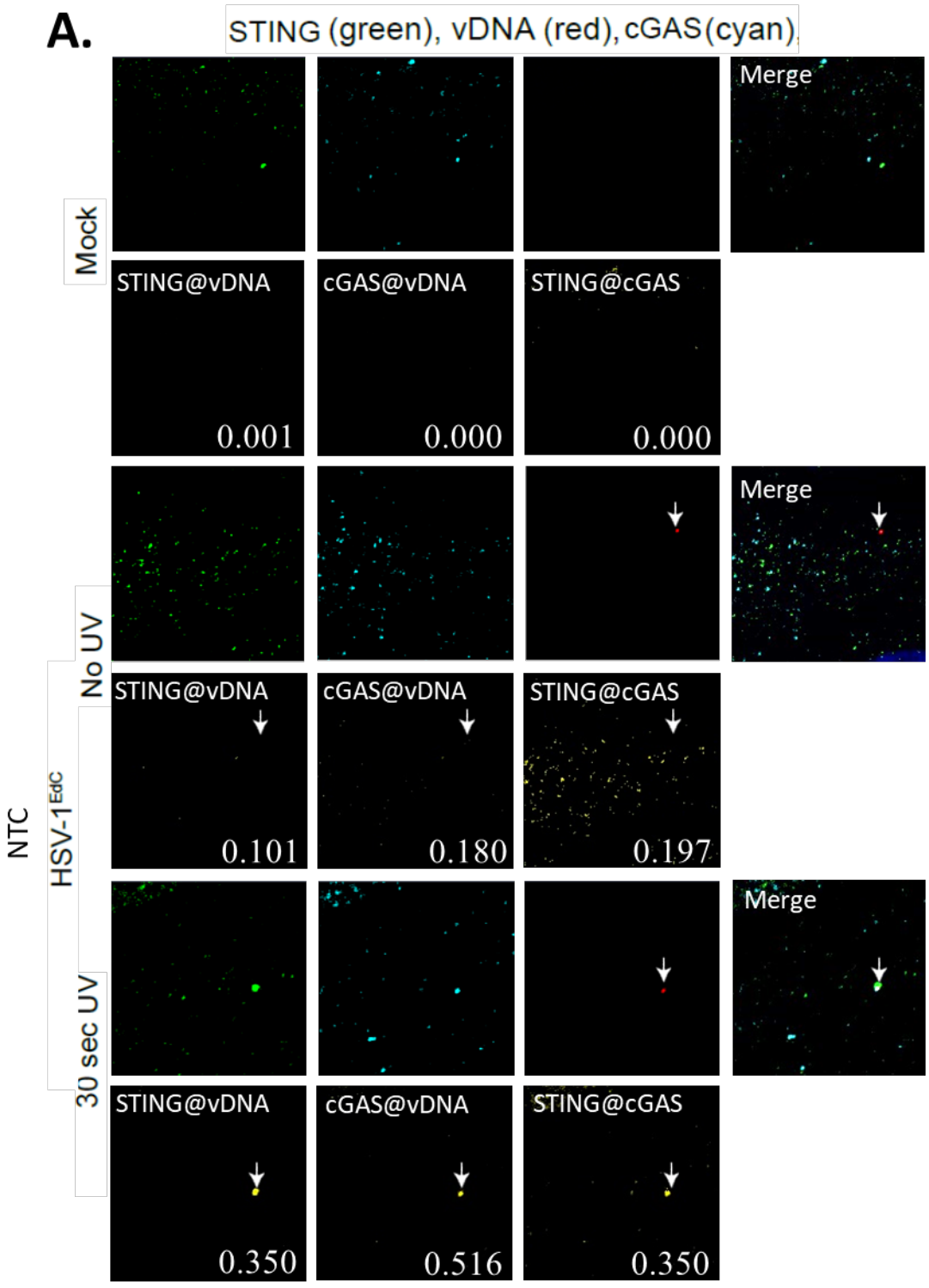
A.
STING (green), vDNA (red), cGAS (cyan)
Merge
Mock
STING@vDNA
cGAS@vDNA
STING@cGAS
0.001
0.000
0.000
Merge
No UV
STING@vDNA
cGAS@vDNA
STING@cGAS
0.101
0.180
0.197
NTC
HSV-1 EdC
Merge
30 sec UV
STING@vDNA
cGAS@vDNA
STING@cGAS
0.350
0.516
0.350

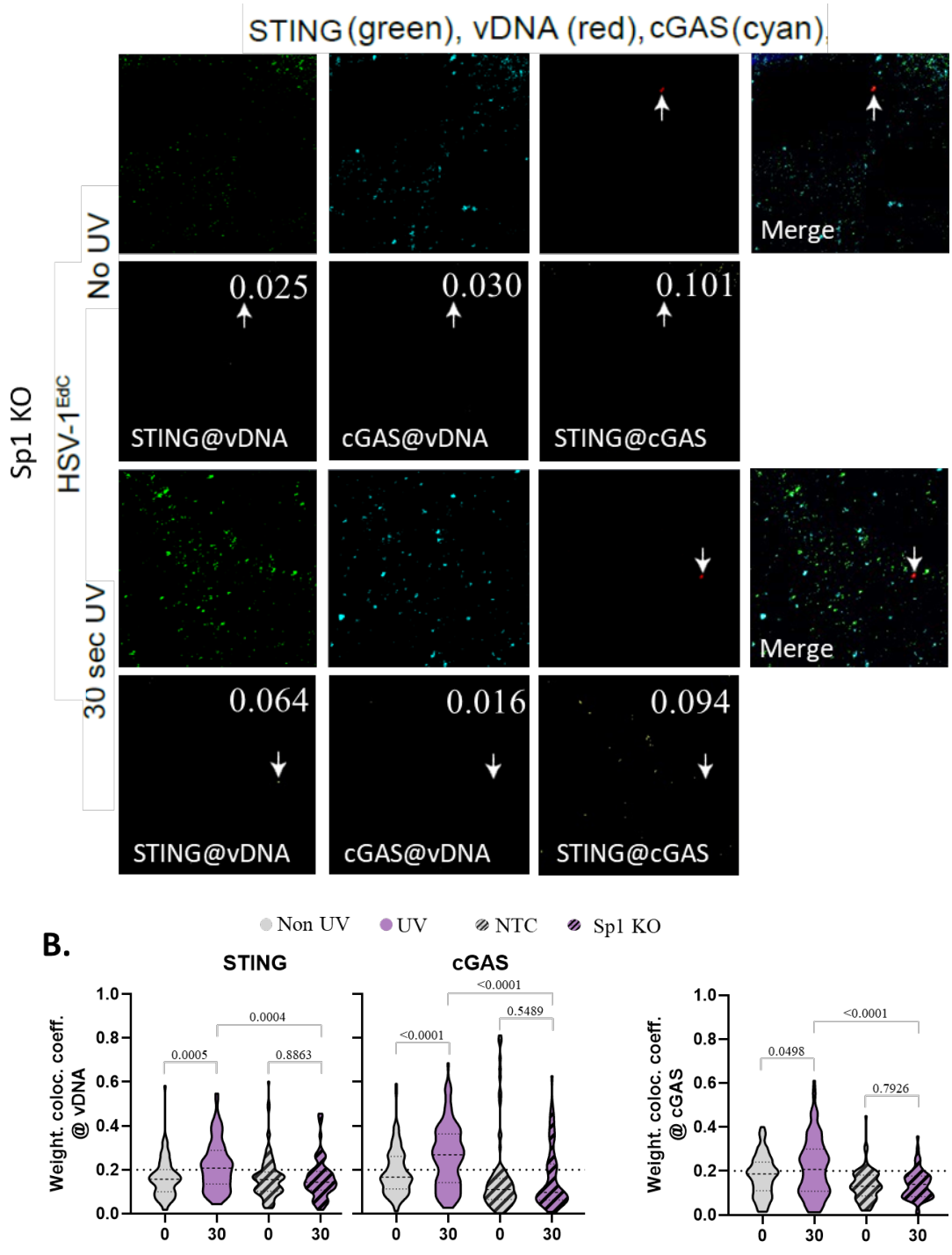

Figure 36. Sp1 KO affects the localization of cGAS and STING to UV irradiated HSV-1 genomes. NTC or Sp1 KO HFt cells were infected with 3 PFU/cell of non-UV or UV irradiated HSV-1. Cells were fixed and permeabilized at 90 mpi. vDNA was detected using click chemistry. STING and cGAS were detected by indirect immunofluorescence. Nuclei were stained with DAPI. (A) Localization of STING (green) and cGAS (cyan) recruitment to infecting viral genomes (red), indicated by white arrows. Cut mask (yellow) highlights the regions of colocalization between the cellular proteins of interest and non-UV or UV irradiated HSV-1 genomes. Weighted colocalization coefficient shown. White arrows indicate individual HSV-1 genome foci. (B) Quantitation of cellular protein recruitment to infecting vDNA or STING to cGAS in the cytoplasm at 90 mpi. Black line: median weighted (w.)

colocalization coefficient; dashed lines: SD. n>90 nuclei per sample population derived from a minimum of three independent repeats. P value shown; Mann-Whitney *U*-test.

6.3. Summary

The detection of viral PAMPs, such as vDNA, by cellular PRRs is critical for the activation of immune signalling. Following pathogen invasion, the PRR molecules recognise specific pathogen-associated motifs and ultimately lead to the production of signalling molecules, such as cGAMP, that stimulate signal transduction cascades that ultimately lead to cytokine expression to control infection (Abe, Marutani & Shoji, 2019; Ma, Ni & Damania, 2018). Since its discovery in 2013 (Zhang et al., 2013; Sun et al., 2009), the cGAS-STING pathways has been extensively researched in its role to detect vDNA. Recent reports have shown that it is heavily antagonized during HSV-1 infection, for example UL37 deaminates cGAS to inhibit cGAMP production or UL36 which binds directly to STING to promote deubiquitination, resulting in the decreased production of IFNβ and ISGs (Royer & Carr, 2016; Reinert et al., 2016; Yamashiro et al., 2020; Wang et al., 2020; Huang et al., 2018a, 2018b; Orzalli et al., 2015; Su & Zheng, 2017; Zhang et al., 2018a, 2018b). However, the spatiotemporal kinetics of this disruption have yet to be described. In the previous chapters we demonstrated that UV irradiation of HSV-1 caused the premature uncoating of HSV-1 genomes in the cytosol that led to enhanced levels of immune signalling leading to IFNβ transcription (Figures 10, 12 and 14). In this chapter, we investigated the interaction between cytoplasmic cellular PRR molecules and HSV-1 DNA in the context of UV irradiated virus infection.

Characterizing the recruitment profiles of cGAS and STING, we found both proteins to increase in their relative localization to vDNA in the cytoplasm (Figures 26 and 17). Notably, we could not observe cGAS or STING localization to vDNA in the nucleus. With respect to cGAS, our data are in line with the well characterized role of cGAS in cytosolic vDNA detection (Zhou et al., 2018; Civril et al., 2013; Luecke et al., 2017; Du & Chen, 2018). On the other hand, STING's recruitment was unexpected, as STING is an ER bound dimer that interacts with cGAS indirectly via cGAMP following cGAS activation upon DNA binding (Zhang et al., 2013; Shang et

al., 2019; Diner et al., 2013; Shang et al., 2012; Burdette et al., 2011; Ishikawa & Barber, 2008). It has been shown that STING is capable of binding DNA directly, so a more direct role in DNA detection is plausible (Abe et al., 2013b). However, we failed to observe STING binding to vDNA by ChIP (Figure 33).

STING localization to cGAS during HSV-1 infection was present and was enhanced in the context of a UV irradiated HSV-1 infection, although direct contact with DNA was rare (Figure 33). Both of these PRRs are crucial for the induction of the type-I IFN response to UV irradiated HSV-1 (Figure 30) (Stetson & Medzhitov, 2006). Our high-resolution analysis demonstrated cGAS and STING to localize in close proximity to cytosolic vDNA, with cGAS making direct contact (Figure 28). cGAS localized closer to vDNA than STING, consistent with its reported DNA binding properties (Zhou et al., 2018; Civril et al., 2013; Luecke et al., 2017). KO of cGAS inhibited the recruitment of STING to HSV-1 DNA, demonstrating that cGAS promotes the accumulation of STING at vDNA (Figure 32). Direct interaction with vDNA was only observed for cGAS, indicating that STING is unlikely to directly interact with vDNA in our model system. Notably, cGAS binding to vDNA in the presence of UV irradiation was significantly enhanced compared to non-UV irradiated HSV-1 DNA (Figure 33). These findings demonstrated that cGAS recruitment is enhanced when HSV-1 is UV irradiated. Whether cGAS and STING form a complex at the site of vDNA is an interesting area of investigation for future research.

Although Sp1 is a well described nuclear transcription factor that influences the expression of many cellular genes, our data identified Sp1 as a cellular factor being recruited to cytoplasmic vDNA foci (Figure 34) (Jackson et al., 1990; Chu, 2012). The high level of colocalization observed for Sp1 at HSV-1 genomes was site specific and only present in the cytoplasm and not in the nucleus at 90 mpi (Figure 34). Additionally, the recruitment of Sp1 was affected upon UV irradiation of HSV-1 genomes, showing an inverse correlation between the level of Sp1 recruitment and

UV irradiation (Figure 36). These observations may explain the enhanced recruitment of the cytoplasmic DNA sensors cGAS and STING in the context of UV irradiated virus infection, as the potential steric inhibition by Sp1 would be lost. HFt cells that were KO for Sp1 were unable to recruit cGAS or STING to sites of HSV-1 DNA irrespective of UV irradiation. Moreover, the colocalization between both cellular proteins in the absence of Sp1 was lacking (Figure 36). These findings provide evidence that cGAS may require Sp1 recruitment to vDNA prior to cGAS localization and further STING recruitment during HSV-1 infection. However, the levels of cGAS protein expression were affected in the absence of Sp1, indicating an indirect role of Sp1 via its transcript regulatory function. Notably, there is an Sp1 binding site present on the cGAS gene upstream of the promoter region. This remains an interesting hypothesis for future research, as many herpesviruses influence the expression of Sp1 during infection.

Collectively, these findings shed light into the mechanisms of DNA detection during UV irradiated virus infection and provide an explanation for the intense IFN response of cells produced in response to UV virus infection. The cGAS-STING pathway is crucial in mediating the DNA recognition during UV HSV-1 infection. The mechanism that this pathway utilizes to recognize UV irradiated foreign nucleic acid differs from the canonical pathway and may be masked by antagonistic HSV-1 proteins during infection (e.g., UL37, UL46). The exact detail of this mechanism is not fully clear and warrants further experimentation.

7. Optimizing CLICK labelling of hCMV and characterizing the cellular intrinsic immune response

7.1. Overview

HCMV is a betaherpesvirus that, similar to HSV-1, has a dsDNA genome that replicates in the nucleus of infected cells (Shenk & Stinski, n.d.; Landolfo et al., n.d.). Following membrane fusion and cellular uptake, the capsid binds to microtubules to transit through the cytoplasm to the nucleus (Ogawa-Goto et al., 2003). However, unlike HSV-1, the intrinsic immune response to hCMV infection has not been as well studied. It has been reported that hCMV DNA localizes to PML-NBs, which are disrupted following the de novo expression of IE1 (Ishov, Stenberg & Maul, 1997; Wilkinson et al., 1998; Korioth et al., 1996). PML knockdown alleviates the intrinsic repression of hCMV and enhances lytic replication, whilst the transient expression of PML reverses the phenotype (Tavalai et al., 2006). Sp100 has also been shown to play a role in hCMV restriction, as Sp100 KD results in increased viral plaque formation (Adler et al., 2011). Daxx and ATRX repress IE1 gene expression, and their individual knock down has a positive effect on hCMV replication and plaque formation (Tavalai, Rechter & Stamminger, 2008; Lukashchuk et al., 2008; Woodhall et al., 2006). The proteasomal-mediated degradation of Daxx and displacement of ATRX by the tegument protein pp71 alleviates IE1 gene silencing to promote IE1 gene expression and the onset of lytic replication (Hofmann, Sindre & Stamminger, 2002; Hwang & Kalejta, 2007; Lukashchuk et al., 2008; Saffert & Kalejta, 2006). One of the reasons for the poor understanding in the spatiotemporal kinetics of these initial nuclear events to hCMV infection events is due to a lack of a suitable model system that would allow for the direct visualization of host factor recruitment to vDNA. Studies looking into the association of intrinsic immune factors have historically utilized indirect labelling methods, for example the use of viral DNA binding proteins, or in situ hybridization to visualize vDNA (Ishov, Stenberg & Maul, 1997). Such methods typically rely on the use of high MOIs to be able to successfully detect viral genomes as well as harsh processing conditions, which ultimately lead to the saturation of

intrinsic immune defences, cytotoxicity, and poor detection of cellular host factors. In order to circumvent these issues, we optimized a CLICK labelling protocol to visualize hCMV DNA that would be applicable to investigate the PML-NB intrinsic immune response. Unlike HSV-1, hCMV required different labelling conditions as the kinetics of infection is much slower and studies have shown that the incorporation of nucleoside analogues to be significantly different (Manska, Octaviano & Rossetto, 2020). To date there is only one microscopy-based study currently under review using this method to investigate the role of PML-NBs and other intrinsic restriction factors to hCMV utilizing click chemistry (Scherer et al., 2021).

In this chapter a combination of EdC/EdA labelling of hCMV genomes and indirect immunofluorescence confocal microscopy was used to characterize the recruitment of nuclear intrinsic immune factors (PML-NB major constituent proteins) to hCMV genomes. This analysis was performed up to 360 mpi and an MOI of 3 FFU/cell. hCMV viral genome translocation into the nucleus occurred at a much slower rate compared to HSV-1, with 360 mpi being optimal for vDNA delivery into the nucleus. Key PML-NB protein constituents, but not SUMO proteins, were observed to be recruited to sites of infecting hCMV DNA and exhibited a genome entrapment mechanism of viral inhibition, similar to that observed for HSV-1 (Alandijany et al., 2018). IE1 and pp71 expression was enough to overcome the intrinsic immune response, which dispersed PML and Daxx from vDNA. These findings provide further evidence that the PML-NB intrinsic immune response is conserved against Herpesviruses from multiple subfamilies.

7.2. Results

7.2.1. Optimization of EdC/A-labelling of hCMV in IMR-90 cells

EdC/EdA labelling of hCMV (AD169) was carried out in IMR-90 cells as the viral titre yields were the highest in this cell line and the nucleoside analogues did not induce observable cytotoxicity. A combination of EdC and EdA was utilized due to poor incorporation of EdC into hCMV genomes alone (Manska, Octaviano & Rossetto, 2020). IMR-90 flasks were infected with hCMV stocks and incubated until visible CPE was observed, indicative of a productive infection to ensure the uptake of the click nucleotides. This typically occurred between 4-6 dpi, when daily pulsing with EdC/EdA at 5 mM (final concentration) commenced. Virus harvesting was performed when CPE reached 80-90% cell death to achieve the highest viral titres possible. This was usually seen between 12-14 dpi (Figure 37). Labelled hCMV was not processed through a NAP column due to a significant drop in virus during this cleaning-up step (Figure 38). This remained a limitation, as the free nucleotides present in the viral supernatant could be uptaken by cells and incorporated into cellular chromatin during cell division. This resulted in obstructed visualization of hCMV genomes within a population of cells. These labelled cells were excluded from our preliminary analysis, in order to begin to investigate if hCMV click labelling could be applicable to investigating nuclear intrinsic host immune defences (Figure 39). These labelling conditions worked, but a degree of variability was observed between the different viral preparations. To limit the effect of the difference in labelling efficiency on data interpretation, we utilized a single hCMV virus stock for all of the presented experiments below. Further optimising is ongoing within the lab, which has now established a column purification step and the labelling of more clinically relevant strains of hCMV (e.g., TB40E).

Initially experiments were aimed at characterising the labelling efficiency of the viral stock to ensure that the vDNA signal is detectable. To determine the virus concentration, we utilized a Foci Forming Unit (FFU) assay to estimate the concentration of the virus stock for future infections, as normal PFU assays take upto 14 days to perform (Figure 39A). HFt cells were infected with two MOIs of virus – 0.01 and 0.1 FFU/cell and fixed at 360 mpi. Samples were stained by click chemistry and cellular nuclei were stained with DAPI stain. The number of viral genomes per FoV, genomes per nucleus and percentage of infected cells all increased at the higher MOI of 0.1 FFU/cell compared to 0.01 FFU/cell (Figure 39B, C and D). Quantitation of microscopy images demonstrated that there was no difference in the percentage of nuclear and cytoplasmic genomes between the two different MOIs used (Figure 39E). These data demonstrated that the CLICK-labelled virus stock (hCMV$^{EdC/EdA}$) was readily detectable and suitable for the purpose of our investigations.

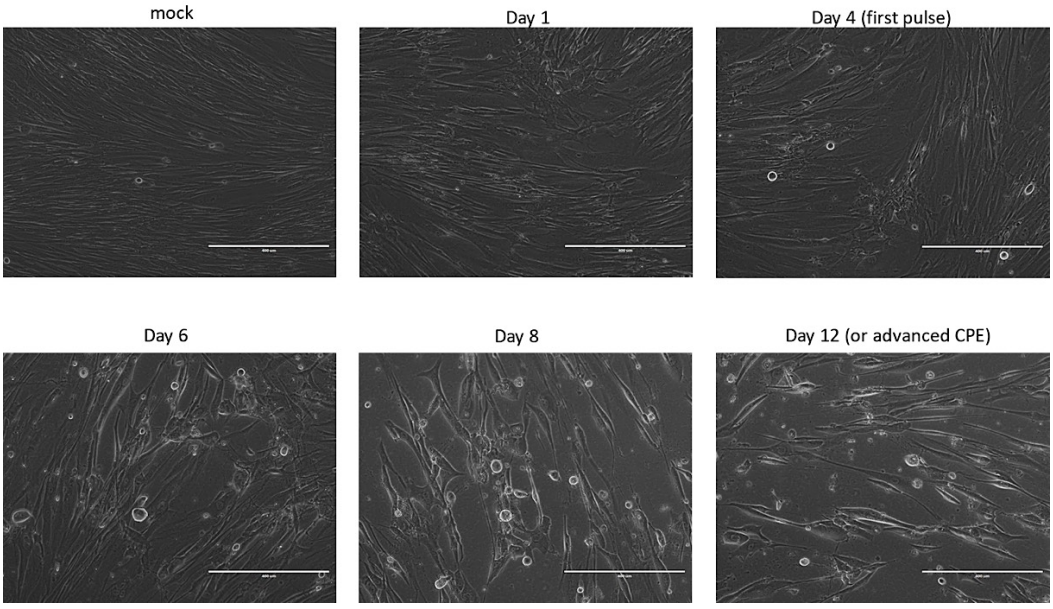

Figure 37. Pulsing and harvesting of EdC/EdA labelled hCMV.

Flasks of IMR-90 cells were mock infected (negative control) or infected with hCMV (strain AD169) at an MOI of 0.01 PFU/cell. Following absorption, flasks were incubated for 4-5 days until CPE was observed. Pulsing with EdC/EdA (final concentration of 5μM) was initiated every 24 hrs. Virus was harvested when advanced CPE was observable.

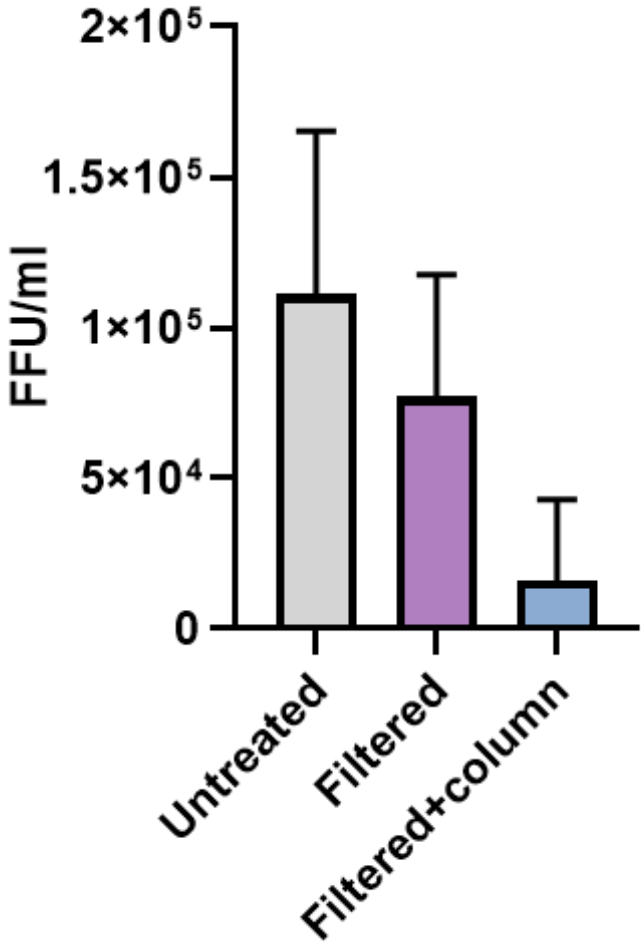

Figure 38. Clean-up and titration of labelled hCMV virus.
HFF cells were seeded overnight prior to infection with neat labelled hCMV, filtered (0.45 μM filter) labelled hCMV or NAP column purified filtered hCMV. At 24 hours post-infection, cells were fixed and permeabilized, and immunostained for hCMV foci formation using an anti-pp72 monoclonal antibody. Cells were analysed using a Celigo Image Cytometer and the FFU titre was then calculated.

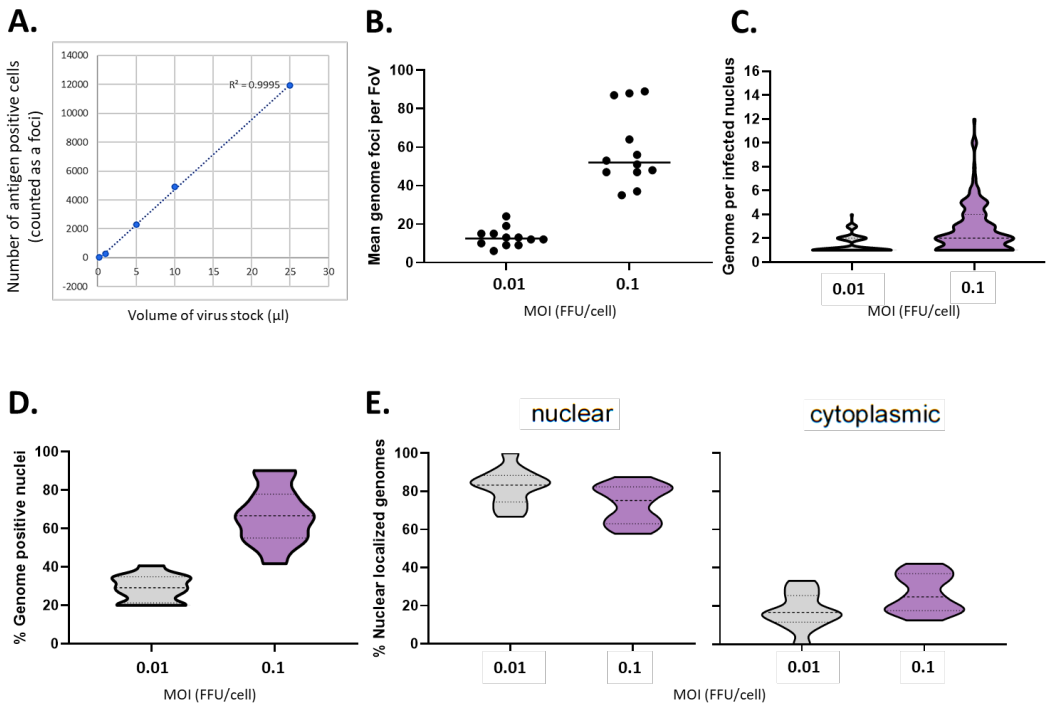

Figure 39. Characterization of labelled hCMV virus stock.
(A) HFF cells were seeded overnight prior to infection with labelled hCMV with indicated volumes. At 24 hours post-infection, cells were fixed and permeabilized, and immunostained for hCMV foci formation using an anti-pp72 monoclonal antibody. Cells were analysed using a Celigo Image Cytometer and the FFU titre was then calculated. (B) HFF cells were seeded overnight prior to infection with hCMV at an MOI of 0.5 FFU/cell. Cell monolayers were fixed and permeabilized at 90 mpi. Viral DNA was visualized with click chemistry. Nuclei were stained with DAPI stain (blue). Number of genomes per FoV. Individual points shown; black line: median. n=3 fields of view per condition derived from a minimum of 3 independent experiments conducted in duplicate. (C) Total number of genomes per nucleus. Minimum of 3 independent experiments conducted in duplicate. (D) Percentage of genome positive nuclei per FoV over time. (E) Quantitation of the genome distribution (nuclear or cytoplasmic).

7.2.2. Direct visualization of hCMV$^{EdC/EdA}$ genomes demonstrate the dynamics of genome deposition

Having confirmed the hCMV genome labelling to have worked, we were able to utilize EdC-EdA labelled virus to directly detect input genomes prior to the onset of viral gene expression. Similar to HSV-1, CLICK chemistry was used to detect vDNA and indirect immunolabelling used to detect host cell restriction factors. HFF cells were seeded onto glass coverslips prior to infection with hCMV$^{EdC/EdA}$ at an MOI of 0.5 FFU/cell. Coverslips were fixed at different timepoints following the addition of virus (45, 90, 180 and 360 mpi), prior to staining for vDNA and nuclei with DAPI (Figure 40A).

Viral genomes could be detected as early as 45 mpi, with the majority of these being cytoplasmic (80%) at this time point. The sub-cellular localization of vDNA gradually shifted over time, with around 70% of hCMV$^{Edc/EdA}$ genomes being detected in the nucleus at 360 mpi (Figure 40A). Viral genome foci could be detected in approximately 30% of infected cells per FoV by 360 mpi (Figure 40B). The number of detectable genomes per nucleus remained consistent throughout the time course (Figure 40B). Collectively, these data demonstrate hCMV to have slower kinetics of genome transport to the nucleus compared to HSV-1 and identify 360 mpi as an initial timepoint to investigate nuclear genome association with PML-NBs. We therefore utilized 360 mpi as the experimental timepoint for the remainder of this chapter.

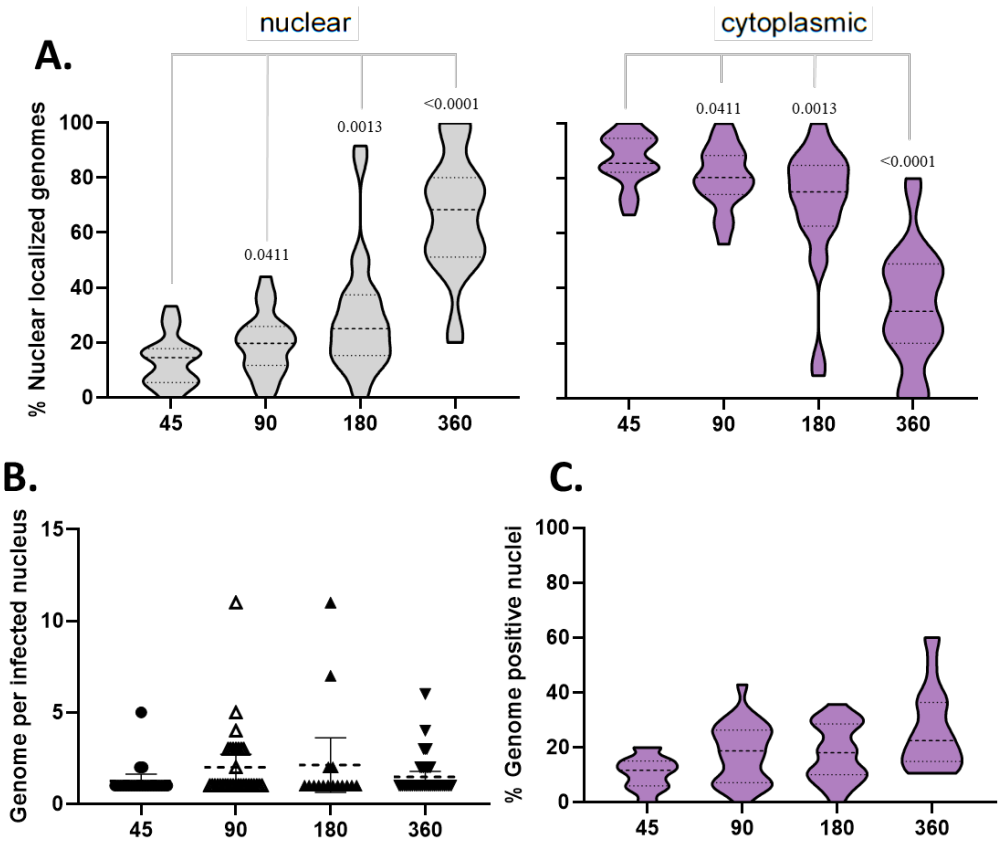

Figure 40. Time course of hCMV genome deposition in the nucleus.

HFF cells were seeded overnight prior to infection with hCMV at an MOI of 0.5 FFU/cell. Cell monolayers were fixed and permeabilized at 90 mpi. Viral DNA was visualized by click chemistry. Nuclei were stained with DAPI (blue). (A) Quantitation of the genome distribution (nuclear or cytoplasmic) over time per FoV expressed as a percentage (%). Black line: median with 95% CI; n=3 FoV per condition derived from a minimum of 3 independent experiments conducted in duplicate. P value shown; One-way ANOVA (Kruskal-Wallis). (B) Total number of genomes per nucleus. n≥100 genome foci per condition derived from 3 independent experiments conducted in duplicate. Individual points shown; black line: median with 95% CI. n=3 fields of view per condition derived from a minimum of 3 independent experiments conducted in duplicate. (C) Percentage of genome positive nuclei per FoV over time.

7.2.3. PML-NB proteins entrap hCMV vDNA from the outset of nuclear infection

Core constituent proteins that reside within PML-NBs can act as intrinsic host immune factors in the cellular restriction of herpesviruses, which in the case of HSV-1 can entrap vDNA leading tot its epigenetic silencing (Alandijany et al., 2018). However, it is not known if this mechanism of PML-NB entrapment is a panherpesvirus mechanism of restriction or Alphaherpesvirus specific (Reichelt et al., 2012, 2011a; Alandijany et al., 2018). PML-NBs have been described to associate with hCMV genome foci in the nucleus prior to IE1 expression (Ishov, Stenberg & Maul, 1997; Kelly, Driep & Wilkinson, 1995; Wilkinson et al., 1998; Korioth et al., 1996; Lee et al., 2004; Hou et al., 2017; Schilling et al., 2017). In order to investigate the recruitment of PML-NB proteins to hCMV vDNA following nuclear entry we utilized the CLICK labelled hCMV$^{EdC/EdA}$ (Figure 39) (Manska, Octaviano & Rossetto, 2020; Scherer et al., 2021).

HFF cells were seeded onto glass coverslips prior to infection with hCMV$^{EdC/EdA}$ at an MOI of 0.5 FFU/cell. Coverslips were fixed at 360 mpi, prior to staining for cellular proteins (PML, Daxx, ATRX and histone H3), DAPI and vDNA (Figure 41A). Infected cells exhibited a high degree of colocalization efficiency (w. coloc. coeff. ≤0.6) between PML and viral genome foci (Figure 41B). In contrast, histone H3, ATRX and Daxx were all demonstrated significantly lower levels of colocalization with hCMV vDNA less efficiently. Z-series imaging revealed hCMV genomes to be entrapped within PML-NBs, similar to that observed for HSV-1 and VZV (Figure 41C) (Alandijany et al., 2018; Reichelt et al., 2011a). Quantitative analysis of microscopy images demonstrated that Daxx, ATRX and histone H3 to have reduced localization to PML, during hCMV infection (Figure 41B). The hCMV tegument protein pp71 is known to target Daxx for dispersal from PML-NBs by mediating Daxx proteasomal degradation, which influences the recruitment of ATRX and histone H3 at PML-NBs through the histone H3.3 chaperone properties of Daxx (Ishov, Vladimirova & Maul, 2002; Cantrell & Bresnahan, 2006; Hwang & Kalejta, 2007). These data demonstrate PML-NBs

entrapment of vDNA to be a conserved host response to herpesvirus infection, although key mediators of intrinsic immunity (e.g., Daxx and ATRX) are missing from these structures that promote transcriptional silencing (Cantrell & Bresnahan, 2006; Ishov, Vladimirova & Maul, 2002; Woodhall et al., 2006).

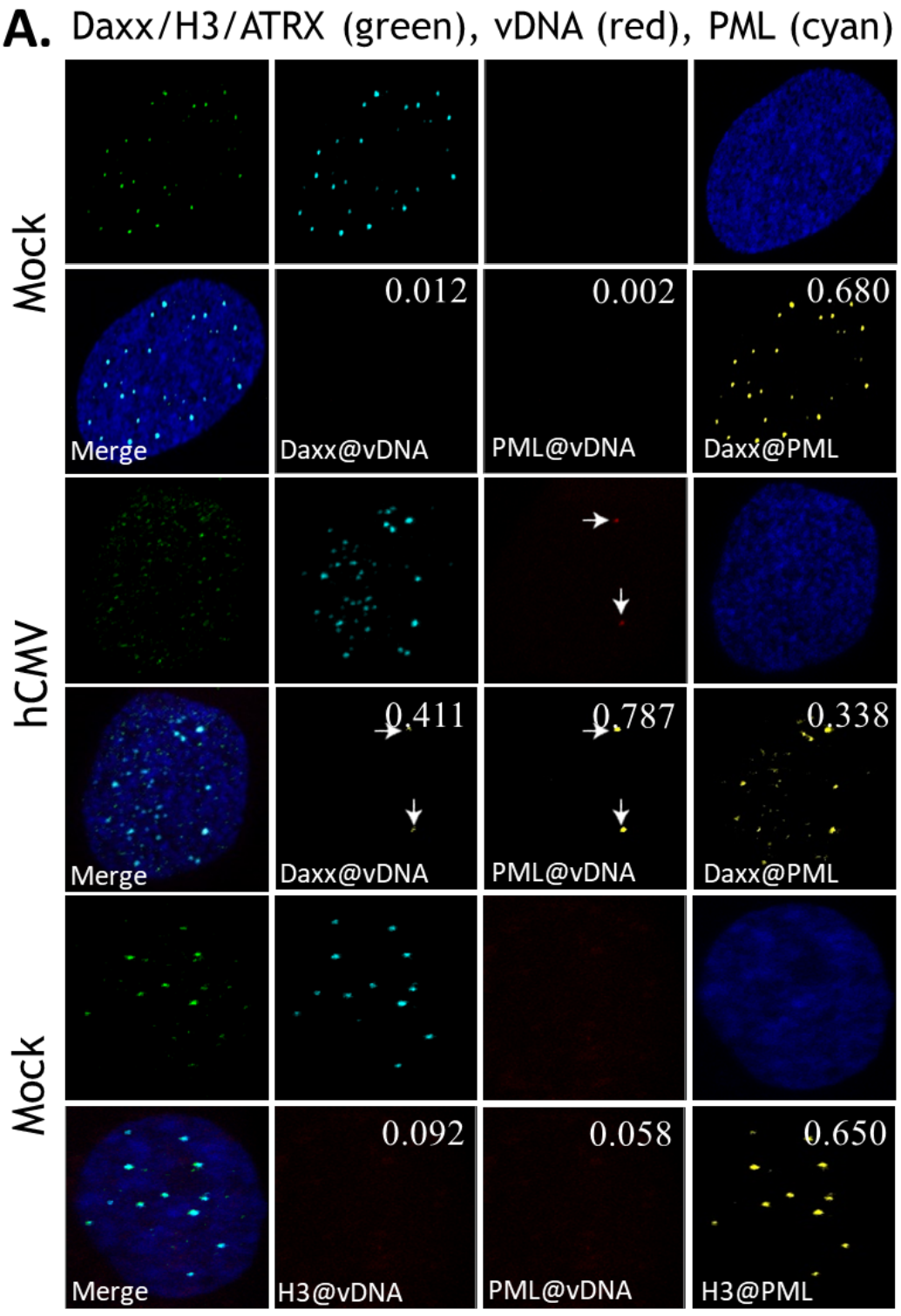
A. Daxx/H3/ATRX (green), vDNA (red), PML (cyan)
Mock
hCMV
Mock
Merge
0.012
Daxx@vDNA
0.002
PML@vDNA
0.680
Daxx@PML
Merge
0.411
Daxx@vDNA
0.787
PML@vDNA
0.338
Daxx@PML
Merge
0.092
H3@vDNA
0.058
PML@vDNA
0.650
H3@PML

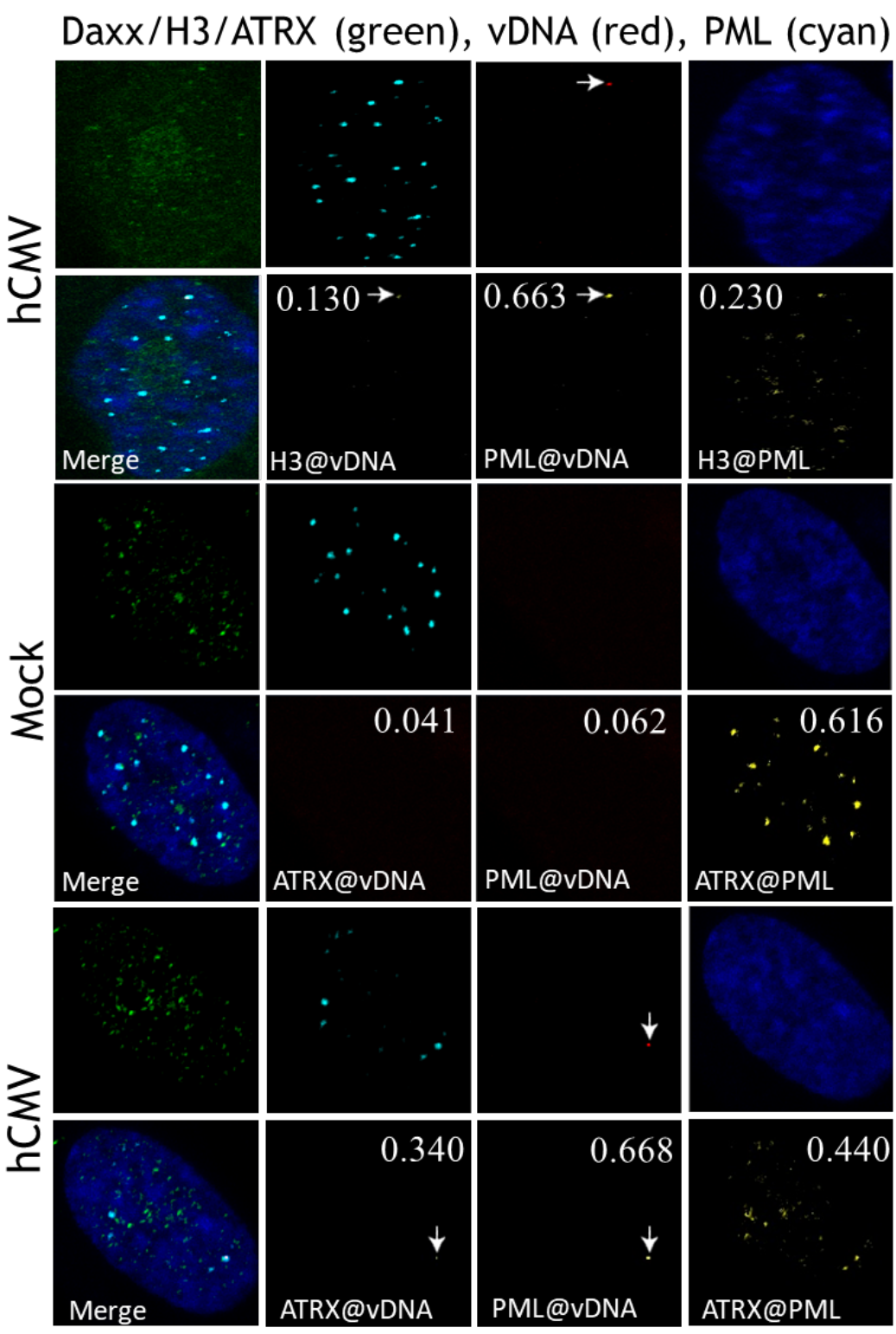
Daxx/H3/ATRX (green), vDNA (red), PML (cyan)
hCMV
Merge
0.130
H3@vDNA
0.663
PML@vDNA
0.230
H3@PML
Mock
Merge
0.041
ATRX@vDNA
0.062
PML@vDNA
0.616
ATRX@PML
hCMV
Merge
0.340
ATRX@vDNA
0.668
PML@vDNA
0.440
ATRX@PML

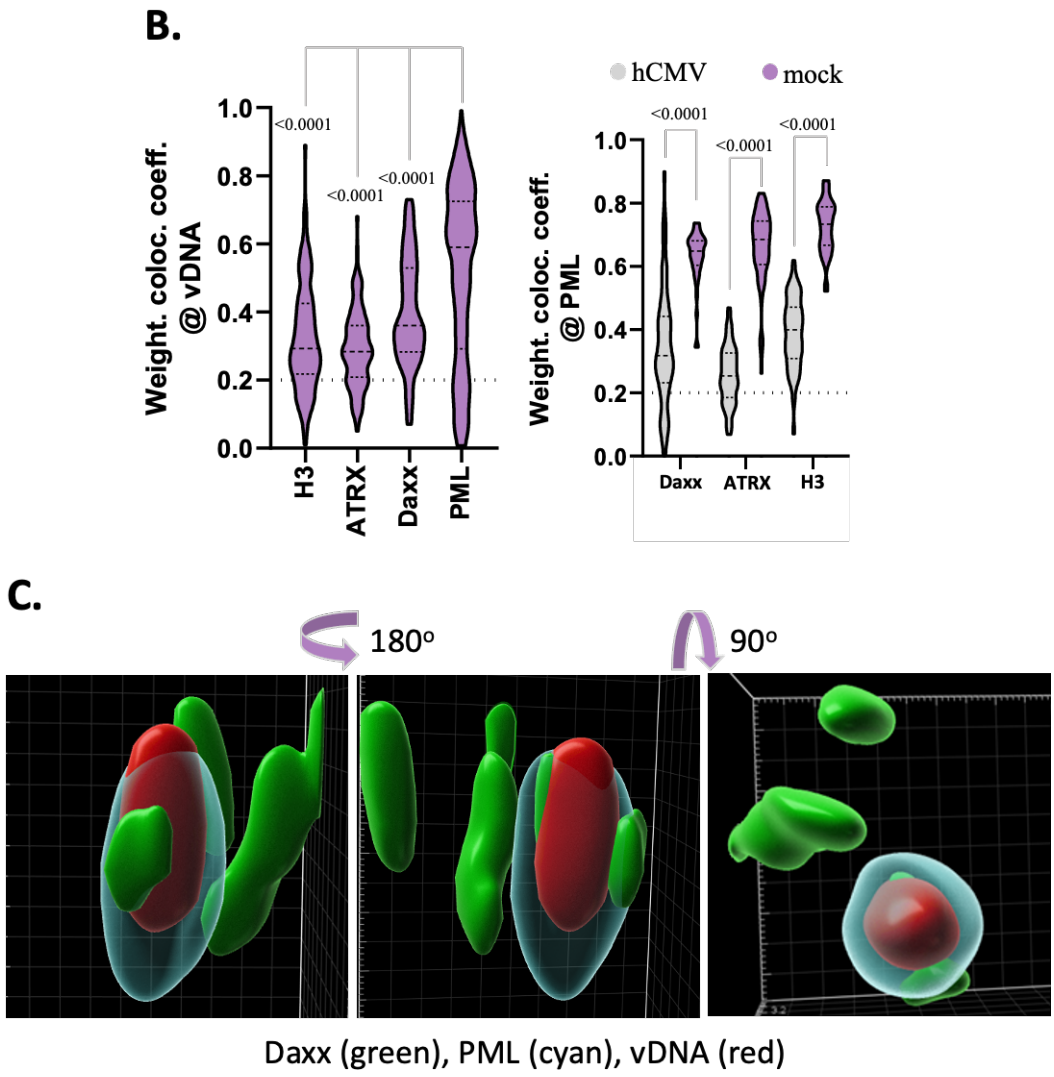

Figure 41. PML-NB constituent proteins colocalization and entrapment of hCMV genomes upon nuclear entry.

HFF cells were infected with hCMV at an MOI of 0.5 FFU/cell. Cells were fixed and permeabilized at 360 mpi. Infecting labelled viral DNA was detected by click chemistry. PML, Daxx, histone H3, and ATRX were detected by indirect immunofluorescence. Nuclei were stained with DAPI. (A) Localization of Daxx/ATRX/histone H3 (green) and PML (cyan) to nuclear viral genomes (red), indicated with white arrows. Cut mask (yellow) highlights the regions of colocalization between the cellular proteins of interest and hCMV genomes. Weighted colocalization coefficient shown. (B) Quantitation of cellular protein recruitment to infecting vDNA or PML in the nucleus at 360 mpi. Black line: median weighted (w.) colocalization coefficient; dashed lines: 95% CI. n>80 nuclei per sample population derived from a minimum of three independent repeats. P value shown; Mann-Whitney U-test. (C) Super-resolution Images were rendered and analysed using Imaris Imaging Software. Representative 3D images of localization of Daxx (green) and PML (cyan) recruitment to hCMV genomes (red). Purple arrows indicate direction of the 90/180-degree rotation of the image.

7.2.4. hCMV IE1 disperses PML to antagonize PML-NB entrapment of vDNA

Unlike HSV-1 (Figure 20 and 21), the weighted colocalization coefficient for PML at hCMV DNA significantly varied between genomes, representative of a long narrow violin plot (Figure 42). IE1 is known to inhibit the *de novo* PML SUMOylation, leading to the nuclear diffusion of PML-NBs which alleviates viral genome repression (Lee et al., 2004; Hou et al., 2017; Schilling et al., 2017). We therefore investigated the role of IE1 in disrupting the localization of PML at hCMV vDNA during initial stages of nuclear infection. HFF cells were seeded onto glass coverslips prior to infection with $hCMV^{EdC/EdA}$ at an MOI of 0.5 FFU/cell. Coverslips were fixed at different times (120, 180 and 360 mpi), prior to staining for PML, hCMV IE1, and vDNA (Figure 42A). PML exhibited a high level of colocalization at DNA (w. coloc. coeff. ≥0.6) at 120 mpi, which reduced over time (Figure 42B). There was a clear inverse correlation between the localization of PML to vDNA and IE1 cell positivity, indicative of IE1 mediated PML dispersal (Figure 42B). Quantitative analysis indicated that the colocalization coefficient of IE1 recruitment to vDNA also increased over time, opposite to the recruitment profile of PML (Figure 42B). Interestingly, IE1 did not localize to PML foci at any of the timepoints (Figure 42C). Collectively, these data demonstrate that the expression of IE1 is sufficient to disassociate PML from PML-NBs in order to relieve viral genome silencing.

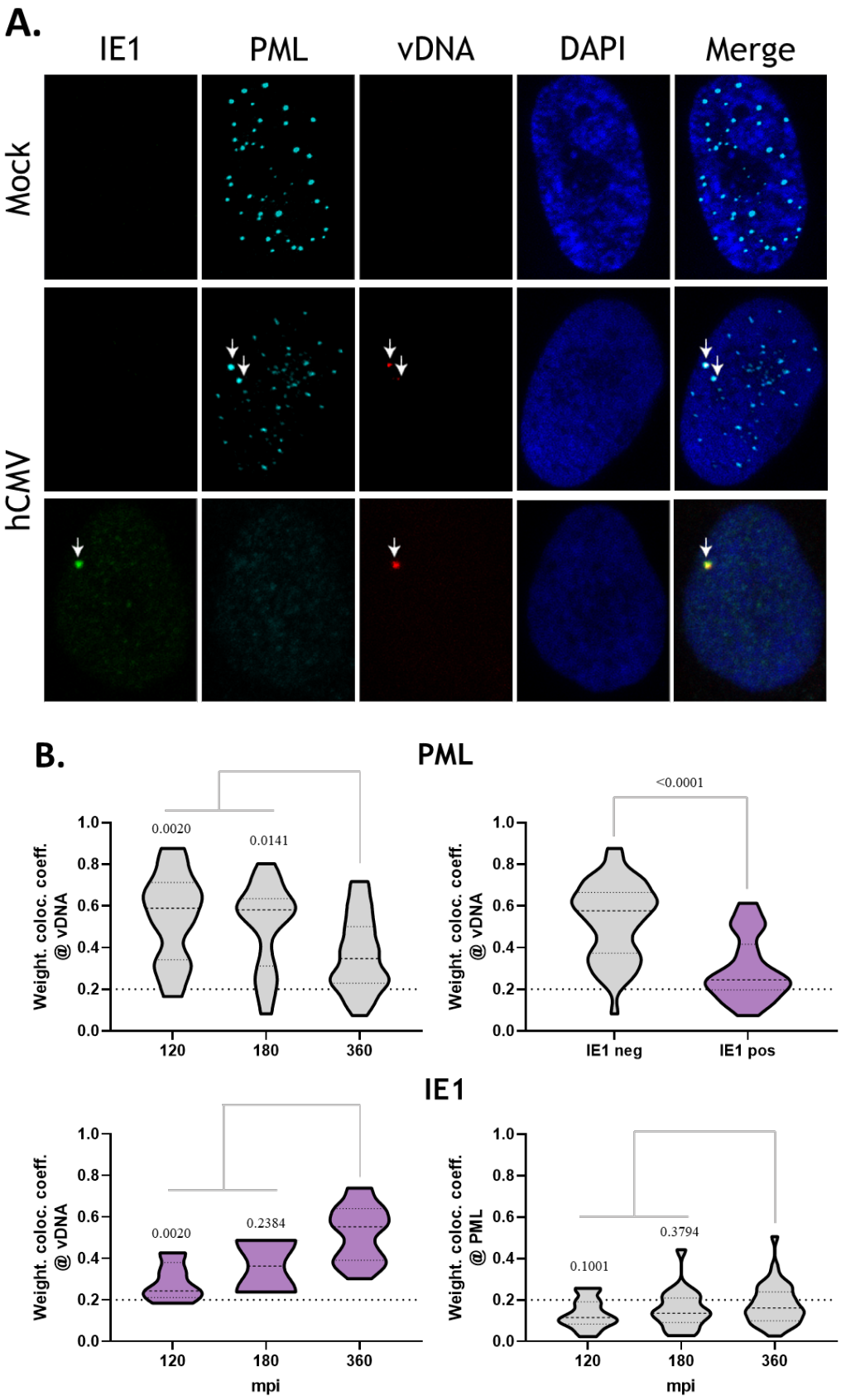

Figure 42. IE1 induces the dispersal of PML from sites of vDNA.

(A) HFF cells were mock infected or infected with hCMV at an MOI of 0.5 FFU/cell. Cells were fixed and permeabilized at the indicated time. Infecting labelled vDNA (red) was detected using click

chemistry, indicated by white arrows. IE1 (green) and PML (cyan) were detected via indirect immunofluorescence. Nuclei were stained with DAPI. (B) Localization of PML to nuclear viral genomes (left) and dependent on IE1 positivity (right). Black line: median weighted (w.) colocalization coefficient; dashed lines: 95% CI shown. n>200 nuclei per sample population derived from a minimum of three independent repeats. P value shown; Mann-Whitney U-test. (C) Localization of IE1 to nuclear viral genomes (left) or PML (right). Black line: median weighted (w.) colocalization coefficient; dashed lines: 95% CI shown. Minimum of three independent repeats. P value shown; Mann-Whitney *U*-test.

7.2.5. SUMO1/2/3 do not stably associate with nuclear hCMV genomes

SUMO proteins are involved in regulating a wide range of cellular processes such as transcription, cell cycle regulation and immune response pathways (Rivas et al., 2021b; Wilkinson & Henley, 2010). IE1 has evolved to hijack the SUMO pathways by either exploiting the SUMO machinery or targeting cellular or viral proteins for SUMOylation to promote the viral infection (Tripathi, Chatterjee & Das, 2021; Lee et al., 2004; Schilling et al., 2017). Considering the role SUMO proteins play during hCMV infection, we investigated the recruitment of SUMO proteins to infecting hCMV genomes following genome entry into the nucleus. HFF cells were seeded onto glass coverslips prior to infection with $hCMV^{EdC/EdA}$ at an MOI of 0.5 FFU/cell. Coverslips were fixed at 360 mpi, prior to staining for PML, Sp100, SUMO1 and SUMO2/3, and vDNA (Figure 43A). Both Sp100 and PML were strongly associated with hCMV genome foci (w. coloc. coeff. ≥0.6), whilst SUMO1 and SUMO2/3 were not readily detected at vDNA, but rather in close proximity to genome foci (Figure 43B). From these data we cannot conclude if SUMO1/2/3 play a role in the entrapment of hCMV genomes during early time points of infection, as their function may be antagonized by IE1 expression. Further investigation is required to study the involvement of SUMO proteins in the entrapment of hCMV genomes.

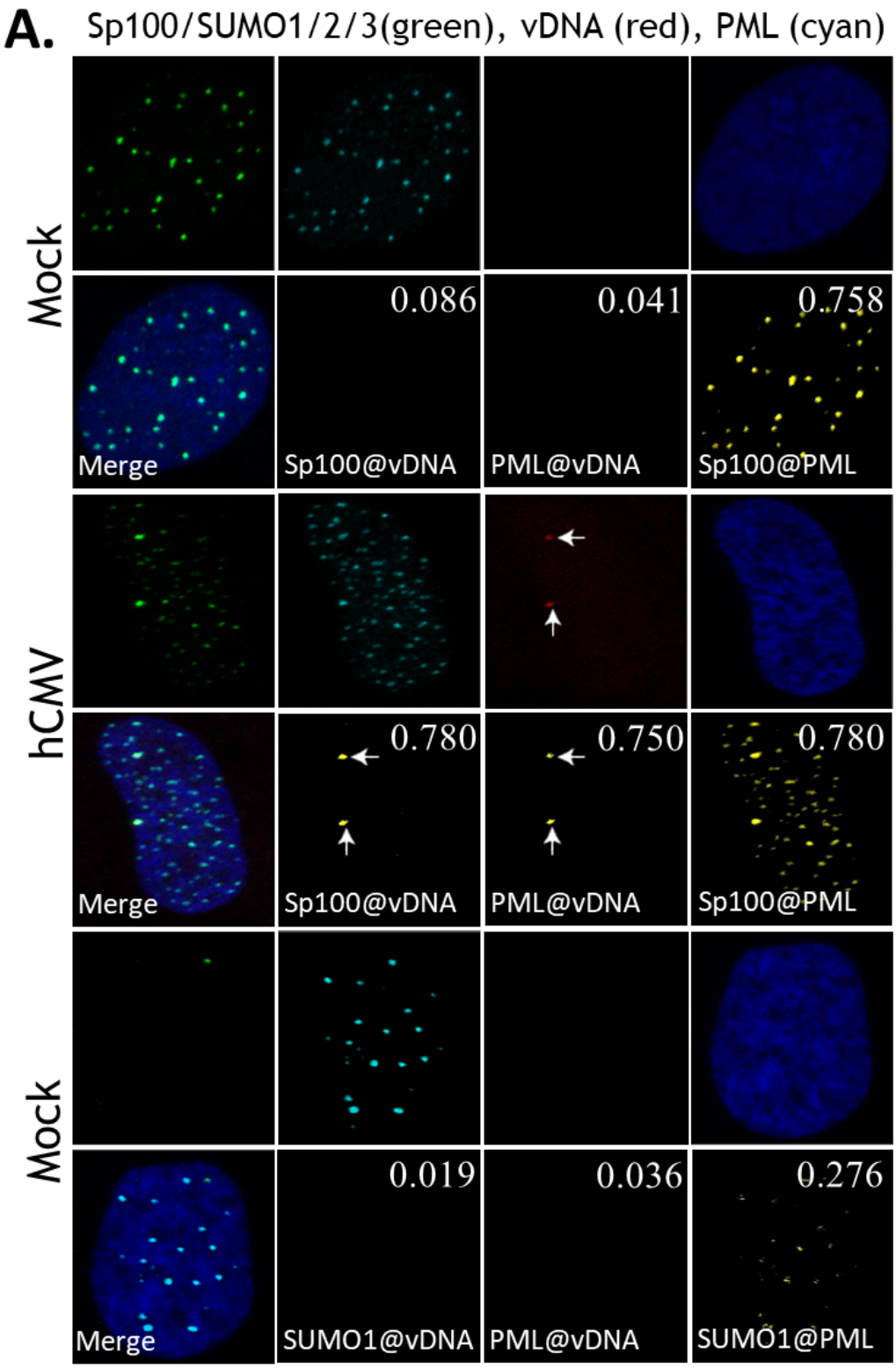
A.
Sp100/SUMO1/2/3(green), vDNA (red), PML (cyan)
Mock
Merge
0.086
Sp100@vDNA
0.041
PML@vDNA
0.758
Sp100@PML
hCMV
Merge
0.780
Sp100@vDNA
0.750
PML@vDNA
0.780
Sp100@PML
Mock
Merge
0.019
SUMO1@vDNA
0.036
PML@vDNA
0.276
SUMO1@PML

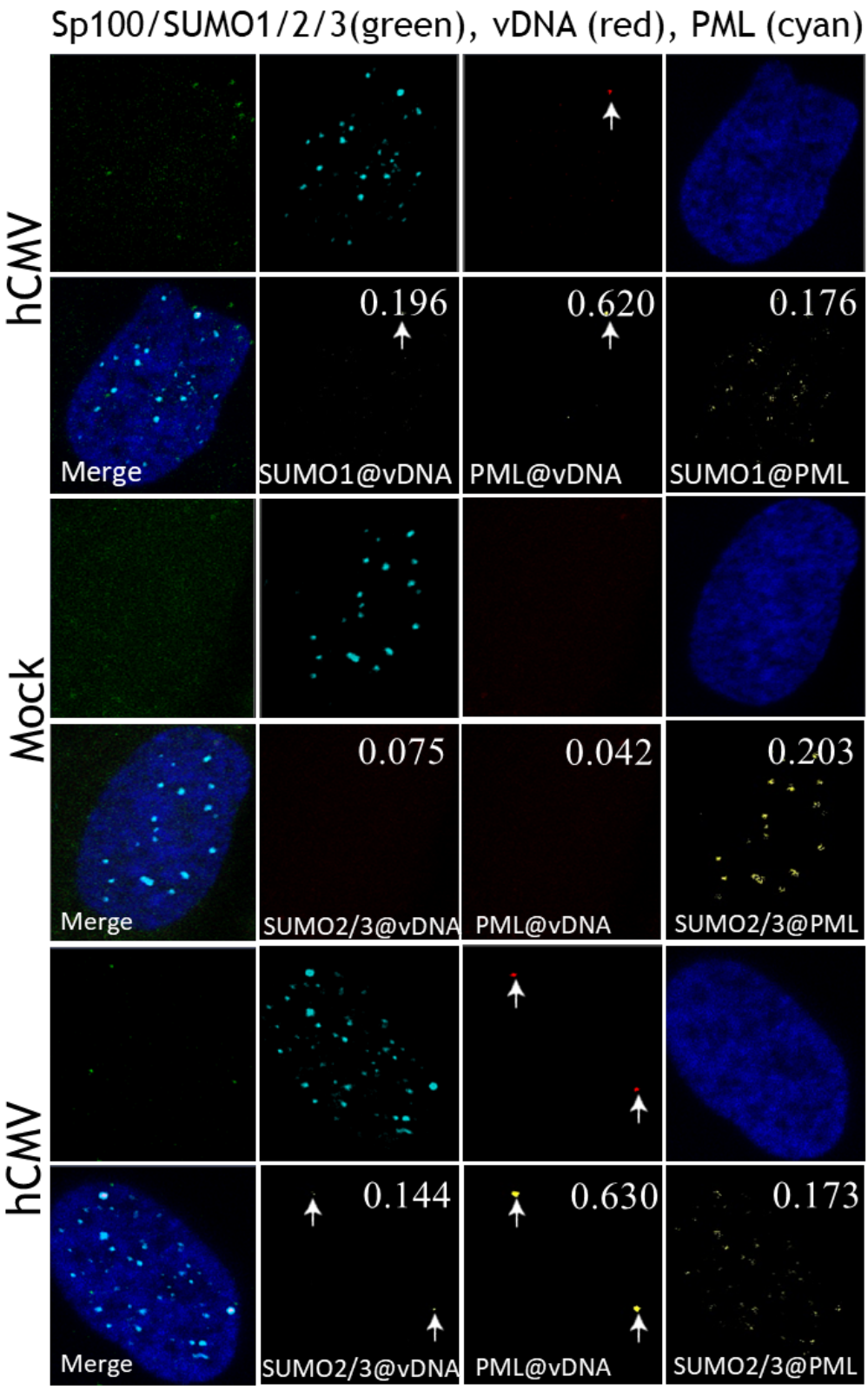
Sp100/SUMO1/2/3(green), vDNA (red), PML (cyan)
hCMV
Merge
0.196
SUMO1@vDNA
0.620
PML@vDNA
0.176
SUMO1@PML
Mock
Merge
0.075
SUMO2/3@vDNA
0.042
PML@vDNA
0.203
SUMO2/3@PML
hCMV
Merge
0.144
SUMO2/3@vDNA
0.630
PML@vDNA
0.173
SUMO2/3@PML

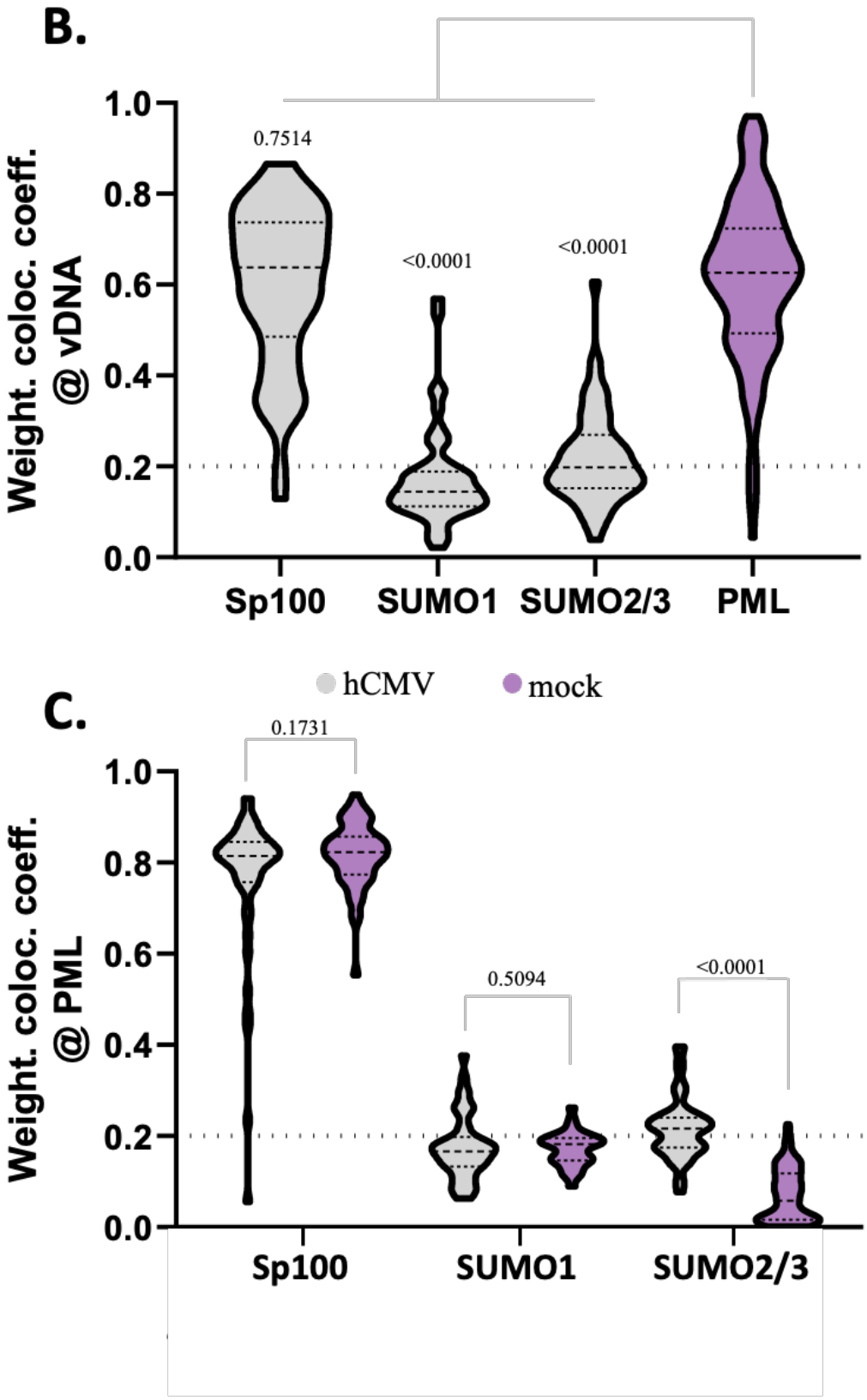

Figure 43. Recruitment of PML-NB constituent proteins to infecting viral genomes.
HFF cells were infected with hCMV at an MOI of 0.5 FFU/cell. Cells were fixed and permeabilized at 90 mpi. Infecting labelled viral DNA was detected using click chemistry. PML, Sp100, SUMO1, and SUMO2/3 were detected via indirect immunofluorescence. Nuclei were stained with DAPI. (A)

Localization of Sp100/SUMO1/SUMO2/3 (green) and PML (cyan) to nuclear viral genomes (red), indicated with white arrows. Cut mask (yellow) highlights the regions of colocalization between the cellular proteins of interest and hCMV genomes. Weighted colocalization coefficient shown. (B) Quantitation of cellular protein recruitment to infecting vDNA in the nucleus at 90 mpi. Black line: median weighted (w.) colocalization coefficient; dashed lines: 95% CI. n>120 nuclei per sample population derived from a minimum of three independent repeats. P value shown; Mann-Whitney *U*-test. (C) Quantitation of cellular protein recruitment to PML in the nucleus at 90 mpi. Black line: median weighted (w.) colocalization coefficient; dashed lines: 95% CI. n>120 nuclei per sample population derived from a minimum of three independent repeats. P value shown; Mann-Whitney *U*-test

7.3. Summary

The rapid recruitment of host restriction factors is key for mounting an effective antiviral immune response to infection. As such, PML-NB consituent proteins have been the subject of intensive research over the last 30 years, due to their known role in modulating the onset of hCMV infection. However, a large gap in our understanding of the spatiotemporal kinetics of how these proteins are recruited to herpesviruses outwith of the alphaherpesviruses, such as hCMV, has remained limited. This is due to the limitations and technical challenges in the detection of vDNA during the initial phase of nuclear infection. In the previous chapters we demonstrated an optimized protocol for DNA labelling of HSV-1 that has provided a non-invasive method to analyse the recruitment efficiency of host immune factors to HSV-1 (Sekine et al., 2017; Alandijany et al., 2018). This protocol was applied to visualizing hCMV vDNA to enable the investigation of the temporal recruitment of host intrinsic immune factors to vDNA to determine these host intrinsic immune responses were conserved between herpesvirus family members.

Labelling of hCMV DNA using nucleoside analogues required optimization to ensure the highest efficiency of incorporation within the viral DNA backbone. Recent studies have shown that the different nucleotides- deoxyuridine (EdU), deoxyadenine (EdA), deoxycytidine (EdC) and deoxythymidine (EdT) are incorporated into the different herpesviruses at various efficiencies in specific cell lines (Manska, Octaviano & Rossetto, 2020). It was shown that EdC alone was insufficient to pulse label hCMV DNA (Manska, Octaviano & Rossetto, 2020). To bypass the reduced incorporation efficiency and increase the labelling efficiency we utilized a combination of two nucleotide analogues, EdC and EdA. The time at which pulsing was initiated was also optimised to ensure efficient uptake by the virus without inhibiting the progress of hCMV infection. Due to the slow replication cycle of hCMV, with progeny virus being detected after 50 hours post-infection, it was important to allow virus replication to be well initiated to avoid the

nucleotides be solely uptaken into cellular chromatin during cell division. As a limitation to this method additional post-infection clean-up of the virus stock to remove the free nucleotides resulted in significant reduction in virus titre (Figure 37, 38 and 39). Consequently, using the virus stock to infect cells resulted in nucleotides being taken up by bystander cells and adding additional signal that would increase some of the background during the analysis. This could be overcome by increasing the number of samples (n) and exclude the labelled cells. However, work is currently ongoing in the lab to further optimise hCMV$^{EdC/EdA}$ clean up. Overall, this method allows for the generation of a labelled virus stock that is consistent in its labelling for subsequent experimentation (Scherer et al., 2021).

The microscopy observations in this study show the dynamics of genome deposition of hCMV DNA during infection, indicating that most viral genomes reach the nucleus by 360 mpi (Figure 40). Compared to the 90 mpi of HSV-1, hCMV genome traverse the cytosol with different kinetics. While it remains to be determined as to why this may be the case, it may reflect the size of the virus particle or mixed modes of entry. Notably, hCMV has been shown to enter cells through fusion and endocytosis, which may account for the differences observed. Additionally, there might be other cytoplasmic intrinsic immune factors that may be slowing down the transport of viral capsids, such as IFI16 (Dell'Oste et al., 2014). Once the viral genome is released into the nucleus, PML-NBs were initially proposed to be beneficial sites for viral replication. However, it has been revealed that core constituent proteins of PML-NBs such as PML, Sp100, and Daxx are hCMV restriction factors (Landolfo et al., n.d.; Shenk & Stinski, n.d.). PML-NBs have shown to associate with hCMV DNA immediately after nuclear entry, which promote the transcriptional silencing of IE promoters that is the actions of the Daxx-ATRX complex and histone deacetylases (Saffert & Kalejta, 2006; Woodhall et al., 2006). The exact mechanism of restriction of other major constituent proteins, such as PML and Sp100, remains to be elucidated. The data presented here demonstrates PML and Sp100 to entrap the viral genome up to 360 mpi (Figure 41), similar to that observed for HSV-1 and Varicella-Zoster Virus (Sekine et al., 2017; Alandijany et al.,

2018; Reichelt et al., 2011b). This entrapment promotes genome silencing, which is antagonized by the expression of IE1 destabilising PML SUMOylation (Figure 42) (Wilkinson et al., 1998; Korioth et al., 1996). The mechanism by which hCMV evades chromatin repression is by the removal of Daxx, and consecutively ATRX, by the viral pp71 from the MIE sites, which allows for the generation of IE1/IE2 (Hofmann, Sindre & Stamminger, 2002; Ishov, Vladimirova & Maul, 2002; Cantrell & Bresnahan, 2005; Ishov, Vladimirova & Maul, 2002; Cantrell & Bresnahan, 2005; (Hwang & Kalejta, 2007). These observations are further supported by a recent report also showing the entrapment phenotype of hCMV DNA exerted by PML-NBs (Scherer et al., 2021).

In summary, the data presented in this chapter demonstrates the spatiotemporal regulation of the intrinsic immune response during hCMV infection. PML-NB constituent proteins are rapidly recruited to vDNA genomes upon the nuclear deposition of the vDNA leading to the silencing of the virus via genome entrapment. The viral protein-mediated degradation of PML-NB proteins is required to alleviate this restriction and initiate viral gene transcription.

8. Discussion

The host intrinsic and innate immune response play a key role in controlling HSV-1 replication. UV irradiation of viruses has provided a useful tool to study the innate immune response, as it robustly activates the IFN immune response under relatively low MOI. The key findings of this study are that intrinsic and innate immune responses to UV irradiated HSV-1 infection are inversely activated by virtue of premature cytoplasmic deposition of viral genomes and opposing effects of UV irradiation on vDNA interactions with cellular PRRs and host restriction factors. The intrinsic immune response to HSV-1 is mediated by pre-existing nuclear restriction factors (e.g. PML-NB proteins) which recognize vDNA immediately after nuclear entry that attempt to represses the onset of viral transcription (Tavalai & Stamminger, 2009; Boutell & Everett, 2013; Everett & Chelbi-Alix, 2007; Scherer & Stamminger, 2016). In contrast, the induction of innate immune response is reliant on the recognition of viral genomes that have been inappropriately deposited in the cytoplasm by PRRs (e.g., cGAS). This initiates signalling cascades that ultimately results in the production of type I IFNs that act to prime neighbouring cells into an antiviral state to limit the spread of infection (Abe, Marutani & Shoji, 2019; Ma, Ni & Damania, 2018; Lurie & Platanias, 2005). The secretion of IFNs is also critical for the activation and recruitment of different immune cells, such as macrophages and Natural Killer cells (Paolini et al., 2015; Rizza et al., 2015), which restrict replication through the induction of apoptosis or phagocytosis of infected cells (Nainu, Shiratsuchi & Nakanishi, 2017; Rodriguez et al., 2017; Bayliss & Piguet, 2018).

This study advanced our understanding as to why UV irradiated herpesviruses are strong inducers of the type I IFN response. Additionally, it provides evidence that some of these pathways, like PML-NB entrapment, are conserved between different herpesvirus families, which and warrants further optimisation and investigation. These findings are discussed below.

8.1. The effects of UV irradiation on viral genome deposition during infection

UV irradiation has been a method utilized routinely in virology to inactivate viruses and induce IFN responses for immunological studies (Laycock et al., 1991; Dalai et al., 2002; Leblanc et al., 1999; Gary, Rosenberg & Louis, 1974). The use of UV inactivated viruses enables cellular immune response to infection to be studied at an organismal or cellular level independently of the expression of viral proteins that may otherwise counteract host immune response to infection. However, it remains to be determined what direct influence UV irradiation has on the presentation of PAMPs or detection by cellular PRRs. In order to investigate these virus host interactions at single-molecule resolution, we utilized a protocol that allowed for the specific detection of EdC-labeled vDNA under low MOI (Figure 6) (Sekine et al., 2017; Alandijany et al., 2018). Plaque assay data showed that UV irradiated HSV-1 was unable to establish a productive infection due to a lack of viral IE protein synthesis (Figure 7,8 and 9) (Eglin, Gugerli & Wildy, 1980; Ross, Cameron & Wildy, 1972; Fridlender et al., 1978). We find considerable evidence demonstrating UV irradiation to induce the premature deposition of HSV-1 vDNA into the cytoplasm of cells. This phenotype was observed independently of UV light sources. (Figure 13 and 20) (Miyamoto' And & Morgan, 1971). Correspondingly, these cells induced a much stronger type I IFN immune response compared to non-UV irradiated HSV-1 infected cells (Figure 10) (Gary, Rosenberg & Louis, 1974; Taylor & O'brien, 1985; Hendricks et al., 2021; Eloranta, Sandberg & Alm, 1996). Our observations are consistent with EM observations that have shown a block to viral infection at a pre-replication step (Ross, Cameron and Wildy, 1972; Fridlender, Asher, Weinberg-Zahlering and Becker, 1978). Thus, in contrast to normal infection, UV irradiation promotes the premature activation of type I IFN mediated signalling by significantly increasing the cytoplasmic deposition of viral genomes.

Following entry, viral capsids bind to microtubules to traverse the cytoplasm to the nucleus, where they interact with component proteins of

the NPC to deposit their genomes into the nucleus (Kristensson et al., 1986; Sodeik; Topp, Meade and LaVail, 1994; Ebersold and Helenius, 1997). Studies carried out in macrophages have shown a role of the proteasome-mediated degradation in processing HSV-1 capsids that contributes to the releasing of vDNA into the cytoplasm for subsequent detection by cellular PRRs, such cGAS (Horan et al., 2013; Sun et al., 2019). These findings are inconsistent with our data, which show the chemical inhibition of the cellular proteasome in fibroblasts not to affect the levels of detectable vDNA in the cytoplasm irrespective of UV treatment (Figure 15 and 16). We therefore did not identify a role for the proteasome in the premature uncoating of UV-irradiated HSV-1 genomes. This difference may be attributable to the difference in cell type, as fibroblasts have lower expression levels of the 26s proteasome compared to myeloid cells (Human Protein Atlas). Cytoskeletal disruption, specifically microtubule disruption, is known to influence capsid transport to the nucleus that reduces HSV-1 viral titre yields (Kristensson et al., 1986; Ebersold and Helenius, 1997). These data are consistent with our findings, which show Nocodazole treatment of cells to significantly increases the levels of cytoplasmic HSV-1 genomes independently of UV irradiation (Figures 17 and 18). We propose that UV irradiation of HSV-1 virions inhibits the association with microtubules, which enhances the rate of premature vDNA deposition observed in untreated cells upon infection with UV irradiated virus. Further investigation is warranted to determine the specific mechanism of disassociation of UV-irradiated HSV-1 capsids from cellular microtubules but is likely to involve changes to capsid or tegument proteins involved in cytoskeletal transport, such as UL34 and VP26 (Reynolds et al., 2002; Döhner, Nagel and Sodeik, 2005). Collectively, our data demonstrate that the failure of HSV-1 to establish a productive infection following UV irradiation is, at least in part, caused by the ineffective delivery of genomes to the nucleus due to the premature release of vDNA into the cytoplasm. These data have implications on our understanding of the effects of UV irradiation on viral infection and the localization of the UV irradiated vDNA within the cell following entry. In turn, the cytoplasmic deposition of vDNA explains the enhanced innate immune response elicited by cells in response to UV irradiated herpesviruses (Rosenberg and Notkins, 1974; Taylor and

O'Brian, 1985; Hendricks et al., 1991; ELORANTA, SANDBERG and ALM, 1996).

The major limitation of bio-orthogonal nucleic acid labelling is that it requires for the alkyne group to be available for the binding of the fluorophore-bound azide molecule, which could be disrupted by the UV cross-linking of the vDNA, thus resulting in the reduced number of detectable viral genomes in infected cells (Figure 12 and 14). It is also possible that there may be a population of genomes that have not been labelled and therefore cannot be detected during the analysis. However, the reduced number of viral genomes reaching the nucleus to initiate viral replication fall in line with previously reported data (Eglin, Gugerli and Wildy, 1980, Fridlender, Asher, Weinberg-Zahlering and Becker, 1978), with electron microscopy data showing a similar decrease in detectable intracellular capsids (Miyamoto and Morgan, 1971).

8.2. Viral genome decompaction plays a role in PML-NB recognition of infecting HSV-1 DNA

PML-NBs are comprised of numerous cellular proteins and play a key role in many cellular processes, including antiviral immune responses (Tavalai & Stamminger, 2009). This is mediated via the *de novo* recruitment of constituent proteins to sites of infecting nuclear viral genomes (Glass & Everett, 2013; Everett & Murray, 2005). Work from our group has revealed that vDNA is entrapped within PML-NBs, a phenotype that promotes the repression of viral gene expression prior to ICP0 synthesis and disruption of PML-NBs (Alandijany et al., 2018). With respect to non-irradiated HSV-1 genomes, our findings were consistent with the stable recruitment of key PML-NB associated proteins (PML, Sp100 and Daxx) to vDNA as previously reported (Figure 19). In contrast, UV irradiation of HSV-1 genomes resulted in a UV dose-dependent decrease in the localization of PML, Daxx and Sp100 to nuclear infecting HSV-1 DNA (Figure 19). This decrease in localization

was independent of the UV source (Figure 20). Additionally, the stability and composition of PML-NBs within infected cells was not visibly affected during infection with UV irradiated HSV-1 (Figure 19 and 20). Importantly, the direct interaction between PML and vDNA was negatively affected by UV irradiation, reducing the interaction between PML and vDNA (Figure 23). Since the exact recognition mechanism of vDNA by PML remains to be elucidated, the disruption of vDNA recognition by PML-NBs by UV irradiation could be down to numerous factors. Studies have shown that PML itself can associate with cellular ssDNA in response to exogenous DNA damage and PML-NBs can sequester DNA molecules during DNA processing events associated with DNA synthesis (Jul-Larsen et al., 2004; Boe et al., 2006). Our data indicates that the structure of vDNA is affected by UV irradiation, which induces TD and impaired genome decompaction following its release from the capsid (Figure 24 and 25). This finding likely accounts for the reduced recruitment of PML-NB associated proteins to UV irradiated vDNA. The damage induced by UV irradiation has been extensively studied over the last 70 years (Rörsch, Beukers, Iljstra and Berends, 1958; Beukers and Berends, 1960) and shown to induce the formation of various DNA lesions (Rastogi et al., 2010; Schreier, Gilch and Zinth, 2015). The main photoproducts are cyclobutene pyrimidine dimers (CPDs) and 6-4 photoproducts (Carell and Epple, 1998), that alter DNA structure and base-pairing. These data are consistent with the increased concentration of thymine dimers found in UV irradiated HSV-1 samples in a UV dose-dependent manner compared to control samples (Figure 25). Consequently, the structure of the HSV-1 genome was altered, along with its ability to decompact, following capsid uncoating (Figure 24). This changed conformation of viral genomes may mask a PML-specific binding sequence that may be revealed upon genome decompaction required to promote recruitment of PML-NB proteins. Equally, the altered structure of the DNA molecule may inhibit the binding of accessory proteins required for PML binding. These data indicate that nuclear genome delivery alone is insufficient to initiate a robust PML-NB mediated intrinsic immune response. Further investigation is required to identify the specific mechanism by which decompaction affects the recruitment of PML-NBs, as these structures have shown to influence the outcome of infection for many

DNA viruses (Doucas et al., 1996; Wu, Ceccarelli & Frappier, 2000; Bell, Lieberman & Maul, 2000; Scherer et al., 2021; Reichelt et al., 2011b, 2011a).

Genome deposition in the cytoplasm or nucleus was insufficient to stimulate the recruitment of IFI16 (Figure 21). IFI16 has been reported to recognize infecting DNA and initiate the production of IFNβ via the STING-IRF3 axis (Unterholzner et al., 2010; Horan et al., 2013). However, most of these studies rely on vDNA binding proteins and high MOIs that saturate intrinsic host defences to detect the association of IFI16 with viral genomes. These observations are in line with previously published data, which show that active viral DNA replication promotes IFI16 localization to HSV-1 DNA (Alandijany et al., 2018). However, we cannot discount a more transient role for IFI16 in cytosolic PRR sensing as our experiments were carried at a single timepoint of 90 mpi.

8.3. The cGAS-STING pathway plays a key role in mediating the innate immune response to UV irradiated HSV-1 infection

The innate immune response is initiated in response to pathogen infection by the recognition of specific PAMPS by cellular PRRs. This tightly regulated process results in the production of cytokines and chemokines, including IFNs, which are key regulators of innate immunity. As one of the most potent activators of the IFN response, foreign DNA is detected by a large number of DNA sensing molecules, including cGAS and IFI16 (Leib et al., 1999; Zawatzky et al., 1982; Luker et al., 2003; Stetson & Medzhitov, 2006; Wilcox et al., 2016; Abe, Marutani & Shoji, 2019; Ma, Ni & Damania, 2018). However, most studies have focused on nuclear IFI16 DNA sensing due to the fact that genomes in the cytoplasm are protected from detection by the viral capsid. In recent years, following the discovery of the cGAS-STING sensing pathway, numerous studies have identified a variety of different HSV-1 proteins that act to repress cytosolic sensing, for example the targeting of PTMs of the cGAS pathway being by UL37, VP22, VP1-2 (Zhang et al., 2018; Huang et al.,

2018; Ye et al., 2017; Xu et al., 2017; Su & Zheng, 2017b; Deschamps & Kalamvoki, 2017; Bodda et al., 2020; Pan et al., 2018; Christensen et al., 2016). However, the spatiotemporal recruitment and localization of these PRRs to infecting HSV-1 DNA remains largely uninvestigated. The detection of vDNA by CLICK chemistry enabled recruitment studies of host DNA sensing proteins to viral genomes under infection conditions that have not oversaturated the host immune response at high MOI, thereby enabling a comparison between effector molecules of the induction of the intrinsic and innate immunity.

Our microscopy analysis clearly demonstrates that cGAS-STING pathway plays an important role in the detection of viral DNA as the enhanced localization of both cGAS and STING to infecting vDNA was observed (Figure 26, 27 and 28) as well as the induction of IFNβ production (Figure 30) (Hopfner & Hornung, 2020; Diner et al., 2013; Liu et al., n.d., 2015; Ishikawa & Barber, 2008b). This association appeared to be specifically cytoplasmic (Figure 27 and 28) and was not detected in the nucleus (Figure 27 and 28), even though it has been reported that cGAS plays a role in stabilizing IFI16 in the nuclear PRR sensing pathway during HSV-1 infection (Orzalli et al., 2015). Our data is consistent with studies which have shown cGAS in detecting cytoplasmic vDNA in macrophages (Sun et al., 2019) and the induction of an enhanced type I IFN response (Taylor and O'Brian, 1985; Hendricks et al., 1991; Eloranta, Sandberg and Alm, 1996). Interestingly, the localization of STING to cytoplasmic UV-irradiated vDNA has not been previously reported, thus we identify for the first-time a recruitment of STING to vDNA in the cytosol, in contrast to the reported role for STING in the canonical cGAS-STING pathway. This correlates with studies that have identified STING to complex with intracellular foreign ssDNA or dsDNA without the need of any accessory molecules (Abe et al., 2013). Our ChIP analysis revealed that cGAS interacted directly with HSV-1 DNA, and that this interaction was enhanced upon UV irradiation even though chromatin extracts contained equivalent genome copies of HSV-1 DNA (Figure 33). This could be a result of the increased number of cytoplasmic viral genomes or decreased binding of competing host factors to vDNA factor, reducing steric inhibition of cGAS binding to vDNA. Our ChIP analysis failed to detect an

interaction between STING and vDNA, irrespective of UV irradiation. These data are in line with its canonical role of interacting with cGAMP produced by cGAS following activation by DNA sensing (Figure 26, 27, 28 and 30) (Ishikawa & Barber, 2008b; Burdette et al., 2011b). However, our data demonstrate that STING is not stationary localized to the ER and ERGIC compartments, through an unknown mechanism (Burdette et al., 2011b; Sun et al., 2009). Our high-resolution image analysis provided further confirmation, as the number of STING foci to vDNA significantly increased upon UV irradiation (Figure 28). Collectively, these findings identify a potential complex between at least a subset of cGAS-STING molecules associated with cytoplasmic vDNA, which may subsequently contribute to activation of the type I IFN response. It is plausible therefore to speculate that STING is likely to play a more direct role in DNA detection than previously thought. Further investigation is warranted to determine what contribution this complex may have on the regulation of cytosolic DNA sensing, using engineered cell lines which express tagged proteins to perform ChIP experiments and dissect this interaction further.

Sp1 is a ubiquitously expressed cellular transcription factor that binds to multiple binding sites within the HSV-1 genome to enhance the transcriptional initiation of viral IE and E genes (Pande, Petroski & Wagner, 1998; Tuan Nguyen-huynh & Schaffer, 1998; Gu, Huang & Hyward, 1995; Jones & Tjian, 1985). This interaction typically occurs in the nucleus (Kuwahara et al., 2000). We identified strong cytoplasmic Sp1 recruitment to vDNA in the cytoplasm during non-UV irradiated HSV-1 infection (Figure 34). The recruitment of Sp1 to vDNA was directly affected by UV-irradiation (Figure 34). We hypothesise that the accumulation of pyrimidine dimers within the genome may inhibit genome decompaction and reduce the ability of Sp1 to effectively bind dsDNA (Figure 24) (Goodsell, 2001; Rastogi et al., 2010; Schreier, Gilch & Zinth, 2015). This would potentially allow for the increased binding of cGAS and STING to HSV-1 DNA due to the reduction of steric competition for DNA surface binding. Interestingly, KO of Sp1 resulted in the abrogated recruitment of cGAS and STING to cytoplasmic HSV-1 genomes, with or without UV irradiation (Figure 35 and 36). It would be plausible to speculate

that Sp1 localization may be a pre-requisite for cGAS and STING binding, however more data is required to make such a conclusion. Notably, however, the levels of cGAS were significantly reduced in Sp1 KO HFt cells, which revealed a potential role for Sp1 in regulating cGAS expression. Correspondingly, we identify one Sp1 binding site in the promoter region of the gene (Appendix C) (Kuwahara et al., 2000). Thus, our recruitment analysis cannot discount the possibility that a loss in cGAS/STING recruitment to vDNA in Sp1 KO cells is not an indirect consequence of reduced levels of cGAS expression.

Collectively our data shows that the enhanced innate immune response in fibroblasts to UV irradiated HSV-1 is carried out by the cellular PRRs cGAS and STING, where both proteins associate with vDNA within the cytosol as early as 90 mpi. These data have important implications on our understanding of the cGAS-STING pathway with respect to the specific sequence of events that mediate cytosolic DNA detection required to promote downstream signalling events that activate innate immune defences to HSV-1 infection.

8.4. PML-NB restriction by entrapment of genomes in response to Herpesviruses is conserved

The discovery of PML-NBs and their role in herpesvirus restriction was initially identified during hCMV infection (Ishov, Stenberg & Maul, 1997). SUMOylated PML recruits other component proteins of PML-NBs from the nucleoplasm, including Daxx and ATRX, that ultimately create a condensed chromatin repressive environment on the IE1 promoter (Woodhall et al., 2006; Saffert & Kalejta, 2006). Knockdown of individual PML-NB protein components enhances the plaque formation of hCMV, while overexpression limits hCMV replication (Tavalai et al., 2006, 2011; Adler et al., 2011; Tavalai, Rechter & Stamminger, 2008; Lukashchuk et al., 2008). However, few studies have examined the spatiotemporal kinetics of PML-NB recruitment to vDNA and

whether entrapment of HSV-1 DNA is a conserved mechanism across the Herpesviridae family (Sekine et al., 2017; Alandijany et al., 2018). Click chemistry labelling of hCMV DNA and its association with PML-NBs has very recently been reported (Figure 39) (Manska, Octaviano & Rossetto, 2020; Scherer et al., 2021). Our analysis presented here is in agreement with these studies and show PML to play an important role in the regulation of hCMV infection upon genome delivery to the nucleus.

We demonstrate that the majority of nuclei are infected with at least 1 genome by 360 mpi (Figure 40) (Ogawa-Goto et al., 2003; Alandijany et al., 2018). Our microscopy analysis demonstrated that PML localizes to hCMV DNA foci at this time point, although recruitment phenotype was variable in comparison to HSV-1 infection at 90 mpi (Figure 41) (Scherer et al., 2021). Daxx-mediated repression of the MIEP is antagonised by pp71, which displaces Daxx from PML-NBs, and concurrently induces the loss of ATRX and H3 from vDNA (Figure 42) (Ishov, Vladimirova & Maul, 2002; Cantrell & Bresnahan, 2005; Hwang & Kalejta, 2007; Lukashchuk et al., 2008). HCMV vDNA remains entrapped in PML-NBs until IE1 induces the dispersal of PML-NBs to promote the full onset of lytic replication (Figure 42) (Lee et al., 2004; Hou et al., 2017; Schilling et al., 2017; Reuter et al., 2021). Collectively these data demonstrate the spatiotemporal kinetics of PML-NB entrapment of infecting hCMV vDNA during early stages on infection are a conserved antiviral response to herpesvirus infection.

9. Conclusion remarks and future work

9.1. Conclusion remarks

Intrinsic and innate immunity are two distinct arms of immunity that act to limit initiation, propagation, and spread of HSV-1. Intrinsic immunity

is the first line of defence that entraps Herpesvirus genomes almost immediately after nuclear entry. It is mainly mediated by PML-NB protein constituents that are stably recruited to viral genomes that require genome decompaction for efficient binding. The innate immune response limits viral propagation by DNA sensing that stimulates the synthesis of IFN and the induction of an antiviral state through the expression of ISGs. The cGAS-STING pathway plays a key role in detecting infecting vDNA. Here we show the UV irradiation of HSV-1 induces a switch in the sequential regulation of the intracellular immune defences to HSV-1infection that promotes the induction of the type I IFN response. Our analysis shows multiple host factors to alter their respective recruitment and/or DNA binding properties in response to UV irradiation.

9.2. Recommendations for future work

Many different avenues or key tests and experiments have been left for the future due to lack of time (i.e. the experiments with IF data are usually very time consuming, requiring even weeks to finish a single repeat), specifically due to the COVID-19 pandemic outbreak, which further limited my time in the lab and required me to prioritise specific avenues of experimentation. Future work concerns deeper analysis of particular mechanisms, new proposals to try different methods, or simply curiosity.

There are several areas in the studies undertaken in this thesis that would require further investigation or development. Some avenues that would be interesting to pursue would be in relation to section 4.2.5. and the interaction between UV irradiated HSV-1 capsids and the cellular microtubule network. These include the further examination of the phenomenon of UV irradiated HSV-1 capsids disassociating from the MT network and what mechanisms are at play. How does UV irradiation affect the specific viral tegument proteins that are involved in microtubule association, for example VP22, and if UV exposure affects tegument protein

function by crosslinking? Specifically, is their interaction with cellular motor proteins, such as dynein-1 and kinesin-1, responsible for the transport of capsids to the nucleus during UV irradiated virus infection. Additionally, it would be interesting to research the viral capsid uncoating as a process and identify the reasons that lead to its occurrence specifically following HSV-1 capsid disassociation from the microtubules, since the proteasome was not found to be involved in the experiments presented in this thesis and cytoplasmic deposition in the literature is mostly mentioned as genome leaking.

This study has investigated the interaction between PML and non-UV or UV irradiated HSV-1 DNA, demonstrating there is direct interaction between PML and viral genomes during infection and the importance of genome decompaction of HSV-1 DNA in its recognition by PML. Similar approaches can be taken, for example by ChIP-Seq, to investigate if there is a specific consensus sequence that is specifically recognised by cellular PML. Additionally, the identification of the specific PML isoform that is responsible for this direct interaction would be an intriguing direction to take, including mutations in the specific domains within PML to identify the domain responsible for DNA binding.

An analogous approach can be applied to investigate if these cellular intrinsic and innate immune defences to UV irradiated HSV-1 is a conserved herpesvirus mechanism utilizing the labelled hCMV virus or if they are HSV-1 specific.

10. References

Abe, T., Harashima, A., Xia, T., Konno, H., Konno, K., Morales, A., Ahn, J., Gutman, D. & Barber, G.N. (2013a) STING Recognition of Cytoplasmic DNA Instigates Cellular Defense. Molecular Cell. 50 (1), 5–15. doi:10.1016/j.molcel.2013.01.039.

Abe, T., Marutani, Y. & Shoji, I. (2019) Cytosolic DNA-sensing immune response and viral infection. Microbiology and Immunology.63 (2) pp.51–64. doi:10.1111/1348-0421.12669.

Adler, M., Tavalai, N., Mü, R. & Stamminger, T. (2011) Human cytomegalovirus immediate-early gene expression is restricted by the nuclear domain 10 component Sp100. Journal of General Virology. 92, 1532–1538. doi:10.1099/vir.0.030981-0.

Ahn, J.-H. & Hayward, G.S. (1997) The Major Immediate-Early Proteins IE1 and IE2 of Human Cytomegalovirus Colocalize with and Disrupt PML-Associated Nuclear Bodies at Very Early Times in Infected Permissive Cells. JOURNAL OF VIROLOGY.71

Alandijany, T., Roberts, A.P.E., Conn, K.L., Loney, C., McFarlane, S., Orr, A. & Boutell, C. (2018) Distinct temporal roles for the promyelocytic leukaemia (PML) protein in the sequential regulation of intracellular host immunity to HSV-1 infection. PLoS Pathogens. 14 (1). doi:10.1371/journal.ppat.1006769.

Al-Khatib, K., Williams, B.R.G., Silverman, R.H., Halford, W. & Carr, D.J.J. (2003) The murine double-stranded RNA-dependent protein kinase PKR and the murine 2′,5′-oligoadenylate synthetase-dependent RNase L are required for IFN-β-mediated resistance against herpes simplex virus type 1 in primary trigeminal ganglion culture. Virology. 313 (1), 126–135. doi:10.1016/S0042-6822(03)00298-8.

Almine, J.F., O'Hare, C.A.J., Dunphy, G., Haga, I.R., Naik, R.J., Atrih, A., Connolly, D.J., Taylor, J., Kelsall, I.R., Bowie, A.G., Beard, P.M. & Unterholzner, L. (2017) IFI16 and cGAS cooperate in the activation of STING during DNA sensing in human keratinocytes. Nature Communications. 8. doi:10.1038/ncomms14392.

Amelio, A.L., Mcanany, P.K., Bloom, D.C., Kubat, N.J., Tran, R.K., Mcanany, P., Bloom, D.C. & Virol, J. (2006) A Chromatin Insulator-Like Element in the Herpes Simplex Virus Type 1 Latency-Associated Transcript Region Binds CCCTC-Binding Factor and Displays Enhancer-Blocking and Silencing Activities. JOURNAL OF VIROLOGY. 80 (5), 2358–2368. doi:10.1128/JVI.80.5.2358-2368.2006.

Andreeva, L., Hiller, björn, Kostrewa, D., Lässig, C., de Oliveira mann, C.C., Jan Drexler, D., maiser, A., Gaidt, moritz, Leonhardt, H., Hornung, V. & Hopfner, K. (2017) cGAS senses long and HMGB/TFAM-bound U-turn DNA by forming protein-DNA ladders. Nature Publishing Group. doi:10.1038/nature23890.

Avitabile, E., Forghieri, C. & Campadelli-Fiume, G. (2007) Complexes between Herpes Simplex Virus Glycoproteins gD, gB, and gH Detected in Cells by Complementation of Split Enhanced Green Fluorescent Protein. JOURNAL OF VIROLOGY. 81 (20), 11532–11537. doi:10.1128/JVI.01343-07.

Baczyk, D., Audette, M.C., Drewlo, S., Levytska, K. & Kingdom, J.C. (2017) SUMO-4: A novel functional candidate in the human placental protein SUMOylation machinery. doi:10.1371/journal.pone.0178056.

Batterson, W., Roizman, B. & Kovler, M.B. (1983) Characterization of the Herpes Simplex Virion-Associated Factor Responsible for the Induction of ot Genes. JOURNAL OF VIROLOGY.46 (2).

Bauer, D.W., Huffman, J.B., Homa, F.L. & Evilevitch, A. (2013) Herpes virus genome, the pressure is on. Journal of the American Chemical Society. 135 (30), 11216–11221. doi:10.1021/ja404008r.

Bayliss, R.J. & Piguet, V. (2018) Masters of manipulation: Viral modulation of the immunological synapse. Cellular Microbiology.20 (10). doi:10.1111/cmi.12944.

Bell, P., Lieberman, P.M. & Maul, G.G. (2000) Lytic but Not Latent Replication of Epstein-Barr Virus Is Associated with PML and Induces Sequential Release of Nuclear Domain 10 Proteins. JOURNAL OF VIROLOGY.74 (24).

Bernardi, R. & Pandolfi, P. (2007) Structure, dynamics and functions of promyelocytic leukaemia nuclear bodies. Nature Reviews. 8, 1006–1016. doi:10.1038/nrm2277.

Beukers, R., Ijlstra, J. & Berends, W. (1960) THE EFFECT OF ULTRAVIOLET LIGHT ON SOME COMPONENTS OF THE NUCLEIC ACIDS. VI The origin of the U.V. sensitivity of deoxyribonucleic acid.

Biasin, M., Bianco, A., Pareschi, G., Cavalleri, A., Cavatorta, C., Fenizia, C., Galli, P., Lessio, L., Lualdi, M., Tombetti, E., Ambrosi, A., Redaelli, E.M.A., Saulle, I., Trabattoni, D., Zanutta, A. & Clerici, M. (2021) UV-C irradiation is highly effective in inactivating SARS-CoV-2 replication. Scientific Reports. 11 (1). doi:10.1038/s41598-021-85425-w.

Biasin, M., Strizzi, S., Bianco, A., Macchi, A., Utyro, O., Pareschi, G., Loffreda, A., Cavalleri, A., Lualdi, M., Trabattoni, D., Tacchetti, C., Mazza, D. & Clerici, M. (2022) UV and violet light can Neutralize SARS-CoV-2 Infectivity. Journal of Photochemistry and Photobiology. 10, 100107. doi:10.1016/j.jpap.2021.100107.

Birkmann, A. & Zimmermann, H. (2016) HSV antivirals-current and future treatment options. doi:10.1016/j.coviro.2016.01.013.

Bodda, C., Reinert, L.S., Fruhwürth, S., Richardo, T., Sun, C., Zhang, B.C., Kalamvoki, M., Pohlmann, A., Mogensen, T.H., Bergström, P., Agholme, L.,

O'Hare, P., Sodeik, B., Gyrd-Hansen, M., Zetterberg, H. & Paludan, S.R. (2020) Hsv1 vp1-2 deubiquitinates sting to block type i interferon expression and promote brain infection. Journal of Experimental Medicine. 217 (7). doi:10.1084/jem.20191422.

Bøe, S.O., Haave, M., Jul-Larsen, Å., Grudic, A., Bjerkvig, R. & Lønning, P.E. (2006) Promyelocytic leukemia nuclear bodies are predetermined processing sites for damaged DNA. Journal of Cell Science. 119 (16), 3284–3295. doi:10.1242/jcs.03068.

Bonneau, R.H. (1996) Stress-Induced Effects on Integral Immune Components Involved in Herpes Simplex Virus (HSV)-Specific Memory Cytotoxic T Lymphocyte Activation. BRAIN, BEHAVIOR, AND IMMUNITY.10.

Booy, F.P., Newcomb, W.W., Trus, B.L., Brown, J.C., Baker, T.S. & Steven, A.C. (1991) Liquid-Crystalline, Phage-like Packing of Encapsidated DNA in Herpes Simplex Virus.

Booy, F.P., Trus, B.L., Newcomb, W.W., Browns, J.C., Conway, J.F. & Steven, A.C. (1994) Finding a needle in a haystack: Detection of a small protein (the 12-kDa VP26) in a large complex (the 200-MDa capsid of herpes simplex virus). Proc. Natd. Acad. Sci. USA.91.

Borst, E.-M. & Messerle, M. (2005) Analysis of Human Cytomegalovirus oriLyt Sequence Requirements in the Context of the Viral Genome. JOURNAL OF VIROLOGY. 79 (6), 3615–3626. doi:10.1128/JVI.79.6.3615-3626.2005.

Boshart, M., Weber, F., Jahn, G., Dorsch-Hiisler, K., Fleckenstein, B. & Schaffnert, W. (1985) A Very Strong Enhancer Is Located Upstream of an Immediate Early Gene of Human Cytomegalovirus. Cell.41.

Boutell, C., Cuchet-Lourenço, D., Vanni, E., Orr, A., Glass, M., Mcfarlane, S. & Everett, R.D. (2011) A Viral Ubiquitin Ligase Has Substrate Preferential

SUMO Targeted Ubiquitin Ligase Activity that Counteracts Intrinsic Antiviral Defence. PLoS Pathogens. doi:10.1371/journal.ppat.1002245.

Boutell, C. & Everett, R.D. (2013) Regulation of alphaherpesvirus infections by the ICP0 family of proteins. Journal of General Virology.94 (PART3) pp.465–481. doi:10.1099/vir.0.048900-0.

Boutell, C., Sadis, S. & Everett, R.D. (2002) Herpes Simplex Virus Type 1 Immediate-Early Protein ICP0 and Its Isolated RING Finger Domain Act as Ubiquitin E3 Ligases In Vitro. JOURNAL OF VIROLOGY. 76 (2), 841–850. doi:10.1128/JVI.76.2.841-850.2002.

Broniarczyk, J., Massimi, P., Bergant, M. & Banks, L. (2015) Human Papillomavirus Infectious Entry and Trafficking Is a Rapid Process. Journal of virology. 89 (17), 8727–8732. doi:10.1128/JVI.00722-15.

Burdette, D.L., Monroe, K.M., Sotelo-Troha, K., Iwig, J.S., Eckert, B., Hyodo, M., Hayakawa, Y. & Vance, R.E. (2011a) STING is a direct innate immune sensor of cyclic di-GMP. Nature. 478. doi:10.1038/nature10429.

Burdette, D.L., Monroe, K.M., Sotelo-Troha, K., Iwig, J.S., Eckert, B., Hyodo, M., Hayakawa, Y. & Vance, R.E. (2011b) STING is a direct innate immune sensor of cyclic di-GMP. Nature. 478. doi:10.1038/nature10429.

Butcher, S.J., Aitken, J., Mitchell, J., Gowen, B. & Dargan, D.J. (1998a) Structure of the Human Cytomegalovirus B Capsid by Electron Cryomicroscopy and Image Reconstruction.

Butcher, S.J., Aitken, J., Mitchell, J., Gowen, B. & Dargan, D.J. (1998b) Structure of the Human Cytomegalovirus B Capsid by Electron Cryomicroscopy and Image Reconstruction.

Cantrell, S.R. & Bresnahan, W.A. (2006) Human Cytomegalovirus (HCMV) UL82 Gene Product (pp71) Relieves hDaxx-Mediated Repression of HCMV Replication. JOURNAL OF VIROLOGY. 80 (12), 6188–6191. doi:10.1128/JVI.02676-05.

Cantrell, S.R. & Bresnahan, W.A. (2005) Interaction between the Human Cytomegalovirus UL82 Gene Product (pp71) and hDaxx Regulates Immediate-Early Gene Expression and Viral Replication. Journal of Virology. 79 (12), 7792–7802. doi:10.1128/jvi.79.12.7792-7802.2005.

Carell, T. & Epple, R. (1998) MICROREVIEW Repair of UV Light Induced DNA Lesions: A Comparative Study with Model Compounds.

Carrozza, M.J. & Deluca, N.A. (1996) Interaction of the Viral Activator Protein ICP4 with TFIID through TAF250. MOLECULAR AND CELLULAR BIOLOGY.16 (6). https://journals.asm.org/journal/mcb.

Challberg, M.D. (1986) A method for identifying the viral genes required for herpesvirus DNA replication (plasmid transfection/transient assay/herpes simplex virus OrL and oris). Genetics.83.

Chee, A. v, Lopez, P., Pandolfi, P.P. & Roizman, B. (2003) Promyelocytic Leukemia Protein Mediates Interferon-Based Anti-Herpes Simplex Virus 1 Effects. JOURNAL OF VIROLOGY. 77 (12), 7101–7105. doi:10.1128/JVI.77.12.7101-7105.2003.

Chehrehasa, F., Meedeniya, A.C.B., Dwyer, P., Abrahamsen, G. & Mackay-Sim, A. (2009) EdU, a new thymidine analogue for labelling proliferating cells in the nervous system. Journal of Neuroscience Methods. 177 (1), 122–130. doi:10.1016/j.jneumeth.2008.10.006.

Chen, I.-H.B., Sciabica, K.S. & Sandri-Goldin, R.M. (2002) ICP27 Interacts with the RNA Export Factor Aly/REF To Direct Herpes Simplex Virus Type 1 Intronless mRNAs to the TAP Export Pathway. Journal of Virology. 76 (24), 12877–12889. doi:10.1128/jvi.76.24.12877-12889.2002.

Christensen, M.H., Jensen, S.B., Miettinen, J.J., Luecke, S., Prabakaran, T., Reinert, L.S., Mettenleiter, T., Chen, Z.J., Knipe, D.M., Sandri-Goldin, R.M., Enquist, L.W., Hartmann, R., Mogensen, T.H., Rice, S.A., Nyman,

T.A., Matikainen, S. & Paludan, S.R. (2016) HSV -1 ICP 27 targets the TBK 1-activated STING signalsome to inhibit virus-induced type I IFN expression . The EMBO Journal. 35 (13), 1385–1399. doi:10.15252/embj.201593458.

Chu, S. (2012) Transcriptional regulation by post-transcriptional modification-Role of phosphorylation in Sp1 transcriptional activity. doi:10.1016/j.gene.2012.07.022.

Civril, F., Deimling, T., de Oliveira Mann, C.C., Ablasser, A., Moldt, M., Witte, G., Hornung, V. & Hopfner, K.P. (2013) Structural mechanism of cytosolic DNA sensing by cGAS. Nature. 498 (7454), 332–337. doi:10.1038/nature12305.

Cliffe, A.R. & Knipe, D.M. (2008) Herpes Simplex Virus ICP0 Promotes both Histone Removal and Acetylation on Viral DNA during Lytic Infection. Journal of Virology. 82 (24), 12030–12038. doi:10.1128/jvi.01575-08.

Cockrell, S.K., Huffman, J.B., Toropova, K., Conway, J.F. & Homa, F.L. (2011) Residues of the UL25 Protein of Herpes Simplex Virus That Are Required for Its Stable Interaction with Capsids. JOURNAL OF VIROLOGY. 85 (10), 4875–4887. doi:10.1128/JVI.00242-11.

Compton, T., Nepomuceno, R.R. & Nowlin, D.M. (1992) Human Cytomegalovirus Penetrates Host Cells by PH-Independent Fusion at the Cell Surface. VIROLOGY.191.

Compton, T., Nowlin, D.M. & Cooper, N.R. (1993) Initiation of Human Cytomegalovirs Infection Requires Initial Interaction with Cell Surface Heparan Sulfate. Virology. 193, 834–841.

Conley, A.J., Knipe, D.M., Jones, P.C. & Roizman, B. (1981) Molecular Genetics of Herpes Simplex Virus Characterization of a Temperature-Sensitive Mutant Produced by In Vitro Mutagenesis and Defective in DNA Synthesis and Accumulation of y Polypeptides. JOURNAL OF VIROLOGY.37 (1). https://journals.asm.org/journal/jvi.

Connolly, S.A., Jardetzky, T.S. & Longnecker, R. (2021) The structural basis of herpesvirus entry. Nature Reviews. 19, 110–121. doi:10.1038/s41579-020-00448-w.

Conway, J.F., Cockrell, S.K., Copeland, A.M., Newcomb, W.W., Brown, J.C. & Homa, F.L. (2010) Labeling and Localization of the Herpes Simplex Virus Capsid Protein UL25 and Its Interaction with the Two Triplexes Closest to the Penton. Journal of Molecular Biology. 397 (2), 575–586. doi:10.1016/j.jmb.2010.01.043.

Copeland, A.M., Newcomb, W.W. & Brown, J.C. (2009a) Herpes Simplex Virus Replication: Roles of Viral Proteins and Nucleoporins in Capsid-Nucleus Attachment. Journal of Virology. 83 (4), 1660–1668. doi:10.1128/jvi.01139-08.

Copeland, A.M., Newcomb, W.W. & Brown, J.C. (2009b) Herpes Simplex Virus Replication: Roles of Viral Proteins and Nucleoporins in Capsid-Nucleus Attachment. JOURNAL OF VIROLOGY. 83 (4), 1660–1668. doi:10.1128/JVI.01139-08.

Corrales, L., Glickman, L.H., McWhirter, S.M., Kanne, D.B., Sivick, K.E., Katibah, G.E., Woo, S.R., Lemmens, E., Banda, T., Leong, J.J., Metchette, K., Dubensky, T.W. & Gajewski, T.F. (2015) Direct Activation of STING in the Tumor Microenvironment Leads to Potent and Systemic Tumor Regression and Immunity. Cell Reports. 11 (7), 1018–1030. doi:10.1016/j.celrep.2015.04.031.

Courey, A.J. & Tjian, R. (1988) Analysis of Spl In Vivo Reveals Mutiple Transcriptional Domains, Including a Novel Glutamine-Rich Activation Motif. Cell.55.

Crameri, M., Bauer, M., Caduff, N., Walker, R., Steiner, F., Franzoso, F.D., Gujer, C., Boucke, K., Kucera, T., Zbinden, A., Münz, C., Fraefel, C., Greber, U.F. & Pavlovic, J. (2018) MxB is an interferon-induced restriction

factor of human herpesviruses. Nature Communications. 9, 1980–1996. doi:10.1038/s41467-018-04379-2.

Cuchet-Lourenço, D., Anderson, G., Sloan, E., Orr, A. & Everett, R.D. (2013) The Viral Ubiquitin Ligase ICP0 Is neither Sufficient nor Necessary for Degradation of the Cellular DNA Sensor IFI16 during Herpes Simplex Virus 1 Infection. doi:10.1128/JVI.02474-13.

Cuchet-Lourenço, D., Boutell, C., Lukashchuk, V., Grant, K., Sykes, A., Murray, J., Orr, A. & Everett, R.D. (2011) SUMO pathway dependent recruitment of cellular repressors to herpes simplex virus type 1 genomes. PLoS Pathogens. 7 (7). doi:10.1371/journal.ppat.1002123.

Cui, Y., Yu, H., Zheng, X., Peng, R., Wang, Q., Zhou, Y., Wang, R., Wang, J., Qu, B., Shen, N., Guo, Q., Liu, X. & Wang, C. (2017) SENP7 Potentiates cGAS Activation by Relieving SUMO-Mediated Inhibition of Cytosolic DNA Sensing. PLoS Pathogens. 13 (1). doi:10.1371/journal.ppat.1006156.

Dalai, S.K., Pesnicak, L., Miller, G.F. & Straus, S.E. (2002) Prophylactic and therapeutic effects of human immunoglobulin on the pathobiology of HSV-1 infection, latency, and reactivation in mice. Journal of NeuroVirology.8.

Davis' And, D.B. & Kingsbury, D.T. (1976) Quantitation of the Viral DNA Present in Cells Transformed by UV-Irradiated Herpes Simplex Virus. JOURNAL OF VIROLOGY.17 (3). https://journals.asm.org/journal/jvi.

Delaloye, J., Roger, T., Steiner-Tardivel, Q.G., le Roy, D., Reymond, M.K., Akira, S., Petrilli, V., Gomez, C.E., Perdiguero, B., Tschopp, J., Pantaleo, G., Esteban, M. & Calandra, T. (2009) Innate immune sensing of modified vaccinia virus Ankara (MVA) is mediated by TLR2-TLR6, MDA-5 and the NALP3 inflammasome. PLoS Pathogens. 5 (6). doi:10.1371/journal.ppat.1000480.

Dell'Oste, V., Gatti, D., Gugliesi, F., de Andrea, M., Bawadekar, M., lo Cigno, I., Biolatti, M., Vallino, M., Marschall, M., Gariglio, M. & Landolfo,

S. (2014) Innate Nuclear Sensor IFI16 Translocates into the Cytoplasm during the Early Stage of In Vitro Human Cytomegalovirus Infection and Is Entrapped in the Egressing Virions during the Late Stage . Journal of Virology. 88 (12), 6970–6982. doi:10.1128/jvi.00384-14.

Deschamps, T. & Kalamvoki, M. (2017) Evasion of the STING DNA-Sensing Pathway by VP11/12 of Herpes Simplex Virus 1. doi:10.1128/JVI.

Diner, B.A., Lum, K.K., Toettcher, J.E. & Cristea, I.M. (2016) Viral DNA sensors IFI16 and cyclic GMP-AMP synthase possess distinct functions in regulating viral gene expression, immune defenses, and apoptotic responses during herpesvirus infection. mBio. 7 (6). doi:10.1128/mBio.01553-16.

Diner, E.J., Burdette, D.L., Wilson, S.C., Monroe, K.M., Kellenberger, C.A., Hyodo, M., Hayakawa, Y., Hammond, M.C. & Vance, R.E. (2013) The Innate Immune DNA Sensor cGAS Produces a Noncanonical Cyclic Dinucleotide that Activates Human STING. Cell Reports. 3 (5), 1355–1361. doi:10.1016/j.celrep.2013.05.009.

Döhner, K., Nagel, C.H. & Sodeik, B. (2005) Viral stop-and-go along microtubules: Taking a ride with dynein and kinesins. Trends in Microbiology.13 (7) pp.320–327. doi:10.1016/j.tim.2005.05.010.

Doucas, V., Ishov, A.M., Romo, A., Juguilon, H., Weitzman, M.D., Evans, R.M. & Maul, G.G. (1996) Adenovirus replication is coupltd e with the dynamic propernes of PML nuclear structure.

Drané, P., Ouararhni, K., Depaux, A., Shuaib, M. & Hamiche, A. (2010) The death-associated protein DAXX is a novel histone chaperone involved in the replication-independent deposition of H3.3. Genes and Development. 24, 1253–1265. doi:10.1101/gad.566910.

Du, M. & Chen, Z.J. (2018) DNA-induced liquid phase condensation of cGAS activates innate immune signaling. http://science.sciencemag.org/.

Du, T., Zhou, G., Roizman, B. & Kovler, M.B. (2011) HSV-1 gene expression from reactivated ganglia is disordered and concurrent with suppression of latency-associated transcript and miRNAs. PNAS. 108 (46), 18820–18824. doi:10.1073/pnas.1117203108.

Duff, R. & Rapp, F. (1973) Oncogenic Transformation of Hamster Embryo Cells After Exposure to Inactivated Herpes Simplex Virus Type 1. JOURNAL OF VIROLOGY.12 (2). https://journals.asm.org/journal/jvi.

Dutrieux, J., Maarifi, G., Portilho, D.M., Arhel, N.J., Chelbi-Alix, M.K. & Nisole, S. (2015) PML/TRIM19-Dependent Inhibition of Retroviral Reverse-Transcription by Daxx. PLoS Pathogens. 11 (11). doi:10.1371/journal.ppat.1005280.

Dynan, W.S. & Tjian, R. (1983) Isolation of Transcription Factors That Discriminate between Different Promoters Recognized by RNA Polymerase II. Cell.32.

Eglin, R.P., Gugerli, P. & Wildy, P. (1980) Ultraviolet Irradiation of Herpes Simplex Virus (Type 1): Delayed Transcription and Comparative Sensitivities of Virus Functions.49. www.microbiologyresearch.org.

Elias, P., O'donnell, M.E., Mocarskit, E.S. & Lehman, I.R. (1986) A DNA binding protein specific for an origin of replication of her'pes simplex virus type 1. Proc. Nati. Acad. Sci. USA.83.

Eloranta, M.-L., Sandberg, K. & Alm, G. v (1996) The Interferon-/ Responses of Mice to Herpes Simplex Virus Studied at the Blood and Tissue Level In Vitro and In Vivo.

El-Sagheer, A.H. & Brown, T. (2010) Click chemistry with DNA. Chemical Society Reviews. 39 (4), 1388–1405. doi:10.1039/b901971p.

Everett, R.D. (2015) Dynamic Response of IFI16 and Promyelocytic Leukemia Nuclear Body Components to Herpes Simplex Virus 1 Infection. doi:10.1128/JVI.02249-15.

Everett, R.D. (2014) HSV-1 biology and life cycle. Methods in Molecular Biology. 1144, 1–17. doi:10.1007/978-1-4939-0428-0_1.

Everett, R.D. (2006) Interactions between DNA viruses, ND10 and the DNA damage response. Cellular Microbiology. 8 (3), 365–374. doi:10.1111/j.1462-5822.2005.00677.x.

Everett, R.D., Boutell, C. & Hale, B.G. (2013) Interplay between viruses and host sumoylation pathways. Nature Reviews Microbiology.11 (6) pp.400–411. doi:10.1038/nrmicro3015.

Everett, R.D., Boutell, C. & Orr, A. (2004) Phenotype of a Herpes Simplex Virus Type 1 Mutant That Fails To Express Immediate-Early Regulatory Protein ICP0. Journal of Virology. 78 (4), 1763–1774. doi:10.1128/jvi.78.4.1763-1774.2004.

Everett, R.D. & Chelbi-Alix, M.K. (2007) PML and PML nuclear bodies: Implications in antiviral defence. Biochimie.89 (6–7) pp.819–830. doi:10.1016/j.biochi.2007.01.004.

Everett, R.D. & Murray, J. (2005) ND10 Components Relocate to Sites Associated with Herpes Simplex Virus Type 1 Nucleoprotein Complexes during Virus Infection. Journal of Virology. 79 (8), 5078–5089. doi:10.1128/jvi.79.8.5078-5089.2005.

Everett, R.D., Murray, J., Orr, A. & Preston, C.M. (2007) Herpes Simplex Virus Type 1 Genomes Are Associated with ND10 Nuclear Substructures in Quiescently Infected Human Fibroblasts. JOURNAL OF VIROLOGY. 81 (20), 10991–11004. doi:10.1128/JVI.00705-07.

Everett, R.D., Parada, C., Gripon, P., Sirma, H. & Orr, A. (2008) Replication of ICP0-Null Mutant Herpes Simplex Virus Type 1 Is Restricted by both PML and Sp100. JOURNAL OF VIROLOGY. 82 (6), 2661–2672. doi:10.1128/JVI.02308-07.

Everett, R.D., Rechter, S., Papior, P., Tavalai, N., Stamminger, T. & Orr, A. (2006) PML Contributes to a Cellular Mechanism of Repression of Herpes Simplex Virus Type 1 Infection That Is Inactivated by ICP0. Journal of Virology. 80 (16), 7995–8005. doi:10.1128/jvi.00734-06.

Falkenberg, M., Bushnell, D.A., Elias, P. & Lehman, I.R. (1997) The UL8 subunit of the heterotrimeric herpes simplex virus type 1 helicase-primase is required for the unwinding of single strand DNA-binding protein (ICP8)-coated DNA substrates. Journal of Biological Chemistry. 272 (36), 22766–22770. doi:10.1074/jbc.272.36.22766.

Fan, D., Wang, M., Cheng, A., Jia, R., Yang, Q., et al. (2020) The Role of VP16 in the Life Cycle of Alphaherpesviruses. Frontiers in Microbiology.11. doi:10.3389/fmicb.2020.01910.

Fan, W.H., Roberts, A.P.E., Mcelwee, M., Bhella, D., Rixon, F.J. & Lauder, R. (2015) The Large Tegument Protein pUL36 Is Essential for Formation of the Capsid Vertex-Specific Component at the Capsid-Tegument Interface of Herpes Simplex Virus 1. doi:10.1128/JVI.02887-14.

Feire, A.L., Koss, H. & Compton, T. (2004) Cellular integrins function as entry receptors for human cytomegalovirus via a highly conserved disintegrin-like domain. www.pnas.orgcgidoi10.1073pnas.0406821101.

Fierer, D.S. & Challberg, M.D. (1992) Purification and Characterization of UL9, the Herpes Simplex Virus Type 1 Origin-Binding Protein. JOURNAL OF VIROLOGY.66 (7). https://journals.asm.org/journal/jvi.

Fortunato, E.A., Sommer, M.H., Yoder, K. & Spector, D.H. (1997) Identification of Domains within the Human Cytomegalovirus Major Immediate-Early 86-Kilodalton Protein and the Retinoblastoma Protein Required for Physical and Functional Interaction with Each Other. JOURNAL OF VIROLOGY.71 (11). https://journals.asm.org/journal/jvi.

Fortunato, E.A. & Spector, D.H. (1999) REGULATION OF HUMAN CYTOMEGALOVIRUS GENE EXPRESSION Vast Array of Cis-Acting Sequences Defining IElIIE2 Promoter Physical Properties of IEUIE2 Proteins Delineation of Transacting Functions of IEl/IE2 Gene Products Importance of IE1 72 in Growth and Replication of HCMV Signal Transduction Events Important for Early Gene Expression Transcriptional Control of HCMV Early Promoters Establishment of Replication Centers by Early Genes Sequestration of Several Cellular Proteins into Replication Centers.

Frappier, L. (2016) Manipulation of PML Nuclear Bodies and DNA Damage Responses by DNA Viruses.

Fridlender, B., Asher, Y., Weinberg-Zahlering, E. & Becker, Y. (1978) Interaction of Ultraviolet-irradiated Herpes Simplex Virus Type 1 with BSC-1 cells.

Frobert, E., Burrel, S., Ducastelle-Lepretre, S., Billaud, G., Ader, F., Casalegno, J.S., Nave, V., Boutolleau, D., Michallet, M., Lina, B. & Morfin, F. (2014) Resistance of herpes simplex viruses to acyclovir: An update from a ten-year survey in France. Antiviral Research. 111, 36–41. doi:10.1016/j.antiviral.2014.08.013.

Furlong, D., Swift, H. & Roizman, B. (1972) Arrangement of Herpesvirus Deoxyribonucleic Acid in the Core. JOURNAL OF VIROLOGY. https://journals.asm.org/journal/jvi.

Further, V., Batterson, W., Furlong, D., Roizman, B. & Kovler, M.B. (1983) Molecular Genetics of Herpes Simplex Virus Characterization of a Temperature-Sensitive Mutant Defective in Release of Viral DNA and in Other Stages of the Viral Reproductive Cycle. JOURNAL OF VIROLOGY.45 (1). https://journals.asm.org/journal/jvi.

le Gac, N.T., Villani, G. & Boehmer, P.E. (1998) Herpes Simplex Virus Type-1 Single-strand DNA-binding Protein (ICP8) Enhances the Ability of the Viral

DNA Helicase-primase to Unwind Cisplatin-modified DNA*. THE JOURNAL OF BIOLOGICAL CHEMISTRY.273 (22). http://www.jbc.org.

Gao, D., Li, T., Li, X.-D., Chen, X., Li, Q.-Z., Wight-Carter, M., Chen, Z.J., Casanova, J.-L., Jung, J.U. & P-Y Ting, J. (2015) Activation of cyclic GMP-AMP synthase by self-DNA causes autoimmune diseases. PNAS. doi:10.1073/pnas.1516465112.

Gao, P., Ascano, M., Wu, Y., Barchet, W., Gaffney, B.L., Zillinger, T., Serganov, A.A., Liu, Y., Jones, R.A., Hartmann, G., Tuschl, T. & Patel, D.J. (2013) Cyclic [G(2′,5′)pA(3′,5′)p] is the metazoan second messenger produced by DNA-activated cyclic GMP-AMP synthase. Cell. 153 (5), 1094–1107. doi:10.1016/j.cell.2013.04.046.

Gary, N., Rosenberg, L. & Louis, A. (1974) Induction of Cellular Immunity to Herpes Simplex Virus: Relationship to the Humoral Immune Response. http://www.jimmunol.org/content/112/3.

Geraghty, R.J., Krummenacher, C., Cohen, G.H., Eisenberg, R.J. & Spear, P.G. (1998) Entry of Alphaherpesviruses Mediated by Poliovirus Receptor-Related Protein 1 and Poliovirus Receptor. http://science.sciencemag.org/.

Gianni, T., Amasio, M. & Campadelli-Fiume, G. (2009) Herpes simplex virus gD forms distinct complexes with fusion executors gB and gH/gL in part through the C-terminal profusion domain. Journal of Biological Chemistry. 284 (26), 17370–17382. doi:10.1074/jbc.M109.005728.

Gibson, W. (1983) Protein Counterparts of Human and Simian Cytomegaloviruses'. VIROLOGY.128.

Gibson, W., Baxter, M.K. & Clopper, K.S. (1996) Cytomegalovirus "Missing" Capsid Protein Identified as Heat-Aggregable Product of Human Cytomegalovirus UL46. JOURNAL OF VIROLOGY.70 (11). https://journals.asm.org/journal/jvi.

Gibson, W., van Breemen, R., Fields, A., Lafemina, R. & Irmiere, A. (1984) D,L-OL-Difluoromethylornithine Inhibits Human Cytomegalovirus Replication. JOURNAL OF VIROLOGY.50 (1). https://journals.asm.org/journal/jvi.

Gibson, W., Clopper, K.S., Britt, W.J. & Baxter, M.K. (1996) Human Cytomegalovirus (HCMV) Smallest Capsid Protein Identified as Product of Short Open Reading Frame Located between HCMV UL48 and UL49. JOURNAL OF VIROLOGY.70 (8). https://journals.asm.org/journal/jvi.

Glass, M. & Everett, R.D. (2013) Components of Promyelocytic Leukemia Nuclear Bodies (ND10) Act Cooperatively To Repress Herpesvirus Infection. doi:10.1128/JVI.02950-12.

Glauser, D.L., Strasser, R., Laimbacher, A.S., Saydam, O., Clément, N., Linden, R.M., Ackermann, M. & Fraefel, C. (2007) Live Covisualization of Competing Adeno-Associated Virus and Herpes Simplex Virus Type 1 DNA Replication: Molecular Mechanisms of Interaction. Journal of Virology. 81 (9), 4732–4743. doi:10.1128/jvi.02476-06.

Goff, S.P., Cabral, J.M., Oh, H.S. & Knipe, D.M. (2018) ATRX promotes maintenance of herpes simplex virus heterochromatin during chromatin stress. doi:10.7554/eLife.40228.001.

Goldberg, A.D., Banaszynski, L.A., Noh, K.M., Lewis, P.W., Elsaesser, S.J., et al. (2010) Distinct Factors Control Histone Variant H3.3 Localization at Specific Genomic Regions. Cell. 140 (5), 678–691. doi:10.1016/j.cell.2010.01.003.

Goodrum, F. (2016) Human Cytomegalovirus Latency: Approaching the Gordian Knot. Annual Review of Virology.3 pp.333–357. doi:10.1146/annurev-virology-110615-042422.

Goodsell, D. (2001) The Molecular Perspective: Ultraviolet Light and Pyrimidine Dimers. http://theoncologist.alphamedpress.org/.

Granzow, H., Klupp, B.G., Fuchs, W., Veits, J., Osterrieder, N. & Mettenleiter, T.C. (2001) Egress of Alphaherpesviruses: Comparative Ultrastructural Study. JOURNAL OF VIROLOGY. 75 (8), 3675–3684. doi:10.1128/JVI.75.8.3675-3684.2001.

Griffiths, P., Baraniak, I. & Reeves, M. (2015) The pathogenesis of human cytomegalovirus. Journal of Pathology J Pathol. 235, 288–297. doi:10.1002/path.4437.

Grünewald, K., Desai, P., Winkler, D.C., Heymann, J.B., Belnap, D.M., Baumeister, W. & Steven, A.C. (2003) Three-Dimensional Structure of Herpes Simplex Virus from Cryo-Electron Tomography. www.sciencemag.org/cgi/content/full/302/5649/1396/DC1.

Gu, B., Rivera Gonzalez, R., Smith, C.A. & Deluca, N.A. (1993) Herpes simplex virus infected cell polypeptide 4 preferentially represses Spl-activated over basal transcription from its own promoter (TATA binding protein/in vitro transcription/DNA-protein interactions/regulation of transcription). Proc. Natl. Acad. Sci. USA.90.

Gu, W., Huang, Q. & Hyward, G.S. (1995) Multiple Tandemly Repeated Binding Sites for the YY1 Repressor and Transcription Factors AP-1 and SP-1 Are Clustered within Intron-1 of the Gene Encoding the IE 110 Transactivator of Herpes simplex Virus Type I. J Biomed Sci.2.

Hall, J.D., Featherston, J.D. & Almy, R.E. (1980) Evidence for Repair of Ultraviolet Light-Damaged Herpes Virus in Human Fibroblasts by a Recombination Mechanism. VIROLOGY.105.

Hannoun, Z., Maarifi, G. & Chelbi-Alix, M.K. (2016) The implication of SUMO in intrinsic and innate immunity. Elsevier. 29, 3–16. doi:10.1016/j.cytogfr.2016.04.003.

Hardwicke, M.A. & Schaffer, P.A. (1995) Cloning and Characterization of Herpes Simplex Virus Type 1 oriL: Comparison of Replication and Protein-

DNA Complex Formation by oriL and oriS. JOURNAL OF VIROLOGY.69 (3). https://journals.asm.org/journal/jvi.

Held, K. & Derfuss, T. (2011) Control of HSV-1 latency in human trigeminal ganglia-current overview. Journal of Neurovirology. (17), 518–527. doi:10.1007/s13365-011-0063-0.

Heming, J.D., Conway, J.F. & Homa, F.L. (2017) Herpesvirus capsid assembly and DNA packaging. Adv Anat Embryol Cell Biol. 223, 119–142. doi:10.1007/978-3-319-53168-7_6.

Hendricks, R.L., Freeman, M.L., Sheridan, B.S. & Bonneau, R.H. (2021) Type 1 Infections Cell Control of Latent Herpes Simplex Virus T + Psychological Stress Compromises CD8. doi:10.4049/jimmunol.179.1.322.

Hendricks, R.L., Weber, P.C., Taylor, J.L., Koumbis, A., Tmnpey I, T.M. & Gloriosoa, J.C. (1991) Endogenously produced interferon • protects mice from herpes simplex virus type 1 corneal disease. Journal of General Virology.72.

Hidmark, A.S., McInerney, G.M., Nordstrom, E.K.L., Douagi, I., Werner, K.M., Liljestrom, P. & Hedestam, G.B.K. (2005) Early Alpha/Beta Interferon Production by Myeloid Dendritic Cells in Response to UV-Inactivated Virus Requires Viral Entry and Interferon Regulatory Factor 3 but Not MyD88. Journal of Virology. 79 (16), 10376–10385. doi:10.1128/jvi.79.16.10376-10385.2005.

Hoey, T., Weinzierl, J., Gill, G., Chen, J.-L., David Dynlacht, B. & Tjian, R. (1993) Molecular Cloning and Functional Analysis of Drosophila TAF110 Reveal Properties Expected of Coactivators. Cell.72.

Hofmann, H., Sindre, H. & Stamminger, T. (2002) Functional Interaction between the pp71 Protein of Human Cytomegalovirus and the PML-Interacting Protein Human Daxx. JOURNAL OF VIROLOGY. 76 (11), 5769–5783. doi:10.1128/JVI.76.11.5769-5783.2002.

Hollinshead, M., Johns, H.L., Sayers, C.L., Gonzalez-Lopez, C., Smith, G.L. & Elliott, G. (2012) Endocytic tubules regulated by Rab GTPases 5 and 11 are used for envelopment of herpes simplex virus. EMBO Journal. 31 (21), 4204–4220. doi:10.1038/emboj.2012.262.

Honess, R.W. & Roizman, B. (1974) Regulation of Herpesvirus Macromolecular Synthesis I. Cascade Regulation of the Synthesis of Three Groups of Viral Proteins. JOURNAL OF VIROLOGY.14 (1). https://journals.asm.org/journal/jvi.

Hopfner, K.-P. & Hornung, V. (2020) Molecular mechanisms and cellular functions of cGAS–STING signalling. Nature Reviews Molecular Cell Biology. 21, 501–521. doi:10.1038/s41580-020-0244-x.

Horan, K.A., Hansen, K., Jakobsen, M.R., Holm, C.K., Søby, S., Unterholzner, L., Thompson, M., West, J.A., Iversen, M.B., Rasmussen, S.B., Ellermann-Eriksen, S., Kurt-Jones, E., Landolfo, S., Damania, B., Melchjorsen, J., Bowie, A.G., Fitzgerald, K.A. & Paludan, S.R. (2013) Proteasomal Degradation of Herpes Simplex Virus Capsids in Macrophages Releases DNA to the Cytosol for Recognition by DNA Sensors. The Journal of Immunology. 190 (5), 2311–2319. doi:10.4049/jimmunol.1202749.

Hou, W., Cruz-Cosme, R., Wen, F., Ahn, J.-H., Reeves, I., Luo, M.-H., Tang, Q. & Jung, J.U. (2017) Expression of Human Cytomegalovirus IE1 Leads to Accumulation of Mono-SUMOylated PML That Is Protected from Degradation by Herpes Simplex Virus 1 ICP0 VIRUS-CELL INTERACTIONS crossm. J Virol. 91, 1452–1470. doi:10.1128/JVI.

Hsu, K.-S. & Kao, H.-Y. (2018) PML: Regulation and multifaceted function beyond tumor suppression. 8, 5. doi:10.1186/s13578-018-0204-8.

Hu, B., Li, X., Huo, Y., Yu, Y., Zhang, Q., Chen, G., Zhang, Y., Fraser, N.W., Wu, D. & Zhou, J. (2016a) Cellular responses to HSV-1 infection are linked

to specific types of alterations in the host transcriptome. Scientific Reports. 6. doi:10.1038/srep28075.

Hu, M.M., Yang, Q., Xie, X.Q., Liao, C.Y., Lin, H., Liu, T.T., Yin, L. & Shu, H.B. (2016b) Sumoylation Promotes the Stability of the DNA Sensor cGAS and the Adaptor STING to Regulate the Kinetics of Response to DNA Virus. Immunity. 45 (3), 555–569. doi:10.1016/j.immuni.2016.08.014.

Huang, J., You, H., Su, C., Li, Y., Chen, S. & Zheng, C. (2018) Herpes Simplex Virus 1 Tegument Protein VP22 Abrogates cGAS/STING-Mediated Antiviral Innate Immunity. doi:10.1128/JVI.00841-18.

Huet, A., Makhov, A.M., Huffman, J.B., Vos, M., Homa, F.L. & Conway, J.F. (2016) Extensive subunit contacts underpin herpesvirus capsid stability and interior-to-exterior allostery. Nature Structural & Molecular Biology. 23 (6), 531–540. doi:10.1038/nsmb.3212.

Hwang, J. & Kalejta, R.F. (2009) Human Cytomegalovirus Protein pp71 Induces Daxx SUMOylation †. JOURNAL OF VIROLOGY. 83 (13), 6591–6598. doi:10.1128/JVI.02639-08.

Hwang, J. & Kalejta, R.F. (2007) Proteasome-dependent, ubiquitin-independent degradation of Daxx by the viral pp71 protein in human cytomegalovirus-infected cells. Virology. 367 (2), 334–338. doi:10.1016/j.virol.2007.05.037.

Imbalzano, A.N., Coen, D.M. & Delucal12, N.A. (1991) Herpes Simplex Virus Transactivator ICP4 Operationally Substitutes for the Cellular Transcription Factor Spl for Efficient Expression of the Viral Thymidine Kinase Gene. JOURNAL OF VIROLOGY.65 (2). https://journals.asm.org/journal/jvi.

Imbalzanot, A.N. & Delucat, N.A. (1992) Substitution of a TATA Box from a Herpes Simplex Virus Late Gene in the Viral Thymidine Kinase Promoter Alters ICP4 Inducibility but Not Temporal Expression. JOURNAL OF VIROLOGY.66 (9). https://journals.asm.org/journal/jvi.

Imbert, F. & Langford, · Dianne (2021) Viruses, SUMO, and immunity: the interplay between viruses and the host SUMOylation system. Journal of NeuroVirology. 1, 3. doi:10.1007/s13365-021-00995-9.

Irmiere, A. & Gibson, W. (1985) Isolation of Human Cytomegalovirus Intranuclear Capsids, Characterization of Their Protein Constituents, and Demonstration that the B-Capsid Assembly Protein Is Also Abundant in Noninfectious Enveloped Particles. JOURNAL OF VIROLOGY.56 (1). https://journals.asm.org/journal/jvi.

Ishikawa, H. & Barber, G.N. (2008a) STING is an endoplasmic reticulum adaptor that facilitates innate immune signalling. Nature. 455, 674–679. doi:10.1038/nature07317.
Ishikawa, H. & Barber, G.N. (2008b) STING is an endoplasmic reticulum adaptor that facilitates innate immune signalling. Nature. 455 (7213), 674–678. doi:10.1038/nature07317.

Ishikawa, H., Ma, Z. & Barber, G.N. (2009) LETTERS STING regulates intracellular DNA-mediated, type I interferon-dependent innate immunity. Nature. doi:10.1038/nature08476.

Ishov, A.M. & Maul, G.G. (1996) The Periphery of Nuclear Domain 10 (ND10) as Site of DNA Virus Deposition.

Ishov, A.M., Stenberg, R.M. & Maul, G.G. (1997) Human Cytomegalovirus Immediate Early Interaction with Host Nuclear Structures: Definition of an Immediate Transcript Environment. The Journal of Cell Biology.138 (1).

Ishov, A.M., Vladimirova, O. v & Maul, G.G. (2002) Daxx-Mediated Accumulation of Human Cytomegalovirus Tegument Protein pp71 at ND10 Facilitates Initiation of Viral Infection at These Nuclear Domains. JOURNAL OF VIROLOGY. 76 (15), 7705–7712. doi:10.1128/JVI.76.15.7705-7712.2002.

Iwahori, S., Shirata, N., Kawaguchi, Y., Weller, S.K., Sato, Y., Kudoh, A., Nakayama, S., Isomura, H. & Tsurumi, T. (2007) Enhanced Phosphorylation of Transcription Factor Sp1 in Response to Herpes Simplex Virus Type 1 Infection Is Dependent on the Ataxia Telangiectasia-Mutated Protein. Journal of Virology. 81 (18), 9653–9664. doi:10.1128/jvi.00568-07.

Iwahori, S., Yasui, Y., Kudoh, A., Sato, Y., Nakayama, S., Murata, T., Isomura, H. & Tsurumi, T. (2008) Identification of phosphorylation sites on transcription factor Sp1 in response to DNA damage and its accumulation at damaged sites. Cellular Signalling. 20 (10), 1795–1803. doi:10.1016/j.cellsig.2008.06.007.

Jackson, S.P., MacDonald, J.J., Lees-Miller, S. & Tjian, R. (1990) GC Box Binding Induces Phosphorylation of Spl by a DNA-Dependent Protein Kinase. Cell.63.

Jaguva Vasudevan, A.A., Bähr, A., Grothmann, R., Singer, A., Häussinger, D., Zimmermann, A. & Münk, C. (2018) MXB inhibits murine cytomegalovirus. Virology. 522, 158–167. doi:10.1016/j.virol.2018.07.017.

Jakobse, M.R., Bak, R.O., Anderson, A., Berg, R.K., Jensen, S.B., Jin, T., Laustsen, A., Hensen, K., Ostergaard, L., Fitzgerald, K.A., Xiao, S.T., Mikkelsen, J.G., Mogensen, T.H. & Paludan, S.R. (2013) IFI16 senses DNA forms of the lentiviral replicationcycle and controls HIV-1 replication. Proceedings of the National Academy of Sciences of the United States of America. 41 (14), 6358–6363. doi:10.1073/pnas.1314303110.

Jaworska, A.M., Nikola, |, Wlodarczyk, A., Mackiewicz, | Andrzej & Czerwinska, P. (2020) The role of TRIM family proteins in the regulation of cancer stem cell self-renewal. Stem Cells. 38, 165–173. doi:10.1002/stem.3109.

Jensen, E. (2014) Technical Review: In Situ Hybridization.

Jensen, K., Shiels, C. & Freemont, P.S. (2001) PML protein isoforms and the RBCC/TRIM motif. www.nature.com/onc.

Jiang, H., Xue, X., Panda, S., Kawale, A., Hooy, R.M., Liang, F., Sohn, J., Sung, P. & Gekara, N.O. (2019) Chromatin-bound cGAS is an inhibitor of DNA repair and hence accelerates genome destabilization and cell death . The EMBO Journal. 38 (21). doi:10.15252/embj.2019102718.

Johnson, K.E., Bottero, V., Flaherty, S., Dutta, S. & Singh, V. v (2014) IFI16 Restricts HSV-1 Replication by Accumulating on the HSV-1 Genome, Repressing HSV-1 Gene Expression, and Directly or Indirectly Modulating Histone Modifications. PLoS Pathog. 10 (11), 1004503. doi:10.1371/journal.ppat.1004503.

Johnson, K.E., Chikoti, L. & Chandran, B. (2013) Herpes Simplex Virus 1 Infection Induces Activation and Subsequent Inhibition of the IFI16 and NLRP3 Inflammasomes. Journal of Virology. 87 (9), 5005–5018. doi:10.1128/jvi.00082-13.

Johnston, C., Gottlieb, S.L. & Wald, A. (2016) Status of vaccine research and development of vaccines for herpes simplex virus. Vaccine. 34 (26), 2948–2952. doi:10.1016/j.vaccine.2015.12.076.

Jones, K.A. & Tjian, R. (1985) Spl binds to promoter sequences and activates herpes simplex virus “immediate-early” gene transcription in vitro.

Jønsson, K.L., Laustsen, A., Krapp, C., Skipper, K.A., Thavachelvam, K., et al. (2017) IFI16 is required for DNA sensing in human macrophages by promoting production and function of cGAMP. Nature Communications. 8. doi:10.1038/ncomms14391.

Jovasevic, V., Liang, L. & Roizman, B. (2008) Proteolytic Cleavage of VP1-2 Is Required for Release of Herpes Simplex Virus 1 DNA into the Nucleus. JOURNAL OF VIROLOGY. 82 (7), 3311–3319. doi:10.1128/JVI.01919-07.

Jul-Larsen, Å., Visted, T., Karlsen, B.O., Rinaldo, C.H., Bjerkvig, R., Lønning, P.E. & Bøe, S.O. (2004) PML-nuclear bodies accumulate DNA in response to polyomavirus BK and simian virus 40 replication. Experimental Cell Research. 298 (1), 58–73. doi:10.1016/j.yexcr.2004.03.045.

Kabani, N. & Kimberlin, D.W. (2018) Neonatal Herpes Simplex Virus Infection. NeoReviews. 19 (2). doi:10.1542/neo.19-2-e89.

Kahle, T., Volkmann, B., Eissmann, K., Herrmann, A., Schmitt, S., Wittmann, S., Merkel, L., Reuter, N., Stamminger, T. & Gramberg, T. (2016) TRIM19/PML restricts HIV infection in a cell type-dependent manner. Viruses. 8 (1). doi:10.3390/v8010002.

Kamitani, T., Kito, K., Nguyen, H.P., Fukuda-Kamitani, T. & Yeh, E.T.H. (1998a) Characterization of a Second Member of the Sentrin Family of Ubiquitin-like Proteins*. http://www.jbc.org.

Kamitani, T., Kito, K., Nguyen, H.P., Wada, H., Fukuda-Kamitani, T. & Yeh, E.T.H. (1998b) Identification of Three Major Sentrinization Sites in PML*. http://www.jbc.org.

Kari, B. & Gehrz, R. (1993) Structure, composition and heparin binding properties of a human cytomegalovirus glycoprotein complex designated gC-II. Journal of General Virology.

Kelly, B.J., Fraefel, C., Cunningham, A.L. & Diefenbach, R.J. (2009) Functional roles of the tegument proteins of herpes simplex virus type 1. Virus Research. 145, 173–186. doi:10.1016/j.virusres.2009.07.007.

Kelly, C., Driep, R. van & Wilkinson, G.W.G. (1995) Disruption of PML-associated nuclear bodies during human cytomegalovirus infection. Journal of General Virology.76.

Kerur, N., Veettil, M.V., Sharma-Walia, N., Bottero, V., Sadagopan, S., Otageri, P. & Chandran, B. (2011) IFI16 acts as a nuclear pathogen sensor to induce the inflammasome in response to Kaposi Sarcoma-associated

herpesvirus infection. Cell Host and Microbe. 9 (5), 363–375. doi:10.1016/j.chom.2011.04.008.

Khanna, K.M., Bonneau, R.H., Kinchington, P.R. & Hendricks, R.L. (2003) Herpes simplex virus-specific memory CD8+ T cells are selectively activated and retained in latently infected sensory ganglia. Immunity.18.

Kieff, E.D., Bachenheimer, S.L. & Roizman, B. (1971) Size, Composition, and Structure of the Deoxyribonucleic Acid of Herpes Simplex Virus Subtypes 1 and 2. JOURNAL OF VIROLOGY.8 (2). https://journals.asm.org/journal/jvi.

Kim, D.-B. & Deluca, N.A. (2002) Phosphorylation of Transcription Factor Sp1 during Herpes Simplex Virus Type 1 Infection. JOURNAL OF VIROLOGY. 76 (13), 6473–6479. doi:10.1128/JVI.76.13.6473-6479.2002.

Knipe, D. & Howley-Fields, P. (2013) Fields Virology (Sixth Edition).

Komatsu, T., Dacheux, D., Kreppel, F., Nagata, K. & Wodrich, H. (2015) A Method for Visualization of Incoming Adenovirus Chromatin Complexes in Fixed and Living Cells. doi:10.1371/journal.pone.0137102.

Komatsu, T., Nagata, K. & Wodrich, H. (2016) The role of nuclear antiviral factors against invading DNA viruses: The immediate fate of incoming viral genomes. Viruses.8 (10). doi:10.3390/v8100290.

Korioth, F., Maul, G.G., Plachter, B., Stamminger, T., Ju¨, J. & Frey, J. (1996) The Nuclear Domain 10 (ND10) Is Disrupted by the Human Cytomegalovirus Gene Product IE1. EXPERIMENTAL CELL RESEARCH.229.

Kristensson, K., Lycke, E., Roytta, M., Svennerholm, B.O. & Vahlne, A. (1986) Neuritic Transport of Herpes Simplex Virus in Rat Sensory Neurons in vitro. Effects of Substances Interacting with Microtubular Function and Axonal Flow [Nocodazole, Taxol and Erythro-9-3-(2-hydroxynonyl)adenine]. J. gen. Virol.67.

Kristie, T.M. & Sharp, P.A. (1990) Interactions of the Oct-1 POU subdomains with specific DNA sequences and with the HSV a-tr^ns-activator protein.

Ku, C.C., Che, X.B., Reichelt, M., Rajamani, J., Schaap-Nutt, A., Huang, K.J., Sommer, M.H., Chen, Y.S., Chen, Y.Y. & Arvin, A.M. (2011) Herpes simplex virus-1 induces expression of a novel MxA isoform that enhances viral replication. Immunology and Cell Biology. 89 (2), 173–182. doi:10.1038/icb.2010.83.

Kuwahara, J., Watanabe, Y., Kayasuga, T. & Itoh, K. (2000) Zn finger and nuclear localization of transcription factor Sp1. Nucleic Acids Symposium Series.44. https://academic.oup.com/nass/article/44/1/265/1019707.

Kwiatkowski, D.L., Thompson, H.W. & Bloom, D.C. (2009) The Polycomb Group Protein Bmi1 Binds to the Herpes Simplex Virus 1 Latent Genome and Maintains Repressive Histone Marks during Latency. JOURNAL OF VIROLOGY. 83 (16), 8173–8181. doi:10.1128/JVI.00686-09.

Laboissie`re, S. & O'hare, P. (2000) Analysis of HCF, the Cellular Cofactor of VP16, in Herpes Simplex Virus-Infected Cells. JOURNAL OF VIROLOGY.74 (1). https://journals.asm.org/journal/jvi.

Landolfo, S., Gariglio, M., Gribaudo, G. & Lembo, D. (n.d.) The human cytomegalovirus. doi:10.1016/S0163-7258(03)00034-2.

Laquerre, S., Argnani, R., Anderson, D.B., Zucchini, S., Manservigi, R. & Glorioso, J.C. (1998) Heparan Sulfate Proteoglycan Binding by Herpes Simplex Virus Type 1 Glycoproteins B and C, Which Differ in Their Contributions to Virus Attachment, Penetration, and Cell-to-Cell Spread. JOURNAL OF VIROLOGY.72 (7). https://journals.asm.org/journal/jvi.

Laycock, K.A., Lee, S.F., Brady, R.H. & Pepose, J.S. (1991) Characterization of a Murine Model of Recurrent Herpes Simplex Viral Keratitis Induced by Ultraviolet B Radiation. Investigative Ophthalmology & Visual Science.32 (10).

Leblanc, R.A., Pesnicak, L., Godleski, M. & Straus, S.E. (1999) Treatment of HSV-1 Infection with Immunoglobulin or Acyclovir: Comparison of Their Effects on Viral Spread, Latency, and Reactivation. http://www.idealibrary.com.

Lee, H.-R., Kim, D.-J., Lee, J.-M., Choi, C.Y., Ahn, B.-Y., Hayward, G.S. & Ahn, J.-H. (2004) Ability of the Human Cytomegalovirus IE1 Protein To Modulate Sumoylation of PML Correlates with Its Functional Activities in Transcriptional Regulation and Infectivity in Cultured Fibroblast Cells. Journal of Virology. 78 (12), 6527–6542. doi:10.1128/jvi.78.12.6527-6542.2004.

Lee, J.S., Raja, P. & Knipe, D.M. (2016) Herpesviral ICP0 protein promotes two waves of heterochromatin removal on an early viral promoter during lytic infection. mBio. 7 (1). doi:10.1128/mBio.02007-15.

Leib, D.A., Harrison, T.E., Laslo, K.M., Machalek, M.A., Moorman, N.J. & Virgin, H.W. (1999) Interferons Regulate the Phenotype of Wild-type and Mutant Herpes Simplex Viruses In Vivo. J. Exp. Med.189 (4). http://www.jem.org.

Lenschow, D.J., Lai, C., Frias-Staheli, N., Giannakopoulos, N. v, Lutz, A., Wolff, T., Osiak, A., Levine, B., Schmidt, R.E., García-Sastre, A., Leib, D.A., Pekosz, A., Knobeloch, K.-P., Horak, I. & Whiting Virgin, H.I. (2007) IFN-stimulated gene 15 functions as a critical antiviral molecule against influenza, herpes, and Sindbis viruses. www.pnas.org/cgi/content/full/.

Li, Z., Zhao, D., Xiang, B. & Li, H. (2017) LETTER Structural and biochemical characterization of DAXX-ATRX interaction Protein & Cell Protein & Cell. Protein Cell. 8 (10), 762–766. doi:10.1007/s13238-017-0463-x.

Liang, Y.-C., Lee, C.-C., Yao, Y.-L., Lai, C.-C., Lienhard Schmitz, M. & Yang, W.-M. (2016b) SUMO5, a Novel Poly-SUMO Isoform, Regulates PML Nuclear Bodies. doi:10.1038/srep26509.

Lin, D.Y., Huang, Y.S., Jeng, J.C., Kuo, H.Y., Chang, C.C., Chao, T.T., Ho, C.C., Chen, Y.C., Lin, T.P., Fang, H.I., Hung, C.C., Suen, C.S., Hwang, M.J., Chang, K.S., Maul, G.G. & Shih, H.M. (2006) Role of SUMO-Interacting Motif in Daxx SUMO Modification, Subnuclear Localization, and Repression of Sumoylated Transcription Factors. Molecular Cell. 24 (3), 341–354. doi:10.1016/j.molcel.2006.10.019.

Liu, F. & Roizman, B. (1993) Characterization of the Protease and Other Products of Amino-Terminus-Proximal Cleavage of the Herpes Simplex Virus 1 UL26 Protein. JOURNAL OF VIROLOGY. https://journals.asm.org/journal/jvi.

Liu, H., Zhang, H., Wu, X., Ma, D., Wu, J., et al. (2018) Nuclear cGAS suppresses DNA repair and promotes tumorigenesis. Nature. doi:10.1038/s41586-018-0629-6.

Liu, S., Cai, X., Wu, J., Cong, Q., Chen, X., Li, T., Du, F., Ren, J., Wu, Y.-T., Grishin, N. v & Chen, Z.J. (n.d.) Phosphorylation of innate immune adaptor proteins MAVS, STING, and TRIF induces IRF3 activation. doi:10.1126/science.aaa2630.

Loret, S., Guay, G. & Lippé, R. (2008) Comprehensive Characterization of Extracellular Herpes SimplexVirus Type 1 Virions. JOURNAL OF VIROLOGY. 82 (17), 8605–8618. doi:10.1128/JVI.00904-08.

Luecke, S., Holleufer, A., Christensen, M.H., Jønsson, K.L., Boni, G.A., Sørensen, L.K., Johannsen, M., Jakobsen, M.R., Hartmann, R. & Paludan, S.R. (2017) cGAS is activated by DNA in a length-dependent manner . EMBO reports. 18 (10), 1707–1715. doi:10.15252/embr.201744017.

Lukashchuk, V. & Everett, R.D. (2010) Regulation of ICP0-Null Mutant Herpes Simplex Virus Type 1 Infection by ND10 Components ATRX and hDaxx. JOURNAL OF VIROLOGY. 84 (8), 4026–4040. doi:10.1128/JVI.02597-09.

Lukashchuk, V., McFarlane, S., Everett, R.D. & Preston, C.M. (2008) Human Cytomegalovirus Protein pp71 Displaces the Chromatin-Associated Factor ATRX from Nuclear Domain 10 at Early Stages of Infection. Journal of Virology. 82 (24), 12543–12554. doi:10.1128/jvi.01215-08.

Luker, G.D., Prior, J.L., Song, J., Pica, C.M. & Leib, D.A. (2003) Bioluminescence Imaging Reveals Systemic Dissemination of Herpes Simplex Virus Type 1 in the Absence of Interferon Receptors. Journal of Virology. 77 (20), 11082–11093. doi:10.1128/jvi.77.20.11082-11093.2003.

Lurie, R.H. & Platanias, L.C. (2005) MECHANISMS OF TYPE¤I¤ AND TYPE¤II¤INTERFERON¤MEDIATED SIGNALLING. doi:10.1038/nri1604.

Lye, M.F., Sharma, M., el Omari, K., Filman, D.J., Schuermann, J.P., Hogle, J.M. & Coen, D.M. (2015) Unexpected features and mechanism of heterodimer formation of a herpesvirus nuclear egress complex. The EMBO Journal. 34 (23), 2937–2952. doi:10.15252/embj.201592651.

Ma, Z., Ni, G. & Damania, B. (2018) Innate Sensing of DNA Virus Genomes. doi:10.1146/annurev-virology.

Mahmud, I. & Liao, D. (2019) DAXX in cancer: Phenomena, processes, mechanisms and regulation. Nucleic Acids Research. 47 (15), 7734–7752. doi:10.1093/nar/gkz634.

Manska, X.S., Octaviano, R. & Rossetto, X.C.C. (2020) 5-Ethynyl-2-deoxycytidine and 5-ethynyl-2-deoxyuridine are differentially incorporated in cells infected with hsv-1, hcmv, and kshv viruses. Journal of Biological Chemistry. 295 (18), 5871–5890. doi:10.1074/jbc.RA119.012378.

Marcus, P.I., Rojek, J.M. & Sekellick, M.J. (2005) Interferon Induction and/or Production and Its Suppression by Influenza A Viruses †. JOURNAL OF VIROLOGY. 79 (5), 2880–2890. doi:10.1128/JVI.79.5.2880-2890.2005.

Matic, I., van Hagen, M., Schimmel, J., Macek, B., Ogg, S.C., Tatham, M.H., Hay, R.T., Lamond, A.I., Mann, M. & Vertegaal, A.C.O. (2008) In vivo identification of human small ubiquitin-like modifier polymerization sites by high accuracy mass spectrometry and an in vitro to in vivo strategy. Molecular and Cellular Proteomics. 7 (1), 132–144. doi:10.1074/mcp.M700173-MCP200.

Maul, G.G., Guldner, H.H. & Spivack, J.G. (1993) Modification of discrete nuclear domains induced by herpes simplex virus type 1 immediate early gene 1 product (ICP0). Journal of General Virology.74.

Maurer, U.E., Sodeik, B. & Grü, K. (2008) Native 3D intermediates of membrane fusion in herpes simplex virus 1 entry. PNAS.

McFarlane, S., Orr, A., Roberts, A.P.E., Conn, K.L., Iliev, V., Loney, C., Filipe, A.D.S., Smollett, K., Gu, Q., Robertson, N., Adams, P.D., Rai, T.S. & Boutell, C. (2019) The histone chaperone hira promotes the induction of host innate immune defences in response to HSV-1 infection. PLoS Pathogens. 15 (3). doi:10.1371/journal.ppat.1007667.

Mcgeoch, D.J., Dalrymple, M.A., Davison, A.J., Dolan, A., Frame, M.C., Mcnab, D., Perry, L.J., Scott, J.E. & Taylor, P. (1988) The Complete DNA Sequence of the Long Unique Region in the Genome of Herpes Simplex Virus Type 1. J. gen. Virol.69.

Mcgregor, F., Phelan, A., Dunlop, J. & Clements, J.B. (1996) Regulation of Herpes Simplex Virus Poly(A) Site Usage and the Action of Immediate-Early Protein IE63 in the Early-Late Switch. JOURNAL OF VIROLOGY.70 (3). https://journals.asm.org/journal/jvi.

Mcvoy, M.A. & Adler, S.P. (1994) Human Cytomegalovirus DNA Replicates after Early Circularization by Concatemer Formation, and Inversion Occurs within the Concatemer. JOURNAL OF VIROLOGY.68 (2). https://journals.asm.org/journal/jvi.

Merkl, P.E., Orzalli, M.H. & Knipe, D.M. (2018) Mechanisms of Host IFI16, PML, and Daxx Protein Restriction of Herpes Simplex Virus 1 Replication. Journal of Virology. 92 (10). doi:10.1128/jvi.00057-18.

Mettenleiter, T.C. (2002) Herpesvirus Assembly and Egress. Journal of Virology. 76 (4), 1537–1547. doi:10.1128/jvi.76.4.1537-1547.2002.

Mettenleiter, T.C. & Minson, T. (2006) Egress of Alphaherpesviruses. Journal of Virology. 80 (3), 1610–1612. doi:10.1128/jvi.80.3.1610-1612.2006.

Millhouse, S., Wang, X., Fraser, N.W., Faber, L. & Block, T.M. (2012) Direct evidence that HSV DNA damaged by ultraviolet (UV) irradiation can be repaired in a cell type-dependent manner. Journal of NeuroVirology. 18 (3), 231–243. doi:10.1007/s13365-012-0105-2.

Milne, R.S.B., Nicola, A. v, Whitbeck, J.C., Eisenberg, R.J. & Cohen, G.H. (2005) Glycoprotein D Receptor-Dependent, Low-pH-Independent Endocytic Entry of Herpes Simplex Virus Type 1. JOURNAL OF VIROLOGY. 79 (11), 6655–6663. doi:10.1128/JVI.79.11.6655-6663.2005.

Miyamoto' And, K. & Morgan, C. (1971) Structure and Development of Viruses as Observed in the Electron Microscope XI. Entry and Uncoating of Herpes Simplex Virus Downloaded from. JOURNAL OF VIROLOGY. http://jvi.asm.org/.

Mocarski, E.S., Kemblet, G.W., Lyle, J.M. & Greaves, R.F. (1996) A deletion mutant in the human cytomegalovirus gene encoding IE1491aa is replication defective due to a failure in autoregulation.93.

Montgomery, R.I., Warner, M.S., Lum, B.J. & Spear, P.G. (1996) Herpes Simplex Virus-1 Entry into Cells Mediated by a Novel Member of the TNF/NGF Receptor Family. Cell.87.

Morrone, S.R., Wang, T., Constantoulakis, L.M., Hooy, R.M., Delannoy, M.J. & Sohn, J. (2013) Cooperative assembly of IFI16 filaments on dsDNA provides insights into host defense strategy. PNAS. 62–71. doi:10.1073/pnas.1313577111.

Mu¨ller, S. & Dejean, A. (1999) Viral Immediate-Early Proteins Abrogate the Modification by SUMO-1 of PML and Sp100 Proteins, Correlating with Nuclear Body Disruption. JOURNAL OF VIROLOGY.73 (6). https://journals.asm.org/journal/jvi.

Mukhopadhyay, D. & Dasso, M. (2007) Modification in reverse: the SUMO proteases. Trends in Biochemical Sciences.32 (6) pp.286–295. doi:10.1016/j.tibs.2007.05.002.

Muller, M.T. (1987) Binding of the Herpes Simplex Virus Immediate-Early Gene Product ICP4 to Its Own Transcription Start Site. JOURNAL OF VIROLOGY.61 (3). https://journals.asm.org/journal/jvi.

Nainu, F., Shiratsuchi, A. & Nakanishi, Y. (2017) Induction of apoptosis and subsequent phagocytosis of virus-infected cells as an antiviral mechanism. Frontiers in Immunology.8 (SEP). doi:10.3389/fimmu.2017.01220.

Negorev, D.G., Vladimirova, O. v, Ivanov, A. & Maul, G.G. (2006) Differential Role of Sp100 Isoforms in Interferon-Mediated Repression of Herpes Simplex Virus Type 1 Immediate-Early Protein Expression. JOURNAL OF VIROLOGY. 80 (16), 8019–8029. doi:10.1128/JVI.02164-05.

Newcomb, W.W., Homa, F.L., Thomsen, D.R., Booy, F.P., Trus, B.L., Steven, A.C., Spencer, J. v & Brown, J.C. (1996) Assembly of the Herpes Simplex Virus Capsid: Characterization of Intermediates Observed During Cell-free Capsid Formation. J. Mol. Biol.263.

Newcomb, W.W., Homa, F.L., Thomsen, D.R., Trus, B.L., Cheng, N., Steven, A., Booy, F. & Brown, J.C. (1999) Assembly of the Herpes Simplex Virus Procapsid from Purified Components and Identification of Small

Complexes Containing the Major Capsid and Scaffolding Proteins. JOURNAL OF VIROLOGY.73 (5). https://journals.asm.org/journal/jvi.

Newcomb,', W.W., Homa, F.L., Thomsen, D.R., Ye, Z. & Brown', J.C. (1994) Cell-Free Assembly of the Herpes Simplex Virus Capsid. Molecular Biology Research.68 (9). https://journals.asm.org/journal/jvi.

Newcomb, W.W., Juhas, R.M., Thomsen, D.R., Homa, F.L., Burch, A.D., Weller, S.K. & Brown, J.C. (2001) The UL6 Gene Product Forms the Portal for Entry of DNA into the Herpes Simplex Virus Capsid. JOURNAL OF VIROLOGY. 75 (22), 10923–10932. doi:10.1128/JVI.75.22.10923-10932.2001.

Newcomb, W.W., Trus, L.B., Booy, P.F., Steven, C.A., Wall, S.J. & Brown, C.J. (1993) Structure of the Herpes Simplex Virus Capsid Molecular Composition of the Pentons and the Triplexes. Journal of Molecular Biology. (232), 499–511.

Nicola, A. v. (2016) Herpesvirus Entry into Host Cells Mediated by Endosomal Low pH. Traffic.17 (9) pp.965–975. doi:10.1111/tra.12408.

Nicola, A. v, Hou, J., Major, E.O. & Straus, S.E. (2005) Herpes Simplex Virus Type 1 Enters Human Epidermal Keratinocytes, but Not Neurons, via a pH-Dependent Endocytic Pathway. JOURNAL OF VIROLOGY. 79 (12), 7609–7616. doi:10.1128/JVI.79.12.7609-7616.2005.

Ogawa-Goto, K., Tanaka, K., Gibson, W., Moriishi, E., Miura, Y., Kurata, T., Irie, S. & Sata, T. (2003) Microtubule Network Facilitates Nuclear Targeting of Human Cytomegalovirus Capsid. JOURNAL OF VIROLOGY. 77 (15), 8541–8547. doi:10.1128/JVI.77.15.8541-8547.2003.

Olesky, M., McNamee, E.E., Zhou, C., Taylor, T.J. & Knipe, D.M. (2005) Evidence for a direct interaction between HSV-1 ICP27 and ICP8 proteins. Virology. 331 (1), 94–105. doi:10.1016/j.virol.2004.10.003.

Orzalli, M.H., Broekema, N.M., Diner, B.A., Hancks, D.C., Elde, N.C., Cristea, I.M. & Knipe, D.M. (2015) cGAS-mediated stabilization of IFI16 promotes innate signaling during herpes simplex virus infection. PNAS. 1773–1781. doi:10.1073/pnas.1424637112.

Orzalli, M.H., Broekema, N.M. & Knipe, D.M. (2016) Relative Contributions of Herpes Simplex Virus 1 ICP0 and vhs to Loss of Cellular IFI16 Vary in Different Human Cell Types. Journal of Virology. 90 (18), 8351–8359. doi:10.1128/jvi.00939-16.

Orzalli, M.H., Conwell, S.E., Berrios, C., Decaprio, J.A. & Knipe, D.M. (2013) Nuclear interferon-inducible protein 16 promotes silencing of herpesviral and transfected DNA. PNAS. 4492–4501. doi:10.1073/pnas.1316194110.

Orzalli, M.H., Conwell, S.E., Berrios, C., Decaprio, J.A. & Knipe, D.M. (n.d.) Nuclear interferon-inducible protein 16 promotes silencing of herpesviral and transfected DNA. doi:10.1073/pnas.1316194110.

Orzalli, M.H., DeLuca, N.A. & Knipe, D.M. (2012) Nuclear IFI16 induction of IRF-3 signaling during herpesviral infection and degradation of IFI16 by the viral ICP0 protein. Proceedings of the National Academy of Sciences of the United States of America. 109 (44). doi:10.1073/pnas.1211302109.

Osorio, Y. & Ghiasi, H. (2003) Comparison of Adjuvant Efficacy of Herpes Simplex Virus Type 1 Recombinant Viruses Expressing T H 1 and T H 2 Cytokine Genes. JOURNAL OF VIROLOGY. 77 (10), 5774–5783. doi:10.1128/JVI.77.10.5774-5783.2003.

Pa¨, P., Ojala, P.M., Sodeik, B., Ebersold, M.W., Kutay, U. & Helenius, A. (2000) Herpes Simplex Virus Type 1 Entry into Host Cells: Reconstitution of Capsid Binding and Uncoating at the Nuclear Pore Complex In Vitro. MOLECULAR AND CELLULAR BIOLOGY.20 (13).

Paludan, S.R., Xing, J., Zheng, C. & Alandijany, T. (2019) Host Intrinsic and Innate Intracellular Immunity During Herpes Simplex Virus Type 1 (HSV-1) Infection. doi:10.3389/fmicb.2019.02611.

Pan, S., Liu, X., Ma, Y., Cao, Y. & He, B. (2018) Herpes Simplex Virus 1 1 34.5 Protein Inhibits STING Activation That Restricts Viral Replication. doi:10.1128/JVI.

Pande, N.T., Petroski, M.D. & Wagner, E.K. (1998) Functional Modules Important for Activated Expression of Early Genes of Herpes Simplex Virus Type 1 Are Clustered Upstream of the TATA Box.

Paolini, R., Bernardini, G., Molfetta, R. & Santoni, A. (2015) NK cells and interferons. Cytokine and Growth Factor Reviews. 26 (2), 113–120. doi:10.1016/j.cytogfr.2014.11.003.

Papavassiliou, A.G. & Silverstein, S.J. (1990) Characterization of DNA-Protein Complex Formation in Nuclear Extracts with a Sequence from the Herpes Simplex Virus Thymidine Kinase Gene*.265 (3).

Parker, Z.M., Murphy, A.A. & Leib, D.A. (2015) Role of the DNA Sensor STING in Protection from Lethal Infection following Corneal and Intracerebral Challenge with Herpes Simplex Virus 1. doi:10.1128/JVI.00954-15.

Pasdeloup, D., Blondel, D., Isidro, A.L. & Rixon, F.J. (2009) Herpesvirus Capsid Association with the Nuclear Pore Complex and Viral DNA Release Involve the Nucleoporin CAN/Nup214 and the Capsid Protein pUL25. JOURNAL OF VIROLOGY. 83 (13), 6610–6623. doi:10.1128/JVI.02655-08.

Peng, L., Ryazantsev, S., Sun, R. & Zhou, Z.H. (2010) Three-Dimensional Visualization of Gammaherpesvirus Life Cycle in Host Cells by Electron Tomography. Structure. 18 (1), 47–58. doi:10.1016/j.str.2009.10.017.

Pietropaolo, R.L. & Compton, T. (1997) Direct Interaction between Human Cytomegalovirus Glycoprotein B and Cellular Annexin II. JOURNAL OF VIROLOGY.71 (12). https://journals.asm.org/journal/jvi.

Pizzorno, M.C. & Hayward, G.S. (1990) The IE2 Gene Products of Human Cytomegalovirus Specifically Down-Regulate Expression from the Major Immediate-Early Promoter through a Target Sequence Located near the Cap Site. JOURNAL OF VIROLOGY.64 (12). https://journals.asm.org/journal/jvi.

Platanias, L.C. (2005) Mechanisms of type-I- and type-II-interferon-mediated signalling. Nature Reviews Immunology.5 (5) pp.375–386. doi:10.1038/nri1604.

Purifoy, D.J., Lewis, R.B. & Powell, K.L. (1977) Identification of the herpes simplex virus DNA polymerase gene.

Quinian, M.P., Chen, L.B. & Knipe, D.M. (1984) The lntranuclear Location of a Herpes Simplex Virus DNA-Binding Protein Is Determined by the Status of Viral DNA Replication. Cell.36.

Rabkin, S.D. & Hanlon, B. (1990) Herpes Simplex Virus DNA Synthesis at a Preformed Replication Fork In Vitro.64 (10). https://journals.asm.org/journal/jvi.

Rabson, A.S., Tyrrell, S.A. & Legallais, F.Y. (1969) Growth of Ultraviolet-Damaged Herpesvirus in Xeroderma Pigmentosum Cells (34312.

Radtke, K., Kieneke, D., Wolfstein, A., Michael, K., Steffen, W., Scholz, T., Karger, A. & Sodeik, B. (2010) Plus-and Minus-End Directed Microtubule Motors Bind Simultaneously to Herpes Simplex Virus Capsids Using Different Inner Tegument Structures. PLoS Pathogens. 6 (7), 1–20. doi:10.1371/journal.ppat.1000991.

Rastogi, R.P., Richa, Kumar, A., Tyagi, M.B. & Sinha, R.P. (2010) Molecular mechanisms of ultraviolet radiation-induced DNA damage and repair. Journal of Nucleic Acids.2010. doi:10.4061/2010/592980.

Regad, T., Saib, A., Lallemand-Breitenbach, V., Pandolfi, P., de The, H. & Chelbi-Alix, M. (2001) PML mediates the interferon-induced antiviral stateagainst a complex retrovirus via its association withthe viral transactivator. The EMBO Journal. 20 (13), 3495–3505.

Reichelt, M., Joubert, L., Perrino, J., Koh, A.L., Phanwar, I. & Arvin, A.M. (2012) 3D reconstruction of VZV infected cell nuclei and PML nuclear cages by serial section array scanning electron microscopy and electron tomography. PLoS Pathogens. 8 (6). doi:10.1371/journal.ppat.1002740.

Reichelt, M., Wang, L., Sommer, M., Perrino, J., Nour, A.M., Sen, N., Baiker, A., Zerboni, L. & Arvin, A.M. (2011b) Entrapment of viral capsids in nuclear PML cages is an intrinsic antiviral host defense against Varicella-zoster virus. PLoS Pathogens. 7 (2). doi:10.1371/journal.ppat.1001266.

Reinert, L.S., Lopušná, K., Winther, H., Sun, C., Thomsen, M.K., Nandakumar, R., Mogensen, T.H., Meyer, M., Vægter, C., Nyengaard, J.R., Fitzgerald, K.A. & Paludan, S.R. (2016) Sensing of HSV-1 by the cGAS-STING pathway in microglia orchestrates antiviral defence in the CNS. Nature Communications. 7. doi:10.1038/ncomms13348.

Research; P, C.D.A.W.L. (2010) Daxx is an H3.3-specific histone chaperone and cooperates with ATRX in replication-independent chromatin assembly at telomeres. 107 (32), 14075–14080. doi:10.1073/pnas.1008850107/-/DCSupplemental.

Reske, A., Pollara, G., Krummenacher, C., Chain, B.M. & Katz, D.R. (2007) Understanding HSV-1 entry glycoproteins. Rev. Med. Virol. 17, 205–215. doi:10.1002/rmv.531.

Reuter, N., Schilling, E.-M., Scherer, M., Müller, R., Stamminger, T. & Sandri-Goldin, R.M. (2021) The ND10 Component Promyelocytic Leukemia Protein Acts as an E3 Ligase for SUMOylation of the Major Immediate Early Protein IE1 of Human Cytomegalovirus VIRUS-CELL INTERACTIONS crossm. jvi.asm.org 1 Journal of Virology Downloaded. 91, 2335–2351. doi:10.1128/JVI.02335-16.

Reynolds, A.E., Wills, E.G., Roller, R.J., Ryckman, B.J. & Baines, J.D. (2002) Ultrastructural Localization of the Herpes Simplex Virus Type 1 U L 31, U L 34, and U S 3 Proteins Suggests Specific Roles in Primary Envelopment and Egress of Nucleocapsids Downloaded from. JOURNAL OF VIROLOGY. 76 (17), 8939–8952. doi:10.1128/JVI.76.17.8939-8952.2002.

Rivas, C., Lopitz Otsoa, F., bioGUNE, C., Shirin Bonni, S., K, S.T., Joshi, G., Arya, P., Mahajan, V., Chaturvedi, A. & Kumar Mishra, R. (2021b) SUMO and SUMOylation Pathway at the Forefront of Host Immune Response. doi:10.3389/fcell.2021.681057.

Rizza, P., Moretti, F., Capone, I. & Belardelli, F. (2015) Role of type I interferon in inducing a protective immune response: Perspectives for clinical applications. Cytokine and Growth Factor Reviews.26 (2) pp.195–201. doi:10.1016/j.cytogfr.2014.10.002.

Rodriguez, S., Roussel, M., Tarte, K. & Amé-Thomas, P. (2017) Impact of chronic viral infection on T-cell dependent humoral immune response. Frontiers in Immunology.8 (OCT). doi:10.3389/fimmu.2017.01434.

Roizman, B. (2011) The Checkpoints of Viral Gene Expression in Productive and Latent Infection: the Role of the HDAC/CoREST/LSD1/REST Repressor Complex. JOURNAL OF VIROLOGY. 85 (15), 7474–7482. doi:10.1128/JVI.00180-11.

Roizman, B. & Whitley, R.J. (2013) An inquiry into the molecular basis of HSV latency and reactivation. Annual Review of Microbiology. 67, 355–374. doi:10.1146/annurev-micro-092412-155654.

Rorsch', A., Beukers'), R., Ijlstra, J. & Berends, W. (1958) THE EFFECT OF U.V.-LIGHT ON SOME COMPONENTS OF THE NUCLEIC ACIDS I. Uracil, thymine.

Ross, L.J.N., Cameron, K.R. & Wildy, P. (1972) Ultraviolet Irradiation of Herpes Simplex Virus: Reactivation Processes and Delay in Virus Multiplication. J. gen. Virol. (I972).6.

Royer, D.J. & Carr, D. (2016) A STING-dependent innate-sensing pathway mediates resistance to corneal HSV-1 infection via upregulation of the antiviral effector tetherin. doi:10.1038/mi.2015.124.

Ryckman, B.J., Jarvis, M.A., Drummond, D.D., Nelson, J.A. & Johnson, D.C. (2006) Human Cytomegalovirus Entry into Epithelial and Endothelial Cells Depends on Genes UL128 to UL150 and Occurs by Endocytosis and Low-pH Fusion. JOURNAL OF VIROLOGY. 80 (2), 710–722. doi:10.1128/JVI.80.2.710-722.2006.

Ryu, S., Zhou, S., Ladurner, A.G. & Tjian, R. (1999) The transcriptional cofactorcomplex CRSP is required foractivity of the enhancer-binding protein Sp1. www.nature.com.

Sacks, W.R., Greene, C.C., Aschman, D.P. & Schaffer, P.A. (1985) Herpes Simplex Virus Type 1 ICP27 Is an Essential Regulatory Protein. JOURNAL OF VIROLOGY.55 (3). https://journals.asm.org/journal/jvi.

Sacks, W.R. & Schaffer, P.A. (1987) Deletion Mutants in the Gene Encoding the Herpes Simplex Virus Type 1 Immediate-Early Protein ICPO Exhibit Impaired Growth in Cell Culture. JOURNAL OF VIROLOGY.61 (3).

Saffert, R.T. & Kalejta, R.F. (2006) Inactivating a Cellular Intrinsic Immune Defense Mediated by Daxx Is the Mechanism through Which the Human Cytomegalovirus pp71 Protein Stimulates Viral Immediate-Early Gene Expression. JOURNAL OF VIROLOGY. 80 (8), 3863–3871. doi:10.1128/JVI.80.8.3863-3871.2006.

Sahin Umut, U., Ferhi, O., Jeanne, M., Benhenda, S., Berthier, C., Jollivet, F., Niwa-Kawakita, M., Faklaris, O., Setterblad, N., de Thé, H. & Lallemand-Breitenbach, V. (2014) Oxidative stress-induced assembly of PML nuclear bodies controls sumoylation of partner proteins. Journal of Cell Biology. 204 (6), 931–945. doi:10.1083/jcb.201305148.

Salic, A. & Mitchison, T.J. (2008) A chemical method for fast and sensitive detection of DNA synthesis in vivo. PNAS.105 (7). www.pnas.orgcgidoi10.1073pnas.0712168105.

Samaniego, L.A., Webb, A.L. & Deluca, N.A. (1995) Functional Interactions between Herpes Simplex Virus Immediate-Early Proteins during Infection: Gene Expression as a Consequence of ICP27 and Different Domains of ICP4. JOURNAL OF VIROLOGY.69 (9). https://journals.asm.org/journal/jvi.

Samudio, I., Hofs, E., Cho, B., Li, M., Bolduc, K., Bu, L., Liu, G., Lam, V., Rennie, P., Jia, W., Elisia, I. & Krystal, G. (2019) UV Light-inactivated HSV-1 Stimulates Natural Killer Cell-induced Killing of Prostate Cancer Cells. http://links.

Samudio, I., Rezvani, K., Shaim, H., Hofs, E., Ngom, M., Bu, L., Liu, G., Lee, J.T.C., Imren, S., Lam, V., Poon, G.F.T., Ghaedi, M., Takei, F., Humphries, K., Jia, W. & Krystal, G. (2016) UV-inactivated HSV-1 potently activates NK cell killing of leukemic cells. doi:10.1182/blood-2015-04.

Sànchez, R. & Mohr, I. (2007) Inhibition of Cellular 2-5 Oligoadenylate Synthetase by the Herpes Simplex Virus Type 1 Us11 Protein. JOURNAL OF VIROLOGY. 81 (7), 3455–3464. doi:10.1128/JVI.02520-06.

Sanchez, V., Greis, K.D., Sztul, ‡ Elizabeth & Britt, W.J. (2000) Accumulation of Virion Tegument and Envelope Proteins in a Stable Cytoplasmic Compartment during Human Cytomegalovirus Replication: Characterization of a Potential Site of Virus Assembly. JOURNAL OF VIROLOGY.74 (2). https://journals.asm.org/journal/jvi.

Sandri-Goldin, R.M. (1995) ICP27 mediates HSV RNA export by shuttling through a leucine-rich nuclear export signal and binding viral intronless RNAs through an RGG motif. Fridell et al. www.genesdev.org.

Santiago, A., Godsey, A.C., Hossain, J., Zhao, L.Y. & Liao, D. (2009) Cell Cycle Identification of two independent SUMO-interacting motifs in Daxx: Evolutionary conservation from Drosophila to humans and their biochemical functions. doi:10.4161/cc.8.1.7493.

Satoh, T., Arii, J., Suenaga, T., Wang, J., Kogure, A., Uehori, J., Arase, N., Shiratori, I., Tanaka, S., Kawaguchi, Y., Spear, P.G., Lanier, L.L. & Arase, H. (2008) PILRα Is a Herpes Simplex Virus-1 Entry Coreceptor That Associates with Glycoprotein B. Cell. 132 (6), 935–944. doi:10.1016/j.cell.2008.01.043.

Scherer, M., Otto, V., Stump, J.D., Klingl, S., Müller, R., Reuter, N., Muller, Y.A., Sticht, H. & Stamminger, T. (2016) Characterization of Recombinant Human Cytomegaloviruses Encoding IE1 Mutants L174P and 1-382 Reveals that Viral Targeting of PML Bodies Perturbs both Intrinsic and Innate Immune Responses. J Virol. 90. doi:10.1128/JVI.01973-15.

Scherer, M., Read, C., Neusser, G., Kranz, C., Müller, R., Wörz, S., Reichel, A., Schilling, E.-M., Walther, P. & Stamminger, T. (2021) Dual signaling via interferon and DNA damage response elicits entrapment 3 by giant PML nuclear bodies 4 5. BioRXive. doi:10.1101/2021.08.24.457524.

Scherer, M. & Stamminger, T. (2016) Emerging Role of PML Nuclear Bodies in Innate Immune Signaling. doi:10.1128/JVI.01979-15.

Schilling, E.-M., Scherer, M., Reuter, N., Schweininger, J., Muller, Y.A., Stamminger, T. & Sandri-Goldin, R.M. (2017) The Human Cytomegalovirus IE1 Protein Antagonizes PML Nuclear Body-Mediated Intrinsic Immunity via the Inhibition of PML De Novo SUMOylation VIRUS-CELL INTERACTIONS crossm. 91, 2049–2065. doi:10.1128/JVI.02049-16.

Schilling, M., Bulli, L., Weigang, S., Graf, L., Naumann, S., Patzina, C., Wagner, V., Bauersfeld, L., Goujon, C., Hengel, H., Halenius, A., Ruzsics, Z., Schaller, T. & Kochs, G. (2018) Human MxB Protein Is a Pan-herpesvirus Restriction Factor. doi:10.1128/JVI.

Schneweis, K.E., Gruber, J., Hilfenhaus, J., M~slein, A., Kayser, M. & Wolff, M.H. (1981) Medical Microbiology and Immunology The Influence of Different Modes of Immunization on the Experimental Genital Herpes Simplex Virus Infection of Mice. Med Microbiol Immunol.169.

Schreier, W.J., Gilch, P. & Zinth, W. (2015) Early events of DNA photodamage. Annual Review of Physical Chemistry. 66, 497–519. doi:10.1146/annurev-physchem-040214-121821.

Schulte, B., Buffone, C., Opp, S., di Nunzio, F., de Souza Aranha Vieira, D.A., Brandariz-Nuñez, A. & Diaz-Griffero, F. (2015) Restriction of HIV-1 Requires the N-Terminal Region of MxB as a Capsid-Binding Motif but Not as a Nuclear Localization Signal. Journal of Virology. 89 (16), 8599–8610. doi:10.1128/jvi.00753-15.

Sekine, E., Schmidt, N., Gaboriau, D. & O'Hare, P. (2017) Spatiotemporal dynamics of HSV genome nuclear entry and compaction state transitions using bioorthogonal chemistry and super-resolution microscopy. PLoS pathogens. 13 (11), e1006721. doi:10.1371/journal.ppat.1006721.

Shahin, V., Hafezi, W., Oberleithner, H., Ludwig, Y., Windoffer, B., Schillers, H. & Kühn, J.E. (2006) The genome of HSV-1 translocates through the nuclear pore as a condensed rod-like structure. Journal of Cell Science. 119 (1), 23–30. doi:10.1242/jcs.02705.

Shang, G., Zhang, C., Chen, Z.J., Bai, X.-C. & Zhang, X. (2019) Cryo-EM structures of STING reveal its mechanism of activation by cyclic GMP-AMP. Nature. 567, 389–393. doi:10.1038/s41586-019-0998-5.

Shang, G., Zhu, D., Li, N., Zhang, J., Zhu, C., Lu, D., Liu, C., Yu, Q., Zhao, Y., Xu, S. & Gu, L. (2012) Crystal structures of STING protein reveal basis

for recognition of cyclic di-GMP. Nature Structural & Molecular Biology. 19 (7). doi:10.1038/nsmb.2332.

Sharma, M., Bender, B.J., Kamil, J.P., Lye, M.F., Pesola, J.M., Reim, N.I., Hogle, J.M. & Coen, D.M. (2015) Human Cytomegalovirus UL97 Phosphorylates the Viral Nuclear Egress Complex. Journal of Virology. 89 (1), 523–534. doi:10.1128/jvi.02426-14.

Sharma, M., Kamil, J.P., Coughlin, M., Reim, N.I. & Coen, D.M. (2014) Human Cytomegalovirus UL50 and UL53 Recruit Viral Protein Kinase UL97, Not Protein Kinase C, for Disruption of Nuclear Lamina and Nuclear Egress in Infected Cells. Journal of Virology. 88 (1), 249–262. doi:10.1128/jvi.02358-13.

Shen, G., Wang, K., Wang, S., Cai, M., Li, M.-L. & Zheng, C. (2014) Herpes Simplex Virus 1 Counteracts Viperin via Its Virion Host Shutoff Protein UL41. doi:10.1128/JVI.01380-14.

Shen, T.H., Lin, H.K., Scaglioni, P.P., Yung, T.M. & Pandolfi, P.P. (2006a) The Mechanisms of PML-Nuclear Body Formation. Molecular Cell. 24 (3), 331–339. doi:10.1016/j.molcel.2006.09.013.

Shen, T.H., Lin, H.K., Scaglioni, P.P., Yung, T.M. & Pandolfi, P.P. (2006b) The Mechanisms of PML-Nuclear Body Formation. Molecular Cell. 24 (3), 331–339. doi:10.1016/j.molcel.2006.09.013.

Shenk, T. & Stinski, M.F. (n.d.) Human Cytomegalovirus. CURRENT TOPICS IN MICROBIOLOGY AND IMMUNOLOGY.

Shieh, M.-T., Wudunn, D., Montgomery, R. 1, Esko, J.D. & Spear, P.G. (1992) Cell SurfaceReceptors for Herpes Simplex Virus Are Heparan Sulfate Proteoglycans. http://rupress.org/jcb/article-pdf/116/5/1273/1062607/1273.pdf.

Shukla, D., Liu, J., Blaiklock, P., Shworak, N.W., Bai, X., Esko, J.D. & Cohen, G.H. (1999) Viral entry University of Pennsylvania may require interactions with other cell surface recep-Philadelphia, Pennsylvania 19104 tors as well. Cell.99.

Silva, M.C., Yu, Q.-C., Enquist, L. & Shenk, T. (2003) Human Cytomegalovirus UL99-Encoded pp28 Is Required for the Cytoplasmic Envelopment of Tegument-Associated Capsids. Journal of Virology. 77 (19), 10594–10605. doi:10.1128/jvi.77.19.10594-10605.2003.

Simmen, K.A., Newell, A., Robinson, M., Mills, J.S., Canning, G., Handa, R., Parkes, K., Borkakoti, N. & Jupp, R. (1997) Protein Interactions in the Herpes Simplex Virus Type 1 VP16-Induced Complex: VP16 Peptide Inhibition and Mutational Analysis of Host Cell Factor Requirements. JOURNAL OF VIROLOGY.71 (5). https://journals.asm.org/journal/jvi.

Sinclair, J. & Sissons, P. (2006) Latency and reactivation of human cytomegalovirus. Journal of General Virology.87 (7) pp.1763–1779. doi:10.1099/vir.0.81891-0.

Skepper, J.N., Whiteley, A., Browne, † H & Minson, A.A. (2021) Herpes Simplex Virus Nucleocapsids Mature to Progeny Virions by an Envelopment 3 Deenvelopment 3 Reenvelopment Pathway. JOURNAL OF VIROLOGY. 75 (12), 5697–5702. doi:10.1128/JVI.75.12.5697-5702.2001.

Smith, C.A., Bates, P., Rivera-Gonzalez, R., Gu,', B. & Deluca", N.A. (1993) ICP4, the Major Transcriptional Regulatory Protein of Herpes Simplex Virus Type 1, Forms a Tripartite Complex with TATA-Binding Protein and TFIIB. JOURNAL OF VIROLOGY.67 (8). https://journals.asm.org/journal/jvi.

Sodeik, B., Ebersold, M.W. & Helenius, A. (1997) Microtubule-mediated Transport of Incoming Herpes Simplex Virus 1 Capsids to the Nucleus. The Journal of Cell Biology.136 (5). http://rupress.org/jcb/article-pdf/136/5/1007/1270058/14462.pdf.

Sommer, M.H., Scully, A.L. & Spector, D.H. (1994) Transactivation by the Human Cytomegalovirus IE2 86-Kilodalton Protein Requires a Domain That Binds to both the TATA Box-Binding Protein and the Retinoblastoma Protein. JOURNAL OF VIROLOGY.68 (10). https://journals.asm.org/journal/jvi.

Spencer, J. v, Newcomb, W.W., Thomsen, D.R., Homa, F.L. & Brown, J.C. (1998) Assembly of the Herpes Simplex Virus Capsid: Preformed Triplexes Bind to the Nascent Capsid. JOURNAL OF VIROLOGY.72 (5). https://journals.asm.org/journal/jvi.

Sternsdorf, T., Guldner, H.H., Szostecki, C., Grotzinger, T. & Will, H. (1995) Two Nuclear Dot-Associated Proteins, PML and SplOO, are Often Co-Autoimmunogenic in Patients with Primary Biliary Cirrhosis. Scand. J. Immunol.42.

Sternsdorf, T., Jensen, K., Reich, B. & Will, H. (1999) The Nuclear Dot Protein Sp100, Characterization of Domains Necessary for Dimerization, Subcellular Localization, and Modification by Small Ubiquitin-like Modifiers*. http://www.jbc.org.

Stetson, D.B. & Medzhitov, R. (2006) Recognition of cytosolic DNA activates an IRF3-dependent innate immune response. Immunity. 24 (1), 93–103. doi:10.1016/j.immuni.2005.12.003.

Stevens, J.G. & Cook, M.L. (1971) Latent Herpes Simplex Virus in Spinal Ganglia of Mice. Science. 173, 843–845. doi:10.1126/science.173.3999.843.

Stow, N.D. & Stow, E.C. (1986) Isolation and Characterization of a Herpes Simplex Virus Type 1 Mutant Containing a Deletion within the Gene Encoding the Immediate Early Polypeptide Vmw110. gen. Virol.67.

Su, C., Zhang, J. & Zheng, C. (2015) Herpes simplex virus 1 UL41 protein abrogates the antiviral activity of hZAP by degrading its mRNA. doi:10.1186/s12985-015-0433-y.

Su, C. & Zheng, C. (2017a) Herpes Simplex Virus 1 Abrogates the cGAS/STING-Mediated Cytosolic DNA-Sensing Pathway via Its Virion Host Shutoff Protein, UL41. doi:10.1128/JVI.02414-16.

Su, C. & Zheng, C. (2017b) Herpes Simplex Virus 1 Abrogates the cGAS/STING-Mediated Cytosolic DNA-Sensing Pathway via Its Virion Host Shutoff Protein, UL41. Journal of Virology. 91 (6). doi:10.1128/jvi.02414-16.

Sugimoto, K., Uema, M., Sagara, H., Tanaka, M., Sata, T., Hashimoto, Y. & Kawaguchi, Y. (2008) Simultaneous Tracking of Capsid, Tegument, and Envelope Protein Localization in Living Cells Infected with Triply Fluorescent Herpes Simplex Virus 1. JOURNAL OF VIROLOGY. 82 (11), 5198–5211. doi:10.1128/JVI.02681-07.

Sun, C., Luecke, S., Bodda, C., Jønsson, K.L., Cai, Y., Zhang, B.C., Jensen, S.B., Nordentoft, I., Jensen, J.M., Jakobsen, M.R. & Paludan, S.R. (2019) Cellular Requirements for Sensing and Elimination of Incoming HSV-1 DNA and Capsids. Journal of Interferon and Cytokine Research. 39 (4), 191–204. doi:10.1089/jir.2018.0141.

Sun, L., Wu, J., Du, F., Chen, X. & Chen, Z.J. (2013) Cyclic GMP-AMP Synthase Is a Cytosolic DNA Sensor That Activates the Type I Interferon Pathway. http://science.sciencemag.org/.

Sun, W., Li, Y., Chen, L., Chen, H., You, F., Zhou, X., Zhou, Y., Zhai, Z., Chen, D. & Jiang, Z. (2009) ERIS, an endoplasmic reticulum IFN stimulator, activates innate immune signaling through dimerization. www.pnas.orgcgidoi10.1073pnas.0900850106.

Taddeo, B., Esclatine, A. & Roizman, B. (2002) The patterns of accumulation of cellular RNAs in cells infected with a wild-type and a mutant herpes simplex virus 1 lacking the virion host shutoff gene. www.pnas.orgcgidoi10.1073pnas.252588599.

Takahashi, H., Hatakeyama, S., Saitoh, H. & Nakayama, K.I. (2005a) Noncovalent SUMO-1 binding activity of thymine DNA glycosylase (TDG) is required for its SUMO-1 modification and colocalization with the promyelocytic leukemia protein. Journal of Biological Chemistry. 280 (7), 5611–5621. doi:10.1074/jbc.M408130200.

Takahashi, H., Hatakeyama, S., Saitoh, H. & Nakayama, K.I. (2005b) Noncovalent SUMO-1 binding activity of thymine DNA glycosylase (TDG) is required for its SUMO-1 modification and colocalization with the promyelocytic leukemia protein. Journal of Biological Chemistry. 280 (7), 5611–5621. doi:10.1074/jbc.M408130200.

Tang, J., Wu, S., Liu, H., Stratt, R., Barak, O.G., Shiekhattar, R., Picketts, D.J. & Yang, X. (2004) A Novel Transcription Regulatory Complex Containing Death Domain-associated Protein and the ATR-X Syndrome Protein. Journal of Biological Chemistry. 279 (19), 20369–20377. doi:10.1074/jbc.M401321200.

Tao, H., Simmons, B.N., Singireddy, S., Jakkidi, M., Short, K.M., Cox, T.C. & Massiah, M.A. (2008) Structure of the MID1 tandem B-boxes reveals an interaction reminiscent of intermolecular ring heterodimers. Biochemistry. 47 (8), 2450–2457. doi:10.1021/bi7018496.

Tatham, M.H., Jaffray, E., Vaughan, O.A., Desterro, J.M.P., Botting, C.H., Naismith, J.H. & Hay, R.T. (2001) Polymeric Chains of SUMO-2 and SUMO-3 are Conjugated to Protein Substrates by SAE1/SAE2 and Ubc9. Journal of Biological Chemistry. 276 (38), 35368–35374. doi:10.1074/jbc.M104214200.

Tavalai, N., Adler, M., Scherer, M., Riedl, Y. & Stamminger, T. (2011) Evidence for a Dual Antiviral Role of the Major Nuclear Domain 10 Component Sp100 during the Immediate-Early and Late Phases of the Human Cytomegalovirus Replication Cycle. JOURNAL OF VIROLOGY. 85 (18), 9447–9458. doi:10.1128/JVI.00870-11.

Tavalai, N., Papior, P., Rechter, S., Leis, M. & Stamminger, T. (2006) Evidence for a Role of the Cellular ND10 Protein PML in Mediating Intrinsic Immunity against Human Cytomegalovirus Infections. Journal of Virology. 80 (16), 8006–8018. doi:10.1128/jvi.00743-06.

Tavalai, N., Rechter, S. & Stamminger, T. (2008) Nuclear Domain 10 Components Promyelocytic Leukemia Protein and hDaxx Independently Contribute to an Intrinsic Antiviral Defense against Human Cytomegalovirus Infection. JOURNAL OF VIROLOGY. 82 (1), 126–137. doi:10.1128/JVI.01685-07.

Tavalai, N. & Stamminger, T. (2009) Interplay between herpesvirus infection and host defense by PML nuclear bodies. Viruses.1 (3) pp.1240–1264. doi:10.3390/v1031240.

Taylor, J.L. & O'brien, W.J. (1985) Interferon Production and Sensitivity of Rabbit Corneal Epithelial and Stromal Cells.

Taylort, H.P. & Cooper, N.R. (1990) The Human Cytomegalovirus Receptor on Fibroblasts Is a 30-Kilodalton Membrane Proteint. JOURNAL OF VIROLOGY.64 (6). https://journals.asm.org/journal/jvi.

Theil, D., Derfuss, T., Paripovic, I., Herberger, S., Meinl, E., Schueler, O., Strupp, M., Arbusow, V. & Brandt, T. (2003) Short Communication Latent Herpesvirus Infection in Human Trigeminal Ganglia Causes Chronic Immune Response. American Journal of Pathology.163 (6).

Toropova, K., Huffman, J.B., Homa, F.L. & Conway, J.F. (2011) The Herpes Simplex Virus 1 UL17 Protein Is the Second Constituent of the Capsid Vertex-Specific Component Required for DNA Packaging and Retention. Journal of Virology. 85 (15), 7513–7522. doi:10.1128/jvi.00837-11.

Tripathi, V., Chatterjee, K.S. & Das, R. (2021) Non-covalent Interaction With SUMO Enhances the Activity of Human Cytomegalovirus Protein IE1. Frontiers in Cell and Developmental Biology. 9. doi:10.3389/fcell.2021.662522.

Trus, B.L., Booy, F.P., Newcomb, W.W., Brown, J.C., Homa, F.L., Thomsen, D.R. & Steven, A.C. (1996) The Herpes Simplex Virus Procapsid: Structure, Conformational Changes Upon Maturation, and Roles of the Triplex Proteins VP19c and VP23 in Assembly. J. MoL BioL.263.

Trus, B.L., Newcomb, W.W., Cheng, N., Cardone, G., Marekov, L., Homa, F.L., Brown, J.C. & Steven, A.C. (2007) Allosteric Signaling and a Nuclear Exit Strategy: Binding of UL25/UL17 Heterodimers to DNA-Filled HSV-1 Capsids. Molecular Cell. 26 (4), 479–489. doi:10.1016/j.molcel.2007.04.010.

Tuan Nguyen-huynh, A. & Schaffer, P.A. (1998) Cellular Transcription Factors Enhance Herpes Simplex Virus Type 1 oriS-Dependent DNA Replication. JOURNAL OF VIROLOGY.72 (5). https://journals.asm.org/journal/jvi.

Turcotte, S., Letellier, J. & Lippé, R. (2005) Herpes Simplex Virus Type 1 Capsids Transit by the trans-Golgi Network, Where Viral Glycoproteins Accumulate Independently of Capsid Egress. JOURNAL OF VIROLOGY. 79 (14), 8847–8860. doi:10.1128/JVI.79.14.8847-8860.2005.

Unterholzner, L., Keating, S.E., Baran, M., Horan, K.A., Jensen, S.B., Sharma, S., Sirois, C.M., Jin, T., Latz, E., Sam Xiao, T., Fitzgerald, K.A., Paludan, S.R. & Bowie, A.G. (2010) IFI16 is an innate immune sensor for intracellular DNA. Nature Publishing Group. doi:10.1038/ni.1932.

Uprichard, S.L. & Knipe, D.M. (1996) Herpes Simplex ICP27 Mutant Viruses Exhibit Reduced Expression of Specific DNA Replication Genes. JOURNAL OF VIROLOGY.70 (3). https://journals.asm.org/journal/jvi.

Vanni, E., Gatherer, D., Tong, L., Everett, R.D. & Boutell, C. (2012) Functional Characterization of Residues Required for the Herpes Simplex Virus 1 E3 Ubiquitin Ligase ICP0 To Interact with the Cellular E2 Ubiquitin-

Conjugating Enzyme UBE2D1 (UbcH5a). 86, 6323–6333. doi:10.1128/JVI.07210-11.

Varnum, S.M., Streblow, D.N., Monroe, M.E., Smith, P., Auberry, K.J., Paša-Tolic, L., Wang, D., Camp II, D.G., Rodland, K., Wiley, S., Britt, W., Shenk, T., Smith, R.D. & Nelson, J.A. (2004) Identification of Proteins in Human Cytomegalovirus (HCMV) Particles: the HCMV Proteome †. JOURNAL OF VIROLOGY. 78 (20), 10960–10966. doi:10.1128/JVI.78.20.10960-10966.2004.

de Veer, M.J., Holko, M., Frevel, M., Walker, E., Der, S., Paranjape, J.M., Silverman, R.H. & Williams, B.R.G. (2001) Functional classification of interferon-stimulated genes identified using microarrays. doi:10.1189/jlb.69.6.912.

Wang, I.H., Suomalainen, M., Andriasyan, V., Kilcher, S., Mercer, J., Neef, A., Luedtke, N.W. & Greber, U.F. (2013) Tracking viral genomes in host cells at single-molecule resolution. Cell Host and Microbe. 14 (4), 468–480. doi:10.1016/j.chom.2013.09.004.

Wang, Q.-Y., Zhou, C., Johnson, K.E., Colgrove, R.C., Coen, D.M. & Knipe, D.M. (2005a) Herpesviral latency-associated transcript gene promotes assembly of heterochromatin on viral lytic-gene promoters in latent infection. www.pnas.orgcgidoi10.1073pnas.0505850102.

Wang, W., 2, H., Wu, C., Feng, Y., Li, A., Liu, W., Wang, Y., Chen, K., Tian, M., Xiao, F., Zhang, Q., Shereen, M.A., Chen, W., Pan, P., Wu, K. & Wuid, J. (2020) STING promotes NLRP3 localization in ER and facilitates NLRP3 deubiquitination to activate the inflammasome upon HSV-1 infection. doi:10.1371/journal.ppat.1008335.

Wang, X., Huang, D.Y., Huong, S.-M. & Huang, E.-S. (2005b) Integrin αvβ3 is a coreceptor for human cytomegalovirus. NATURE MEDICINE. 11, 515. doi:10.1038/nm1236.

Whitbeck, J.C., Peng, C., Lou, H., Xu, R., Willis, S.H., Ponce De Leon, M., Peng, T., Nicola, A. v, Montgomery, R.I., Warner, M.S., Soulika, A.M., Spruce, L.A., Moore, W.T., Lambris, J.D., Spear, P.G., Cohen, G.H. & Eisenberg, R.J. (1997) Glycoprotein D of Herpes Simplex Virus (HSV) Binds Directly to HVEM, a Member of the Tumor Necrosis Factor Receptor Superfamily and a Mediator of HSV Entry. JOURNAL OF VIROLOGY.71 (8). https://journals.asm.org/journal/jvi.

Whitley, R. & Baines, J. (2018) Open Peer Review Clinical management of herpes simplex virus infections: past, present, and future [version 1; referees: 2 approved]. doi:10.12688/f1000research.16157.1.

Wilcox, D.R., Folmsbee, S.S., Muller, W.J. & Longnecker, R. (2016) The type I interferon response determines differences in choroid plexus susceptibility between newborns and adults in herpes simplex virus encephalitis. mBio. 7 (2). doi:10.1128/mBio.00437-16.

Wildy, P., Russell, W.C., And, ~ & Horne, R.W. (1960) The Morphology of Herpes Virus. VIROLOGY.12.

Wilkinson, G.W.G., Kelly, C., Sinclair, J.H. & Rickards, C. (1998) Printed in Great Britain Disruption of PML-associated nuclear bodies mediated by the human cytomegalovirus major immediate early gene product. Journal of General Virology.79.

Wilkinson, K.A. & Henley, J.M. (2010) Mechanisms, regulation and consequences of protein SUMOylation. Biochemical Journal.428 (2) pp.133–145. doi:10.1042/BJ20100158.

Woodhall, D.L., Groves, I.J., Reeves, M.B., Wilkinson, G. & Sinclair, J.H. (2006) Human Daxx-mediated repression of human cytomegalovirus gene expression correlates with a repressive chromatin structure around the major immediate early promoter. Journal of Biological Chemistry. 281 (49), 37652–37660. doi:10.1074/jbc.M604273200.

Wu,', C.A., Nelson, N.J., Mcgeoch, D.J., Challbergl, M.D. & 20892, M. (1988) Identification of Herpes Simplex Virus Type 1 Genes Required for Origin-Dependent DNA Synthesis. JOURNAL OF VIROLOGY.62 (2). https://journals.asm.org/journal/jvi.

Wu, H., Ceccarelli, D.F.J. & Frappier, L. (2000) The DNA segregation mechanism of Epstein-Barr virus nuclear antigen 1. EMBO Reports.1 (2).

Wu, J., Dobbs, N., Yang, K. & Yan, N. (2020) Interferon-Independent Activities of Mammalian STING Mediate Antiviral Response and Tumor Immune Evasion. Immunity. 53 (1), 115-126.e5. doi:10.1016/j.immuni.2020.06.009.

Wu, J., Sun, L., Chen, X., Du, F., Shi, H., Chen, C. & Chen, Z.J. (2013) Cyclic GMP-AMP Is an EndogenousSecond Messenger in Innate ImmuneSignaling by Cytosolic DNA. Science. 339, 826–830. doi:10.1126/science.1232033.

Xu, H., Su, C., Pearson, A., Mody, C.H. & Zheng, C. (2017) Herpes Simplex Virus 1 UL24 Abrogates the DNA Sensing Signal Pathway by Inhibiting NF-B Activation. doi:10.1128/JVI.00025-17.

Yamashiro, L.H., Wilson, S.C., Morrison, H.M., Karalis, V., Chung, J.-Y.J., Chen, K.J., Bateup, H.S., Szpara, M.L., Lee, A.Y., Cox, J.S. & Vance, R.E. (2020) Interferon-independent STING signaling promotes resistance to HSV-1 in vivo. Nature Communications. 11, 1–11. doi:10.1038/s41467-020-17156-x.

Yan, N. & Chen, Z.J. (2012) Intrinsic antiviral immunity. Nature Publishing Group. doi:10.1038/ni.2229.

Yang, K., Homa, F. & Baines, J.D. (2007) Putative Terminase Subunits of Herpes Simplex Virus 1 Form a Complex in the Cytoplasm and Interact with Portal Protein in the Nucleus. Journal of Virology. 81 (12), 6419–6433. doi:10.1128/jvi.00047-07.

Yang, M., Hsu, C.T., Ting, C.Y., Liu, L.F. & Hwang, J. (2006) Assembly of a polymeric chain of SUMO1 on human topoisomerase I in vitro. Journal of Biological Chemistry. 281 (12), 8264–8274. doi:10.1074/jbc.M510364200.

Yang, Q. & Shu, H.B. (2020) Deciphering the pathways to antiviral innate immunity and inflammation. In: Advances in Immunology. Academic Press Inc. pp. 1–36. doi:10.1016/bs.ai.2019.11.001.

Yao, F. & Schaffer, P.A. (1995) An Activity Specified by the Osteosarcoma Line U2OS Can Substitute Functionally for ICP0, a Major Regulatory Protein of Herpes Simplex Virus Type 1. JOURNAL OF VIROLOGY.69 (10).

Ye, R., Su, C., Xu, H. & Zheng, C. (2017) Herpes Simplex Virus 1 Ubiquitin-Specific Protease UL36 Abrogates NF-B Activation in DNA Sensing Signal Pathway. doi:10.1128/JVI.02417-16.

Yu, D., Smith, G.A., Enquist, L.W. & Shenk, T. (2002) Construction of a Self-Excisable Bacterial Artificial Chromosome Containing the Human Cytomegalovirus Genome and Mutagenesis of the Diploid TRL/IRL13 Gene. Journal of Virology. 76 (5), 2316–2328. doi:10.1128/jvi.76.5.2316-2328.2002.

Zawatzky, R., Gresser, I., Demaeyer, E. & Kirchner, H. (1982) The Role of Interferon in the Resistance of CS7BL/6 Mice to Various Doses of Herpes Simplex Virus Type 1. THE JOURNAL OF INFECTIOUS DISEASES •.146 (3). https://academic.oup.com/jid/article/146/3/405/853542.

Zenner, H.L., Mauricio, R., Banting, G. & Crump, C.M. (2013) Herpes Simplex Virus 1 Counteracts Tetherin Restriction via Its Virion Host Shutoff Activity. Journal of Virology. 87 (24), 13115–13123. doi:10.1128/jvi.02167-13.

Zhang, C., Shang, G., Gui, X., Zhang, X., Bai, X.-C. & Chen, Z.J. (2019) Structural basis of STING binding with and phosphorylation by TBK1. Nature. 567, 394–398. doi:10.1038/s41586-019-1000-2.

Zhang, J., Zhao, J., Xu, S., Li, J., He, S., Zeng, Y., Xie, L., Xie, N., Liu, T., Lee, K., Seo, G.J., Chen, L., Stabell, A.C., Xia, Z., Sawyer, S.L., Jung, J., Huang, C. & Feng, P. (2018) Species-Specific Deamidation of cGAS by Herpes Simplex Virus UL37 Protein Facilitates Viral Replication. Cell Host and Microbe. 24 (2), 234-248.e5. doi:10.1016/j.chom.2018.07.004.

Zhang, X., Shi, H., Wu, J., Zhang, X., Sun, L., Chen, C. & Chen, Z.J. (2013) Cyclic GMP-AMP containing mixed Phosphodiester linkages is an endogenous high-affinity ligand for STING. Molecular Cell. 51 (2), 226–235. doi:10.1016/j.molcel.2013.05.022.

Zheng, Y., Samrat, S.K. & Gu, H. (2016) A Tale of Two PMLs: Elements Regulating a Differential Substrate Recognition by the ICP0 E3 Ubiquitin Ligase of Herpes Simplex Virus 1. Journal of Virology. 90 (23), 10875–10885. doi:10.1128/jvi.01636-16.

Zhong, B., Yang, Y., Li, S., Wang, Y.Y., Li, Y., Diao, F., Lei, C., He, X., Zhang, L., Tien, P. & Shu, H.B. (2008) The Adaptor Protein MITA Links Virus-Sensing Receptors to IRF3 Transcription Factor Activation. Immunity. 29 (4), 538–550. doi:10.1016/j.immuni.2008.09.003.

Zhong, S., Mü, S., Ronchetti, S., Freemont, P.S., Dejean, A. & Pandolfi, P.P. (2000) Role of SUMO-1-modified PML in nuclear body formation.

Zhou, W., Whiteley, A.T., de Oliveira Mann, C.C., Morehouse, B.R., Nowak, R.P., Fischer, E.S., Gray, N.S., Mekalanos, J.J. & Kranzusch, P.J. (2018) Structure of the Human cGAS–DNA Complex Reveals Enhanced Control of Immune Surveillance. Cell. 174 (2), 300-311.e11. doi:10.1016/j.cell.2018.06.026.

Zhou, Z.H., Venkataram Prasad, B.V., Jakana, J., Rixon, F.J. & Chiu, W. (1994) Protein Subunit Structures in the Herpes Simplex Virus A-capsid Determined from 400 kV Spot-scan Electron Cryomicroscopy. Journal of Nolecular Biology . (242), 456–469.

Appendix A: Mx2 recruitment to UV irradiated HSV-1 DNA

Mx2 is an IFN-induced restriction factor that has been found to confer panherpesvirus restriction (Schilling et al., 2018; Crameri et al., 2018; Schulte et al., 2015). The exact mechanism is unknown, but it was shown to disrupt capsid transport to the nucleus and reduce viral transport (Crameri et al., 2018; Jaguva Vasudevan et al., 2018). Based on the profile of UV irradiated HSV-1 and the increase in cytosolic genomes we investigated the potential involvement of Mx2 in this process. During UV irradiated HSV-1 infection, Mx2 was upregulated to similar levels as IFNb only treated cells, and Mx2 production was absent in non-UV irradiated infection (Figure 31). HFt cells were seeded overnight prior to infection with HSV-1 +/- UV at an MOI of 3 PFU/cell. Coverslips were fixed and permed at 90 mpi. Cells were stained for Mx2 and PML, whereas vDNA was detected via click chemistry. The microscopy observations for PML were reproducible and exhibited a reduced recruitment of PML to UV irradiated HSV-1(>0.5) compared to non-UV irradiated HSV-1 DNA (>0.7). On the other hand, there was no indication of recruitment of Mx2 to HSV-1 vDNA in either the cytoplasm or nucleus, irrespective of UV irradiation (Figure 32). These data suggest that there is no involvement of Mx2 in controlling the UV irradiated HSV-1 immune response during early timepoint of infection.

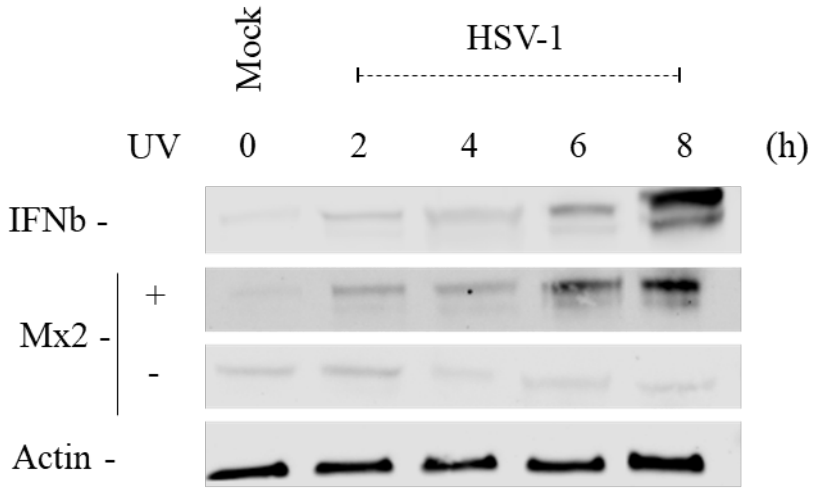

Mx2 induction is stimulated during UV irradiated HSV-1 infection.

HFt cells were seeded overnight then infected with either no UV WT HSV-1 or UV-irradiated HSV-1 (UV irradiation length indicated in secs) at an MOI of 3 PFU/cell. At the indicated timepoints lysates were collected, and protein levels were measured using Western blot. Membrane was probed for the cellular protein Mx2 to track its production during viral infection or IFNb treatment (positive control). Actin levels was used as loading control.

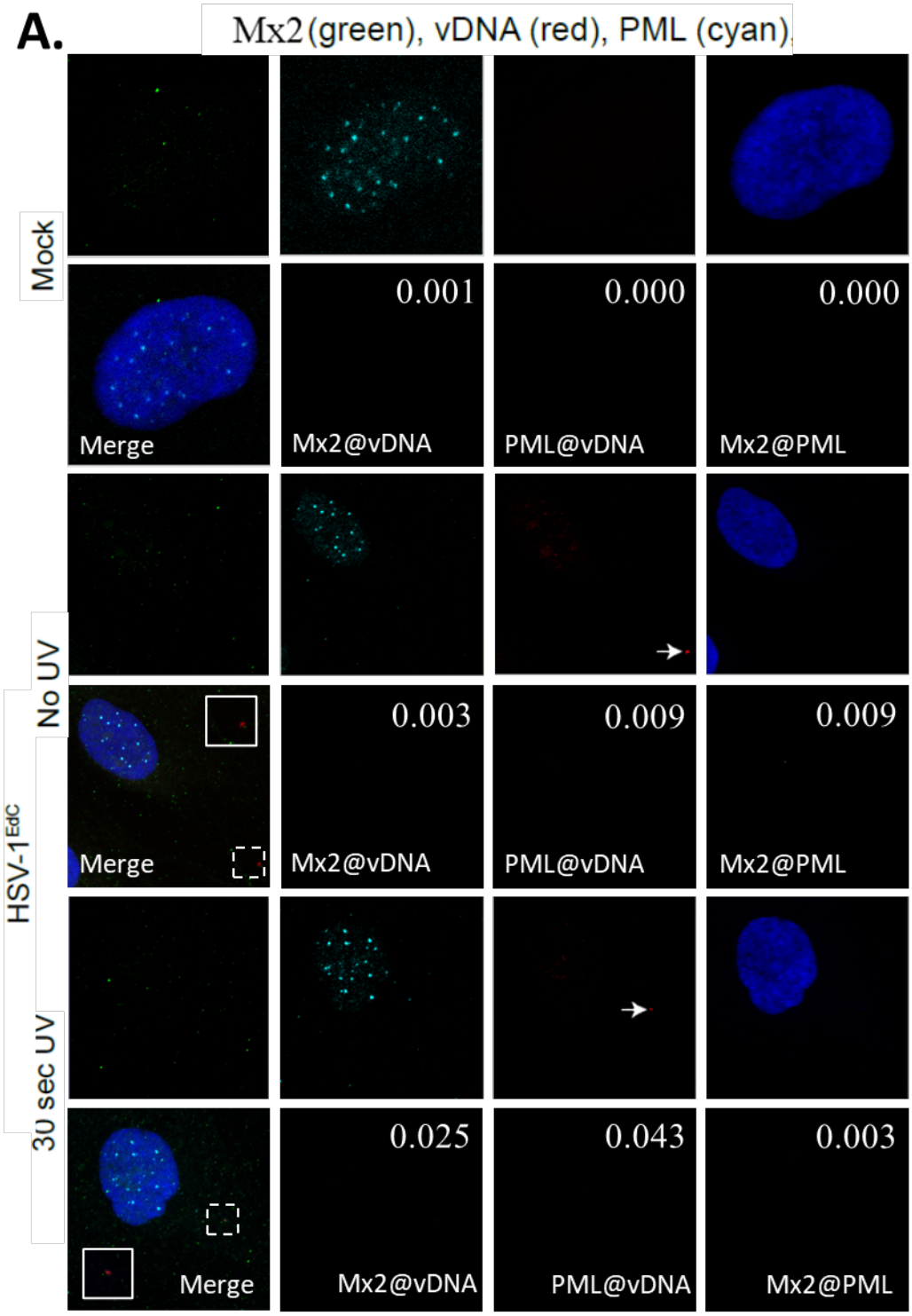
A.
Mx2 (green), vDNA (red), PML (cyan)
Mock
HSV-1EdC
No UV
3U sec UV
Merge
Mx2@vDNA
PML@vDNA
Mx2@PML
0.001
0.000
0.000
0.003
0.009
0.009
0.025
0.043
0.003

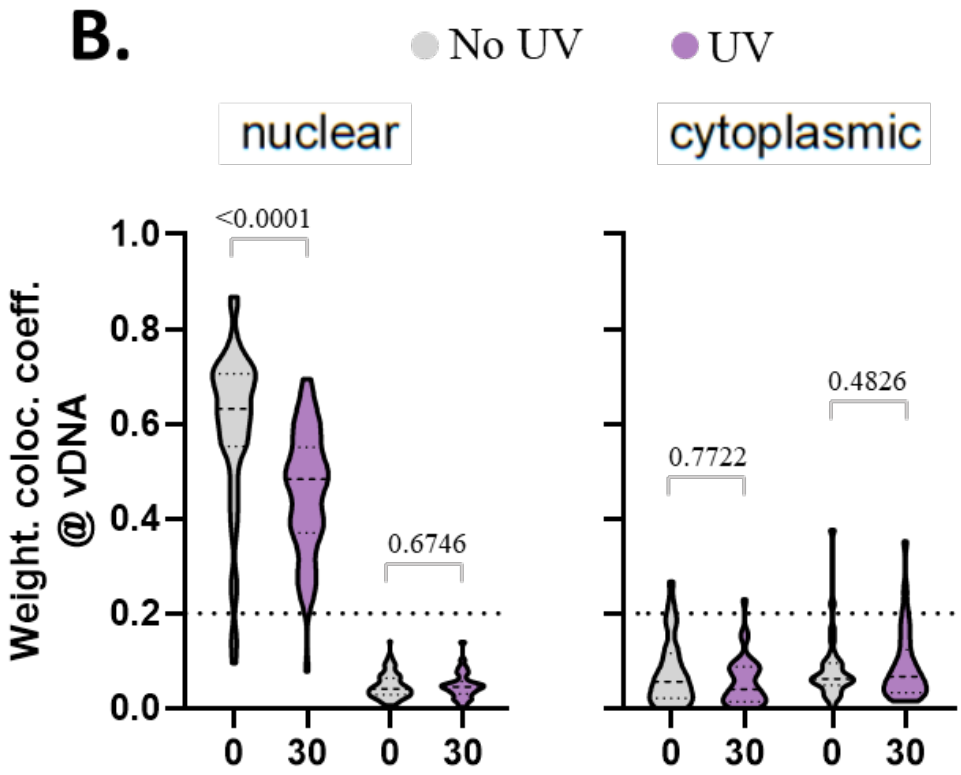

Mx2 is not recruited to HSV-1 genomes during early time points of infection.

HFt cells were mock infected or infected with 3 PFU/cell of HSV-1^{EdC} or UV HSV-1^{EdC}. Cells were fixed and permeabilized at 90 mpi. Infecting labelled viral DNA was detected using click chemistry. Mx2 and PML were detected via indirect immunofluorescence. Nuclei were stained with DAPI. (A) Localization of sub-nuclear recruitment of Mx2 (green) and PML (cyan) to infecting viral genomes (red). White boxes show zoomed areas of interest. Cut mask (yellow) highlights the regions of colocalization between the cellular proteins of interest and non-UV or UV irradiated HSV-1^{EdC} genomes. Weighted colocalization coefficient shown. (B) Quantitation of cellular protein recruitment to infecting vDNA in the cytoplasm or nucleus at 90 mpi. Black line: median weighted (w.) colocalization coefficient; dashed lines: SD. n>50 nuclei per sample population derived from a minimum of three independent repeats. ****P< 0.0001, ns (not significant); Kruskal-Wallis.

Appendix B: SUMO1/2/3 recruitment to UV irradiated HSV-1 DNA.

SUMO proteins can carry out a PTM process called SUMOylation, similar to ubiquitination, that targets lysine residues of proteins and can have an effect on protein stability or subcellular localization (Wilkinson & Henley, 2010). A recent study showed that SUMOylation via TRIM38 plays a role in regulating the activity of both cGAS and STING by increasing protein stability (Hu et al., 2016b). In contrast, SENP7 has been reported to deSUMOylate cGAS to activate its DNA binding activity by alleviating SUMO-mediated inhibtion (Cui et al., 2017). This raised the hypothesis that SUMO proteins may be recruited onto sites of cGAS/STING and HSV-1 genome foci localization and play a role in the DNA sensing pathway. To address this, we investigated the recruitment profile of SUMO1, SUMO2 and SUMO3 to cytosolic vDNA. HFt cells were infected with either non-UV or UV irradiated HSV-1 at an MOI of 3 PFU/cell. Samples were fixed at 90 mpi and stained for SUMO1 and SUMO2/3 (antibody able to stain both isoforms due to their high level of homology). PML was used as a reference protein (Figure 33A). Neither SUMO1 or SUMO2/3 was observed to be localizing to sites of vDNA foci in the cytoplasm, similar to PML and irrespective of UV irradiation. Quantitation of these microscopy observations confirmed this phenotype (Figure 33B). These results suggest that SUMO proteins are not playing a direct role in the cytoplasmic detection of HSV-1 DNA by the cGAS-STING pathway.

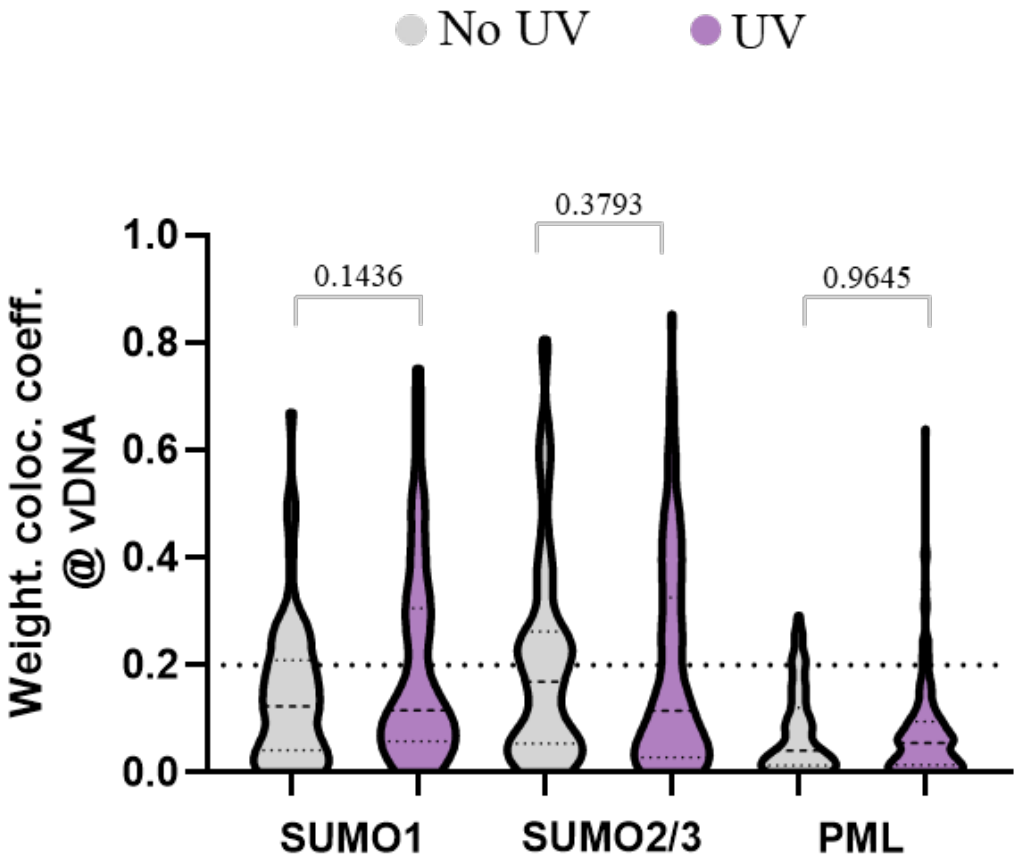

SUMO1/2/3 are not recruited to HSV-1 genomes during early time points of infection.
HFt cells were mock infected or infected with 3 PFU/cell of HSV-1^{EdC} or UV HSV-1^{EdC}. Cells were fixed and permeabilized at 90 mpi. Infecting labelled viral DNA was detected using click chemistry. SUMO1, SUMO2/3 and PML were detected via indirect immunofluorescence. Nuclei were stained with DAPI. (A) Localization of sub-nuclear recruitment of SUMO1 or2/3 (green) and PML (cyan) to infecting viral genomes (red). White boxes show zoomed areas of interest. Cut mask (yellow) highlights the regions of colocalization between the cellular proteins of interest and non-UV or UV irradiated HSV-1^{EdC} genomes. Weighted colocalization coefficient shown. (B) Quantitation of cellular protein recruitment to infecting vDNA in the cytoplasm or nucleus at 90 mpi. Black line: median weighted (w.) colocalization coefficient; dashed lines: SD. n>50 nuclei per sample population derived from a minimum of three independent repeats. ns (not significant); Kruskal-Wallis.

Appendix C: cGAS gene contains an Sp1 binding site

GCAGACTCTTGTGTGCCCGCCAGTAGTGCTTGGTTTCCAACAGCTGCTGCTGGCTCTTCCTCTTGCGGCC
TTTTCCTGAAACGGATTCTTCTTTCGGGGAACAGAAAGCGCCAGCCATGCAGCCTTGGCACGGAAAGGCC
ATGCAGAGAGCTTCCGAGGCCGGAGCCACTGCCCCCAAGGCTTCCGCACGGAATGCCAGGGGCGCCCCGA
TGGATCCCACCGAGTCTCCGGCTGCCCCCGAGGCCGCCCTGCCTAAGGCGGGAAAGTTCGGCCCCGCCAG
GAAGTCGGGATCCCGGCAGAAAAAGAGCGCCCCGGACACCCAGGAGAGGCCGCCCGTCCGCGCAACTGGG
GCCCGCGCCAAAAAGGCCCCTCAGCGCGCCCAGGACACGCAGCCGTCTGACGCCACCAGCGCCCCTGGGG
CAGAGGGGCTGGAGCCTCCTGCGGCTCGGGAGCCGGCTCTTTCCAGGGCTGGTTCTTGCCGCCAGAGGGG
CGCGCGCTGCTCCACGAAGCCAAGACCTCCGCCCGGGCCCTGGGACGTGCCCAGCCCCGGCCTGCCGGTC
TCGGCCCCCATTCTCGTACGGAGGGATGCGGCGCCTGGGGCCTCGAAGCTCCGGGCGGTTTTGGAGAAGT
TGAAGCTCAGCCGCGATGATATCTCCACGGCGGCGGGGATGGTGAAAGGGGTTGTGGACCACCTGCTGCT
CAGACTGAAGTGCGACTCCGCGTTCAGAGGCGTCGGGCTGCTGAACACCGGGAGCTACTATGAGCACGTG
AAGGTGAGCTGCTTGGCGCCCTCCCGCCGAGCCCCGCTGCTCGGCCTTCCGCAATCCGCAGTCCCTACCT
TCCCCGGGTCGCGCCCCTCACTTCCCTTCGGAAGTAACTTAGACTTTTGCATGTTTTTCGGTAGCCTAGT
CTAAGTAAAACGACAAACCGTTCGTTTATTCATCTACACATCCAACGATCAGACAACCAACCGGTACTGA
TTGCTGGCTAATTTCAAGACACTGCTCCCGGGGGAATTCAAATGTATGGGTTCATTCATGCAAGCCGACA
TGTATCGAGTTTCCGTAACAGGGCAGTGTTTGATGGTGTGGACCTGAGGTCCCGAGTCAGATATTGACTT
GGATAATTTGAAGTGGTCTGTTAAAAATTCCACGTAGACTTTTTCCTATGAGGAAGACCTCTTACTCCAT
AGAAAAAAAGATCTTCAGTTTCTCTCCCCCTCTTCCTCCCTGCCCCCTCTCCTGCTATCCCGTCTGACCC
CAATTTCTTTTTTTTCTTTTTTCTTTTCTTTTCTTTTTTTTTTTTTTTGAGGCGGAGTCTCGCTGCGTCC
CCCAGGCTGGAGTGCAGTGGCGCTATCTCGGCTCACTGCAAGCTCCGCCTCCCGGGTTCACGCCATTCTC
CTGCCTCAGCTTCCCGAGTAGCTGGGACTACAGGCGCCCGCCACCATGCCCGGCTAATTTTTTTTGTATT
TTTAGTAGAGACGGTGTTTCACCGTGTTAGCCAGGATGGTCTCGATCTCCTGACCTCTTGATTCGCTCGT
CTCGGCCTCTCAAAGTGCTGGGATTACAGGCGTGAGCTACCGCGCCCGGCCGTCTGTCCCCAGTTTCTTA
CACAGAAATCATGGGAAGCTTACAGTATAATGTTAAACAAACAAATAAGAATATCTCCTACAGATACTAA
AACGCTTTCTAGATACACATTCCGTATAATTGCTTCGACGTGTGTATTACACAGCTCCATTTGCTTGTGG
GTGATTGAGTCATTAATCATTCCTGTGTAAATTGAAAGTTTAGAAGCAGGTTCCTGACTGGAGCGTGTTT
CTTGCCCAGCAAGAGATTTGTTTCTTTTTCTTTTTCTTTCTTTCTTTCTTTTTTTTTTTTTTGAGACGGA
GTTTCGCTCTTGTTACCCAGGCTGGAGTGCAATGGCGCGATCTCAGCTCACCTCAACCTCCACCTCCCAG
GTTCAAGCGATTCTCCTGTCTCAGCCTCCTGAGTAGATGGGATTACAAGCATGAGCCTCCACCCTGGCTA
ATTTTGTATTTTTAGTAGAGACGGGCTTTCTCCATGTTGGTCAGGCTGGTCTAGAACTCCCGACCTCAGG
TGATCTGCCAGCCTCAGCCTCCCAAAGTGCTGGGATTACAGGCGTGAGCCACCACACCCGGCTTCTTTTC
TCTTCTTTTTTCTCTTCTCTTCTCTTCTCTCTATCTCTCTGTCTCTCTCTTTTCCTCCCTCCCTCTCTTC
CTCTCTCTCTCTCTCTCTTTATTTTGTTCTTTCTTTCTTTTCTTTCTTCTTTCTTCTTTTTTTGATGGAG
TTTCACTCTTGTTGCCCAGGCTGTAGTGCAGTGGTGCCATCTAGGTTTCGCTGCAACCTCCGGCTTCCAG
GTTCAAGCGATTCTCCTGCTTCAGCCTTCCAAATAGCAGGGATTACAGGTGCCTGCCCCCACTCCCGGCT
AATTTATGTATTTTTAGTAGAGACGGGGTTTCACCATGTTGGCCAGGCTGGTCTCGAACTCTGACCTCAG
ATGATCCACCTGCCTCGGCCTCCCTAAGTGCTGGGATTACAGGCTTGAGCCACGGCACCCAGCCCAGACT
GTGTCTTGAGCATGATTCTTTTTAATTAACTAATTTACTTTTCAGCATCAGATATGTCTCTGATTGAGCA
TGATTCTTATTATGTAAGTATCAATTCAGTTCAATTACTGTATATGGCGGGTCCAAAGGAAAAAGAAAGT
TACTAGTTAGAATTAGAGAACAAGACATTCAGAAGACAGTCTCCATTCAGAACCACTTTGTGTGTGTGTG
TGTGTGTGTGTGTGTGTGTTTGAGACAGAGTCTCACTCTGTCACCCAGGCTGGAGTGCAGTGGCGCGA
TCTCGGCTCACTGCAAGCCCTGCCTACTGGGTTCACACCATTCTCCTGCCTCAGCCTCCCAAGTAGCTGG
GACTACAGGCGCCCGCCACCATGCCCAGCTAATTTTTGTATTTTTAGTAGAGACGGGGTTTCACCGTGTT
AGCCAGGCTGGTCTCTATCTCCTGACCTCATGATCTTCCCGCCTTGGCCTCCCAAAGTGCTGGGATTACA
GGTGGGAGCCACCATGCCCAGCCCAGAACCACTTTGTTTTTAAAAATTATGCCAATGAAAAGAAATCCAG
TGAAATTTGTTTTATCTAAAACTTTTTCTTTTTTTCTTTTTCTTTTTTCTTTTTTTTTGGGGATGGAGTC
TTGCTCTGTCACCCAGGGTGGAGTGCAGTGATGTGATCTTGGCTCACTGTAACCTCCGCCTCCCGGGTTC
AAGTGAGTCTCCTGCCTCAGCCTCCAGAGTAACTGGGATTACAGGCGGGCGTCACCTCACCTGGCTAATT
TTGTATTTTTAGTAGAGATAAGGTTTCAGCATGTTGGCCAGGCTGGTCTCGAACTCCTGACCTCAAGTGA
TCCACCTGCATCAGCCTTTCAAAGTGCTGGGATTACAGGCGTGAGCCACTACACCCAGCCTAAAACTTTT
TCTATTACTGATTATGAGATATATGTGGGCCAGGTACAGTGGACTCATGCCTGTGATCCTAGCACCATGG
GAGGCTGAGGCGGGAGTTTGAGTCCAGCCTGGACAACATAGTGAGACCCCAGCTCTACCAAAAATAAGTT
AAAAATTAACTGGATGTGGTGGCACACACAGGTAGTCCCAGCTACCTGGGACTACAAATTCTAGGTAAAA
AAAAATCTCGAAAATACATGGGAAGTTTCTTGTAGAAATTCCCTGTAGAATTGTCAGTCCATATGTTCTT
TTCATTCTAAGTGTTAATGTACTTTACTATTTATATAGTTTGGACTCAGTGAAAAGGTTACATAGAAATC
AATTAATTGTAGTTTTTTTTGTTTGTTTGTTTTTTGTTTTGTTTTGTTTTGAGACAGAGTTTCACTCTTG
TTGCCTGGGCTGGAGTACAATGGCGTGGGTGGCCTCAGCTCACTGCAACCTCTGCCTCCCAGGTTCAAGC
GATTCTCCTGCCTCAGCCTCCCGAGTAGCTGGGATTACAGGAATGCACCACCATGCCTGGCTAATTTTTT
GTGTTTTTAGTAGAGATGGGGTTTCTCCATGTTGGTAAGGCTGGTCTCAAACTCCTGACCTCAGGTGATC
CACCCGTCTCAGCCTCCCAAAGTACTGGGATTACAGGCGTGAGCCACTGTGCCCGGCCAGTGGTTTTAAG
TAATGGTATATTAACTGGTAAAGAAAAGGAACAAACTACAGCAACATGAACAGTGAAAATGAATTACATA
AATAATGTTGAACAACAACAAAAAGAACGTAAAGGAATACATACAGCTGATGCAGCAAGACAAGGAAAAT
AAAGGCATAAGATGGGAAAAAGAGTGATGAAATCGTTATGTGTAGATGACTTGATTGGCTTCACATATAA
ACTGTTGGAAATAATTAGTAAATTAGCAAAATTGCTGGTTGCAAAGTCAATAAACAAAAATAAAAATATT
TCAATATACTAACAAGATTAAAAACAAAATGAAAATACCATTTAGAATATCATCAAAAATATCAAACCTA
GGTCCATTGGTGCATTCTGATAGTCCCAGCTATTTGGGAGGCCGAGGTGGGAGAATCACATCAAGTCAGG
AGTTTGAGGCTGCAGTACACTATGATCTATCTGTGAGTAGCCACTGTACTCCAGCCTAGAGACCCCATCT
CTAAAAAATAAAAATTGAAAACTTTGGCCAGGCATGGTGGCTCACGCCTATAATCCCAGCACTTTGGGAG

TAGAGGCAGGCAGATCACTTGAGGTCAGGAGTTTGAGACCAGCCTGGTCAACATGGCAAAACCCTGTCTC
TACTAAAACTACAAAAATTAGCTGGGCGTGTTGGTGCGCGCCTGTATTCCCAGCTACTTGGGAGGCTGAG
GCAGGAGAATTGCTTGAGCCCAGGAAGCTGAGGTTGCAGTGAGCCAAGCTTGCTCCATTGCACTCCAGCC
TCAGTGACAAGCGTGAAACTCTGTCTCAAAAAAAAACAAAAAACTGAAAACTTGAAAAACAATTTAAAAA
TCAAATATTTAGGAATAAATATCACTAAAGATATTCAAAACTTAAAAACATAACTGGGTAAATTTGAAGA
GGAAGTAATTGACAACTATATCGTGTTCATTTTTCCTCAAATTGTTCTAGATTTAATGCAATCAGTTGAA
ATATGATCAGTTTTTTAAATTAAATTGACAAACTGATTAAAATATGTATTCATTTATTTTTTGAGACGGA
GTCTCGCACTGTCGCCCAGGCTGGAGTGCAGTGGTACCATCTCGGCTCACTGCAACCTCCGCCTCCCGGG
TTCAAGCAAGTCTCCTGCCTCAGCCTCCTGAGTAGCTGGAACTACAGGTGCATGCCACCACACCTAGCTA
ATTTTCATATTTTTAATAGAGACGAAGTTCCACCATGTTGGCCAGGATGGCCTTGATCTCTTGACCTTGT
GATTCGCCTGCCTCGTCCTCCCAAAGTACTGGGATTACAAGCGTGAGCCACCGCGCCTGGCTGAAAGGAC
GATTTTTTTTTTTTTTTTTTTTTTTTTTTTTTGAGACGGAGTCTCGCTCTGTCGCCCCGGCGGGACTGC
GGACTGCAGTGGCGCAATCTCGGCTCACTGCAAGCTCCGCTTCCCGGGTTCACGCCATTCTCCTGCCTCA
GCCTCCCGAGTAGCTGGGACTACAGGCGCCCGCCACCGCGCCCGGCTAATTTTTTTTTGTATTTTTAGTA
GAGACGGGGTTTCACCTTGTTAGCCAGGATGGTCTCGATCTCCTGACCTCATGATCCACCCGCCTCGGCC
TCCCAAAGTGCTGGGATTACAGGCGTGAGCCACCGCGCCCGGCCCGATTTTTTTTTTTCAATAAATAATG
CTGGGTCAATTGGATATCTATGTAGGAAAAACATGAACCTTGATTCCCTACCACATATCATACACAAATT
TTTTTTTTTTTTTTTTTTGAGATGGAGTCTTGCTCTGTTGCCCAGGCTGGAGTACAGTGACACTATTTTG
GCTCACTGCAACATCTGCCTTCTAGGTTCAAGCAATTCTCCTGCTTCAGCCTCCTGAGTAGCTGGGATTA
CAGGCGCATGCCACTATGCCCGGCTAATTTTTGTATTTTTAGTAGAGACGGGGTTTCACCATGTTGGACC
AGGCTGGTCTCGAACACCTGACCTCAGGTGAATCGCCCGCCTTGGCCTCCCAAAGTGCTGGGATTACAGG
CATGAGCCACTGCACCTGGCCCCACAAAATTTAATTATAGGTGTGAGCCACTGCACTTGGCCTAAAATCA
TTTTTAGTTATAAAAATAATACTAGGTCATGGTAAAAAAAATTAATTGAGTGTAGAACCTACAAAATGAA
ACTGGTAATACTCTTCCACCTCCTGCCAGCTCCACTAGTCCCACTCCCAGAGGGTATATATAGACATTAT
GAATCTTGCTTTTTAAAGTAAAGTTTTAAGTGGAAATTTTTTAAAAAGTTCCAGTCACTTGGAAAATATT
CATAAGCAAATATTTCAGTACTATTTTTACTGTTTCTTAGATTTCTGCACCTAATGAATTTGATGTCATG
TTTAAACTGGAAGTCCCCAGAATTCAACTAGAAGAATATTCCAACACTCGTGCATATTACTTTGTGAAAT
TTAAAAGAAATCCGAAAGAAAATCCTCTGAGTCAGTTTTTAGAAGGTGAAATATTATCAGCTTCTAAGAT
GCTGTCAAAGTTTAGGAAAATCATTAAGGAAGAAATTAACGACATTAAAGGTAAGACTTTTGCCTTTTGA
TTCTTAAAGGTTTAATTATACCTAGTAATTGCCAATGTACACTCCCATTCTCATGTTTCTTGACCTCTCT
GCAGTAAGAAAAAGTGCAGTAGAGAGGTCAAGAAACATCAGTAGAGGAGTGTACATTGGCAATTACTTAT
AATATGATTACAAGATTATAAAGTACAGAAGGGTAGAGGTCTTTATCTATTTGTTCTCTAATGAATCCTA
AATAACTAGAACACCTACACATTAGATAATCAATGAATATTGATTAAATTAAATGATTAAATTATATGAA
ATAATCAATGAATATTTATTAAATTGATGGATAAATGAATCTACACTCTCTGCCTAGGTATTTCATCCAT
TCCCAATGCCACCTATATGATGATGACTCCCAAATGTTTACTTGCAGCCCAAATATATCCTTTGCACTCC
AAACCTATATCCAGCTACGTCCTTAACATATCCACTTTGATGTTGATGTACCACAGGAATCTATAACCAA
ACATATCCAAAGCGAATAAACATAACTTAATTCATATACCAAACTATGTTTTGCCTCAGTCCTTCCCATC
TCAGAAAATGGCACAATCAATCCACCCAGACGCACCATCCAGAAACCTGGGAACCATCTTAATTTAATCC
TCTCTGTTACCCCCTACGCTTAATCCAGATGCAAGTGCTGCTACAGCTTGGACCTGTCTGCTGCTTCAAT
CCCAGCACCCTACTCCCACCCCACCTAAGCTGCCACCATCTTTTACCTGAACTATTACATCATTTTCCTT
TCTAATCTCCCTATTTGCCTTCTTATAATATCTGTCCTTAGAAGCCAGAGTAAATGTTTTAAAATACAAA
GCCAGTCATTACTCTCTGATGAAAACCTGGCTTCTCAATGATCAGATAATAAAATCTGGTGCCAGGCGCA
GTGGCTCACACCTGTAATCCCAGCACTTTGGGAGGCTGAGGTGCGTGGATCACCTGAGCTCAGGAGTTTG
AGACCAGCCTGGCCAACATGGAGAAACCCCATCTCTACTAAAAATACAAAAATTAGCCGGGTGTGGTGGC
ACATGTCTGTAATCCCAGCTACTTGGGAGGCTGAGGCAGGAGAATTGCTTCAACCTGGGAGGCAGAGGTT
GCAGTAAGCCGAGATCGGGGCATTGCACTCCAGCCTGAGTGACAAGAGCGAAACTCCATCTCAAAATAAA
ATAAAATTAAATTAAATTAAATTAAAATCTGGCCAGGCGCAGTGGCTCACACCTGTAATCCCAGCACTTT
GGGAAGCTGAGGTAGGTATATCACGAGGTCAGGAGTTCAAGACCAGCCTGGCTAAGATGGTGAAACCCCA
TCTATACTAAAAATACAAAAATTAGCCAGGCGTGGTGGTGGATGCCTGTAATCCCAGCTACTCGGGAGGC
TGAGGCAGGAGAATCGCTTGAACCCGAGAGGTGGAGGTTGCAGTGAGCCGAGATCGTGCCACTGCACTCC
AGCCTGGGCGACAGAGCAAGACTCCGTCTCAAAAATAAAATGAAATCTAAAGTCCTTTTCAGGGTCTACA
AGTCAGTACAGAATCTGGTCCCTGGCTGCCTCTTCAGCTTCATTTCATATAACTTCATCTTTTCCGAAAG
AGTCTCTTTTTGTTCCTAGATCTTTCCAAGCTCTTTTTTTCTGCCTCAGGGCTTGGCTCCACCACCCCAT
TCCACCCTAATTGCTATCACTTTTCCCAGTTTATTCCCTTCAGAGCACTCACTGCAATTTGTGTTGTATG
TTATTACGCTATTAGATTAAGAGCTTTATCTTGCAAGCACAGACGTACAATTAATAACAAATGGAAAAAA
TGATTATCTTGTATACTGGAAAGTAGTAAGTGCTGTTGTGAAGAAGTATAGCAAAGTGAGAGGGATCAGG
AATGTGGGAGATGGAGGTGGGGGGGAAGTTGCAATGTTAAGTAGAGTGGTAAGAAGAGAATTCCATTAGA
GTTTGGGAAGAGCCAGGCGCCGTGGCTCACGCCTGTAATCCCAACACTTTGGGAGGCCGAGGCGGGTGGA
TCACGAGGTCAGGAGTTCAAGACCAGCCTGGCCAAGATGGTGAAACCCCGTCTTGACTAAAAATACAAAA
AACTAGCCGGGCGTGGTGGCGGGTGCCTGTAATCCCAGCTACTTGGGAGGCTGAGGCAGAGAATTTCTTG
AACCCAGAAGGCGGAGGTTGCAGTGAGCTGAGACCGCGCCACTGAACTCCAGCCTGGGCGACAGAGTGAG
ACCCTGTCTCAGAAAAAAAAAAAAAAAAAAAAAGAGTTTGGGAAGAAGAGAATGAACAAAAGGAGACTATG
AGTGTTTTGTAGAAGGAGCGGTCAGTGTTTGGAATGCTACTGACATCCAGAAATCCAATGGATTTGTTCT
TTGGTCTTGTGGGGTTGACAAGAGAAATGTCAGTGGGGTGATGGACACAGAGTGAAAAGGCAGGGTTGCA
GTGGAGATAACATGTGTAGGCCACTCTAGAAAGTTCTGTCTGGGCTAACTGTGGTGTCTCAGCACTTTGG
GAGGCCAAGGCAGAAGGATTGCTTGAGCCCAGGAGTTCAAGACCAGCCTGGGCAACAAAGTGAGAGTCCA
TCTCTACAAAAAAAAATTTTAGGCCAGGTATGGTGGCTCATGCCTGTAATCCCAGCACTTTGGGAGGCCA
AGGTGGGCGGATCACAAGGTCAGGAGTTCAAGACCAGCCTGGCCAAGATGATGAAACCCCGTCTGTACTA
AAAATACAAAAATTAGCCAGGCGTGGTGGCAGACACCTATAATCATAGCTACTCAGGAAGTTGAGGCAAA
AGAATTGCTTGAGCCTGGGAGACAGAGGTTGCAGTGAGCTGAGATTGCGCCACTGCACTCCAGCCTGAGC
GACAGAGCAAGACTGTCTCAGAAAAAAAAAAAAAAAAAAAAGAAAGAAAAAAGAAAAAAACATTTTTTTAA
TTAGCCAGGAGTGGTGGCATGTGCCTGTGGTCCCAGCTACATACGATGCTGAGGCAAGAGGATTGCTTGA

ACCTAGGAGGTTGAGGCTGCAGTGAGCCATGTTCACGCTACTGCACTCCAGCCTGGGTGACAGAACGGGA
CCCTGTCTCAAAAAAAAAAAAAAAGTTTGGGCTGGAAGGAAGCAGAAAGATGGGTGAGTATGGAGAGGAGG
AAGATGTGGGGTGAAAGGAGAGGTATACCCTATAACCCTTTGTATGAATTTCAGAATAATCTAGCAGGGA
GGGAGAGATGGCTGATGTAGGAGAGGAAATACTTGAAGAGCATGGTACTTGAGAAGTTGAGAAGGAAGGG
ATCCAGAGACTATGGGCAGAGGTGGCCTTTGAAAGGTAGATGGAGGGCCAGGCACAGTGGCTCACACTTG
TAACCCTAGCACTTTGGGAGGCCAAGGTAGGCAGATCATTTGAGCTCAAGAGTTCAAGACCAGCCTGGCC
AACATGGTGAAACCCTGTCTCTACTAAAAATACAAAAATTAGCCAGGTGTGGTGGTGCATGCCTGTAATC
CCAGCGACTCAGGAGGTTGAGGCAGGAGAATCACTTGAAGCTGGGAGGTGGAGTTTGCAGTGAGCTGATA
TCACACCACTGCACTGCATCCAGCCTGGGCTACAGAGCAAGACTTTGTCTCAAAAAAAAGTAAGGTAGAT
GGACACTTACTTCCTCAGTGGTAACAGGAGAGGTGGCCAGGTTTGGGTAACAGGTGGCCAGGTTTGCAGA
TTTTTCTAGCATTTTCTCCTTTGTGCTCTACTTCGTCACTGTGGAAGTCTTATCTGACAGTAGTAGTCTT
TACTGCTTATAAACCCCCAACTCCCAAAGCCATCTAAATTTCTGACCATAGCCACCCACCCAGCAGCCAT
CTCCACTTGAGTGTCCCACAGGTATCTAGAGCTCATTGTATCTCATGAAGTTCAGCTTGGCCCAATCTTT
CTTCTTCCTGCTTATTCTATTTTGAGGAATGGAACCAACATCAGCCATTAGGCCTAGGAAGGCCAAGATC
CTGGGATGGCATCCCAAGGCTCCTACTTTCCTCCTCACATCGTAGCCTCAACTCATGACCACTTATGTTG
ATTTGGACTTCTTTAGTTGCTCTCACTTCTTCCCCGTGTCTTGATGCTCACTACCTCTGTGCTGCCGTGG
CACCCAGCCTCTGTGCCAGGCTGTTGCTGTGGTCTTTTTGCTGCCTGTCTCTTCCCTCTTGCCCATCTGG
CCTCTCCTCTAGGCTTCCCTCCATTCTGCCATCTATAATTTGTAATGAAAATTTAACCAGGCACAGTGGC
ACATGCCTGTAATCCCAGCTACTCAGGAAGCTGAGGCAGGAGGATCAATTGAACCCGGGAGGCAGAAGTT
GCAGTGAGCCGAGATCGTGCCACTGCACTCCAGCCTGGGCAACAAGACAATAAGAGTGAAACTCTGTCTC
AAAAAAAAAAAAAAAGAAAAAGAAAAAGAAAAAAGAAAAGAAAAGAAAAGAAGAAAATTTAATCACAGCA
CTCTTAAACCTCAAAGTCTACAGAGACCCCTTCATCATATATGCCCCACACCATCTTGACAATGCCTCCC
AATGGGAGATATCAGTAATTATTGTGTTTTTTGTTTTTTGTTTTTTTTTCTTTTTTGAGACAGAGTCTTA
ATCTGTCGCCCAGGCTGGAGTGCAGTCATGTGATCTCGGCTCACTGCAACCTCCGCCTCCTGGGTTCAAG
TGATTCTCATGCCTCAGCCTCCCGAGTAGCTGGGATTACAGGCATTCGCCACCATGCCCGGCTAATTTTT
GTATTTTTAGTAGAGATGGGGTTCCACCATGTTGGCCAGGCTGGTCTCGAACTCCTGACCTCAAGTGATC
CACCTGTCTCGGCCTCCCAAAGTGCTGCGATTACAGGCATGAGCCATCATGCCCAGCCAATATTGGTTTA
GTAAAATACTTTGCCTTTTAGAGCCAGTTTCTGTTTTACCACTAATGTTTACTTCATACTTAGCACACCA
GAGATCTTCAATTATAGTTACATTATTTCCCCTGTATTTCCAGAGAAAATTGGATTAATAAATACTTTCT
TTTCTTTTATATGTTCAACCAGATACAGATGTCATCATGAAGAGGAAAAGAGGAGGGAGCCCTGCTGTAA
CACTTCTTATTAGTGAAAAAATATCTGTGGATATAACCCTGGCTTTGGAATCAAAAAGTAGCTGGCCTGC
TAGCACCCAAGAAGGCCTGCGCATTCAAAACTGGCTTTCAGCAAAAGTTAGGAAGCAACTACGACTAAAG
CCATTTTACCTTGTACCCAAGCATGCAAAGGAAGGAAATGGTTTCCAAGGTATTTTAAATATTAAAGTTA
ACTTAAAGAAGTAAAAGAGTTGTTAATGTTATATGTTCAGGCAGTAAAAGATCAACAGCCAACCAATGCT
GTTGTCATTTCAAGAGCCATCAGGCAAAATAGGTTATAAGATGGGAGTCTGGTGACAGACAGAATTGAAA
AGGGCAAAGTTGTAGTATTAATATCAAATACTCAGCTTTAAAATGTCTAGCAATCCATATTTGAATTTTA
TTTTATTTTTTTCGGTAAAGAAAAGCAGTATTGGCCTTGGAGTCAGACTGCCCTGGTTCTGAATCCTGAG
GCTCCTTCTACTAGTTGTGTGAATTCGAGCTAGTTATGATGCTTTCTAAACCCATTTGCTCATCCGTACA
CTGTGTTAACCAAAAGTACTTGAAAAATTCTGGAAAGATAAAATGTGCATGCAGTTCTGTGGCCAATTCT
GTTCATGCCAGTTATACGTTATTACATATTAATATTATCATTAGAGTCTAGACTCTCATTCTCAGCCCTG
GTTCTCTCTTTCCTTCATCTTCCCATTCCACTGCTCCTATGCAGCGTGTCTCAGCCTCACAGATCAGGAC
GGGTTTTCAGGCTGTGCTCTTGGGTAAAATTCAACTTCCAAGAAACAGACTGAGTTGGTCTACAGCTAAA
ACTTTATAATGGTGATATTTTTGAAGGTAGAAGGAAGTAACTTTTTTTTTTCTTTCTTTCTTTTTTTTTT
TTTCCTGAGACAGAGTTTTGCTCTTGTTGCCCAGGCTGAAGTGCAGTGGCACAATCTCAGCTTGCTGCAA
CCTCTGCCTCCCGGGTTAAAGCGATTCTCCTGCCCCATCCTCCCGAGTAGCTGGGACTACAGGTGCCCGC
TACCATGCCTGGCTAATTTTTTGTATTTTTAGTAGAGACGGGGTTTCACCATGTTGGCCAGGCTGGTCTC
AAACTCCTGGGAAGTAGCTTTTTTCCTTGTGATTTAGTCTAAAAAAAAAAAGAAAGTAGCTGATTATTTT
CATTTTCTCCCATAGATTTATATAGGACTTTTGGCACCTACTACTATTGGATTCCAGGGAAATTGAAGGA
GACCATAAAACAAATGAACCAAGTTATAAATGAGTATTGCTGAAAAAAGCCCAGAAATAGTCAATCATGC
TTAGTTTGATGGTTTGTGTTTTTGTGGACACACATCATAACTTCATATATTGCATACATAGAGGAATCAT
TTTCTGTAAGAAAAATAGTCTATGAAGGGTACTTACATATATCATTATTCATGTTTTTACAAAATGAATT
ATAGCTTTCTGCAAAGAGGTTGTTCTGCAAACTGAACAATTTTTAGAATAGCTGCCCCAGGAAACCCTCA
CTGTAAGTGATACAAAAATTGCAACAGGACCCCATACCATCTCTTGCTGACCCCATACTGTCCTGAGGAA
CACTGGAAGGTAAATCACCTTAGAGATGAAGAAGAGTCCTTTGGTGGCCCTGTGGCCTATGTGGTTAGGC
AGTTCTTTTTTTTTTTTTTTTTTTTGAGACGGATTCTTGCTTTGTTGCCCAGGCTGGAGTGCAGTGGTGTGA
ACTTGGCTCACTGCAACCTCTGCCTCCTGGCTCAAGCGATTCTCCTGCCTCAGCCTCATGAGTAGCTGGG
ACTACAGGCGCATGCCACCACGCGAGGCTAATTTTTGTATTTTTAGTAGAGACAGGGTTTCATTATGTTG
GCCAGGATGGTCTCCATCTCTTGACCTCGTGATCCACCCGCCTCAGCCTCCCAAAGTGCTGGGATTACAG
GCGTGAGCCACTGCATCTAGCCATGGTTAGGGAGTTCTTTTCATTCTTCCATTAAAATGAAAGAAAGTGA
AGGCTGGTGCTGGATGCTTAGCTTCACCTCTGCTTTCTGTTACCCTTGGCTGTTCTGCATCTGCCATCAT
TCCAGATTATGTATAATTAGACAAAACTCTGCTTCTGTGTATGTGTGTGAGTGTATGTGAACAGAGGGAC
TTAACAGTGAAAATACTTGTACTAGATTGGAGACACTTATAACACCTGCTATATCTTTTCTTTCTCTAAA
CATTCTACTAGAAATTCCCTGGTCTCACAAGCTATATTTTTAAAAATATTATGTTTTTGTTTTTATTTAT
TTTTATTTGTTTATTTTTTGAGACAGAGTCTCGCTGTGTCGCCCAGGCTGGAGTGCAGTGGTGCAATCTT
GGCTCACTGCAACCTCCACCTCCTGGGTTCAAAAGATTCTCCCACTTCAGCATCTCGAGTAGCTGGGACT
ACAGGTGCGTGCCACCATGCCCAGCTAATTTTTTGTATTTTTAGTAGAGACTGGGTTTCACCATATTGGC
CAGGCTGATCTCGAACTCCCAACTTCAGGTGATCCACCCATCTCCATCTCCCAAAGATTACAGGCATGAG
CCACTGTGCCTGGCCTTGTTTTTATTGATTTTTGATTAAAAATTTTAAATTTTAAAAATTTACCTGTTGC
AAAATAATACTAGTTTTATTACCAAGGATATAATTTATTTAAAGAACAGTTTATGATTTACTTGCAGTTT
TTTTGTTCTTAAGATAAAAGGACAGTCAAAATATGAGGTTTTTAACCCACTCAAAAAAATGTTCAGCCAG
GCGCAGTGGCCCATGCCTATAGTCTCAGCTACTCAGGAAGTTGAGGCGGGAGGATTGCTTGAGCCCAGGG
GTTCAGGGCTGTAGTGAGCTATGATCATGCCACTGCACTCCATCCTGGGTAACATAGCAAGAAGTCCTCT

ATACCCCGCCTGCCAAAAAAAAAGTCTCTGGACAGTTTAACTCAACATAGGTAAATTAACTTGTTTCATT
ATGTTATCTGTTTTTAGATACTGGTTTTTAAATTTTGATTTAATTCGTTTCATAAATTTATAAAGCATAT
ACGTGGTTCCAAAGTCAAAGCTATGGAAAAAGGTACAGTTAGAGAAACATCTTCTGTTCATGTCCTCTCC
ACACTCTTCTCTCCTTCCCTGATTAGAAACCTTTTTAATTGTTTTTAGTTTACCCTTCCATGTTTTATTT
TTTATTTTATTTATTTATTTTTGAGACAGAGTCTCGCTCTGTTGCCCAGGCTGGAGCGCAGTGGGG
CAATCTTGGCTCACTGCAGCCTTCGCCTCCCAGGTTCAAGTGATTCTCCTGCCTCAGCCTCCAGGAGTAG
ATGGGATTACAGGTGTGTGCCACCACGCCTGGCTAATTTTTGTGTTTTTAGTAGAGATGAGGTTTCACCA
CGCTGGCCAGGCTGCTCTTGAACTCCCAACCTCAGGTGGTCCACCCACCTTGGCCTCCCAAAGTACTGGG
ATTACAGGCGTGAGCCACCGTGCCTGGCCTTCCGTGTTTTAAAAGTGTAAGTAAATATATTCTCTCTCTC
TCTCTCTCATTCATGTAATGGCTCAAACCTATAATCCAGTACTTTGGGAGGCTGAAGTGGGTGGATCATT
TGAGCTCAGGAGTTCGAGACCAGCGTGGGCAACATGGTGAAAGCCTGTCTCTACTAAAAATACAAAAATT
AGCCAGGTGTGGTGGTGCAAGCCTGTAGTCCCAACTATTCAAGAGGCTGATGTCAGGGGATCACTTGAGC
CCTGGAGGTTGAGGCTGCAGTGAGCCAAGATGGTGCCACTGCACTCTAGCCTGGGTAACAGAGTGAGACC
CTGTCTCAAAAACAAAGAAAAAGGTGTCCCTTTTATTTTAAAAAGGGGATGGCATATAAATGTGTATATA
GTATATAATATAAATTATATACAATGTTTTATATTATATGACATATTACATATAAATTATACATAATATA
TTACATGTAAATACTTATGTAAATATATTCATATAAATACTTATATTTAATATATATTTTTAAGATAAAG
AAGTCAGGTAAAAACTAAGGAAATCTGGATAAAGTATAGACTTTAGTTAACAATAATGTATCAATATTGG
TTTATTGTACCAATGTATTTTATGAATATGGGATGTTAATAATAGGGAAATGGGGGTGCAGTGGCATGTG
CTTATAGTCCTAGTTTCCTCAGCCTTCGGGAGGCTGAGGCAGGAGGATCATTGAGCCCAGGAGTTAGGGT
TGTTCTTCTTGGAGCTGAACTCCTGGGTTCAAGTGATCCTCCCGTCTCAGTCTCCCACCTCCCAAGTAGC
TGAGATTACAGGTGCACGACACTGTAATCAGTGGACATGTTTTCAAGTGGGTTTAAAACTTGGTATTTTG
ACTGTCCTTTTATCTTAAGGACAAAAAACTGCAAAAAAATTATAAGCTGTTTTTTATAAGTGTATTATTG
GTAATAATACTGGTATTACTTTGAAAAAGGTAGATTGAACATAAATATTAGATAATATAGTAATTTATAT
ACATACAAAATATATTTGTATGCTACCCCCTTTTTAAATAAAAGGTACACTTTTTTTTTTTTTTTTTTA
AAGTAGACACAGGGTCTTGCTATGTTGCCCAGGCTGGTCTCAAACTCCTGGCCTAAAGCAGTCCTCCCAC
TTTGGCCTCCTAAAGTGCTGGGATTATAGGCATGAGCCATCATGGCCAGGACATATGTTTTTCTTTTTAA
TTTTATTAATTTGGTTTATTTTTTAATTTTATAGACGCCCTGCTCTCAGATATAACACTTTTTTTCTTTT
AATTTAACAAGATATTTTCGATCTCACTCCATACCTCTATATAGAGAAAACACCCATTCCTTTTTAAAGT
CTATTTTTACAGCTGGTCAAAGAGTAAATCGTTATGTAATATTGCTAGGCATTTCCCAGATCTCCATAGG
CATCATTCCAATTTGCTTTTCCACAGCAATGTATCAGAGTACCTGTTTCACTCTCAACCTCACTGACTTG
TTAAACTTTTTGCCAATTGAAATTCTTGCCAGTGAGAAAATGATATCTCAAAAAGTAAGAAATGATATCT
CAGTGTAGTTTATTTAAAAATAAACTTTTTGTTTTAGCATAGTTTTGTATTTACAGAAAAATTGTGAAGA
TAGTACAGAGAGTTCCCGTATAACCCCATACCCATTCCCCTGGGGTTTTTTCTGGGGGAGGTAGTGGGGC
AGAGTTTCACTATGTTGCCCATGCTGGTCTTGAACTGAGCTCAATGATCCTCCCACCTCACCTTATCAAG
TAACTGGGACTACAGACACGTGCCACTGCAGCACCCCCATTTTCCTATTATTAATATCTCACATTAATAC
AATACATTTAATAATTAATAAACCAATATTGATATATTATTGTTAGCTAAGGGCTATATCTGCTGGGCAC
AGTGGGTCTTGCCTGTAATCCCAGCACTTTGGGAGGCCGAGGTGGGCAGATCACCTGAAATCAAGAGTTC
GAAACCACCCTGGCCAACATGGCAAAACCCCGTCTCTACTAAAAAAATACAAAAATTAGCCAGGCGTGGT
GGCATGTGACTTAGTCCCAGCTACTCAGGAGGCCGAGACAGGAGAATCACTTGAACTTGGTGGGTGGAGT
TGCAGTGAGCCAAGATCATGCCACTGCACTCCAGTCTAGGAGACACAGCGAGACTCCATTAAAAAAAAAA
ATTATATACTTTATCCAGATTTCCTTAGTTTTTCTTAATGTCCTTTTACTGTTCCAAGATCCCATTTAGG
ATACCATATTGCATTTAGTTGTCATGTCTCCTTAAGCTACTCTTGACTGTGACAGTTTTTTGGTTTTAAC
AGTTTTGAGGAGTACTAGTTAGGTATTTTGTAGAATGTCCTTTACTTGAGATTTCTTTATTATGTTTCTT
ATGATTAGATCAGAGTTATTGGTTTGGGGGAGGAAGGTCACAGAGGCAAAGTGCCATCCTTATCAAATTT
TATCAACGGTACGTGCCACCTTTCTTTACAGTCATGTACAGTTGACCCTCAGGATTGGCTCCAGGGTACC
CTGCAGACACCGAAGTCCACAGATGCTCAAATCCCTTACATAAAATGATATAATACAGTTGGCCCTCCAT
ATCTGTGGGTTTCAATTCACGATTGGTTGAATTCTCAGATGTGAAACCCTCAGATACAGAGGGCCAACCG
TATTGTGTAGCTATCCCTGAACTCTTTATTCTGTCCCATTAAAATCTTTGTCTATCTTTGTACCATGTTG
TTGTACATAATGTAGCTTTATAATTAGTCTCAATATCTTTTAGGGCAAGTTCTACCACTTCGTTTTTCTC
CAAGGGTGTCTGAGAGAGTCTTGACCCTTTACATTCTCATATAAATTTTGAAATCAGCTTTTCAGATTCC
ACAAAATACTTTTTGGAATTTTGATTGAGATAATGTTGAATCTATAGATAAATTTGGGGCCAGGAATGAT
GACTTATGCCTGTAATTCCAGCACTTCAGAAGGCTGAGGAAGGAGAGTTGCTTTAGGTGAGGGGTTCAAG
ACCATCTTGGACAACACTGTGTAAAAACTCTAGCCAGGCGTGGTGGCTCACGCCTGTAATCCCAGCACTT
TGGAAGGCCAAGGTGAGTGGATTACGAGGTCAAGAGATCGAGACCATCCTGGCCAACATGGTAAGACCCC
ATTTCTACTAAAAATACAAAAATTAGCTGGGCATGGTGGCACGTGCCTGTAGTCCTAGCTACTCGGGAGG
CTGAGGCAGGAGAATCGCTTGAACCCAGGAGGCAGAGGTTGCAGTGAGCCAAGATCACGCCATTGCACTC
CAGCCTGGTGACAGAGAGAGACTCCGTCTCAAAAAAAAATTAAAAAAAAAAAAACTCTCTATAAAAGTTTT
TATAGAGAGTTGTGAGTCTTCATCTCTATAAAAACTTTTTAAAAATTAGCCAGGCGTGGTGGTGTGCACT
TGTAGCTTGTAGTCTTAGTTACGCAAGAGAATCACTTAAGCTCAGGAGTTCGAGGTTACAGTGAGCTATG
ATCTTGCCACTGCACTCCAGCCTGGGCAACATAACAAGACACTGTCTGTATTAAAAAAAAAAAAACATGGG
AGAGAGTTGATATGTTAACAATATTGAGTCTCCCAATCCACTTATTTACATCTCCTCTAATACTTCCCAG
CTTCATTCATTAGCATTTTCTCTGCAGAGGTTTTGTATATCTTTTGTTAATTTATTCATAGGTAATTGAT
CTATTTTAAAACTATTTATTTATTTATTTATTTTGAGATGGAGTCTCGCTCTGTCACCCAGGCTGGAGTG
CAGTGGTGCGATCTCGGCTCACTGCACCCTCCACCTCCTGGGTTCAAGCGATTCTCCTGCCTCAGCCTCC
TGAGTAGCTGGGATTACAGGTGCCCACCACCGTGTCTGGCTAGTTTTTGTATTTTTAGTAGAGATAGGGT
TTCACCATGTTGTCCAGGCTGCTCTCAAACTCCTGACCTCAGGTGATCTGCTCACCTCGGCCTCCCAAAG
TACTGGGATGACAGGCGTGAGCCACCGCGCCTGGCCAAAACTTTTTATTATGAAAATTTTAAACCAGTAC
CAAAGGAGACTGGGCCAGGAGTGTTGGCTCATGCTTGTAATACCAGCATTTTGGGAGGCTGAGGTGGGTG
GATCACTTGAGCCCAGGAGTTCAAGCCTGGGCCACGTGACAAAACCCTGTCTCTTCAAAAAATACAAAAT
AAATTAGCTGGGTGTGGTAATATGCACCTGTTGTCCCAGCTATTTGGGGGGCTGAGGTGGGAGAATCACT
TGAGTCTAGGAGGTTGAGGCTTCTGTGAGCCGAGATCATGTCACTGCGCTCCAGCCTGGGTGACAAAGTG
AAACCTTGTCTTAAAAAAATAATCAATGACTGGGAGCGGTGGCTCACACCTGTAATCCAAGCACTTTGGG

AGGCCAAGGCGGGTGGGTCACCTGAGGTCAGGAGTGCGAGACCAGCCTGGCCAACATGGTGAAACCCCAT
CTCTACTAAAAATACAAAATTAGCCGGGCATGGTGGCGCATGCCTGTAATCCCAGCTACTCAGGAGGCTG
AGGCAGGAGAATCACTTGAACCTGGAAGGCAGAGGTTGCAGTGAGCTGAGATGGTGTCACTGCACTCCAG
CCTGGGCAACAGAGCGAGACTCAATCTCAAAAAATAAAAATAAATAAAAATAAATGTATAAACAAATAAT
AATTTTCTTATATTAGCTGGGCACAGTGGCTCACAGCTGTAATTCCAGCACTTTGGGAGGTGGGAGGATT
GCTGGACCCCAGGAGTTTGAGATCAGCCTGGGCAAGGTGGAGAGACCCCGTCTCTACAAAAAAATCCAAA
AATTAGCCAGCCATGGTGATGTATGCTTCTGGTCCCGCTATTGGAACGGCTAACATGAGAAGATTGCTTG
AGGCTGGGAAGTCGAGGTTTCAGTGAGCTGTGTTCACGCACTCCAGCCTGGGTGATAGAGGGAGATCTTG
TCTCAAAAAATGAAAGAAAAAAGTAATAATTCCCTAATATCAAACACCTATTCAGTATTAAAATTTCCGC
TTGTCTTGTAAGTGTCATACTTTTTTTGTATGTTTGGATCAGTCTGTTTGGATCAGGATTCAAATAAGGT
TCATACATTGTGACTGACCAATATGTCTGTTAAATCTCTTTTAACTCATAACTTCCTCTTTCATAACTTT
TTTATTCCTTGAATAAAATTTACTCAATTTACTTCAATTTACTCATTGAAGAAACAGGTTATTTTTCCTG
TAGAGTTTCCCAAAGAGAGTTTGTAGAGTGCATTCTAGAAGTGTCGTTTAGCATGTTCTGCTTTCATCCA
TATTTCTTTTTGTTGTTGTTGTTGTTTTGTTTTTTTGAGAGGGAGTTTTGCTCTTGTTGCCCAGTCTGGA
GTGCAATCGCCCGATCTTGGCTCACTGCAACCTGCGCCTCCCAGGTTTAAGTGATTCTCCTGCCTTAGCC
TCCAGAGTAGCTGGGATTACAGGCTTGTGCCACCATGCCCGGCTAAATGTTTGTATTTTTAGTAGAAATG
GGGTTTCACCATGTTGGTCCGGCTGGTCTCGAACTCCTGACCTCAGGTGATCCACCGCCTCAGCCTCCCA
AAGTGCTGGGATTACAGGAGTGAGCCACTGTGCCTGGCCTCATCCATATTTCATTAGCAGTTAGATCTAG
AAGGTAACTGTTGGGTGTTTTTTTTTGTTTGTTTTTTGTTTTTGTTTTTGTTTTTTGAGACTGAGTCTCA
CTCTGTCATCCAGGCTGGAGTGCAATGGCATGATCTTGGCTCACTGCAACCTCTGCCTCCTGAATTCAAG
CGATTCCCCTGCCTCAGCCTCCTGAGTAGCTGGGATTACAACTGTGTGCCACAATGCCTGGCTAATTTTT
GTATTTTTAGTAGCGACGGAGTTTCGCCATGTTTGCCAGGCTGCTCTTGAACCCCATATCTCAGGTGATC
TGCTCACCTCGGCCTCCCACGGTGCTGGGATTACAGGCATGAGCCACTGCACCTGGCCTAATTGCTAGTT
TTTATACTATTGTAAGTAACATCTTTCTCAAAATTTCATTTTTTGTTTATTACCATATATCAAAATACCT
TTGATTTTTGTATCCACAATCTTGGTAACTCTTTTAATTGATTTGGTGAGTTTATTTACATAATTTTTTT
TTTCTTTTTTCATTTTCTTTCTTTTTTGAGATGGAGCCTCGCTCTGTTGTCCAGGCTGGAGTGCAGTGGC
GTGATCTCGACTCACTGCAACCTCGGCATTCCGGGTTCAAGGGATTCTCCTGCCTCAGCCTCCCAAGTAG
CTGGGACTATATACAAATACATACATACATGTGGTATGTGTAGGCACACGCCACCACACTGGCTAAGCTA
ATCTTTCTATTTTTAGTAGATATGGTGTTTCACCATGTTGGCCAGGCTGGTCTCCTGTCTCGGCCTCCTG
AAGTGCTGGGATTACAGGCGTGAACCACCATGCCCAGCATTGTAGATTCTTTTGTATTTCCTATATATGC
AATTACATCACCTATGAATAATGATGGCTTTGTTTCTCCCTTTCCAGTGTGTAACCCTGTTTTTCCTTCC
CTTACTGTGCTTGCTATGACACCCAGTGCATGTTGAACAGAAATAGAGATAGCAGATGTTTTGCCTTCTT
TCTGATTTCTCTCTCCAACTTTTTACCTCACATAATGATTGTTGCTATAGTTTTCTAAAATCTACCTTTT
ATGGAATCAAGTGTCCATCTAGACTTAGATTGCTAAGAGGTGTTTTTTTAATGATGAACGACTATAGGAT
TTTAAGAGCTTCATTTTCTTCATCTATTGAGACAATCATGTATTTCTCCTCTATTCTGTTAATGTGACAG
ATTATATTGATTGATTTTTCTGAAAAATCATTCAGATTATAAACTACTTATACTTTGCTAGTATAAAACC
ACGAAGTAACAGGGTGGTCAGAGCATAAAAGAGCTAGCCATGGTAAGACTCGGGGAGAAATTTTTTTTTT
TTGAGACAGAGTCTTGTGCTGTTGCCCAGGCTGGAGTGCAGTGGCGCGATCTCCGCTCACTGCAAGCTCC
ACCTCCCGGGTTCGCGCCATTCTCCTGCCTCAGCCTCCCAAGTAGCTGGGATTACAGGCGCCCGCCACCA
CGCCCGGCTAATTTTTTGTATTTTTGGTAGAGGCAGGGTTTCACTGTGTTAGCCAGGATGGTCTTGATCT
CCCGACCTTGTGATCCGCCCACCTTGGCCTCCCAAGGTGCTGGGATTACAGGCGTGAGCCACCGCGCCCA
GGTGAAATCATTCTATATTTACACAAACTCTCATAAATAAGAATAAAGGAAATGGTCCCCAATTCATTTT
GTATTAATATAAAACCTGTAAGGATGGTACAGAAAAAGTGAATAAATTGATTCAAATTATTATTGAAACA
AAATATTTAACAAAGGGAATTTAGCAATATATAAAAGGTAATACATCTTACTATTGCTAACTATATTAAA
CTGTGACTTCCTTTTTTTTTCGGTTAGGCCCATTTTTTGTCTCAGTGTACTTATTTTTATACATAATTAT
TTATCTGTTCACTTCTTTTGATTCACTCCTAAGATTTTTTCAGAATATTTTCTTTTTCTTTCTTTCTTTT
TTTTTTTTTGATGGAGTTTTGCTCTTGTTGCCCAGGCTGGAGTGCAATGGTGCAATCTCGGCTCACTGCA
ACCTCCACCTCCCAGGTTCAAGTGATTCTCCTTCCTCAGCCTCCCGAGTAGCTGGGATTACAGGCATGTG
CCACCATGCCAGGATAACTTTTTTTTTGTATTTTTGGTAGAGATGGGTTTCTCCATGTTGGTCAGGCTGGT
CTCGAACTCCCGACCTCAGGTGACCCACCCTCCTCGGCCTCCCAAAGTACTGAGATTACAGGCGTGAGCC
CCCATGCCCAGCCCCAGGATATTTTCATGAGGGAAACCACTTGAATATTGTTTAGATATGGATGCTTTGG
GTAAAGTGCTTTTTTGTTTTTCTTTTTGAAATTAAGAAGAAACATGGCGGCTATCCTTCTCTCACATCGA
AAAGGAAATTTTGAACAATCATGGAAAATCTAAAACGTGCTGTGAAAACAAAGAAGAGAAATGTTGCAGG
TAACAGCCTTATTTTGTTAAATGACAGATTATCTATGGTATGCTTAATTATTTGTTGACTCCACACCTCA
GACCTGAAGAGCTGAGCTGGGTTGGGTCTGGGGGGCAGGGCAGGATTGGGTTGAGCTGGGGAGAGTGTGA
GTATGAAACCAGAGAAGCTAGATCCAAAGGGCCAAGGAAAGGGTGTTGTTAGAAGGCAAGGCCGGGGAAT
AGTAGTTCTGAACCCTGGATCAGATGAATGTGTTTTTGTATAGATGTATCAGTAGGACAGAGTGAGAGGG
TATGAGCACTAGCCATGACAATTCGATGGGTCTTAGTATTCTGCTTGTTTAAAAGTAATGGATATTAATG
CCATATAATTGGAGGAGGCCAAAAGGTCGCTCTTATTAGATACTGGGCTTGCTTTGGGATAGTTGGGTTG
TGTTGACGGCTAGGGATTGATTGGCCAAACTGAAAACAACACTAAGTGAGTAATTTTTTTTTTTGAGACA
GACTTTCACTCTGTCACCCAGACTGGAGTGCAGTGGCACAATTACGGCTCACCACAGCCTCGATCTCCTG
GGCTCAAGCAATCATCCTACCTCAGCCCCCCAAGTAGCTGAGATTACAGGTGCATGCCACCATGCTCGGC
TAATTTAAAAAAAAATTTTGTAGAGGGCCTGTTGGCTCACACCTGTAATCCCAGCCTAGCAACATGGTGA
GACCCCACCTCCATAAAAAATTTAAAAATTAGCCAGGCATGGTGACTGGTGCCTGTGGTCCCAGCTACTT
GGAAGGCTGAGGTAGGAGAATGGCTCGAGCCCAGAAAATCAAGGCTGCAGTGAGCCATGATCGTGCCACT
GCACTGCAACCTGGGTGACATAGTGACACCCTGTCTCAAAAAAAAATTTTTTTTTATTGGTAGAGATGGTGG
TCTCCCTTTGTTGCCCAGGCAGGCTGGTCACCAACTCCTGGGTTCAAGTAAACTTCCCGCCTTGGCCTCC
CAAAGTCTTGGAAGTACGGGGATGAGACACTGCACCCCACCATTTTTTTTTGTGATGGCATACACACCAT
AAAGAACTAAGATTGAAAAGGAATTGTTCATTTGAGTTTCTAAAGTTGGCCAGTATTGGCCAGGCATGGT
GGCTCAAGGCCTGCAATCCCAGCACTTTGGGAGGCCAGGGCAGGTGGATCACCTGAGGTCAGGAATTCGA
GACCAGCCTGGCCTACGTGGCGAAACCCCGTCTCTACTAAAAATACAAAAATTAGCTGGGCGCAGTGGCA
CGTGCCTGTAATCCCCGCTACTCAGGAGGCTGAGGCAAGAGAATCACCTGAACCCGGGAGACAGAGGTTG

CAATAAGCTGAGATCATGCCACTGCACTCCAGCCTGGGCAACAGAGCAAGACTCCATCTTAAATAAATAA
ATAAATAAATAAATAAATAAATAAATAAAGTAAGTTGGCCAGTATAAAGATCACAAAAGTTAAAAAGTCA
AAACAAAAATGCCCAACATGCAGGCACAGAGGTTCTTTAAGATCTCATATGCAGGCTTTGAAGTAAGCAT
TAAGAAAACTATATTGTTGGCCAGGCACAGTGGCTCACGCCTGTAATCCCAGCACTTTGGGAGGCCGAGG
CAGGTAGATCACCTGAGGTCAGGAGTTCGAGACCAGCCTGGCCAACGTTATGAAACCCCGTCTCTACAAA
AATGCAAAAATTAGCCGGGCGAGGTGGCATGCACCTGTAATCCCAGCTACTTAGGAGGTTGAGGCAGGAG
AATCGCTTGAACCCAGTAGGCAGAGGTTGCGGTGAGCTGAGATCACACCACTGCACTCCAGCCTGGGCAA
CAGAGCGAGACTCCATCTCAAAAAAAAAGGAAAAAGAAAAAAAAAAAGAAATATTGTTGATAAGGCTAAA
TAGTTTCATAAATAGTACATTTTGTCAACTACTAAATAACTAGATGAGATGGCAGATTATCTATGGTACT
CTTAATAATGTAAATAATTCTGTGATACAATCAGTGGATTTTAGAAAAGAAAAAATTTATATTAAATTTG
CAGTTCAATAAAGTAAAATAATTTTATAACAAAACAAGATTTTGGATCGCTTGAGGGGGGTGAGGGGAGG
GTCAGAGGTTGCAGTGAGCCGAGATTGTATCACTGCATCCCAGCCTGGGTGACAGAGTGAGACCCTGTCT
CAAAAAAAAAAAAAAATAGTATAAATATCTGTTAGCTTTATACAGTTGAAGAAATTCATAGAATATATTTA
AGCTAAGAATGGGAAAGAGAGGGAAAAAATGTGTTTTTGAAACTTCAAACCATATATTTGAAAACATAAT
CAGATTTTAGTGTGACTGTTGTATTTATTTTATTTTATTTTATTTTATCATTTCATTTCATTTCATTTAT
TTCATTTTATTTTATTATTTTATTTTATTTTATTTTATTTTATTTTGAGATGGAGTCTCACTTGTTGCCC
AGGCTGGAGTGCAGTGGCATGATCTTGGCTCACTGCAACCTCTGCCTCCTGGGTTCAAGTGATTCTCCTG
CCTCAGCCTCCCGAGTAGCTGGGATTATAGGTGCACGCCACCACACCTGGCTAATTTTTGTATTTTTAGT
AGAGATGGGGTTTCAGCATACTGGCCAGGCTGATCTCGAACTCTTGACCTCGTGATCCGCCTGCCTAGGC
CTCCCAAAGTGCTGGGATTACAGGCATGAGCCACCGCGCCCGGCTTTTTTGTTTTTGTTTTTGTTTTCTG
TGTGTGACAGAGTTTCGTTCTTGTTGCCCAGGCTGGAGTGCAATGACGCGATCTTGGCTCACTGCAACCT
CCGCCTCCTGGCTTCAAGCGATTCTCGTGCCTCAGCCTGCAGAGTAGCTGGGATTACAGGCGTGCGCCAC
CACGCCCAGCTAATTTTGTATTTTTAGTAGAGACGGGGTTTCACCATATTAGTCAGGCTGGACTCAAACT
CTTGATCTTAGGTGATCCCCCTGCCTCAGCCTCCCAAAGTGCTGGGATTACAGGCGTTGTGTCACCACGC
CCGGCCTATATTTATGTTATTATATATCTTTATTGTTTATATTTTTGCTATGAGATGCCTAAAATCCTTT
GTTGAATGTAAATAAGTAAAAATAAGTGTTTTCCTTTTTTATTCAACAGGAAAGATTGTTTAAAACTAAT
GAAATACCTTTTAGAACAGCTGAAAGAAAGGTTTAAAGACAAAAAACATCTGGATAAATTCTCTTCTTAT
CATGTGAAAACTGCCTTCTTTCACGTATGTACCCAGAACCCTCAAGACAGTCAGTGGGACCGCAAAGACC
TGGGCCTCTGCTTTGATAACTGCGTGACATACTTTCTTCAGTGCCTCAGGACAGAAAAACTTGAGAATTA
TTTTATTCCTGAATTCAATCTATTCTCTAGCAACTTAATTGACAAAAGAAGTAAGGAATTTCTGACAAAG
CAAATTGAATATGAAAGAAACAATGAGTTTCCAGTTTTTGATGAATTTTGAGATTGTATTTTTAGAAAGA
TCTAAGAACTAGAGTCACCCTAAATCCTGGAGAATACAAGAAAAATTTGAAAAGGGGCCAGACGCTGTGG
CTCACACCTGTAATCCCAGCTCTTTGGAGGCCGAGGCAGGCGGATCACTTGAGGTCAGGAGTTTGAGACC
AGCCTGACCAACATGGTGAAACTCCATCTCTACTAAAAATATAAAAATTAGCCGGGCATGGTGATGCATG
CCTGTAATCCCAGCTACTCGGGAGGCTTAGACATGAGAATCACTTGAACCCAGGAGGTGGAGGTTGCAGT
GAGTCAAGATGGCACCACTGCACTCCATCCTGGGTGACAGAGCAAGACTTCCTCTCAAAAAATAAATAAA
TAAATAAGAAAAATAAATTAGGAAATTATTAAAATAATTTTTTAGAAAAGCAACAAAATAACAAAAATTA
GTGACTGTAATAATTGGAATGTTTGAAATTTGTCACAGCAATAATTGACTAAAATGAATGTAAATAATTA
TTCAGTTTTCAGTTTGTTGTAATAAACTCTAATCAGTATAAAGGATTGACTATCCTAGGAAAAAGATTAG
TCAAGGAATAAGAAGCAAAAGTAGTATTTGAAATCTAAAAACATTACCATGTTTGCTTTATCATGCAGGC
AAATAAATAAATAAATGACATTTTTAGGTTGGAATAAAAAAAGATAAAGTACATATTGCCTTAATTAAAT
TCATCAAGTTCTTACTGAAAAACAGCTCTCCGCCGTGCCTGGCCAGGAAATACATAATTTTTTTTTTTTT
TTTTTAGATGGAGTCTCGCTCTGTCGCCCAGGCTGGAGTCCAGTGGCATGATCTTGGCTCACTGCAAGCT
CTGCTTCCTGGGTTCATGCCATTCTCCTGCCTCAGCCTTCCGAGTAGCTGGGACTACAGGTGCCCGCCAC
CACATCCGGCTAATTTTTTGTATTTTTAGTAAAGATGGGGTTTCACCATGTTAGCCAGGATGGTCTCGAT
CTCCTTACCTTGTGATCCGCCCGCCTTGGCCTCCCAAAGTGCTGGGATTACAGGTGTGAGCCACCACGCC
TGGCTGAAATACATAATCTTAAAAGAAAACATAAGATACTTTATTTTAATATACGTGACTAAATGTAAAA
CCTAACTTATTTTCTGTTATCTATTTATTTTTACTTTCAGTAACACTTTTTTTATTTTAGGTAGCATTCA
GCCTAGAGGCAACTGCTGTTTGTTAAATATTTCCTGTTCATATATTTTGCACATTTTCTTATGGGTTAGT
TTTCTTCTCATTGTTTTGGGAAGTTCTTAATATATTTGGGGTATTTATCTTTCATTCGTTGTCTGTGTAA
CAAATAACTTCTGCCATATGGGTTGTCTGCACATTTTTTGGTGTCTTTTAGTAAACAAGGTTTTTTTGTT
TTGTATTGTTTTGTTTATTGTAAAGATTTTTAAATTTTAATGGAGTTGATTTCTTTTCTCATTCAAGCTT
TTGAGAATAAATTGGAGTTGAATTTTT

Sp1 binding sequence